UNDERSTANDING PERFORMANCE LIMITS IN WIRELESS SENSOR NETWORKS

BY

HONGHAI ZHANG

B. E., University of Science and Technology of China, 1998
M.S., University of Illinois at Urbana-Champaign, 2001

DISSERTATION

Submitted in partial fulfillment of the requirements
for the degree of Doctor of Philosophy in Computer Science
in the Graduate College of the
University of Illinois at Urbana-Champaign, 2005

Urbana, Illinois

Abstract

In this PhD thesis, we study the fundamental limits of the network performance with respect to coverage, connectivity, lifetime, power, energy, and capacity in wireless sensor networks.

An interesting finding is that many of the performance limits are related to the power level chosen by each node to perform sensing and communication tasks. For example, the choice of sensing power and transmission power determines network coverage, connectivity, and the drain of the battery energy, which in turn decide the network lifetime and capacity. Therefore, most of the performance limits are linked at heart by the power consumption of sensor nodes and sensor networks.

We first address the problem of maintaining sensing coverage and connectivity in large scale wireless sensor networks. We prove a necessary and sufficient condition under which coverage infers connectivity: the radio range is at least twice the sensing range. In addition, we derive a set of optimality conditions that minimize the overlap while maintaining complete coverage. Based on the optimality conditions, we design a localized algorithm OGDC that can form a connected coverage set of sensors using a small number of sensors.

We next analyze the lifetime upper bounds for a wide class of algorithms that maintain coverage and connectivity in sensor networks. Based on the theory of coverage processes, we derive the asymptotic lifetime upper bound in an infinitely large region under several different model assumptions (such as with and without Torus convention) and several different types of node deployment methods (such as Poisson deployment, uniformly random deployment, and regular grid deployment). In addition, we investigate the lifetime upper bound for which only α portion of the area is covered and also devise an algorithm that can approach the derived lifetime upper bound.

We also study the minimum total power required for maintaining k-connectivity. We show that under the assumption that nodes are distributed as a Poisson point process with density λ, the minimum total power required for maintaining k-connectivity is $\Theta(\frac{\Gamma(c/2+k)}{(k-1)!}\lambda^{1-c/2})$, where $2 \leq c \leq 4$ is the path loss exponent. We find that by allowing each node to choose different transmission ranges, the average power consumption can be reduced by an order of $\Theta((\log \lambda)^{c/2})$, compared with the case when all nodes choose a common minimum power to ensure k-connectivity.

Finally, we study the minimum energy required for transporting packets between two arbitrarily chosen source and destination in a random wireless network. We prove that under the assumption that nodes are distributed as a Poisson point process with density λ, the minimum energy is $\Theta(\lambda^{(1-c)/2})$, where c is the path loss exponent. This result can be used to show several network transport capacities. For example, we prove that the network transport capacity with ultra wide band is $\Theta(\lambda^{(c-1)/2})$ under the assumption that nodes are distributed as a Poisson point process and source destination pairs are randomly chosen. Our simulation results show that the minimum energy converges to $l\lambda^{(1-c)/2}$, where l is the distance between the source and destination.

To my parents and my wife, Jing Zhao.

Acknowledges

I would like to express my sincere gratitude to my thesis advisor, Professor Jennifer C. Hou, for her guidance, encouragement, and support throughout my PhD study at University of Illinois. As an academic advisor, she has led me to the networking research area, given invaluable advice and suggestions, provided generous financial support, and offered tremendous encouragement all the time.

I would like to thank Professors P. R. Kumar, Lui Sha, Marco Caccamo, for agreeing to serve on my thesis committee, for much helpful advice, and for their constructive criticism. I especially thank Prof. Kumar for his many insightful discussions.

I also would like to thank my fellow graduate students, friends, and the staff in the Department of Computer Science for their discussions, friendship, and help. The enlightening discussions with Feng Xue and Liang Liang Xie on their related research work have greatly helped me sharpen many ideas crystallized in the thesis. Ning Li, Chunyu Hu, and Guanghui He have discussed and proofread several parts of the work in the thesis. They and several other students have also given me numerous suggestions on organizing the thesis and presenting my work.

Finally, I would like to give special thanks to my wife, parents, brother, and sisters, who endured this long process with me, always offering their unconditional love, support, and encouragement throughout my graduate study. This thesis is dedicated to them.

Table of Contents

List of Tables

List of Figures

Chapter 1

Introduction

Driven by technological advances in MEMS, wireless networking, and embedded processing, ad hoc networks of miniature devices with limited sensing, processing, and wireless communication capabilities are becoming increasing available for civilian and military applications such as environmental monitoring (e.g., traffic, habitat, natural resources), critical infrastructure protection (e.g., power grids, nuclear center, water distribution), industrial sensing and diagnostics (e.g., factory, appliances), and situational awareness for battlefield applications [24, 41, 3, 50].

Interests in wireless sensor networks have opened up many new research vistas and led to a large amount of research activities in the area of sensing tasking and control, tracking and localization, in-network processing, communication protocol design, and system prototyping and implementations. However, relatively less work has been performed on understanding the fundamental performance limits of wireless sensor networks and whether and to what extent the limits can be achieved.

In this thesis, we perform a rigorous study of performance limits for wireless sensor networks with respect to network coverage, connectivity, lifetime, critical power, energy, and network capacity. We also devise algorithms to approach the derived performance limits. An interesting finding is that many of the performance-related attributes are related to the power level chosen by each node to perform sensing and communication tasks (Fig. 1.1). Indeed, the choice of power level determines: (i) the sensing range, (ii) the transmission range, and (iii) the drain of battery energy. The choice of the sensing range and the transmission range determines network coverage and connectivity, which in turn determine the network lifetime and capacity. Thus, the choice of power level influences the physical layer through the quality of the received sensing and communication signal, the MAC layer through the interference and contention caused by communication, the networking layer through the set of wireless links that are formed, and the transport layer through the data transport capacity. Therefore, most of the performance limits studied in this thesis are linked at heart by the power consumption of sensor nodes and sensor networks.

Specifically, we consider the following research issues:

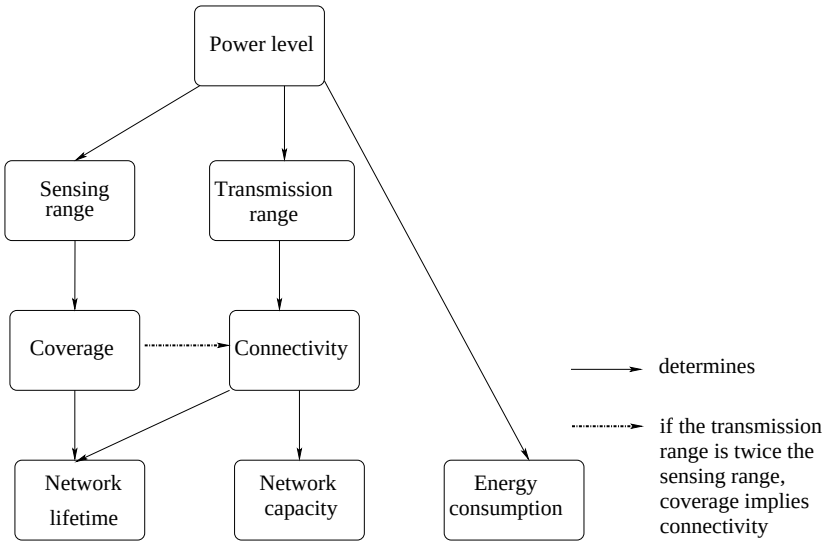

Figure 1.1: The relationship between different node and network attributes in wireless sensor networks.

Density control for maintaining coverage and connectivity: Reducing power consumption and prolonging network lifetime are very important problems in wireless sensor networks because the energy of sensors is often (only) supplied with onboard batteries and it is often impractical or infeasible to replenish energy via replacing or recharging batteries on the sensors. To overcome the problem of limited energy supply and to prolong network lifetime, sensors are often deployed with high density. In such a high-density, energy constrained sensor network, an important issue for saving power is *density control* — the function that controls the density of working sensors to certain level, with the objectives of accomplishing the sensing, monitoring and surveillance tasks [80]. Specifically, density control ensures only a subset of sensor nodes operate in the active mode and put all remaining nodes to sleep in order to save energy and extend network lifetime. The set of working nodes should fulfill the following two requirements: (i) *coverage:* the area that can be monitored is not smaller than that which can be monitored by a full set of sensors; and (ii) *connectivity:* the sensor network remains connected so that the information collected by sensor nodes can be relayed back to data sinks or controllers. Under the assumption that an (acoustic or light) signal can be detected with certain minimum signal to noise ratio by a sensor node if the sensor is within a certain range of the signal source, the first issue essentially boils down to a coverage problem: assuming that each node can monitor a disk (the radius of which is called the *sensing range* of the sensor node) centered at the node on a two dimensional surface, how to choose a subset of nodes that can cover the entire area? Moreover, if the relationship between coverage and connectivity can be well characterized (e.g., under what condition coverage may imply connectivity and vice versa), the connectivity issue can be studied, in conjunction with the first. In addition to the above two requirements, it is desirable to choose

a minimum set of working sensors in order to reduce power consumption and prolong network lifetime. Finally, due to the distributed nature of sensor networks, a practical density control algorithm should be not only distributed but also completely localized (i.e., relies on and makes use of local information only) [24].

In **Chapter 3**, we address the issue of maintaining coverage and connectivity in an analytic framework, and based on the findings, propose a fully decentralized and localized algorithm, called *Optimal Geographical Density Control* (OGDC), in large scale sensor networks. Our goal is to maintain coverage as well as connectivity using a minimum number of sensor nodes. We investigate the relationship between coverage and connectivity by solving the following two sub-problems. First, we prove that under the assumption **(A1)** the radio range is at least twice the sensing range, a complete coverage of a convex area implies connectivity among the set of working nodes. Note that as indicated in Tables A.1 and A.2, **(A1)** holds for a wide spectrum of sensor devices that recently emerge. As a result, the proof allows us to focus only on the coverage problem, as complete coverage implies connectivity. Second, we explore, under the ideal case that the node density is sufficiently high, a set of optimality conditions under which a subset of working nodes can be chosen for complete coverage. Based on the optimality conditions, we then devise a decentralized and localized density control algorithm, OGDC. We also discuss the procedures taken by OGDC in the (infrequent) case that the radio range is smaller than twice the sensing range, thus allowing OGDC to be uniformly applied to all cases. We perform *ns-2* simulations to validate OGDC and compare it against a hexagon-based GAF-like algorithm, the PEAS algorithm presented in [80], and the CCP protocol in [74].

Lifetime analysis: Another important issue that is related to density control is how and to what extent, the network lifetime can be prolonged with all possible density control algorithms.

In **Chapter 4**, we derive the upper bounds of the network lifetime under two classes of density control algorithms, and investigate the tightness of the upper bounds by devising an algorithm that approaches the derived bounds. In the first class, the asymptotic lifetime upper bound is derived under the condition that complete (1-)coverage is maintained in sensor networks that are randomly deployed in large area. The second lifetime upper bound is derived under the condition that partial coverage (or α-coverage) is maintained in sensor networks that are deployed in finite area, where by α-coverage, we mean at least α-portion of the area is covered.

The first class of lifetime upper bounds is determined by the coverage degree because the the lifetime of maintaining complete coverage is upper bounded by the coverage degree multiplied by the lifetime of a single sensor. Therefore, the problem boils down to determining the density requirement in order to obtain

a certain coverage degree k. We consider several different model assumptions for this class of lifetime upper bounds, e.g., with and without Torus convention. In the case that Torus convention is considered, assuming the nodes are distributed according to a Poisson point process with density λ on a square region with side length l, we prove that the target region has k-coverage with probability approaching one if and and if $\lambda = \log l^2 + (k+1)\log\log l^2 + c(l)$ and $c(l) \to \infty$ as $l \to \infty$. In the case that Torus convention is not assumed (i.e., the boundary issue is taken into account), we consider three different methods of node deployment: (i) Poisson process deployment, (ii) uniformly random deployment, (iii) regular grid deployment. In each of the three deployment methods, we obtain a necessary and a sufficient condition for achieving a certain coverage degree k.

For the second class of lifetime upper bounds, we further study two categories of algorithms. The first category of algorithms attempt to maintain complete coverage at system initialization and as sensor nodes die and complete coverage cannot be provided, they will attempt to maintain as large coverage as possible. Most algorithms including our OGDC algorithm fall in this category. The second category of algorithms attempt to provide α-coverage since the system is initialized. Therefore, the lifetime upper bound for the second category of algorithms is universal.

To show that the derived lifetime upper bounds are tight, we also devise an algorithm that approaches the universal α-lifetime upper bound. Conceptually, the algorithm repeatedly chooses a set of nodes that maximizes the α-lifetime upper bound of the *remaining* set of sensor nodes. Our simulation studies show that the algorithm can achieve approximately 90% of the lifetime upper bound, which serves as an evidence that the bounds derived are tight.

Critical total power for maintaining k-connectivity: An alternate method for saving energy in wireless sensor networks is to reduce the transmission power since the transmission power accounts for a large amount of energy consumption of wireless sensors [46]. Reducing transmission power not only saves energy, but also reduces MAC-level collision and hence increases network capacity. However, in order to maintain proper network operations, it is also necessary to ensure network connectivity. In many circumstances (such as in the presence of node failures or mobility), it is important that the networks are k-connected for the sake of robust and fault tolerant communications.

In **Chapter 5**, we derive the critical total power required for maintaining k-connectivity, where the critical total power is defined as the minimum value of the summation of the power of all the nodes required to maintain k-connectivity. Instead of assuming that all nodes use a minimum common transmission power as in previous work [59, 35, 56, 57, 62, 73], we allow each node to choose different transmission power. Under the assumptions that nodes are distributed as a Poisson point process with density λ in a

unit-area square and the transmission power of a node with transmission range r is r^c, where $2 \leq c \leq 4$ is the path loss exponent, we show the critical total power for k-connectivity is $\Theta(\frac{\Gamma(c/2+k)}{(k-1)!}\lambda^{1-c/2})$ with the probability approaching one as the node density $\lambda \to \infty$.

The above result is obtained by deriving a lower bound and an upper bound of the critical total power. The lower bound is derived based on the necessary condition that every node must be able to reach its kth nearest neighbor in order to maintain strong k-connectivity. The upper bound is derived based on an assertion (which is also proved in Chapter 5) that the resulting network is strongly k-connected, if every node can reach at least k nodes in each of its four quadrants, as long as there are at least k nodes in that quadrant. In the case that there are less than k nodes in a quadrant, the transmission power of the node should be sufficiently large to reach all of them.

Our results suggest that the power saved using optimal, non-uniform transmission ranges is in an order of $(\log \lambda)^{c/2}$ compared to that using minimum uniform transmission ranges. By rescaling, we also obtain the critical total and average power in an expanded network (in which the network density is kept constant but the network area increases). We show that, in an expanded network, the average power of each node is bounded if we allow each node to choose its own transmission power to maintain (k-)connectivity, while the power required at every node is unbounded if all nodes have to choose a *common* power to maintain (k-)connectivity. These results are not specific to an algorithm, but rather a fundamental property in wireless networks.

Minimum transporting energy and network capacity: Following the critical total power analysis, we consider the energy efficiency problem from a different angle. Although it is important to maintain connectivity in order to support data transport, maintaining connectivity is merely the underlying mechanism to support data transport. The primary function of a wireless network is to actually transport data packets.

In **Chapter 6**, we study the problem of minimizing energy consumption *while transporting a packet from a source to a destination in a wireless network*. Algorithmically, the problem can be solved using any shortest-path algorithm such as Dijkstra's algorithm. However, it has been left unattended *what is the asymptotic minimum energy*[1] *required to carry a packet from a source to a destination in a wireless network*, and especially, how this quantity scales as the network size goes to infinity. We address this problem under the assumption that nodes are distributed as a Poisson point process with density λ in a unit square area, that the source and the destination are separated by at least a constant distance, and that one hop transport energy is proportional to the hop distance raised to the power loss exponent c.

[1] which is termed as the *minimum transporting energy* in this thesis.

We solve the formulated problem by deriving, based on percolation theory, an upper bound and a lower bound on the asymptotic minimum energy required to transport a packet from a source to a destination in a random network in a unit-square region. We show that if the source-destination distance is of order $\Theta(1)$, both the upper and lower bounds are of order $\Theta(\lambda^{(1-c)/2})$ with the probability approaching one as the network density goes to infinity.

After the bounds are derived, we discuss how to extend the results to accommodate the cases (i) that the network density is kept as constant but the network size goes to infinity, and (ii) that both the transmitting and receiving operations consume power. In particular, we obtain the following more general result in case (i): in a network where nodes are distributed according to a Poisson point process with density λ on an infinite plane, the minimum energy required to carry a packet from a source to a destination with distance l is $\Theta(\lambda^{(1-c)/2}l)$ with high probability if $\lambda l^2 \to \infty$.

We also demonstrate how to apply the derived results to solve other related problems. In particular, we show the derived results can be used to determine the capacity bound in the case that directional antennas are used for spatial reuse and the capacity bound in the case of ultra wide band (UWB) communications. This is because in both cases the limiting factor for the capacity bound is the system energy. In the case of ultra wide band (UWB) communications, we prove the transport network capacity scales in the order of $\Theta(\lambda^{(c-1)/2})$ with high probability as the node density λ goes to infinity. The derived results can also be used to determine an upper bound on the network lifetime of wireless sensor networks.

We carry out simulation to both validate the theoretical derivation and estimate the associated constant in the derived asymptotic function. The simulation results suggest that the minimum energy required for transporting a data packet converges to $l\lambda^{(1-c)/2}$ with high probability, where l is the source-destination distance and λ is the node density.

Major contributions: The major contributions of the thesis are

1. devising an algorithm for maintaining coverage and connectivity based on several theoretical observations;
2. developing the upper bounds of sensor network lifetime for both complete coverage and α-coverage;
3. deriving the critical total power required for maintaining k-connectivity;
4. analyzing the asymptotic minimum energy required for transporting packets from a source to a destination and the transport network capacity under ultra wide band communications or directional antennas.

This is concluded in more details in **Chapter 7** with a list of research avenues for future work.

Chapter 2

Related Work

There are many research activities in wireless sensor networks including density control, tracking and localization, time synchronization, in-network processing, data fusion, system prototyping and implementations, and performance analysis. In this chapter, we give a summary on those that pertain to the research issues addressed in the thesis.

2.1 Density Control

Minimizing energy consumption and prolonging the system lifetime has been a major design objective for wireless ad hoc and sensor networks. An important way of reducing network energy consumption is to put some nodes to sleep and therefore, control the "density" of the active nodes at an adequate, low level.

2.1.1 Density control for maintaining connectivity

Several research activities have focused on density control for *maintaining connectivity* in wireless networks. GAF [77] assumes each node knows its own geographical location and conserves energy by dividing a region into rectangular grids, with the constraint that the maximum distance between any pair of nodes in adjacent grids is within the transmission range of each other. The constraint ensures that a node can communicate with any other node in its neighboring grids. A leader is then elected in each grid to stay awake and relay packets, while all the other nodes are put into sleep. The leader election scheme in each grid takes into account of battery usage at each node.

SPAN [15] is a distributed and randomized protocol in which nodes make local decisions on whether they should sleep or join a forwarding backbone. Nodes that choose to stay awake and maintain network connectivity/capacity are called *coordinators*. A non-coordinator node elects itself as a coordinator if any two of its neighbors cannot communicate with each other directly or indirectly through one or two existing coordinators. The non-coordinator node announces its willingness of being a coordinator via local broadcast, deferred by an interval that reflects the residual power of a node. The information needed for

coordinator election is exchanged among neighbors via HELLO messages.

LEACH [37] is a self-organizing clustering architecture used for large-scale sensor networks. It divides time into rounds and each round into two phases: the setup phase and the steady phase. Clusters are formed during the setup phase and mechanisms are devised to rotate the role of cluster head among nodes to evenly distribute the energy load. In the steady phase, LEACH uses time-division multiple access (TDMA) for intra-cluster communication between the sensors and the cluster-head. Each sensor in a cluster can only transmit in one time-slot within each frame and can sleep in all other time slots.

2.1.2 Density control for maintaining coverage and connectivity

Several centralized and distributed algorithms have been proposed for sensing coverage in sensor networks [67, 14, 69, 79, 80, 33, 74, 76, 38, 39]. Slijepcevic *et al.* [67] addressed the problem of finding the maximal number of covers in a sensor network, where a cover is defined as a set of nodes that can completely cover the monitored area. They proved the NP completeness of this problem, and provide a centralized heuristic solution. They showed that the proposed algorithm approaches the upper bound of the solution under most cases. It is, however, not clear how to implement the solution algorithm in a distributed manner.

Cerpa and Estrin [14] presented ASCENT, to automatically configure sensor network topologies. In ASCENT, each node measures the number of active neighbors and the per-link data loss rate through data traffic. Based on these two values, it decides whether to sleep or keep awake. ASCENT does not consider the issue of completely covering the monitored region either.

Ye *et al.* [79, 80] presented PEAS, a distributed, probing-based density control algorithm for robust sensing coverage. In this work, a subset of nodes operate in the active mode to maintain coverage while others are put into sleep. A sleeping node wakes up occasionally to check if there exist working nodes in its vicinity. If no working nodes are within its probing range, it starts to operate in the active mode; otherwise, it sleeps again. The probing range can be adjusted to achieve different levels of coverage redundancy. The algorithm guarantees that the distance between any pair of working nodes is at least the probing range, but does not ensure that the coverage area of a sleeping node is completely covered by working nodes, i.e., it does not guarantee complete coverage.

Tian *et al.* [69] devised the first algorithm that ensures complete coverage. They defined the "sponsored area" of node j by node i as the maximal sector of node j's coverage disk that is covered by node i. Whenever a sensor node receives a packet from one of its working neighbors, it calculates its sponsored area by that node. If the union of all the sponsored areas of a sensor node covers the coverage disk of the node, the node turns itself off. In general, this method requires quite a lot of working sensors. Moreover,

the authors only address the coverage problem without touching the connectivity problem.

Gupta *et al.* [33] devised both a centralized and a distributed algorithm to find a subset of nodes that ensure both coverage and connectivity. The centralized algorithm guarantees that the size of the formed subset is within $O(\log n)$ factor of the optimal size, where n is the network size. However, the distributed algorithm is heuristic-based and does not guarantee the $O(\log n)$ factor. It is also difficult to implement the distributed algorithm because it requires each node to reliably broadcast messages to all the nodes within $2r$ hops, where r is the maximum number of hops between any two nodes whose sensing regions intersect. In fact, the value of r has to be found out.

Wang *et al.* [74, 76] investigated the same problem and come up with some similar analysis as ours independently. In particular, they also observed that coverage infers connectivity if the radio range is at least twice the sensing range ($r_t \geq 2r_s$), and that if all the crossing points inside a region (or disk) are covered then the region (or disk) is covered. In their Coverage and Configuration Protocol (CCP), each node collects neighboring information and then use this as an eligibility rule to decide if a node can sleep. In the case of radio range is less than twice the sensing range, they combine their protocol with SPAN [15] to form a connected covering set.

Huang and Tseng [38, 39] proposed a new solution to determine whether a sensor network is k-covered. They proved that if the perimeter of each sensor's coverage area is k-covered, the whole network is k-covered. As this solution can be executed by each sensor based on location information of its neighbors, it can be easily translated into a distributed solution. The k-coverage problem can be extended to solve several application-domain problems. For example, it can be used to determine whether a sensor node can sleep but still ensure k-coverage of the network. This can lead to an efficient algorithm for maintaining k-coverage. However, both Wang's and Huang's work [74, 76, 38, 39] did not consider minimizing the overlap or the optimality conditions for minimizing overlap while covering crossings. Therefore, in general, they required more nodes to be active than our work.

It should also be noted that the work reported in [51, 47] gave a totally different definition on coverage. Coverage in these efforts was defined as finding a path through a sensor network, given the location of all sensors. Two coverage problems were studied: the best coverage problem attempted to find the path that minimizes the maximal distance of all points to their closest sensors, while the worst coverage problem attempted to find the path which maximizes the minimum distance of all points on the path to their closest sensors. In particular, Meguerdichian *et al.* [51] presented centralized algorithms for both the best and worst coverage problems, and Li *et al.* [47] gave localized algorithms for both problems. Another related problem is to deploy a minimum number of base stations in cellular networks so as to cover the maximal area. The work reported in [48, 52] approached this problem via devising centralized numerical

methods.

2.2 Fundamental Limits of Network Lifetime

Recently, several research efforts have been made to analyze the upper bound of network lifetime for ad hoc and/or sensor networks [8, 9, 10, 17]. Bhardwaj and Chandrakasan [8, 9] studied the upper bound of network lifetime for data gathering sensor networks [8, 9]. They assumed the data source is randomly distributed in a region with a certain *p.d.f.* function and the data sink is located at a fixed point. They calculated the minimum power required to transmit a bit from the source to the sink and then compute the upper bound of network lifetime based on the minimum power consumption. In [8] they did not consider the network topology or the effect of data aggregation of data streams. In [9] they extended the work in [8] by taking into account of these factors and deriving the upper bound of network lifetime for networks with arbitrarily complex capabilities. However, their model only considered the power consumed in sensing active events and processing/transmitting/receiving data, but not that incurred when the sensor nodes are in the monitoring mode. As shown in the empirical study in [66, 25], power is consumed not only by active communications, but also by wireless devices in the idle and/or sensing state. As a matter of fact, the energy consumed by wireless devices in the idle and/or monitoring state is only a little less than that in the transmitting or receiving states. Thus it makes more sense to derive the network lifetime under the scenario that only a minimum set of sensors are turned on, while the other sensors operate in the low-power mode (or sleep mode).

Blough and Santi [10] studied the upper bound of network lifetime for cell-based energy conservation techniques. While the bound derived does consider energy consumption both in the transmitting/receiving state and in the idle state, it is restricted to the GAF scheme proposed in [77]. In contrast, the lifetime derived in Chapter 4 is independent of the power-saving schemes used.

Coleri *et al.* [17] investigated the lifetime of networked sensor nodes where sensors are organized in a tree-based multi-hop networks. They analyzed the lifetime of nodes in four different groups based on their distance to the data sink using the finite automata technique. However, their analysis was primarily on the lifetime of individual nodes instead of that of the network as a whole.

2.3 Asymptotic Analysis of Coverage, Connectivity, and Node Degree

2.3.1 Coverage

Early research on the density requirement for ensuring coverage focused on 1-coverage. Philips [59] showed that $\pi r^2\lambda \sim \log \ell^2$ is a necessary and sufficient condition for coverage and a necessary condition for connectivity in a random network, where $r(\lambda)$ is the radius of sensing (communication), and nodes are distributed according to a Poisson point process with density λ in a region of area ℓ^2. Hall [36] showed if the nodes are distributed as a Poisson point process with density λ in a unit-area square, then $0.05\min\{1,(1+\lambda^2\pi r^2)e^{-\lambda\pi r^2}\} < P(V_1 > 0) < 3\min\{1,(1+\lambda^2\pi r^2)e^{-\lambda\pi r^2}\}$, where r is the sensing range and V_1 denotes the 1-vacancy area. Both of the above results are consistent with our results in the special case of $k = 1$. In particular, for $k = 1$, boundary conditions do not cause extra density requirement. However, for $k > 1$, adding boundary conditions does require more density for complete k-coverage.

Analysis in the deployment modes other than Poisson process deployment has been performed by Shakkottai *et al.* [65]. They derived necessary and sufficient conditions for 1-coverage and 1-connectivity when n sensors are deployed in a $\sqrt{n} \times \sqrt{n}$ grids and each sensor is active with probability p. Kumar *et al.* [44] studied the issue of k-coverage under three different deployment strategies: grid deployment, uniformly random deployment, and Poisson process deployment. Different from our work [83], they consider the boundary issues. However, in their derivation for k-coverage, they only showed their conclusion holds for the inner regions. As a result, they obtained the same density requirement for k-coverage as in our work [83] in the case that nodes are distributed as a Poisson point process. We have corrected the mistake in Chapter 4, and moreover, proved much sharper bounds on the density requirement in all cases.

Wan and Yi [72] studied the asymptotic node density requirement for maintaining k-coverage in uniformly random deployment and Poisson process deployment. Although the problem studied by Wan and Yi is similar to that to be studied in Chapter 4, as will become clearer, we prove necessary and sufficient asymptotic density requirement for ensuring k-coverage in grid deployment and compare two fundamentally different deployment methods: random and grid distribution, through both analysis and simulation. In addition, the proof techniques in these two works are different. The proof in [72] was based on counting the number of uncovered crossings, while the proof in Chapter 4 is based on counting the number of uncovered small grids. We will demonstrate that this latter approach can be used to obtain different results for grid deployment.

2.3.2 Connectivity

There are two fundamentally different categories of approaches to reduce node transmission power while maintaining (k-)connectivity. In the first category, all nodes use common transmission power but the common transmission power is chosen to be the minimum value such that it guarantees connectivity or k-connectivity. Most of the work in this category [59, 35, 56, 57, 62, 73] studied the asymptotic minimum common transmission range in order to ensure connectivity or k-connectivity.

Philips *et al.* [59] proved that assuming nodes are distributed as a Poisson point process with density λ in a square with area A and each node has transmission range r, for any $\epsilon > 0$, if

$$\lambda \pi r^2 = (1 - \epsilon) \log A,$$

then $\lim_{A \to \infty} P(\text{network is connected}) = 0$.

Gupta and Kumar [35] showed that if n nodes are uniformly randomly placed on a unit disk and the transmission radius $r(n)$ satisfies $\pi r^2(n) = (\log n + c(n)))/n$, it is guaranteed that the network (of large size) is connected with probability approaching 1 if and only if $c(n) \to \infty$ as $n \to \infty$.

Penrose [56] proved that if M_n is the maximum edge length in the minimum spanning tree of a network consisting of n uniformly randomly deployed nodes on a unit-square, then the distribution of $n\pi M_n^2 - \log n$ converges weakly to the double exponential distribution:

$$\lim_{n \to \infty} P(n\pi M_n^2 - \log n \leq \alpha) = \exp(-e^{-\alpha}).$$

This result can be used to obtain the result in [35].

Santi and Blough [62] considered the problem of determining critical transmission range in a sparse, 1, 2, or 3 dimensional space by assuming the side length of the network is l. For example, they showed that assuming that n nodes, each with transmission range r, are distributed uniformly and independently random in $R = [0, l]^d$, for $d = 2, 3$, and that $r^d n = k l^d \log l$ for some constant k with $r = r(l) \ll l$ and $n = n(l) \gg 1$, if $k > d \cdot k_d$, or $k = d \cdot k_d$ and $r = r(l) \gg 1$, then the communication graph is connected with probability approaching one as $l \to \infty$, where $k_d = 2^d d^{d/2}$.

In the second category, each node may choose different levels of transmission power to guarantee connectivity or k-connectivity. The work [11, 30, 60, 16] studied the asymptotic value of the minimum total power required for maintaining connectivity. In particular, Blough *et al.* [11] derived the critical total power only for 1-connectivity based on the results of the total weight of minimal spanning tree [82]. Gomez and Campbell [30] applied Steele's results [68] and showed that for n nodes that are independently,

uniformly distributed in a unit d-dimensional cubic, the total length of minimal spanning tree using the edge weight function $\psi(x) = x^c$ is $\Theta(n^{1-c/d})$ with probability 1 as $n \to \infty$ for $0 < c < d$. As both of the proofs are based on the results on the asymptotic total weight for weighted minimal spanning trees[68, 82], the result cannot be easily generalized to the case of k-connectivity for $k > 1$.

Rengarajan *et al.* [60] computed the expectation of (lower bound and upper bound of) the total power consumption (for 1-connectivity). As will become clearer, although we also focus on computing the critical total power, the results are obtained in the asymptotic sense. Obtaining asymptotic results is significantly more challenging than obtaining expectations.

Clementi *et al.* [16] showed that given the upper bound on the number of hops h, the total power incurred by the n nodes that are independently, uniformly distributed in a unit square region is $\Theta(n^{1/h})$ with high probability. Their result only applies to the path loss exponent $c = 2$ and cannot be readily generalized to the case of $c \neq 2$.

2.3.3 Node degree

Several researchers studied the minimum (common) node degrees that can guarantee network connectivity or k-connectivity. Xue and Kumar [78] showed that in a random ad-hoc network with n nodes, each node should be connected to $\Theta(\log n)$ nearest neighbors in order that the network connectivity is guaranteed in the asymptotic sense. They proved that if each node connects with less than $0.074 \log n$ nearest neighbors, then the network is asymptotically disconnected with probability approaching one as n goes to infinity, while if each node connects with more than $5.1774 \log n$ nearest neighbors then the network is asymptotically connected with probability approaching one.

Wan and Yi [73] proved that for any fixed $k \geq 1$ and any real number $\alpha > 1$, if every node connects with at least $\alpha e \log n$ neighbors (where $e \approx 2.718$ is the natural base), the network is k-connected with probability approaching one.

2.4 Asymptotic Analysis of Network Transport Capacity

In their groundbreaking work [34], Gupta and Kumar first derived the transport capacity of wireless ad hoc network. Specifically, they assumed that n nodes are independently and uniformly randomly distributed, either on the surface of a three-dimensional sphere of unit area, or on a disk of unit area in the plane, that the destination is independently chosen as the node that is closest to a randomly located point (according to the uniform distribution), and that all nodes employ the same transmission range or power. They further assumed two transmission models: protocol model and physical model. In the

protocol model, a transmission from node i to j is successful if and only if (i) $|X_i - X_j| \leq r$ and (ii) $|X_k - X_j| \geq (1+\Delta)r$ for every other simultaneously transmission, where X_i and X_j are the location of node i and j, r is the transmission range, and $\Delta > 0$ is a constant. In the physical model, all nodes choose a common power P for their transmissions. A transmission from node i to node j is successful if and only if

$$\frac{\frac{P}{|X_i - X_j|^\alpha}}{N + \sum_{k \in \Gamma, k \neq i} \frac{P}{|X_k - X_j|^\alpha}} \geq \beta, \tag{2.1}$$

where Γ is the set of simultaneously transmitting nodes, N is the ambient noise power level. In addition, they assume the transmission rate is constant if the transmission is successful.

The authors showed that (i) in the protocol model, the per-node capacity of a wireless network is both upper bounded and lower bounded by $\Theta(1/\sqrt{n \log n})$, and (ii) in the physical model, the per-node capacity is upper bounded by $O(1/\sqrt{n})$ and lower bounded by $\Omega(1/\sqrt{n \log n})$.

Since then, many research efforts have been made to investigate the wireless network capacity. Some of them aimed to improve the capacity bounds in different ways, while others attempted to derive the capacity bounds under different (usually more realistic) assumptions or different traffic patterns. We roughly classify existing works into those that improve the capacity bounds (Section 2.4.1) and those that derive the bounds under different assumptions (Section 2.4.2). In the former category, we further group existing methods for improving the network capacity bounds into four types.

2.4.1 Work that improves the capacity bounds

Improving the network capacity bounds by mobility The first type of methods employs mobility to improve the capacity bounds. Under the assumptions that nodes are mobile and the position of each node is ergodic with stationary uniform distribution on an open disk, Grossglauser and Tse [32] showed that the average long-term throughput per source-destination pair can be kept constant with high probability as the number n of nodes in each unit area goes to infinity. Diggavi *et al.* [21] further showed that even if nodes are only allowed to move in one dimension (every node is constrained to move on a single-dimensional great circle on the unit sphere), each node can still obtain constant capacity as the number of nodes in the unit area increases. Their derivation was based on the physical model.

Following that, several researchers studied the delay incurred using mobility to improve the capacity. Bansal and Liu [7] studied the achievable rate together with the maximum delay incurred. Specifically, under the assumptions that n static nodes and m mobile nodes (that move according to the random mobility model given in [32]) are randomly distributed, and that n sender-receiver pairs are chosen

randomly among the static nodes according to a uniform distribution, they showed that the achievable capacity is at least $\Theta(\frac{\min(m,n)}{n \log^3 n})$ and the maximum delay incurred by packets is at most $2d/v$, where d is the diameter of the network and v is the velocity of the mobile nodes.

Perevalov and Blum [58] obtained an expression for the capacity as a function of the maximum allowable delay in an all mobile network. They showed that there exists a critical value of the delay such that for delays below the critical value, the capacity does not benefit from the motion significantly. For delays d above the critical value, the capacity increases approximately as $d^{2/3}$. In addition, they showed that the value of the critical delay increases approximately as the order of $n^{1/14}$ with the number n of nodes. They assumed the physical model as in [32].

El Gamal *et al.* [28] characterized the optimal throughput-delay tradeoff for both the static network model and the mobile network model. For the static network model, the optimal throughput-delay tradeoff is $D(n) = \Theta(nT(n))$ where $T(n)$ and $D(n)$ are the throughput and delay respectively. For the mobile network model, they showed that the delay scales as $\Theta(n^{1/2}/v(n))$ if the per node capacity scales at $\Theta(1)$. Their derivation was based on a relaxed protocol model where a transmission from node i to j is successful if for any other node k that transmits simultaneously, $d(k,j) \geq (1+\Delta)d(i,j)$ for some fixed $\Delta > 0$, where $d(i,j)$ is the distance between nodes i and j.

Improving the network capacity bounds by infrastructure support The second type of methods used infrastructure support to improve capacity bounds, where a number of wired base stations are deployed in the network to help transport packets. (Networks of this type are called *hybrid* networks.) Liu *et al.* [49] considered the case where m base stations are placed in a regular hexagonal pattern within the ad hoc network with n nodes. Under a deterministic routing strategy, they show that if m grows asymptotically slower than $\sqrt{n}$, the maximum throughput capacity is $\Theta(\sqrt{n/\log \frac{n}{m^2}})$; and if m grows faster than $\sqrt{n}$, the maximum capacity is $\Theta(m)$. Under a probabilistic routing strategy, they show that if m grows slower than $\sqrt{\frac{n}{\log n}}$, the maximum throughput capacity has the same asymptotic behavior as a pure ad hoc network; and if m grows faster than $\sqrt{\frac{n}{\log n}}$, the maximum throughput capacity scales as $\Theta(m)$. Kozat and Tassiulas [43] considered the case where both wireless nodes and base stations are deployed randomly. They showed that the per source node capacity of $\Theta(1/\log(n))$ is achievable, if the ratio of the number n of ad hoc nodes to the number m of the base stations are bounded from above.

Improving the network capacity bounds via directional antennas The third type of methods employs directional antennas to improve the capacity bounds. Yi *et al.* [81] showed that in a random wireless network, use of directional antennas with beamwidth α for transmitters can increase the capacity by a factor of $2\pi/\alpha$ and use of directional antennas with beamwidth β for receivers can increase the

capacity by a factor of $2\pi/\beta$. In addition, if both the transmitter and the receiver employ directional antenna, the capacity can be improved by a factor of $4\pi^2/\alpha\beta$. Peraki and Servetto [5] showed that even if transmitters can generate arbitrarily narrow beams (which essentially removes all wireless interference) and the transmission ranges are set as minimal as possible to maintain connectivity, the capacity can only be improved by an order of $\Theta(\log^2(n))$.

Improving the network capacity bounds with the use of UWB The fourth type of methods leverages unlimited bandwidth resources to improve the network capacity bounds. Negi and Rajeswaran [54] showed that under the limit case when bandwidth $B \to \infty$ and that each node has a power constraint W_0, the per node capacity is upper bounded by $O((n \log n)^{(\alpha-1)/2})$ and lower bounded by $\Omega(\frac{n^{(\alpha-1)/2}}{(\log n)^{(\alpha+1)/2}})$.

Dana and Hassibi [20, 19] considered a different scenario in which there are n relay nodes and $r \leq \sqrt{n}$ source-destination pairs. Assuming unlimited bandwidth, they showed that given the total rate scales as $\Theta(f(n))$, the minimum power required by each node scales as $\Theta(f(n)/\sqrt{n})$. The required bandwidth for achieving the minimum power is $\Theta(f(n))$. In addition to the difference in the scenario, these bounds are based on a simple "listen and transmit" protocol, which may not be optimal in terms of the capacity-power-bandwidth tradeoff.

2.4.2 Work that derives the capacity bound under different assumptions

Several other researchers studied the capacity bounds under different (usually more realistic) assumptions. Dousse and Thiran [23] showed the available rate per node decreases as $\Theta(1/n)$ under the assumption that the attenuation function is uniformly bounded at the origin. Their derivation was based on the physical model. Toumpis and Goldsmith [71] studied the network capacity under a general fading channel model. They showed that in a static network, each node can send data to its destination with a rate of $\Theta(n^{-1/2}(\log n)^{-3/2})$. In a mobile network each of the n mobile nodes can achieve the same order of magnitude throughput with a fixed maximum delay constraint that does not depend on n. If each node is willing to tolerate packet delay $\Theta(n^d)$ where $0 < d < 1$, they showed that each mobile node can send data to its destination with rate $\Theta(n^{(d-1)/2}(\log n)^{-5/2})$.

Xie and Kumar [75] studied the capacity bounds in a setting where nodes can employ sophisticated cooperative strategies to achieve interference cancellation. They showed that the aggregate capacity of an arbitrary network is upper bounded by $O(\sqrt{n})$ (in a large-area network), assuming some natural signal attenuation law, and the upper bound is sharp for regular planar networks where the nodes reside at integer lattice sites in a square.

Research efforts have also been made under different traffic patterns. Gastpar and Vetterli [29]

considered the same physical model as in [34], but a different traffic pattern, namely the *relay traffic pattern*. There exists only one (randomly chosen) source-destination pair and all other nodes serve as relay nodes. They showed that if arbitrarily complex network coding is allowed, the upper bound and lower bound of the capacity of a wireless network with n nodes under the relay traffic pattern meet asymptotically at $\Theta(\log n)$ as the number n of nodes in the network goes to infinity. Marco *et al.* studied the network capacity under the *many-to-one* scenario where there is only one destination and every node needs to transmit packets to the destination. They showed that per node capacity scales as $\Theta(1/n)$ as the number n of nodes increases. This is due to the bottleneck at the single destination.

Toumpis [70] studied the capacity bounds of three classes of wireless networks under fading channels. The first class is asymmetric networks where there are n source nodes and around n^d destination nodes, and each source picks a destination at random. The author showed that if $1/2 < d < 1$, an aggregate throughput of $\Omega(n^{1/2}(\log n)^{-3/2})$ is achievable; and if $0 < d < 1/2$, an aggregate throughput of $\Omega(n^d/\log n)$ is achievable. In both cases, the aggregate throughput is upper bounded by $O(n^d \log n)$. The second class is cluster networks where there are n client nodes and around n^d cluster heads. Each client communicates with one of the cluster heads, but the particular choice of the cluster head is not important. He showed in this setting, the maximum aggregate throughput is lower bounded by $\Omega(n^d(\log n)^{-2})$ and upper bounded by $O(n^d \log n)$. The third class is hybrid networks where there are n wireless nodes and n^d base stations, and the base stations are connected through wired lines and only used to support the operation of wireless nodes. He showed that if $1/2 < d < 1$, the maximum aggregate throughput is lower bounded by $\Omega(n^d(\log n)^{-2})$ and if $0 < d < 1/2$, there is no significant gain of employing the infrastructure. We note the last result is similar to that in [49].

Li *et al.* [45] studied the capacity of small ad hoc networks through extensive simulations, which verified the capacity bounds of order $1/\sqrt{n}$ to some extent. Finally in a very recent work, Franceschetti *et al.* [26, 27] closed the gap between the capacity upper bound and lower bound in Gupta and Kumar's original results [34] under the physical model. They used percolation theory to devise a routing strategy which achieves a per node capacity bounds of $\Theta(1/\sqrt{n})$.

Chapter 3

Maintaining Sensing Coverage and Connectivity in Wireless Sensor Networks

3.1 Introduction

Recent technological advances have led to the emergence of pervasive networks of small, low-power devices that integrate sensors and actuators with limited on-board processing and wireless communication capabilities. These sensor networks open new vistas for many potential applications, such as battlefield surveillance, environment monitoring and biological detection [24, 41, 3, 50].

Since most of the low-power devices have limited battery life and replacing batteries on tens of thousands of these devices is infeasible, it is well accepted that a sensor network should be deployed with high density in order to prolong the network lifetime. In such a high-density network with energy-constrained sensors, if all the sensor nodes operate in the active mode, an excessive amount of energy will be wasted, sensor data collected is likely to be highly correlated and redundant, and moreover, excessive packet collision may occur as a result of sensors intending to send packets simultaneously in the presence of certain triggering events. Hence it is neither necessary nor desirable to have all nodes simultaneously operate in the active mode.

One important issue that arises in such high-density sensor networks is *density control* — the function that controls the density of the working sensors to certain level [80]. Specifically, density control ensures only a subset of sensor nodes operate in the active mode, while fulfilling the following two requirements: (i) *coverage:* the area that can be monitored is not smaller than that which can be monitored by a full set of sensors; and (ii) *connectivity:* the sensor network remains connected so that the information collected by sensor nodes can be relayed back to data sinks or controllers. Under the assumption that an (acoustic or light) signal can be detected with certain minimum signal to noise ratio by a sensor node if the sensor is within a certain range of the signal source, the first issue essentially boils down to a coverage problem: assuming that each node can monitor a disk (the radius of which is called the *sensing range* of the sensor node) centered at the node on a two dimensional surface, what is the minimum set of nodes that can cover the entire area? Moreover, if the relationship between coverage and connectivity can be well characterized (e.g., under what condition coverage may imply connectivity and vice versa), the connectivity issue can be

studied, in conjunction with the first. In addition to the above two requirements, it is desirable to choose a minimum set of working sensors in order to reduce power consumption and prolong network lifetime. Finally, due to the distributed nature of sensor networks, a practical density control algorithm should be not only distributed but also completely localized (i.e., relies on and makes use of local information only) [24].

In this chapter, we address the issue of density control in an analytic framework, and based on the findings, propose a fully decentralized and localized algorithm, called *Optimal Geographical Density Control* (OGDC), in large scale sensor networks. Our goal is to maintain coverage as well as connectivity using a minimum number of sensor nodes. We investigate the relationship between coverage and connectivity by solving the following two sub-problems. First, we prove that under the assumption **(A1)** the radio range is at least twice the sensing range, a complete coverage of a convex area implies connectivity among the set of working nodes. Note that as indicated in Tables A.1 and A.2, **(A1)** holds for a wide class of sensor devices that recently emerge. As a result, the proof allows us to focus only on the coverage problem, as complete coverage implies connectivity. Second, we explore, under the ideal case that the node density is sufficiently high, a set of optimality conditions under which a subset of working nodes can be chosen for complete coverage. Based on the optimality conditions, we then devise a decentralized and localized density control algorithm, OGDC. We also discuss the procedures taken by OGDC in the (infrequent) case that the radio range is smaller than twice the sensing range, thus allowing OGDC to be uniformly applied to all cases. We also perform *ns-2* simulations to validate OGDC and compare it against a hexagon-based GAF-like algorithm, the PEAS algorithm presented in [80] and the CCP protocol in [74].

Several researchers have addressed the same or similar issues, with the work reported in [79, 80, 69, 74, 33] coming closest to ours. (Refer to Chapter 2 for a detailed summary of existing works.) However, the work reported in [79, 80] does not ensure complete coverage. Although the work reported in [69] does attempt to solve the complete coverage problem, it requires a large number of nodes to operate in the active mode (even more than a simple algorithm based on the idea of GAF does [77]). On the other hand, the work in [33] assumes error-free channels and requires reliable broadcasting in a certain range, which is hard to implement in wireless environments. The recent work by Wang *et al.* [74] contains a similar analysis on the relationship between coverage and connectivity, but does not derive optimal conditions for minimizing the number of working nodes as we do in this chapter.

The rest of the chapter is organized as follows. In Section 3.2 we investigate the relationship between coverage and connectivity. In Section 3.3 we derive the optimality conditions for complete coverage under the ideal case. Following that, we present in Section 3.4 the proposed density control algorithm and our

simulation study in Section 3.5. Finally we conclude the chapter in Section 3.6.

3.2 Relationship Between Coverage and Connectivity

In this section, we investigate the relationship between coverage and connectivity. We assume the target region is convex. We assume that each sensor can monitor a circular region centered at itself. The radius of the circular region is called *sensing range*. We also assume each node can communicate with any other node within a certain range from itself. This range is called *radio transmission range*. The sensing range and the radio transmission range are denoted as r_s and r_t, respectively.

Specifically, we derive the necessary and sufficient condition under which coverage implies connectivity — the radio range is at least twice the sensing range.

Lemma 3.2.1 *Assuming the target region is a convex set, the condition of $r_t \geq 2r_s$ is both necessary and sufficient to ensure that complete coverage of a convex region implies connectivity in an arbitrary network.*

Proof. We prove the necessary condition by devising a scenario in which coverage does not imply connectivity if $r_t < 2r_s$. In Figure 3.1, a sensor is located at O and has, respectively, a sensing radius r_s and a radio transmission radius $r_t < 2r_s$. Now we place a sufficient number of sensors on the circle centered at O with radius $r_t + \epsilon < 2r_s$ (where $\epsilon > 0$) such that they together cover the whole disk centered at O and with radius $r_t + \epsilon$. However, this network is not connected since the distance between node O and any other node is more than r_t.

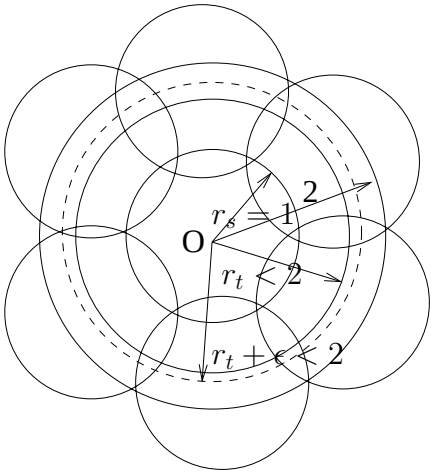

Figure 3.1: A scenario that demonstrates $r_t \geq 2r_s$ is a necessary condition that complete coverage ensures connectivity.

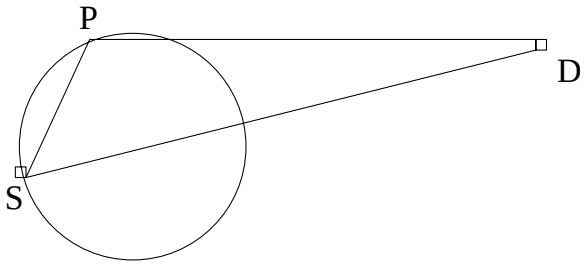

Figure 3.2: A scenario that demonstrates $r_t \geq 2r_s$ is the sufficient condition that complete coverage implies connectivity.

Next we show that $r_t \geq 2r_s$ is also a sufficient condition to ensure that coverage implies connectivity. We prove this by contradiction. If a network is disconnected, there exists a pair of nodes between which no path exists. Let (S, D) be a pair of nodes with the minimum distance among all pairs of disconnected nodes (Fig. 3.2). Considering the circle whose center is on the line from node S to node D and the distance between its center and node S is r_s, we claim that there must exist some other node within or on the circle. Otherwise, since the number of nodes is finite in any finite area, we can move the circle along $\overline{SD}$ toward node D by a minimum distance ϵ in order to make the circle include another node. If we move the circle along $\overline{SD}$ toward node D by a distance $\epsilon/2$, there will be no node within or on the circle. That means the center of the circle is not covered by any node, which violates the condition of coverage. Let node P be such a node that lies within or on the circle (before it is moved). Nodes S and P are connected since their distance is less than $2r_s \leq r_t$. Hence nodes P and D must be disconnected; otherwise nodes S and D are connected. Since $\angle SPD > \pi/2 > \angle PSD$, we have $|\overline{SD}| > |\overline{PD}|$. This contradicts the assumption that nodes S and D have the minimum distance among all the pairs of disconnected nodes. □

Although the above derivation is made on a two dimensional surface, both the lemma and its proof apply to three dimensional space as well. An important implication of Lemma 3.2.1 is that if the radio range is at least twice the sensing range (which holds for a wide variety of applications), then complete coverage implies connectivity. That is, the problem of ensuring both coverage and connectivity can be reduced to that of ensuring coverage only. We will henceforth only consider the coverage problem in the analytical framework. Later in the course of designing our decentralized, localized algorithm, OGDC, we will consider the "extra" procedure taken to deal with the (rare) case that the radio ranges are smaller than twice the sensing ranges.

In a concurrent work[74], It is independently proved that if $r_t \geq 2r_s$, k-coverage implies k-connectivity of the entire network and $2k$-connectivity of the interior network on a convex area. However, we emphasize here that the condition $r_t \geq 2r_s$ is also necessary in the sense that if $r_t < 2r_s$, coverage does not imply connectivity in general.

3.3 Optimal Sensing Coverage in the Ideal Case

Recall that two requirements are implied in density control: first, the subset should completely cover the region R. Specifically, given that the coverage area of a sensor node is a disk centered at itself, we define a *crossing* as an intersection point of two circles (boundaries of disks) or that of a circle and the boundary of region R. A crossing is said to be *covered* if it is an *interior point* of a third disk. The following lemma

from [36] pages 59 and 181 provides a sufficient condition for complete coverage. This condition is also necessary if we assume that the circle boundaries of any three disks do not intersect at a point. The assumption is reasonable as the probability of the circle boundaries of three disks intersecting at a point is zero, if all sensors are randomly placed in a region with uniform distribution. Lemma 3.3.1 serves as an important theoretical base for our distributed density control algorithm in the next section.

Lemma 3.3.1 *Suppose the size of a disk is sufficiently smaller than that of a convex region R. If one or more disks are placed within the region R, and at least one of those disks intersect another disk, and all crossings in the region R are covered, then R is completely covered.*

The second requirement is that the set of working sensors should consume as little power as possible so as to prolong the network lifetime. If each sensor consumes the same amount of power when it is active and has the same sensing range, the requirement of minimizing power consumption boils down to that of minimizing the number of working sensors. On the other hand, if sensors have different sensing ranges (e.g., using different levels of power to sense), a minimum number of working sensors does not necessarily imply minimum power consumption.

To derive conditions under which the second requirement is fulfilled, we first define the *overlap* at a point x as the number of sensors whose sensing ranges can cover the point minus $I_R(x)$, where

$$I_R(x) = \begin{cases} 1 & \text{if } x \in R, \\ 0 & \text{otherwise.} \end{cases}$$

The overlap of sensing areas of all the sensors is then the integral of overlaps of the points over the area covered by all the sensors. In general, the larger the overlap of the sensing areas, the more amount of redundant data will be generated and more power will be consumed. On the other hand, an adequate degree of redundancy may be needed to gather accurate, high-fidelity data in some cases. Although our focus in this chapter is to ensure that every point is covered by at least one sensor, we will discuss how to extend our work to ensure k-coverage (i.e., every point is covered by at least k sensors) in Section 3.5.

We claim that overlap is a better index for measuring power consumption than the number of working sensors for two reasons. First, although the number of working sensors is not directly related to power consumption in the case that sensors have different sensing ranges, the measure of overlap still is, i.e., a larger value of overlap implies more data redundancy and power consumption. Second, as will be proved in the following lemma, minimizing the overlap value is equivalent to minimizing the number of working sensors in the case that all sensors have the same sensing ranges (i.e., the coverage disks of all sensors have the same radius r).

Lemma 3.3.2 *If all sensor nodes (i) completely cover a region R and (ii) have the same sensing range, then minimizing the number of working nodes is equivalent to minimizing the overlap of sensing areas of all the working nodes.*

Proof. See Appendix A.1.

Lemma 3.3.2 is important as it relates the total number of working sensor nodes to the overlapping areas between working nodes. Since the latter is more easily measured from a local point of view, this greatly simplifies the task of designing a decentralized and localized density control algorithm, which will become clear later.

3.3.1 Properties under the ideal case

With Lemmas 3.3.1–3.3.2, we are now in a position to discuss how to minimize the overlap of sensing areas of all the sensor nodes. Our discussion is built upon the following assumptions:

(A1) The sensor density is high enough that a sensor can be found at any desirable point.

(A2) The region R is large enough as compared to the sensing range of each sensor node so that the boundary effects can be ignored.

Assumption (**A2**) is usually valid. Although (**A1**) may not hold in practice, as will be shown in Section 3.4, the result derived under (**A1**) still provides insightful guidance in designing the distributed algorithm.

By Lemma 3.3.1, in order to totally cover the region R, some sensors must be placed inside region R and their coverage areas intersect one another. If two disks A and B intersect, at least one more disk is needed to cover their crossing points. Consider, for example, in Figure 3.3, disk C is used to cover the crossing point O of disks A and B. In order to minimize the overlap while covering the crossing point O (and its vicinity not covered by disks A and B), disk C should also intersect disks A and B at the point O; otherwise, one can always move disk C away from disks A and B to reduce the overlap.

Given that two disks A and B intersect, we now investigate the number of disks needed, and their relative locations, in order to cover a crossing point O of disks A and B and at the same time minimize the overlap. Take the case of three disks (Fig. 3.3) as an example. Let $\angle PAO = \angle PBO \stackrel{\triangle}{=} \alpha_1$, $\angle OBQ = \angle OCQ \stackrel{\triangle}{=} \alpha_2$, and $\angle OCR = \angle OAR \stackrel{\triangle}{=} \alpha_3$. We consider two cases: (i) $\alpha_1, \alpha_2, \alpha_3$ are all variables; and (ii) α_1 is a constant but α_2 and α_3 are variables. Case (i) corresponds to the case where we can choose all the node locations, while case (ii) corresponds to the case where two nodes (A and B) are already fixed and we need to choose the position of a third node C to minimize the overlap. Both of the above two cases can be extended to the general situation in which $k-2$ additional disks are placed to cover one

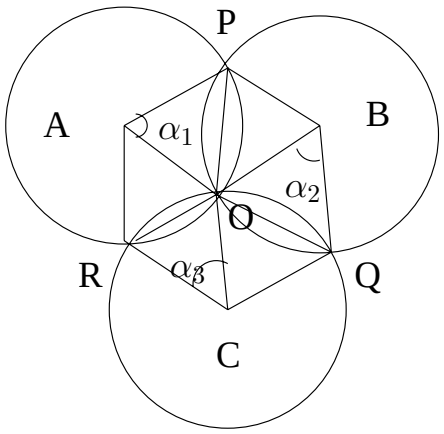

Figure 3.3: An example that demonstrates how to minimize the overlap while covering the crossing point O.

crossing point of the first two disks (that are placed on a two-dimensional plane), and α_i, $1 \leq i \leq k$, can be defined accordingly. Again, the boundaries of all disks should intersect at point O in order to reduce the overlap. In the following discussion we assume for simplicity that the sensing range $r = 1$. Note, however, that the results still hold when $r \neq 1$.

Case 1: α_i, $1 \leq i \leq k$, are all variables We first prove the following Lemma.

Lemma 3.3.3

$$\sum_{i=1}^{k} \alpha_i = (k-2)\pi, \tag{3.1}$$

Proof. See appendix A.2.

Now the overlap between the i^{th} and $(i \bmod k) + 1^{th}$ disks (which are called *adjacent disks*) is $(\alpha_i - \sin\alpha_i)$, $1 \leq i \leq k$. If we ignore the overlap caused by *non-adjacent* disks, then the total overlap is $L = \sum_{i=1}^{k}(\alpha_i - \sin\alpha_i)$. The coverage problem can be formulated as

Problem 3.3.1

$$\text{minimize } \sum_{i=1}^{k}(\alpha_i - \sin\alpha_i)$$
$$\text{subject to} \sum_{i=1}^{k} \alpha_i = (k-2)\pi.$$

The Lagrangian multiplier method can be used to solve the above optimization problem. The solution is $\alpha_i = (k-2)\pi/k, i = 1, 2, \cdots, k$ and the resulting minimum overlap using k disks to cover the crossing

point O is

$$L(k) = (k-2)\pi - k\sin(\frac{(k-2)\pi}{k}) = (k-2)\pi - k\sin(\frac{2\pi}{k}).$$

Note that the overlap per disk

$$\frac{L(k)}{k} = \pi - \frac{2\pi}{k} - sin(\frac{2\pi}{k})$$

monotonically increases with k when $k \geq 3$. Moreover when $k = 3$ (which means that we use one disk to cover the crossing point), the optimal solution is $\alpha_i = \pi/3$ and there is no overlap between *non-adjacent* disks. When $k > 3$, the overlap per disk is always higher than that in the case of $k = 3$, even if we ignore the overlaps between *non-adjacent* disks. This implies that using one disk to cover the crossing point and its vicinity is optimal in the sense of minimizing the overlap. Moreover, the centers of the three disks should form a equilateral triangle with edge $\sqrt{3}$. We state the above result in the following theorem.

Theorem 3.3.1 *To cover one crossing point of two disks with the minimum overlap, only one disk should be used and the centers of the three disk should form a equilateral triangle with side length $\sqrt{3}r$, where r is the radius of the disks.*

Case 2: α_1 is a constant, while α_i, $2 \leq i \leq k$, are variables In this case the problem can still be formulated as in Problem 3.3.1, except that α_1 is fixed. The Lagrangian multiplier method can again be used to solve the problem, and the optimal solution is $\alpha_i = ((k-2)\pi - \alpha_1)/(k-1)$, $2 \leq i \leq k$. Again a similar conclusion can be drawn that using one disk to cover the crossing point gives the minimum overlap. We state the result in the following theorem.

Theorem 3.3.2 *To cover one crossing point of two disks whose locations are fixed (i.e., α_1 is fixed in Fig. 3.3), only one disk should be used and $\alpha_2 = \alpha_3 = (\pi - \alpha_1)/2$.*

In summary, to cover a large region R with the minimum overlap, one should ensure (i) at least one pair of disks intersects; (ii) the crossing points of any pair of disks are covered by a third disk; (iii) if the locations of any three sensor nodes are adjustable, then as stated in Theorem 3.3.1 the three nodes should form an equilateral triangle with side length $\sqrt{3}r$. If the locations of two sensor nodes A and B are already fixed, then as stated in Theorem 3.3.2 the third sensor node should be placed on the line that is perpendicular to the line connecting nodes A and B and have a distance r to the intersection of the two circles (e.g., the optimal point in Fig. 3.4 is C). These conditions are optimal for the coverage problem in the ideal case in which assumptions (**A1**) and (**A2**) hold.

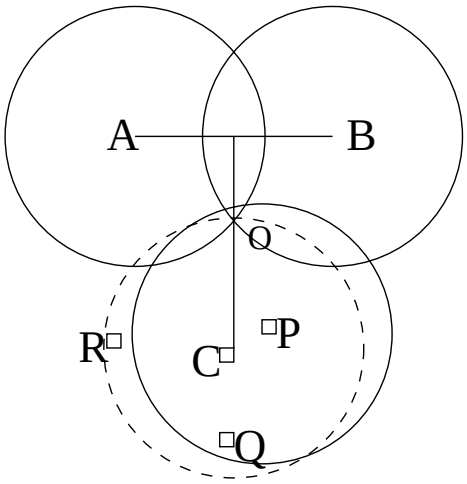

Figure 3.4: Although C is the optimal place to cover the crossing O of A, B, there is no sensor node there. The node closest to C, P, is selected to cover the crossing O.

As mentioned above, the notion of overlap can be extended to the heterogeneous case in which sensors have different sensing ranges. Moreover, Theorem 3.3.1 and 3.3.2 can be generalized to the heterogeneous case. For ease of discussion, we consider the case of using only one extra disk to cover the crossing point O.

Theorem 3.3.3 *Assuming that different nodes have different sensing ranges, to cover one crossing point O of two disks with the minimum overlap, the three disks should be placed such that $\overline{OP} = \overline{OQ} = \overline{OR}$. If disk A and B are already fixed, disk C should be placed such that $\overline{OR} = \overline{OQ}$.*

Proof. We only prove the first part of the theorem where the location of all three disks can change. To prove the second part when node A and B are fixed we only need to take the variable x_1 below as a fixed value.

Refer to Fig. 3.5. Let r_1, r_2 and r_3 denote the radii of disks A, B, and C, let $x_1 = \overline{OP}/2, x_2 = \overline{OQ}/2, x_3 = \overline{OR}/2$, and let $\alpha_1 = \angle OAP, \alpha_2 = \angle OBP, \alpha_3 = \angle OBQ, \alpha_4 = \angle OCQ, \alpha_5 = \angle OCR, \alpha_6 = \angle OAR$. Notice that if $r_1 = r_2 = r_3$, then $\alpha_1 = \alpha_2, \alpha_3 = \alpha_4, \alpha_5 = \alpha_6$. The angles α_i, $1 \leq i \leq 6$, can be expressed as

$$\begin{aligned}
\alpha_1 &= 2\arcsin(x_1/r_1), \quad \alpha_2 = 2\arcsin(x_1/r_2), \\
\alpha_3 &= 2\arcsin(x_2/r_2), \quad \alpha_4 = 2\arcsin(x_2/r_3), \\
\alpha_5 &= 2\arcsin(x_3/r_3), \quad \alpha_6 = 2\arcsin(x_3/r_1).
\end{aligned}$$

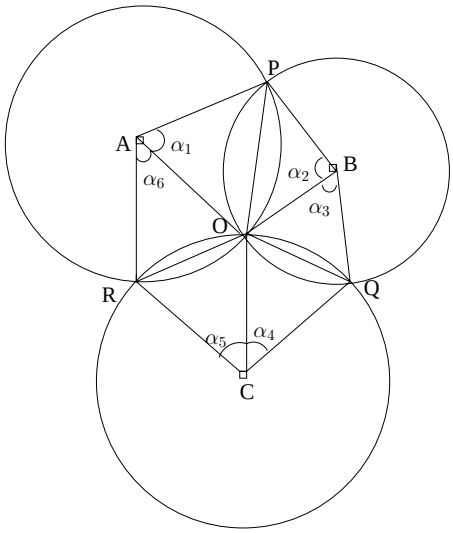

Figure 3.5: Minimizing the overlap while covering the crossing point O when each node has different sensing range.

and the total overlap can be written as

$$\frac{1}{2}\sum_{i=1}^{6} r_i^2(\alpha_i - \sin\alpha_i). \tag{3.2}$$

Now the problem is to minimize Eq. (3.2) subject to the same constraint as in Lemma 3.3.3:

$$\sum_{i=1}^{6} \alpha_i = 2\pi. \tag{3.3}$$

Now we apply Lagrangian multiplier theorem with the Lagrangian function

$$L = \frac{1}{2}\sum_{i=1}^{6}(r_i^2(\alpha_i - \sin\alpha_i) + \lambda(\sum_{i=1}^{6}\alpha_i - 2\pi).$$

Note that the variables α_i's are not independent, e.g., both α_1 and α_2 depend on x_1. Hence we have to apply the Lagrangian multiplier theorem on the independent variables x_i's and regard α_i as $\alpha_i(x_j)$ where x_j is one of the x_k's that α_i depends on. First we apply the first order necessary condition on x_1.

$$\begin{aligned}\frac{\partial L}{\partial x_1} &= \sum_{i=1}^{6}\frac{\partial L}{\partial \alpha_i}\cdot\frac{\partial \alpha_i}{\partial x_1} \\ &= (2x_1^2+\lambda)\left(\frac{1}{\sqrt{r_1^2-x_1^2}}+\frac{1}{\sqrt{r_2^2-x_1^2}}\right) = 0\end{aligned}$$

If $x^* = (x_1^*, x_2^*, x_3^*)$ and λ^* satisfy the first order Lagrangian necessary condition, we have $2x_1^{*2} = -\lambda^*$. Applying the same necessary condition on x_2 and x_3 renders $2x_2^{*2} = 2x_3^{*2} = -\lambda^*$. Thus $x_1^* = x_2^* = x_3^*$

satisfies the first order necessary conditions. To show it also satisfies the second order sufficient conditions, it suffices to verify that

$$\frac{\partial L^2(x^*, \lambda^*)}{\partial x_i \partial x_j} = 0 \text{ for } i \neq j,$$

and

$$\frac{\partial L^2(x^*, \lambda^*)}{\partial x_i^2} > 0 \text{ for all } i$$

to show the Hessian matrix of the Lagrangian is positive definite. That is, (x_1^*, x_2^*, x_3^*) is a local minimum. Since there is only one local minimum, it is also a global minimum. Hence (x_1^*, x_2^*, x_3^*) minimizes the Eq. (3.2) subject to constraint Eq. (3.3), and $\overline{OP} = \overline{OQ} = \overline{OR}$ minimizes the overlap. □

3.4 Optimal Geographical Density Control Algorithm

In this section, we propose a completely localized density control algorithm, called OGDC, that makes use of the optimal conditions derived in Section 3.3. Note that as it may not be possible to locate sensor nodes in any desirable position (i.e., assumption (**A1**) may not hold), OGDC attempts to select as working nodes the sensor nodes that are closest to the optimal locations. We first give an overview of OGDC and then delve into the detailed operations. We also discuss its possible extension and some limitations.

3.4.1 Overview

OGDC is devised under the following assumptions:

(B1) Each node is aware of its own position. This assumption is not impractical, as many research efforts have been made to address the localization problem [63, 51, 22].

(B2) For clarity of algorithm discussion, we assume the radio range is at least twice the sensing range, and will relax this assumption in Section 3.4.3.

(B3) For clarity of algorithm discussion, we assume all sensor nodes are time synchronized, and will relax this assumption in Section 3.4.4.

At any time, a node is in one of the three states: "UNDECIDED," "ON," and "OFF." Time is divided into rounds. Each round has two phases: the *node selection phase* and the *steady state phase*. At the

beginning of the node selection phase, all the nodes wake up, set their states to "UNDECIDED," and carry out the operation of selecting working nodes. By the end of this phase, all the nodes change their states to either "ON" or "OFF". In the steady state phase, all nodes keep their states fixed until the beginning of the next round. The length of each round is so chosen that it is much larger than that of the node selection phase but much smaller than the average sensor lifetime. Our simulation results show that the time it takes to execute the node selection operation for networks of size up to 1000 nodes in an area of $50 \times 50\text{m}^2$ (with timer values appropriately set) is usually well below 1 second and most nodes can decide their states (either "ON" or "OFF") in less than 0.2 second from the time instant when at least one node volunteers to be a starting node. The interval for each round is usually set to approximately hundreds of seconds, and the overhead of density control is small ($\stackrel{<}{\sim} 1\%$).

The node selection phase in each round commences when one or more sensor nodes volunteer to be starting nodes. For example, suppose node A volunteers to be a starting node in Fig. 3.4. Then one of its neighbors with an (approximate) distance of $\sqrt{3}r$, say node B, will be "selected" to be a working node. To cover the crossing point of disks A and B, the node whose position is closest to the optimal position C (e.g., node P in Fig. 3.4) will then be selected, in compliance with Theorem 3.3.2, to become a working node. The process continues until all the nodes change their states to either "ON" or "OFF," and the set of nodes with state "ON" forms the working set. As a node probabilistically volunteers itself to be a starting node (with a probability that is related to its remaining power) in each round, the set of working sensor nodes is not likely to be the same in each round, thus ensuring uniform (and minimum) power consumption across the network, as well as complete coverage and connectivity. In what follows, we give the detailed description of OGDC.

3.4.2 Detailed description of OGDC

Selection of the starting node At the beginning of node election phase, every node is powered on with the "UNDECIDED" state. A node volunteers to be a starting node with probability p if its power exceeds a pre-determined threshold P_t. The power threshold P_t is related to the length of the round and in general is set to a value so as to ensure with high probability the sensor can remain powered on until the end of the round.

If a sensor node volunteers, it sets a backoff timer of τ_1 seconds, where τ_1 is uniformly distributed in $[0, T_d]$. When the timer expires, the node changes its state to "ON", and broadcasts a power-on message. If a node hears other power-on messages before its timer expires, it cancels its timer and does not become a starting node. The power-on message sent by the starting node contains (i) the position of the sender and (ii) the direction α along which the second working node should be located. This direction

is randomly generated from a uniform distribution in $[0, 2\pi]$. Non-starting node may also send power-on message. In this case, the direction field in the power-on message is set to -1 to indicate the sender is a non-starting node.

The use of backoff timers avoids the possibility of multiple neighboring nodes volunteering themselves to be the starting nodes in a round. The selection of T_d is a tradeoff between the performance and the latency. Using a large value of T_d can reduce the number of starting nodes in the network and possibly reduce the level of overlap. However, with fewer starting nodes, it will take a longer time to complete the operations of selecting working nodes. In our simulation, we select T_d to be about 1.5 times of the transmission time of a power-on packet.

If the node does not volunteer itself to be a starting node, it sets a timer of T_s seconds. When the timer T_s[1] expires, it repeats the above volunteering process with p doubled until its value reaches 1. The timer is canceled whenever the state of a node is changed to "ON" or "OFF" in response to other power-on messages. T_s should be set to a sufficiently large value such that if there exists at least one node whose power level qualifies it to be a starting node, the operation of selecting working nodes can be completed in an early stage of each round. The value of p is initially set to p_0. We will discuss how to determine the value of p_0 in Section 3.4.4.

Actions taken when a node receives a power-on message When a sensor node receives a power-on message, if the node is already "ON", or it is more than $2r_s$ away from the sender node, it ignores the message; otherwise it adds this sender to its neighbor list, and checks whether or not all its neighbors' coverage disks completely cover its own coverage disk. If so, the node sets its state to "OFF" and turns itself off. Otherwise, it enters one of the following three cases (as depicted in Fig. 3.6): i) there exists uncovered crossing that is created by its working neighbors and falls in the node's coverage disk; ii) the condition in (i) is not satisfied and at least one neighbor is a starting node; iii) neither (i) nor (ii) satisfies. A node can determine if a neighbor is a starting-node from the direction field of the power-on message sent by that neighbor (a positive value indicates a starting node and vise versa).

In case (i), the node first finds the closest uncovered crossing that falls in its coverage disk. If the closest uncovered crossing is created by the new neighbor (that sends the latest power-on message to the node), the node will cancel existing timer (T_{c1}, T_{c2} or T_{c3}) (if any) and (re-)set a timer of value T_{c1}. Otherwise, the node retains the existing timer. The rationale behind how the value of T_{c1} is calculated is illustrated in Figure 3.7: let O denote the closest uncovered crossing point, A, B the two corresponding sender nodes, C the optimal location of a third sensor node used to cover the crossing point O, R the

[1]With a little abuse of symbols, we will use T_s to refer both the timer and the value of the timer. This applies to other timers.

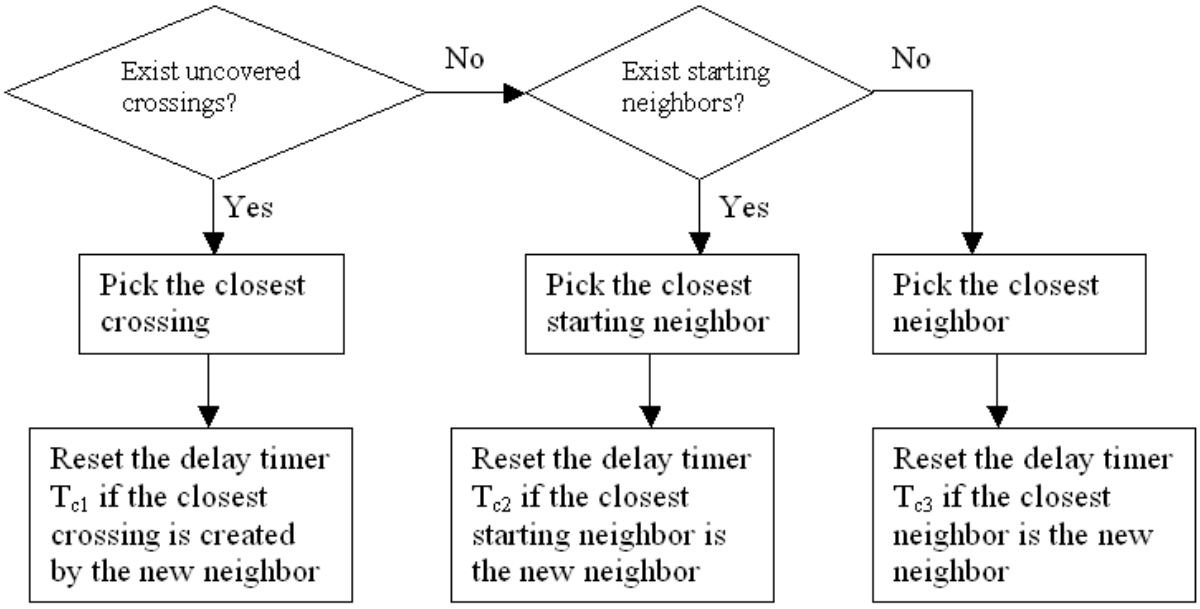

Figure 3.6: The procedure taken when a node receives a power-on message

location of the receiver node, d the distance between the receiver node and the crossing point O, and $\Delta\alpha$ the angle between $\overline{OC}$ and $\overline{OR}$. The value of T_{c1} is set as

$$T_{c1} = t_0(c((r_s - d)^2 + (d\Delta\alpha)^2) + u), \tag{3.4}$$

where t_0 is the time it takes to send a power-on message, c is a constant that determines the backoff scale and is set to $10/r_s^2$ in our simulation study, u is a random number drawn from the uniform distribution on $[0, 1]$. T_{c1} includes two terms: a deterministic term $c((r_s - d)^2 + (d\Delta\alpha)^2)$ and a random term (u). If the receiver is right in the direction α and its distance to the crossing is r_s, the deterministic term is 0; otherwise, $c((r_s - d)^2 + (d\Delta\alpha)^2)$ roughly represents the deviation from the optimal position and a delay is introduced in proportion of this deviation. The random term is introduced to break ties in the case that there exist nodes whose locations yield the same value of the deterministic term.

In case (ii), the node finds the closest starting neighbor. If the closest starting neighbor is the new neighbor, the node cancels the existing backoff timer (T_{c1}, T_{c2} or T_{c3}, if any) and (re-)sets a backoff timer of value T_{c2}. Otherwise, the node retains the existing timer. The value T_{c2} is set as (Fig. 3.8)

$$T_{c2} = t_0(c((\sqrt{3}r_s - d)^2 + (d\Delta\alpha)^2) + u), \tag{3.5}$$

where t_0, c, u are the same as those in Eq. (3.4), d is the distance from the sender to the receiver, $\Delta\alpha$ is

the angle between α and the direction from the sender to the receiver,

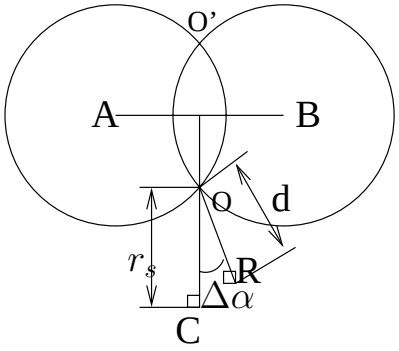

Figure 3.7: A scenario that demonstrates how the value T_{c1} is set (in case (i)).

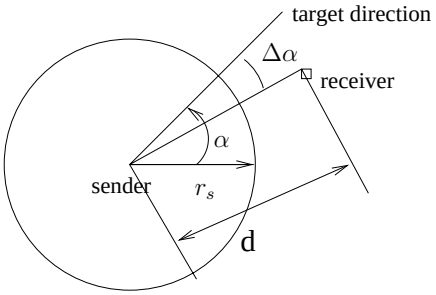

Figure 3.8: A scenario that demonstrates how the value T_{c2} is set (in case (ii)).

In case (iii), the node finds the closest neighbor. If the closest neighbor is the new neighbor, the node cancels the existing backoff timer (T_{c1}, T_{c2} or T_{c3}, if any) and (re-)sets a backoff timer of value T_{c3}, which is much greater than that of the average values of T_{c1}, T_{c2} but much less than the value of T_s. Otherwise, it retains the existing timer. This is because when a node receives only power-on messages from non-starting neighbors, it expects to receive another power-on message and the coverage areas of the two senders will overlap.

In any of the above three cases, when the backoff timer expires, the node sets its state to "ON" and broadcasts a power-on message with the direction field α set to -1 (indicating a message generated by a non-starting node).

3.4.3 Extension to the case of insufficient transmission ranges

Now we extend OGDC to ensure both connectivity and coverage when the radio range is smaller than twice the sensing range. The only issue we need to address is to determine when a node should sleep. A sufficient condition that a node can sleep is that (**C1**) its coverage area is completely covered, and (**C2**) its working neighbors are all connected without it. It is difficult to test in a decentralized manner whether or not the second condition holds, because a node is only aware of its existing working neighbors (from whom it has received power-on messages). As a result we relax the second condition as "its *existing* working neighbors are all connected without it." If two neighbor nodes are within the transmission range of each other, they are necessarily connected. This can be determined by each node under assumption **(B1)**. Moreover, if a starting node propagates a power-on message (possibly via multiple hops) to two workings nodes, clearly they are connected. Hence, two existing working neighbors are connected if either (i) they are within the transmission range of each other, or (ii) they receive power-on messages originated

from some common starting node.

Specifically, we associate each starting node with a unique id, called *netid*, and all nodes receiving power-on messages originated from the same starting node share its *netid*. A node may have multiple *netid*s (which are arranged into a *netid* list), if it receives power-on messages originated from more than one starting node. When a node decides to stay awake, it puts its *netid* list into the power-on message it sends. Each time a node A receives a power-on message from another node B, node A merges node B's *netid* list into its own. Moreover, each node divides its working neighbors into different groups based on their *netid*s. Specifically, each group initially contains working neighbors that share the same *netid*. When a node receives a power-on message, it will first update the groups as follows: if the message contains more than one *netid*, the node will merge all the groups which contain a *netid* in the list of the newly received messages. If the new neighbor is directly connected with another neighbor (as they are within the transmission range of each other) but with non-overlapping *netid* lists, the node will also merge all the groups which contain a *netid* in either of the two *netid* lists. At the end of the group-merging process, the node then decides if it can go to sleep: if there is only one group left and the node's coverage area is covered by the group, the node can go to sleep.

Efficient implementation of the *netid* list Significant overhead may be incurred in the power-on message, if the *netid* list is long. Fortunately, a simple calculation shows that the probability that there are at most 3 starting nodes conditioning on that there exist starting nodes is more than 97%, if each node volunteers to be a starting node with the probability $1/N$, where N is the number of nodes. we efficiently implement the *netid* list as follows. We use a bitmap with the maximum size of k. To put a *netid* into the list, we first hash the "real *netid*" (which could be the starting node id) into an integer j from 1 to k, and then set the jth bit in the bitmap. Clearly the probability of having a hash collision is small with reasonably large k. We choose $k = 8$ in our simulation.

3.4.4 Discussion

After describing the operations of OGDC, we are now in the position to elaborate on several implementation and parameter tuning issues:

Setting of the initial volunteering probability, p_0 Recall that p_0 is the initial probability that a node volunteers itself to be a starting node. In the case that the region to be covered is not large, it is desirable that at one time only one node determines to be a starting node. To this end, we set $p_0 = 1/N$, where N is the total number of sensor nodes in the network, as this maximizes the probability that exactly

one sensor node volunteers itself as a starting node. On the other hand, if the region to be covered is large, it is desirable to have multiple sensor nodes volunteer themselves at one time. In this case, we set $p_0 = k/N$ as this maximizes the probability that exactly k nodes volunteer themselves. We argue that the number of sensor nodes, N, or at least its order is known at the time of network deployment. Even if this is not the case, as the value of p is doubled every time the T_s timer expires, the value of p_0 does not have a significant impact on the performance.

Guidelines of OGDC parameter tuning OGDC has several tunable parameters. We have briefly described how to set the value of each parameter when it is introduced for the first time. Now we outline the set of guidelines for parameter tuning. Table 3.1 lists the parameters, their functions, and their values used in our simulation study.

Table 3.1: Parameter values used in the simulation study.

Parameter	Function	Value Used
r_s	sensing range	10 m
round time	period for executing OGDC	1000 s
P_t	power threshold for volunteering to be a working node	the level that allows a node to be idle for 900 seconds
T_d	maximum timer value used in volunteering to be a starting node	10 ms
T_s	maximum timer value used in re-initiating the process of volunteering to be a starting node	1 s
T_{c3}	timer value used when a node only receives power-on messages from non-starting neighbors and the coverage disks of those neighbors do not intersect in the node's coverage disk	200 ms
t_0	the time it takes to send a power-on packet	6.8 ms
c	constant used in Eqs. (3.4) and (3.5)	$10/r_s^2$
channel capacity		40K bps

Most timing related parameters such as T_d, T_s and c should be set according to the transmission time of a power-on message t_0. As a rule of thumb, the T_d timer used to suppress surplus starting nodes should be in the same order of t_0. The T_s timer should be set to approximately two orders of magnitude larger than t_0 to allow the density control process to be completed before the T_s timer fires, if there exist some starting nodes in the network. T_{c3} should be chosen much larger than the average value of T_{c1}, T_{c2} and much smaller than T_s. The constant c should be chosen such that T_{c1} and T_{c2} are approximately one order of magnitude larger than t_0 on average to avoid packet collision. The round time should be set to a value that is approximately one order of magnitude less than that of the lifetime of a single sensor.

The value of P_t is dependent on the application requirement. If the application requires continuous, complete coverage, P_t should be set to a value such that a sensor can remain active for at least the duration of a round time. If intermittent, incomplete coverage in each round is acceptable, P_t can be set

to a value that is less than the power required to keep the sensor active for the entire round time.

It is worth mentioning that we follow the above guidelines to tune parameters in our simulation and the simulation results are quite satisfactory. Moreover, the performance of OGDC is not particularly susceptible to parameter settings as long as the above guidelines are followed.

Time synchronization For simplicity of algorithm discussion, we have assumed that all nodes are time synchronized (assumption (**B3**)). This assumption can be relaxed as follows. In the first round we designate a sensor node to be the starting node. When the starting node sends a power-on message, it includes in its power-on message a duration δT after which the receivers should wake up for the next round. When a non-starting node broadcasts a power-on message, it reduces the value of δT by the time elapsed since it receives the last power-on message and includes the new value of δT in its power-on message. In this fashion, all the nodes get "synchronized" with the starting node and will all wake up at the beginning of the next round.

If the monitored region is so large that it is not acceptable to have one starting node in a round, we can synchronize a few nodes before deployment, distribute them evenly in the entire region, and designate them to be the starting nodes in the first round. Then we can similarly synchronize other nodes with the starting nodes in the first round as above. In fact it is not unreasonable to assume that multiple synchronized nodes with overlapping coverage areas can serve as reference points of other nodes ([13, 12]). To overcome the small clock drifting over the network lifetime, when a node wakes up, it needs to wait for a short time ($\geq$ the maximum clock drifting) before it starts to send any message.

What if no other sensor nodes volunteer It may occur that the power of a node is less than the threshold power P_t and yet no power-on message is received even after the node sets the value of p to 1. This indicates that all the nodes do not have sufficient power and cannot volunteer themselves to be starting nodes. In this case, the node resets its power threshold P_t to 0 and restarts the density control process.

What if message loss happens If a packet sent from a neighbor is lost for any reasons (transmission errors, collisions, etc), a node is simply not aware of that neighbor's existence. For example, if a starting node's power-on message is lost at all receivers (this will happen with low probability), all other nodes will repeat the process of electing another starting node. Packet loss may increase the number of working nodes. If nodes are deployed in severe environment where transmission error happens frequently, they can send the power-on message multiple times (with a random delay) to increase the receiving probability.

But this has to be done with caution because multiple transmissions may increase packet collisions and worsen the situation.

3.5 Performance Evaluation

3.5.1 Simulation environment setup

To validate and evaluate the proposed design of OGDC, we have implemented it in *ns-2* [2] with the CMU wireless extension, and conducted a simulation study in a $50 \times 50\text{m}^2$ region where up to 1000 sensors are uniformly randomly distributed. Each data point reported below is an average of 20 simulation runs unless specified.

Schemes for comparison In addition to evaluating OGDC, we also evaluate the performance of the PEAS algorithm proposed by Ye *et al.* [80], the CCP algorithm by Wang *et al.* [74] and a hexagon-based GAF-like algorithm. The former two algorithms have been introduced in Section 2.1. The latter (hexagon-based GAF-like) algorithm is built upon GAF [77] and operates as follows. The entire region is divided into square grids and one node is selected to be awake in each grid. To maintain coverage, the grid size must be less than or equal to $r_s/\sqrt{2}$. Thus, for a large area with size $l \times l$, it requires $\frac{2l^2}{r_s^2}$ nodes to operate in the active mode to ensure complete coverage. As pointed out by [42], hexagonal grids are more "homogeneous" than square grids and thus offer more scaling benefits, e.g., the number of working nodes is significantly smaller. To maintain coverage in hexagonal grids, the side length of each hexagon is at most $r_s/2$, and it requires $\frac{8l^2}{3\sqrt{3}r_s^2} \approx \frac{1.54l^2}{r_s^2}$ working nodes to completely cover a large area with size $l \times l$. As will be discussed below, the hexagon-based GAF-like algorithm performs better than the "sponsored area" algorithm [69], and hence the latter is not included in the comparison.

Parameters used We use the energy model in [80], where the power consumption ratio for transmitting, receiving (idling) and sleeping is 20:4:0.01. We define one unit of energy (power) as that required for a node to remain idle for 1 second. Each node has a sensing range of $r_s = 10$ meters, and a lifetime of 5000 seconds if it is idle all the time.

The tunable parameters in OGDC are set as follows: the round time is set to 1000 seconds, the power threshold P_t is set to the level that allows a node to be idle for 900 seconds, the timer values are set to, respectively, $T_d = 10$ ms, $T_s = 1$ s, and $T_e = T_s/5 = 200$ ms, t_0 is set to the time it takes to send a power-on packet, $6.8ms$ (the wireless communication capacity is 40Kbps, the packet size is 34 bytes). The constants used in Eqs. (3.4) and (3.5) are set, respectively, to $c = \frac{10}{r_s^2}$, and p_0 is set to $1/N$ where N

is the total number of sensors. Table 3.1 summarizes all the parameter values used.

Although OGDC involves tuning of several parameters, we have found that its performance is rather insensitive to the parameter values, as long as they are set in compliance with the guidelines discussed in Section 3.4.4. The system parameters, such as the initial energy of a node, the radio transmission rate, and the energy consumption rate, are the same for all the nodes.

Performance metrics The performance metrics of interest are (i) the percentage of coverage, i.e. the ratio of the covered area to the total area to be monitored; (ii) the number of working nodes required to provide the percentage of coverage in (i); and (iii) α-lifetime, defined as the total time during which at least α portion of the total area is covered by at least one node. The conventionally defined network lifetime is then 100%-lifetime. Note that the lifetime definition used in this chapter is slightly different from that in [79], where the lifetime is defined as the time interval until which coverage falls below a pre-determined percentage and never comes back again.

In the first part of the simulation, we assume the transmission range is at least twice the sensing range (which is set to 20m) so that we can focus on coverage alone. In the second part, we simulate the cases in which the transmission range is smaller than twice the sensing range.

3.5.2 Simulation in the case of sufficient transmission ranges

We measure coverage as follows: we divide the area into 50×50 square grids, and a grid is considered covered if the center of the grid is covered, and coverage is defined as the ratio of the number of grids that are covered by at least one sensor to the total number of grids. In the $50 \times 50\text{m}^2$ area, 45 hexagon cells are required to cover the entire area if the hexagon-based GAF-like algorithm is used (Fig 3.9). Hence, the hexagon-based algorithm ensures 100% coverage if at least 45 sensors operate in the active mode in each round, one for each cell. However, at least 47 nodes are required to operate in the active mode under the "sponsored area" algorithm proposed in [69] to ensure the complete coverage. When the number of sensor nodes in the sensor network increases, the sponsored area algorithm requires more nodes to cover the entire area. As the sponsored area algorithm performs worse than the hexagon-based, GAF-like method, we do not include the sponsored area algorithm [69] in the following comparison.

Number of working nodes and coverage Fig. 3.10 shows the number of working nodes and coverage versus the number of sensor nodes deployed in the network. Both metrics are measured after the density control process is completed. Under most cases, OGDC takes less than 1 second to perform density control in each round, while PEAS [80] and CCP [74] may take up to 100 seconds. As shown in Fig. 3.10,

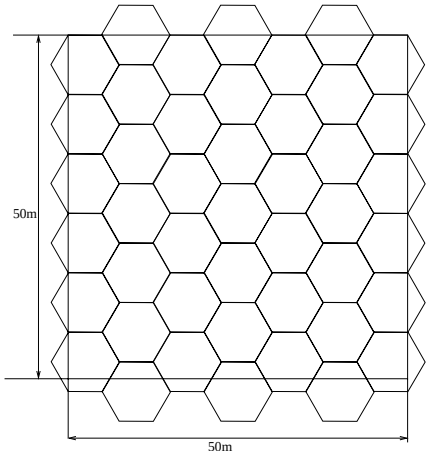

Figure 3.9: 45 hexagons are required to cover a 50 × 50 m^2 area.

OGDC needs only half as many nodes to operate in the active mode as compared to the hexagon-based GAF-like algorithm, but achieves almost the same coverage (in most cases OGDC achieves more than 99.5% coverage). As the PEAS algorithm can control the number of working nodes by using different probing ranges, we tried two different probing ranges: 8m and 9m. (Using a probing range of 10m leads to insufficient coverage, the result of which is thus not reported here.) As shown in Fig. 3.10, using a smaller probing range results in more working nodes. With a probing range of 9m, the resulting coverage is less than that achieved by OGDC, while the number of working nodes is up to 50% more than that of OGDC. Moreover, the number of working nodes required under OGDC modestly increases with the number of sensor nodes deployed, while both PEAS and CCP incur a 50% increase in the number of working nodes, when the number of sensor nodes deployed in the network increases from 100 to 1000. We also observe that when the number of working nodes becomes very large, the coverage ratio of CCP actually decreases. This is because a large number of message exchanges are required in CCP to maintain neighborhood information. When the network density is high, packets incur collision more often and the neighborhood information may be inaccurate. In contrast, in OGDC each working node sends out at most one power-on message in each round, and as a result the packet collision problem is not so serious. The result of CCP reported here is a little different from that is reported in [74] because it assumes error-free channel conditions (no collisions, etc) in [74].

Fig. 3.11 shows the dynamics of coverage and total remaining power over the time in a typical simulation run for a sensor network of 300 sensor nodes in a 50 × 50 m^2 area. OGDC can provide over 95% coverage for appropriately 10 times of the lifetime of a single sensor node and the total power of the network decreases smoothly.

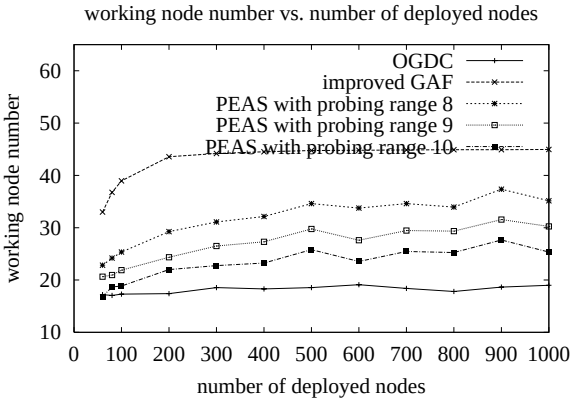

(a) # of working nodes vs. # of deployed nodes

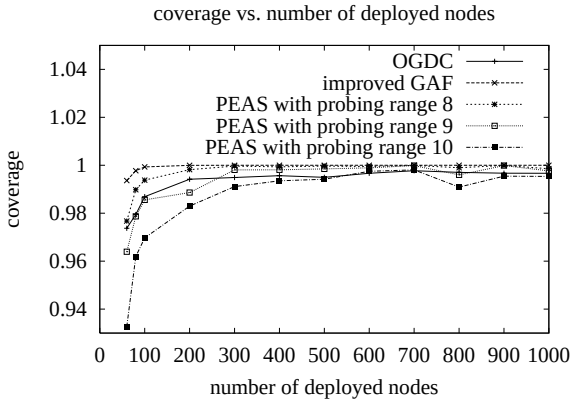

(b) Coverage vs. # of deployed nodes

Figure 3.10: # of working nodes and coverage versus # of sensor nodes in a 50×50 m^2 area.

α-lifetime Fig. 3.12 compares the α-lifetime achieved by OGDC, PEAS and CCP in a sensor network of 300 nodes, where α varies from 98% to 50%. For the PEAS algorithm we again tried two different probing ranges: 8m and 9m. As shown in Fig. 3.12, for a reasonably large α, the α-lifetime of PEAS is much shorter than that of OGDC. Only when α is less than 60%, the lifetime of PEAS using the probing range 9m is longer than that of OGDC. This is because with a relatively small probing range, PEAS requires an excessive number of nodes to operate simultaneously. Hence, its lifetime is consistently shorter than OGDC. On the other hand, with a large probing range of 9m, PEAS only guarantees that no two working nodes are in each other's probing range and does not ensure complete coverage. Moreover, when a node dies, it may take more than 100 seconds for another node to wake up to take its place. During that transition period the network is not completely covered. As a result, the low percentage lifetime is prolonged in PEAS. A nice property of OGDC is that during most of the lifetime, the monitored region is covered with a high percentage. It is clear that OGDC is preferred to PEAS no matter what probing range is used, unless the desired coverage percentage is very low (i.e. less than 60%). Although CCP uses

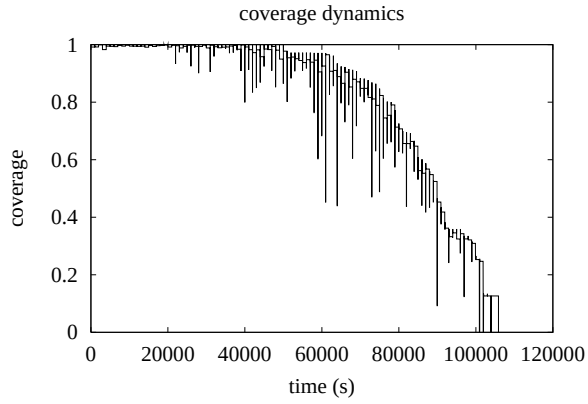

(a) Coverage dynamics vs. time

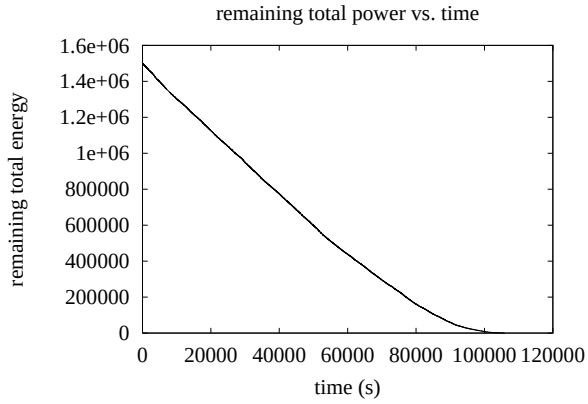

(b) Total remaining power vs. time

Figure 3.11: Dynamics of the sensing coverage and the total remaining power versus time under OGDC in a sensor network of 300 sensor nodes in a 50×50 m^2 area.

less working nodes than PEAS in most cases, its lifetime is much shorter than both PEAS and OGDC. This is due to two reasons. First, CCP needs to periodically broadcast hello messages, the operation of which consumes energy. Second, in CCP when a node wakes up from the sleep mode it must stay awake and wait until it receives hello messages from sufficient number of neighbors that can cover its coverage region.

Fig. 3.13 shows the 98%-lifetime and 90%-lifetime under OGDC, CCP and PEAS with a probing range of 9m, when the number of sensor nodes deployed in a network varies from 100 to 800. The α-lifetime scales linearly as the number of sensors deployed increases for both OGDC and PEAS algorithms. However, OGDC achieves nearly 100% more 98%-lifetime and 40% more 90%-lifetime than PEAS does. Again CCP achieves a much shorter lifetime than OGDC and PEAS.

For applications that require high levels of tracking accuracy and reliability, it may be desirable that each point is covered by multiple sensors. To this end, we define k-coverage as that each point in an

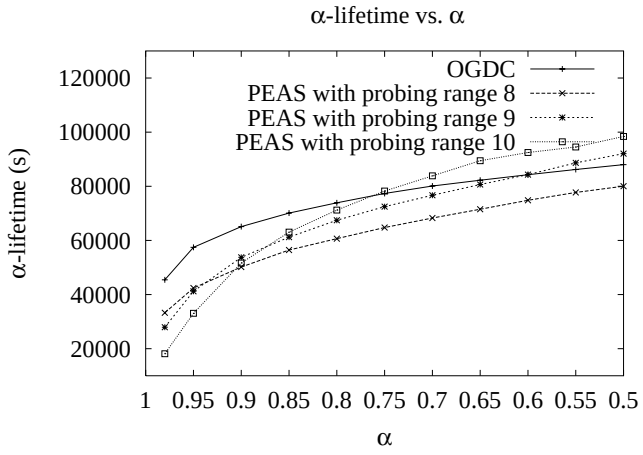

Figure 3.12: Comparison of α-lifetime versus α under OGDC, PEAS and CCP.

area is covered by at least k sensor nodes. OGDC can be readily extended to accommodate k-coverage as follows: a node is only turned off when each grid point in the node's coverage area is covered by at least k other nodes. Figure 3.14 shows the curve of 80%-lifetime with 3-coverage versus the number of sensor nodes. Again the 80%-lifetime linearly increases with the number of sensor nodes deployed in the network. A more in-depth study on k-coverage is a subject of our future research.

3.5.3 Simulation in the case of insufficient transmission ranges

We now investigate the effect of small transmission ranges on coverage and connectivity. Since PEAS does not consider the connectivity issue, we only compare OGDC against CCP. Fig. 3.15 shows the number of working nodes versus the number of sensor nodes deployed with respect to different radio transmission ranges r_t under OGDC and CCP. OGDC uses a much smaller number of working nodes than CCP, especially when the radio range is small. Due to wireless channel errors, the sensor network may not always be connected in the case of small radio ranges, even if all the sensor nodes are powered on. Hence, instead of using the coverage of the network as the performance index, we measure the coverage of the largest connected component and plot the result in Fig. 3.16. The coverage of the largest connected component is very close to 1 under both algorithms, except in the cases that the number of sensor nodes deployed and the radio range are both small (e.g., $n = 100$ and $r_t = 5$). As a matter of fact, in the case of $n = 100$ and $r_t = 5$, the sensor network with all the sensor nodes active is not connected, and has more than 18 connected components with a 45% coverage for the largest connected component in average.

In general we observe that as the radio range decreases, the coverage increases slightly and the number of nodes also increases. This is the cost for maintaining connectivity. However, the number of working

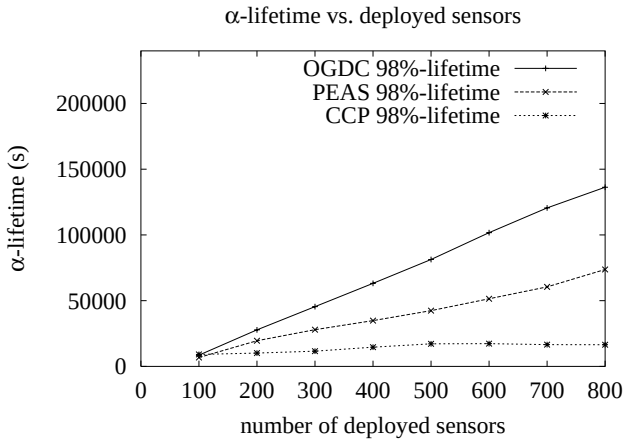

(a) 98%-lifetime

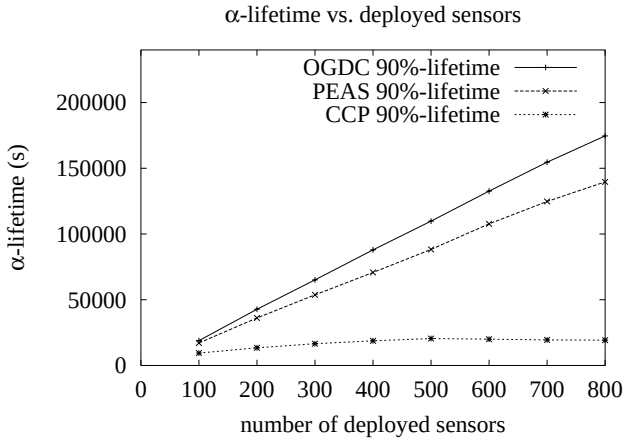

(b) 90%-lifetime

Figure 3.13: Comparison of α-lifetime versus number of sensor nodes under OGDC, PEAS (with probing range 9m) and CCP.

nodes grows far less than the inverse of the square of the radio range.

3.6 Conclusions

In this chapter we have investigated the issues of maintaining coverage and connectivity by keeping a minimum number of sensor nodes to operate in the active mode in wireless sensor networks. We begin with a discussion on the relationship between coverage and connectivity, and show that if the radio range is at least twice the sensing range, then complete coverage implies connectivity. Hence, if the condition holds, we only need to consider the coverage problem. Then, we derive, under the ideal case in which node density is sufficiently high, a set of optimality conditions under which a subset of working sensor nodes can be chosen for complete coverage. Based on the optimality conditions, we then devise a

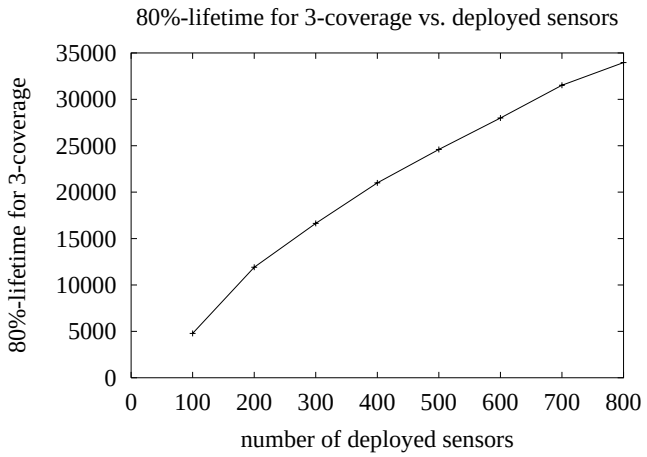

Figure 3.14: 80%-lifetime with 3-coverage versus number of sensor nodes under OGDC.

decentralized and localized density control algorithm, OGDC. OGDC is fully localized and can maintain coverage as well as connectivity, regardless of the relationship between the radio range and the sensing range. *Ns-2* simulations show that OGDC outperforms the PEAS algorithm [80], the CCP algorithm [74], the hexagon-based GAF-like algorithm, and the sponsor area algorithm [69] with respect to the number of working nodes needed and network lifetime (with up to 50% improvement), and achieves almost the same coverage as the best algorithm.

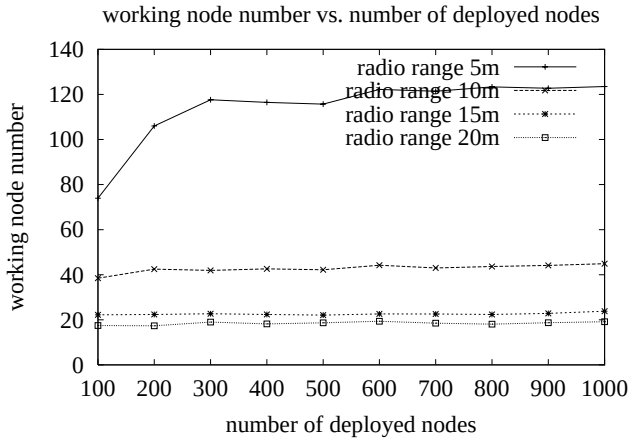

(a) OGDC

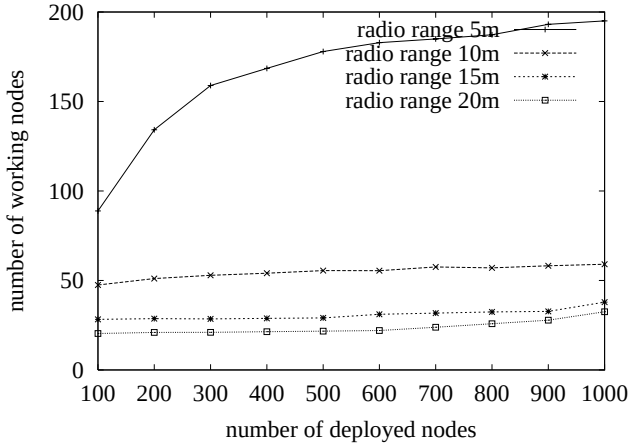

(b) CCP

Figure 3.15: Number of working nodes versus number of sensor nodes deployed with respect to different radio ranges under OGDC and CCP (the sensing range is fixed at 10m).

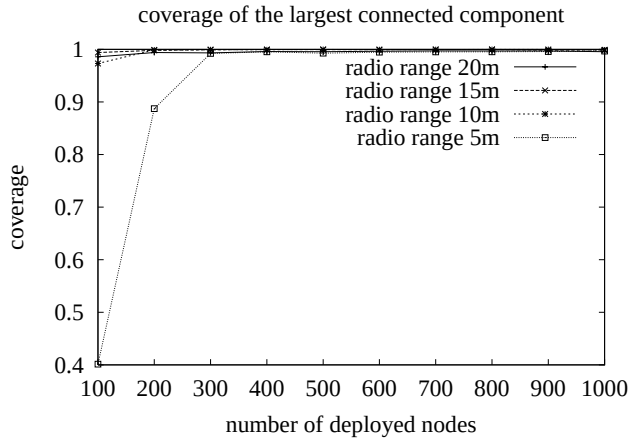

(a) OGDC

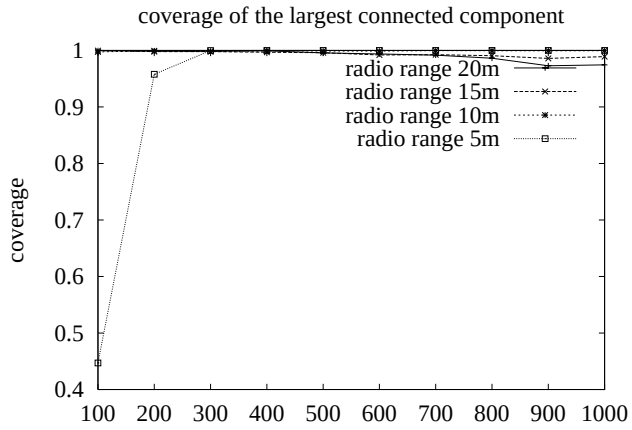

(b) CCP

Figure 3.16: Coverage of the largest connected component versus the number of sensor nodes deployed with respect to different radio ranges under OGDC and CCP (the sensing range is fixed at 10m).

Chapter 4

Lifetime Upper Bounds of Wireless Sensor Networks

4.1 Introduction

In the previous chapter, we design, implement, and evaluate a density control algorithm for maintaining coverage and connectivity. A natural question that remains is whether and to what extent we can still improve the algorithm. In order to answer this question, we need to understand what is the maximum lifetime that can be achieved by all possible algorithms as lifetime is the ultimate performance measurement.

In this chapter, we explore the fundamental limit of sensor network lifetime that all algorithms can possibly achieve. The derivation is based on the theory of coverage processes [36]. We assume sensors are deployed in a square region with side length ℓ. We consider two different kinds of upper bounds. The first is asymptotic upper bound for maintaining complete coverage as $\ell \to \infty$ and the second is actual upper bound for maintaining α-coverage (which means at least α portion of a region is covered) in a finite region. In the case of asymptotic upper bounds, we make several different model assumptions. We investigate the lifetime upper bounds with and without Torus convention (to be explained in the next section). We consider three different node deployment methods: Poisson process deployment, uniformly random deployment, and regular grid deployment.

In each of the deployment methods, we develop a necessary and a sufficient condition on the node density λ in order to guarantee complete k-coverage of a square region with side length ℓ (in the almost sure sense). Therefore, given the density that is not sufficient for maintaining complete $(k+1)$-coverage, the network lifetime for maintaining complete coverage is upper bounded by kT, where T is the lifetime of a single sensor.

The second type of upper bounds is for ensuring only α-portion of the region to be covered. In this scenario, we derive two upper bounds; one holds universally for any possible algorithm, and the other is targeted for a special type of algorithms that intend to completely cover the region initially and maintain as large coverage as possible, until the coverage drops below a certain threshold α.

In order to understand how good the derived upper bounds are (i.e., whether and to what extent

they can be achieved), We also devise an algorithm to approach the derived α-lifetime upper bounds. By numerical simulations, we show that around 90% of the lifetime upper bound can be achieved. This verifies that the lifetime upper bound is tight and the devised algorithm is efficient.

With our derivation and numerical results, we will be able to answer several important questions, e.g., given the lifetime T of a single sensor node, how many sensor nodes have to be deployed in a region (or equivalently what is the sensor density), in order to continuously monitor the region for a period of $k \cdot T$. We also observe that although it is, in general, desirable to deploy a sensor network of high density to achieve a large lifetime per unit of nodal density, the increase in the lifetime per unit of nodal density becomes marginal when the density exceeds certain threshold. This is because the overhead incurred in maintaining coverage in a distributed manner dominates when the sensor density becomes high. In addition, as the universal upper bound of α-lifetime is much larger than that for the special class of algorithms, we conclude that a sensor network should maintain, if allowed by the system requirements, α-coverage from the time the system is initially deployed, rather than maintaining as large coverage as possible at system initialization and operating until the coverage ratio drops below α. Finally the result on the density requirement for k-coverage has another important implication, in addition to its relationship with the network lifetime. In the target tracking application [6], one sensor is usually not enough to correctly track the targets' locations. Thus, it is often required that every point be covered by at least k sensors. Even in applications where one only needs to detect the presence of a certain object (rather than its movement), it may still be desirable to have each point covered by several sensors for fault tolerance of node failure or message loss during the multi-hop transmission to the data sinks. Therefore, it is important to derive the node density required to ensure k-coverage with high probability.

Several research efforts have been made to derive the upper bounds of network lifetime in wireless ad hoc networks and sensor networks [9, 8, 10]. A detailed summary of existing work is given in Section 2.2. Our work differs from existing works in two aspects. First, we consider as the (network) α-lifetime the time interval during which at least α-portion of the region can be continuously monitored. Second, unlike the work reported in [10], the lifetime upper bounds derived in this chapter are independent of the power-saving schemes used.

The rest of the chapter is organized as follows. In Section 4.2, we state the assumptions we make on the system model, and define what we mean by network lifetime in sensor networks. Then we delve into the derivation in Sections 4.3 and 4.4 for 1-lifetime upper bounds and in Section 4.5 for α-lifetime upper bounds. Following that, we present the algorithm that approaches the lifetime upper bounds in Section 4.6 to validate the derived results of the upper bounds of network lifetime. Finally we conclude the chapter in Section 4.7.

4.2 System Model

To facilitate the derivation, in this section we state the assumptions we make on the system model, and define the term of network lifetime that we shall consider throughout the chapter.

4.2.1 Assumptions on the system model

We have some general assumptions throughout the chapter and also some specific assumptions in different sections. The general assumptions are as follows. We assume the region R to be monitored is a square region with side length ℓ. Each sensor node can detect an event of interest within a distance of r, and this distance is termed as the *sensing range*. The disk centered at a sensor node and with a radius of r is termed as the *coverage disk* of this node. Without loss of generality, we assume that each sensor node has a sensing range of $r = \frac{1}{\sqrt{\pi}}$, i.e., each sensor node can cover a disk of unit area, and $\ell >> r$. We assume that each sensor has the same lifetime of T. This assumption is generally made in analyzing the network lifetime, for example, in [10].

As analytically proved in [85], if the radio transmission range is at least twice as large as the sensing range, network coverage implies connectivity. That is, as long as the set of working nodes completely covers the monitored region, the network is connected. We make this assumption so as to facilitate the derivation. As tabulated in Tables A.1–A.2, this assumption holds for most commercially available sensor devices. A study on the network lifetime when the above assumption does not hold (and hence one has to consider both coverage and connectivity in selecting the working set) is a subject of future investigation.

The following are some specific assumptions in each section. In Section 4.3, we further assume the torus convention [36] (a.k.a. the toroidal model [56]), i.e., each disk that protrudes one side of the region R enters R again from the opposite side (Fig. 4.1). This eliminates consideration of boundary effects.

We also assume the deployed sensor nodes in the square region R form a (homogeneous) Poisson point process with density λ in this section. There are several ways of defining a Poisson point process, one of which is stated below. First, for any subset A of the region R, the distribution of the number of nodes in the set is Poisson with mean $\lambda||A||$, where $||A||$ is the area of A. Second, given that the number of nodes in such a set A is m, the node locations in A are m mutually independent random variables, each uniformly distributed over A. It is well known that n nodes whose locations are mutually independent random variables, each with uniform distribution in R, are essentially a Poisson point process with density $\lambda = n/\ell^2$ if R is large ([36], page 39).

In Section 4.4, we do not assume Torus convention and therefore, we consider the boundary effects of maintaining complete k-coverage. We investigate three deployment methods in this section: Poisson

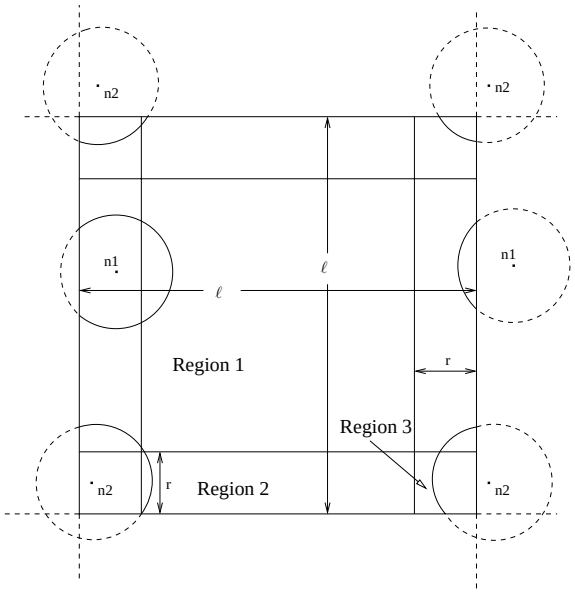

Figure 4.1: The toroidal model. The model can be interpreted by considering R as simply one member of a lattice of squares and assuming that all nodes are repeated in precisely the same relative positions in all squares.

process deployment, uniformly random deployment, and regular grid deployment.

In general, the results in Section 4.5 do not really depend on the node distributions and whether Torus convention is assumed. However, the calculation of the k-vacancy V_k (which is used to calculate the lifetime upper bounds and to be defined in Section 4.5) depends on those assumptions. In order to obtain quick numerical results, we assume Torus convention and Poisson point process. But when calculating the lifetime upper bounds in simulations or experiments, we calculate V_k directly based on the exact node locations and do not assume Torus convention.

4.2.2 Definition of sensor network lifetime

We define α-*lifetime* as length of the time intervals in which at least α portion of the region R is covered by at least one sensor node, where α is a tunable parameter. In the special case of $\alpha = 1$, we mean the lifetime for complete coverage although it can be argued that these two concepts are not exactly equivalent.

A discussion on how the α-lifetime defined above compares against the lifetime defined in [10] and [79] is in order. Blough and Santi [10] define the lifetime of sensor networks as $\min\{t_1, t_2, t_3\}$, where t_1 is the time it takes for the cardinality of the largest connected component to drop below $c_1 \cdot n(t)$, where $n(t)$ is the number of alive nodes at time t, t_2 is the time it takes for $n(t)$ to drop below $c_2 \cdot n(0)$, and t_3 is the time it takes for the covered area to drop below $c_3 \cdot \ell^2$. Here $0 \leq c_1, c_2, c_3 \leq 1$. If we set $c_1 = 0, c_2 = 0$

and $c_3 = \alpha$, then the network lifetime is exactly the same as the α-lifetime defined in this chapter. Under the assumption that the radio range is at least twice as large as the sensing range (and thus network coverage implies connectivity), it makes sense to ignore the connectivity requirement imposed by t_1 and set $c_1 = 0$. The requirement imposed by t_2 is not really necessary in sensor networks, since one is usually not concerned with how many sensors remain alive but with whether or not the remaining sensors can perform certain functions such as monitoring and relaying information back to data sinks.

Ye *et al.* [79] define the lifetime as the time it takes for the coverage (defined as the ratio of the area covered by working nodes to the total area) to drop below, and never exceed again a pre-determined threshold. Due to the network dynamics, the coverage may occasionally drop below a threshold and come back again. They take into account of the time interval when the coverage temporarily drops below the threshold in the network lifetime, while we do not.

4.3 Asymptotic Upper Bound of 1-Lifetime with Torus Convention

In this section, we first investigate the asymptotic lower bound on the density λ required to guarantee full coverage ($\alpha = 1$) for time kT as the monitored region $\ell \to +\infty$. This result can also be interpreted as the asymptotic upper bound of 1-lifetime given the density λ of the sensor nodes. Then we adapt our asymptotic results to a unit-area square (for which other researchers study the problem of maintaining asymptotic 1-coverage and k-connectivity) in Section 4.3.2 in order to compare the results against others. (For ease of understanding, we succinctly summarize several results in coverage processes [36] that pertain to our derivation in Appendix A.3.)

4.3.1 Requirement on the nodal density in square regions of size ℓ^2

The problem of deriving the asymptotic upper bound of 1-lifetime is highly related to the k-coverage problem, where by k-coverage we mean every point in the monitored region is covered by at least k nodes. Let the *coverage degree* denote the maximum value of k such that the sensor network has k-coverage in the monitored region. It is obvious that the coverage degree k times the lifetime T of a single sensor gives a strict upper bound of 1-lifetime.

Let the k-vacancy V_k be defined as the area that is covered by at most $k-1$ nodes. We need to determine the required density λ such that $P(V_k > 0) \to 0$ as $\ell \to +\infty$. Let $\chi_k(x)$ denote the indicator

function of whether a point x is covered by at most $k-1$ sensor nodes, i.e.,

$$\chi_k(x) = \begin{cases} 1, & \text{if at most } k-1 \text{ nodes cover the point } x, \\ 0, & \text{otherwise.} \end{cases} \tag{4.1}$$

The fact that a point x is covered by at most $k-1$ sensor nodes indicates that there are at most $k-1$ sensor nodes within the unit-area disk centered at x (recall that each sensor can cover a unit-area disk centered at itself). Under the assumption that the deployed sensors form a Poisson point process, we have

$$P(\chi_k(x) = 1) = e^{-\lambda} \left(\sum_{i=0}^{k-1} \frac{\lambda^i}{i!} \right). \tag{4.2}$$

Now the random variable V_k can be expressed as

$$V_k = \int_R \chi_k(x) dx. \tag{4.3}$$

To calculate its expectation, we use Fubini's theorem [61] and exchange the order of integral and expectation, i.e.,

$$\begin{aligned} E(V_k) &= \int_R E(\chi_k(x)) dx \\ &= \int_R P(\chi_k(x) = 1)\ dx \\ &= ||R|| P(\chi_k(x) = 1) \\ &= \ell^2 e^{-\lambda} \left(\sum_{i=0}^{k-1} \frac{\lambda^i}{i!} \right), \end{aligned} \tag{4.4}$$

where the third equality results from the fact that $P(\chi_k(x) = 1)$ is a constant for all x.

In order to ensure complete coverage for the duration of kT, each point should be covered by at least k nodes, which implies $V_k = 0$. As nodes form a Poisson point process in the region R, it cannot be guaranteed that this always occurs with a finite density λ, no matter how large λ is. However, with $\lambda \to +\infty$ as $\ell \to +\infty$ we can ensure this occurs with high probability, i.e., $P(V_k = 0) \to 1$ as $\ell \to +\infty$.

In what follows, we establish a tight bound on the density λ that ensures asymptotic complete k-coverage.

Theorem 4.3.1 *Let $\lambda = \log \ell^2 + (k+1) \log\log \ell^2 + c(\ell)$. If $c(\ell) \to +\infty$ as $\ell \to +\infty$, then $P(V_k > 0) \to 0$. If $c(\ell) \le C < +\infty$, then $P(V_k > 0) \ge \epsilon$ as $\ell \to +\infty$, where $\epsilon = 1/(1 + 4e^C(k+1)!)$.*

Proof. First we prove if $c(\ell) \to +\infty$ as $\ell \to +\infty$, $P(V_k > 0) \to 0$. Clearly if the value of λ increases, $P(V_k > 0)$ will decrease. Hence, without loss of generality, we assume that $c(\ell) = o(\log \ell^2)$.

Let a *crossing* be defined as either an intersection point of the boundaries of two disks or an intersection point of the boundary of a disk and the boundary of region R. A crossing is said to be *k-covered* if it is an interior point of at least k disks. By Theorem 4 in [74], region R is completely k-covered if there exist crossing points and every crossing point is k-covered. Equivalently, if R is not completely k-covered and there exist crossings, some of the crossings are not k-covered.

With $\lambda \to +\infty$ as $\ell \to +\infty$ and $\pi r^2 = 1$, we can write

$$P(V_k > 0) = p_1 + p_2 + p_3, \tag{4.5}$$

where

$$\begin{aligned}
p_1 &\equiv P(\text{no disk is centered within } R) = \exp(-\lambda \ell^2) \to 0, \\
p_2 &\equiv P(\text{at least one disk is centered within } R, \text{ but none of the disks intersects any other disk} \\
&\quad \text{and none of the disks intersect the boundary of } R) \\
&\leq P(\text{at least one disk is centered within } R) \times P(\text{a given disk intersects no other disks}) \\
&= (1 - \exp(-\lambda \ell^2)) \times \exp(-\lambda \pi (2r)^2) \\
&\leq \exp(-4\lambda) \to 0,
\end{aligned}$$

and

$$\begin{aligned}
p_3 \equiv\ & P(R \text{ is not completely } k\text{-covered, at least one disk is centered within } R, \text{ and at least} \\
& \text{two disks intersect each other or at least one disk intersects the boundary of } R).
\end{aligned}$$

Therefore, we have

$$P(V_k > 0) \to p_3, \quad \text{as } \ell \to +\infty. \tag{4.6}$$

Next we derive an upper bound of p_3.

If R is not completed k-covered, if one or more disks are centered within R, and if there exist crossings in R, then at least one of the disks has two or more crossings that are not k-covered on its boundary. Let M_k denote the number of crossings that are not k-covered. Then we have

$$p_3 \leq P(M_k \geq 2) \leq E(M_k)/2. \tag{4.7}$$

We first consider crossings created by two disks intersecting each other. The expected number, D, of

nodes in region R is $\lambda\ell^2$. If any two nodes are within a distance of $2r$ from each other, their coverage disks intersect. Hence, the expected number of crossings created by a given node is $2\lambda\pi(2r)^2$. Since each crossing is counted twice, the expected value of the total number, N_1, of crossings created by two disks intersecting each other is given by

$$E(N_1) = \lambda\ell^2 \cdot \lambda\pi(2r)^2 = 4\lambda^2\ell^2. \tag{4.8}$$

Now we consider crossings created by a disk intersecting the boundary of region R. If a node is within a distance of r to the boundary of region R, at most two crossings will be created, except when the node is located on the corner of region R (e.g., Region 3 in Fig. 4.1). In that case, at most 4 crossings will be created. Hence the expected value of the total number, N_2, of crossings created by a disk intersecting the boundary of region R is given by

$$E(N_2) \le 8\lambda\ell r. \tag{4.9}$$

Recall that the probability that a given crossing is not k-covered is $e^{-\lambda}\sum_{i=0}^{k-1}\lambda^i/i!$ (Eq. (4.2)). By Eqs. (4.8) and (4.9), we have

$$\begin{aligned} E(M_k) &= (E(N_1) + E(N_2)) \cdot e^{-\lambda}\sum_{i=0}^{k-1}\frac{\lambda^i}{i!} \\ &\le (4\lambda^2\ell^2 + 8\lambda\ell r)e^{-\lambda}\sum_{i=0}^{k-1}\frac{\lambda^i}{i!} \\ &= 4\lambda^2\ell^2(1+o(1)) \cdot e^{-\lambda}\sum_{i=0}^{k-1}\frac{\lambda^i}{i!}. \end{aligned} \tag{4.10}$$

Since $\lambda \to +\infty$ as $\ell \to +\infty$, by Eqs. (4.7) and (4.10) we have

$$p_3 \le 2\lambda^2\ell^2(1+o(1))e^{-\lambda}\sum_{i=0}^{k-1}\frac{\lambda^i}{i!} = 2\ell^2 e^{-\lambda}\frac{\lambda^{k+1}}{(k-1)!}(1+o(1)). \tag{4.11}$$

If $\lambda = \log\ell^2 + (k+1)\log\log\ell^2 + c(\ell)$, then $\lambda_1 \equiv \lambda - \log\ell^2 = (k+1)\log\log\ell^2 + c(\ell)$. By the reasoning at the beginning of the proof, we can assume $c(\ell) = o(\log\ell^2)$ as $\ell \to +\infty$, and hence $\lambda_1 = o(\log\ell^2)$. This gives $\lambda^{k+1} = (\log\ell^2)^{k+1}(1+o(1))$, and hence

$$p_3 \le \frac{2\lambda^{k+1}}{(\log\ell^2)^{k+1}e^{c(\ell)}(k-1)!}(1+o(1)) = \frac{2(1+o(1))}{e^{c(\ell)}(k-1)!}. \tag{4.12}$$

Since $c(\ell) \to +\infty$ as $\ell \to +\infty$, $p_3 \to 0$ as $\ell \to +\infty$. The first part is proved.

Now we prove that if $c(\ell) \leq C$ for some finite C as $\ell \to +\infty$, $P(V_k > 0) \geq \epsilon$ for $\epsilon = 1/(1+4e^C(k+1)!)$. Let I be the indicator function, by the Cauchy-Schwartz inequality, we have

$$\begin{aligned} E(V_k) &= E(V_k \cdot I(V_k > 0)) \leq \left(E(V_k^2)E(I^2(V_k > 0))\right)^{1/2} \\ &= \left(E(V_k^2)P(V_k > 0)\right)^{1/2}, \end{aligned} \tag{4.13}$$

and

$$P(V_k > 0) \geq \frac{(E(V_k))^2}{E(V_k^2)}. \tag{4.14}$$

The expression of $E(V_k)$ is given in Eq. (4.4), while the bound of $E(V_k^2)$ is given in the following lemma.

Lemma 4.3.1 *Let V_k be defined as in Eq. (4.3). Then,*

$$E(V_k^2) \leq (EV_k)^2 + 4k(k+1)\lambda^{-2}\ell^2 \left(e^{-\lambda}\sum_{i=0}^{k-1}\frac{\lambda^i}{i!}\right). \tag{4.15}$$

Proof: Refer to Appendix A.4 for a detailed account of proof. □.

Combining Eq. (4.14) and Lemma 4.3.1, we have

$$\begin{aligned} P(V_k > 0) &= \frac{(EV_k)^2}{E(V_k^2)} \geq \frac{(EV_k)^2}{(EV_k)^2 + 4k(k+1)\lambda^{-2}\ell^2\left(e^{-\lambda}\sum_{i=0}^{k-1}\frac{\lambda^i}{i!}\right)} \\ &\equiv \frac{1}{1+\beta}, \end{aligned} \tag{4.16}$$

where

$$\begin{aligned} \beta &\equiv \frac{4k(k+1)\lambda^{-2}\ell^2\left(e^{-\lambda}\sum_{i=0}^{k-1}\frac{\lambda^i}{i!}\right)}{(EV_k)^2} = \frac{4k(k+1)\lambda^{-2}\ell^2\left(e^{-\lambda}\sum_{i=0}^{k-1}\frac{\lambda^i}{i!}\right)}{\left(\ell^2 e^{-\lambda}\sum_{i=0}^{k-1}\frac{\lambda^i}{i!}\right)^2} \\ &= \frac{4k(k+1)\lambda^{-2}}{\ell^2 e^{-\lambda}\sum_{i=0}^{k-1}\frac{\lambda^i}{i!}} \leq \frac{4k(k+1)}{\ell^2 e^{-\lambda}\lambda^{k+1}/(k-1)!}. \end{aligned}$$

Let $\lambda_1 \equiv \lambda - \log\ell^2 = (k+1)\log\log\ell^2 + c(\ell)$. By the assumption $c(\ell) \leq C$, with sufficiently large ℓ, we have $\lambda_1 > 0$, and

$$\beta \leq \frac{4e^{c(\ell)}(\log\ell^2)^{k+1}(k+1)!}{(\log\ell^2 + \lambda_1)^{k+1}} \leq 4e^C(k+1)!. \tag{4.17}$$

It then follows from Eqs. (4.16) and (4.17) that

$$P(V_k > 0) \geq \frac{(EV_k)^2}{E(V_k^2)} \geq \frac{1}{1 + 4e^C(k+1)!}. \tag{4.18}$$

This completes the proof. □

Remark 1 If we let $c(\ell) \to -\infty$, and $\lambda = \log \ell^2 + (k+1)\log\log \ell^2 + c(\ell)$, we can conclude $P(V_k > 0) \to 1$ as $\ell \to +\infty$.

Remark 2 If we let $-(k+1)\log\log \ell^2 \leq c(\ell) \leq C$, then $P(V_k > 0) \geq 1/(1 + 4e^C(k+1)!)$ is true for any finite ℓ, since the second part of the proof does not require any asymptotic property in this case.

Remark 3 The terms "complete k-coverage" and "$V_k = 0$" have been used interchangeably, as it has been proved (for the case of $k = 1$) in [36] that the probability of their difference goes to 0 if the region is open and the coverage shape (e.g., the disk in this chapter) is closed. It has also been stated in [36] that the same conclusion holds for any regular region and shape. (The interested reader is referred to the discussions following Theorem 3.3 in [36]). The proof can also be extended to the case of any finite k.

With Theorem 4.3.1 and Remark 1, we reach the following corollary that associates the network lifetime with k-coverage.

Corollary 4.3.1 *If $\lambda = \log \ell^2 + (k+2)\log\log \ell^2 + c(\ell)$, and $c(\ell) \to -\infty$ as $\ell \to +\infty$, then the upper bound of the 1-lifetime is kT with probability approaching 1, where T is the lifetime of each sensor.*

Proof. In order to achieve a network lifetime longer than kT, it is necessary that the entire monitored region R is at least $(k+1)$-covered, i.e., $V_{k+1} = 0$. However, by Remark 1, if $\lambda = \log \ell^2 + (k+2)\log\log \ell^2 + c(\ell)$, and $c(\ell) \to -\infty$ as $\ell \to +\infty$, then $P(V_{k+1} > 0) \to 1$ as $\ell \to +\infty$, i.e., the lifetime cannot be longer than kT (with probability approaching one). Therefore, the 1-lifetime is upper bounded by kT with high probability. □

It is interesting to observe from Corollary 4.3.1 that the node density required to achieve a 1-lifetime of kT is not equal to k times the required density for asymptotic coverage. As a matter of fact, the former is much smaller than the latter. This trend will be confirmed again in the following sections.

In many cases, it may not be necessary to require $P(V_k > 0) \to 0$. One way of relaxing the requirement is to derive the density requirement for $E(V_k) \to 0$ as $\ell \to +\infty$. We give a tight lower bound for this in the following theorem.

Theorem 4.3.2 *Let $\lambda = \log \ell^2 + (k-1)\log\log \ell^2 + c(\ell)$. If $c(\ell) \to +\infty$ as $\ell \to +\infty$, then $E(V_k) \to 0$; if $c(\ell) \leq C < +\infty$, then $E(V_k) \geq e^{-C}/(k-1)!$ as $\ell \to +\infty$.*

Proof. Since $E(V_k)$ decreases as λ increases, we can assume $c(\ell) = o(\log\log\ell^2)$ in the first case ($\ell \to +\infty$) and $c(\ell) = C$ in the second case ($c(\ell) \leq C$). Thus in both cases we have $\lambda \to +\infty$ as $\ell \to +\infty$ and $\lambda^i = o(\lambda^{i+1})$. Let $\lambda_1 \equiv \lambda - \log\ell^2 = (k-1)\log\log\ell^2 + c(\ell)$. When ℓ is sufficiently large, we have $\lambda_1 > 0$ and $\lambda_1 = o(\log\ell^2)$. Therefore,

$$\begin{aligned}
E(V_k) &= \ell^2 \exp(-\lambda)\left(\sum_{i=0}^{k-1}\frac{\lambda^i}{i!}\right) \\
&= \ell^2 \exp(-\lambda)\left(\frac{\lambda^{(k-1)}}{(k-1)!}(1+o(1))\right) \\
&= \ell^2 \exp(-\lambda_1 - log\ell^2)\left(\frac{\lambda^{(k-1)}}{(k-1)!}(1+o(1))\right) \\
&= \exp(-\lambda_1)\left(\frac{\lambda^{(k-1)}}{(k-1)!}(1+o(1))\right) \\
&= \exp(-((k-1)\log\log\ell^2 + c(\ell)))\left(\frac{(\log\ell^2)^{k-1}(1+o(1))}{(k-1)!}(1+o(1))\right) \\
&= \exp(-c(\ell))\left(\frac{1+o(1)}{(k-1)!}\right). \qquad (4.19)
\end{aligned}$$

If $c(\ell) \to +\infty$ as $\ell \to +\infty$, we have $E(V_k) \to 0$ since k is finite. If $c(\ell) \leq C < +\infty$ as $\ell \to +\infty$, we have $E(V_k) \geq e^{-C}/(k-1)!$ as $\ell \to +\infty$. □.

Remark If we let $c(\ell) \to -\infty$, we have $E(V_k) \to +\infty$ as $\ell \to +\infty$.

4.3.2 Requirement on the sensing range in unit-area squares

Several researchers [36, 57] have studied the problem of maintaining asymptotic 1-coverage and k-connectivity on a unit-area disk. In this subsection, we adapt our results in Section 4.3.1 to a unit-area square, in order to make several comparisons. On a unit-area square, the sensing range of each node decreases as the density λ of the network increases. The question is how the sensing range r should scale as the density λ increases in order to ensure complete coverage with the probability approaching one. Our major result is as follows:

Theorem 4.3.3 *In a unit-area square, let $\lambda\pi r^2 = \log\lambda + k\log\log\lambda + c(\lambda)$. If $c(\lambda) \to +\infty$ as $\lambda \to \infty$, then $P(V_k > 0) \to 0$. If $c(\lambda) \leq C < +\infty$, then $P(V_k > 0) \geq \epsilon$ as $\ell \to +\infty$, where $\epsilon = 1/(1+4e^C(k+1)!)$.*

Proof of Theorem 4.3.3. Similar to the proof of Theorem 4.3.1, we can again assume that $c(\lambda) = o(\log\lambda)$ as $\lambda \to \infty$. We re-scale the unit-area square to a square with side length ℓ', such that the coverage disk of each node has a radius $r' = 1/\sqrt{\pi}$. Now if the node density in the unit-area square is λ, the node density in the rescaled network is $\lambda' = \lambda/\ell'^2$. Clearly, the radius and the side length have the same rescaling factor, and hence $\ell' = 1/(\sqrt{\pi}r)$. Table 4.1 gives the corresponding values in both the

Table 4.1: Corresponding values in the unit-area square (Theorem 3) and in the rescaled square.

Values in the unit-area square	Values in the rescaled square
r	$r' = 1/\sqrt{\pi}$
$\ell = 1$	$\ell' = 1/(\sqrt{\pi}r)$
λ	$\lambda' = \lambda/\ell'^2$

unit-area disk and the rescaled (larger) square.

By Theorem 4.3.1, if

$$\lambda' = \log \ell'^2 + (k+1)\log\log \ell'^2 + c'(\ell'), \tag{4.20}$$

then if $c'(\ell') \to +\infty$ as $\ell' \to +\infty$, then $P(V_k > 0) \to 0$; if $c'(\ell') \leq C < +\infty$, then $P(V_k > 0) \geq \epsilon$ as $\ell' \to +\infty$, where $\epsilon = 1/(1 + 4e^C(k+1)!)$. By Table 4.1, we can rewrite Eq. (4.20) as

$$\lambda\pi r^2 = \log \frac{1}{\pi r^2} + (k+1)\log\log \frac{1}{\pi r^2} + c'(\ell'). \tag{4.21}$$

We next show that if

$$\lambda\pi r^2 = \log\lambda + k\log\log\lambda + c(\lambda), \tag{4.22}$$

then as $\lambda \to \infty$, we have

$$(\log\lambda + k\log\log\lambda) - \left(\log \frac{1}{\pi r^2} + (k+1)\log\log \frac{1}{\pi r^2}\right) \to 0. \tag{4.23}$$

If Eq. (4.22) holds (and $c(\lambda) = o(\log\lambda)$ as $\lambda \to 0$), we have

$$\frac{1}{\pi r^2} = \frac{\lambda}{\log\lambda + k\log\log\lambda + c(\lambda)} = \frac{\lambda}{(\log\lambda)(1 + g(\lambda))}, \tag{4.24}$$

where $g(\lambda) \to 0$ as $\lambda \to \infty$, and thus

$$\begin{aligned} \log \frac{1}{\pi r^2} &= \log\lambda - (\log\log\lambda + \log(1 + g(\lambda))) \\ &= (\log\lambda)(1 + h(\lambda)), \end{aligned} \tag{4.25}$$

where $h(\lambda) \to 0$ as $\lambda \to \infty$.

Hence

$$\log\log\frac{1}{\pi r^2} \quad = \quad \log\log\lambda + \log(1+h(\lambda)). \tag{4.26}$$

Combining Eqs. (4.25) and (4.26), we obtain Eq. (4.23). As Eq. (4.22) and Eq. (4.21) differ only in a diminishing term (besides the last term in each equation), the proof is completed. □

Comparison against known results We are now in a position to make several comparisons between results derived so far and existing results in literature. First, in [36], it is shown that $0.05\min\{1,(1+\lambda^2\pi r^2)e^{-\lambda\pi r^2}\} < P(V_1>0) < 3\min\{1,(1+\lambda^2\pi r^2)e^{-\lambda\pi r^2}\}$. This is consistent with our result in the special case of $k=1$. Second, Penrose [57] show that in a network of n independent, uniformly distributed nodes, if r_k is the minimum radius for ensuring k-connectivity, then, $\lim_{n\to\infty} P[n\pi r_{k+1}^2 \le \log n + k\log\log n - \log k! + \alpha] = \exp(-e^{-\alpha})$. Our result shows that the minimum radius required for maintaining asymptotic k-coverage is approximately equal to that required for maintaining $(k+1)$-connectivity.

4.4 Asymptotic Upper Bound of 1-Lifetime without Torus Convention

As the 1-lifetime upper bound is determined by the coverage degree as discussed in the previous section, in this section, we focus on the density requirement in order to ensure k-coverage. The implication on the lifetime upper bound is obvious and therefore ignored.

As mentioned earlier, we assume the region R to be monitored is a square region with side length ℓ. The sensing range of each sensor $r = 1/\sqrt{\pi}$, so the sensing area is a unit-area disk. We assume each sensor has an independent probability $p < 1$ to be active and p may be either a constant or dependent on ℓ. We do not assume Torus convention and therefore, we consider the boundary effects in this section.

We consider sensor nodes are deployed according to one of the three models.

1. *Poisson process deployment:* the nodes form a Poisson point process with density D.
2. *uniformly random deployment:* n nodes are randomly, independently placed with uniform distributions. In this case, we define $D = n/\ell^2$.
3. *grid deployment:* $n = k^2$ nodes are regularly placed on $\sqrt{n}\times\sqrt{n}$ grids. In this case, we define $D = n/\ell^2$.

We assume (i) k is a finite constant value and (ii) most of the variables are functions (which may be constant) of ℓ, and investigate the asymptotic probability as $\ell \to \infty$. For two functions f and g, we denote $f = O(g)$ if $f(\ell) \leq Cg(\ell)$ for some constant $C > 0$ and sufficiently large ℓ, and similarly, $f = \Omega(g)$ if $f(\ell) \geq Cg(\ell)$. We denote $f = o(g)$ if $f(\ell)/g(\ell) \to 0$ as $\ell \to \infty$, and $f \sim g$ if $f(\ell)/g(\ell) \to 1$ as $\ell \to \infty$. Therefore, $f = o(1)$ means f goes to 0 as $\ell \to \infty$, and $f = (1 + o(1))g$ means $f \sim g$. We also denote $f \lesssim g$ if $f(\ell) \leq g(\ell)(1 + o(1))$ and $f \gtrsim g$ if $f(\ell) \geq g(\ell)(1 + o(1))$. Throughout the chapter, the logarithm is of the natural base.

We obtain the following results. Given D and p as defined above,

1. In the case that nodes are deployed according to a Poisson point process, Let $Dp = \log \ell^2 + 2k \log\log \ell^2 + c(\ell)$. As $\ell \to \infty$, if $c(\ell) \to \infty$, then the region R is k-covered with high probability, and if $c(\ell) \leq C$, then

$$\begin{aligned} & P(\text{region } R \text{ is } k\text{-covered}) \\ \leq \quad & 1 - \frac{1}{1 + 32e^{C/2}2^{k-2}(k+1)!/\sqrt{\pi}} < 1. \end{aligned} \tag{4.27}$$

2. In the case that nodes are deployed according to a uniformly random distribution, the results are identical to those in the case that nodes are deployed according to a Poisson point process.

3. In the case of grid deployment, assume $0 < p \leq 1 - \epsilon < 1$ for some constant ϵ. If $-D\log(1-p) = \log \ell^2 + 2k \log\log \ell^2 + 2\sqrt{-2\pi \log \ell^2 \log(1-p)} + c(\ell)$, and $c(\ell) \to \infty$ as $\ell \to \infty$, then the probability that the region R is k-covered tends to 1. If $-D\log(1-p) = \log \ell^2 + 2(k-1)\log\log \ell^2 - 2\sqrt{-2\pi \log \ell^2 \log(1-p)} - c(\ell)$, and $c(\ell) \to \infty$ as $\ell \to \infty$, then the probability that the region R is *not* k-covered tends to 1.

Now we show that using grid deployment requires asymptotically less or equal node density than using uniformly random deployment in all cases of $0 < p \leq 1 - \epsilon < 1$ for any positive constant ϵ $(0 < \epsilon < 1)$. If $p \geq \epsilon > 0$, since $p < -\log(1-p)$, the result follows immediately. If $p = O(\log^{-1} \ell)$, the extra term $2\sqrt{-2\pi \log \ell^2 \log(1-p)}$ in grid deployment is in the order of $\sqrt{p \log \ell^2}$ and bounded by a constant, so the result holds. In the last case, we consider $p \to 0$ but $p \log \ell^2 \to \infty$ as $\ell \to \infty$. By Taylor series expansion, we have $-\log(1-p) = p + \xi p^2$ for $p < \epsilon$ where $\xi > 0$ (since the second order derivative of $-\log(1-p)$ at $p = 0$ is $1 > 0$). Hence, the sufficient condition for grid deployment is

$$\begin{aligned} & Dp + \xi Dp^2 \\ = \; & \log \ell^2 + 2k \log\log \ell^2 + 2\sqrt{-2\pi \log \ell^2 \log(1-p)} + c(\ell). \end{aligned} \tag{4.28}$$

Since $Dp^2 \sim (\log \ell^2)p \to \infty$ and $(\log \ell^2)\log(1-p) \sim (\log \ell^2)p \to \infty$, $\xi Dp^2 >> 2\sqrt{-2\pi \log \ell^2 \log(1-p)}$. Therefore, the density requirement in grid deployment is again less than that in the uniformly random deployment.

4.4.1 Analysis in Poisson process deployment

In this model, the nodes form a Poisson point process with density D and each node is active independently with probability p. By the property of a Poisson point process, the active nodes form a Poisson point process with density $\lambda = Dp$. Therefore in this section, we simply consider a sensor network deployed as a Poisson point process with density λ and every node is active. In the following we establish a sufficient condition and a necessary condition for k-coverage in such a network. We denote $P(k\text{-coverage})$ as the probability that the monitored square region R is k-covered.

Sufficient condition

Theorem 4.4.1 *Let $Dp = \lambda = \log \ell^2 + 2k \log\log \ell^2 + c(\ell)$, where ℓ is the area of the monitored square region. If $c(\ell) \to \infty$ as $\ell \to \infty$, then $P(k\text{-coverage}) \to 1$.*

Before we delve into the proof, we would like to emphasize that the theorem does not require how fast $c(\ell)$ converges to infinity. The theorem is proved under the assumption that $c(\ell) = o(\log\log \ell^2)$ as $\ell \to \infty$. However, if it converges faster, the theorem still holds because $P(k\text{-coverage})$ is clearly an increasing function of λ and $c(\ell)$.

Proof. Let's first divide the area into small grids with side length $s = \sqrt{2}ur$ where $u = 1/(\log \ell^2)$. The area of each grid is s^2 and the number of grids is ℓ^2/s^2. Denote X_i as the indicator function of whether grid i is *not* completely k-covered (i.e., $X_i = 1$ if grid i is *not* completely k-covered and 0 otherwise). Let X denote the number of grids that are not completely k-covered. Therefore $X = \sum_i X_i$. The key idea is to show that as $\ell \to \infty$, $E[X] \to 0$, and therefore by Markov inequality, $P(X > 0) = P(X \geq 1) \leq E[X] \to 0$, and $P(k\text{-coverage}) = P(X = 0) = 1 - P(X > 0) \to 1$ as $\ell \to \infty$.

In order for a grid i to be completely k-covered, it is sufficient that there are at least k sensor nodes within a disk centered at the center of the grid and with radius $r - \frac{\sqrt{2}}{2}s = (1-u)r$, denoted as $B_i((1-u)r)$. Equivalently, if a grid i is not k-covered, then there are less than k nodes in the disk $B_i((1-u)r)$. Note that we assume sensor nodes are located only inside the monitored square region R, and thus we shall only be interested in the region of $B_i((1-u)r) \cap R$ and the nodes inside it. The area of the disk $B_i((1-u)r)$ is $(1-u)^2$.

We consider three types of grids: *inner grids*, *side grids* and *corner grids*, where inner grids are at least $r(= 1/\sqrt{\pi})$ distance away from any side of the square, side grids are at most r distance away from

one side of the square and at least r distance away from any other three sides, corner grids are at most r distance away from two adjacent sides.

Inner grids For an inner grid i, $B_i((1-u)r)$ (the area of which is $(1-u)^2$) is completely contained in the monitored square region, therefore,

$$\begin{aligned} E[X_i] &= P(\text{grid } i \text{ is not } k\text{-covered}) \\ &\leq P(\text{there are less than } k \text{ nodes inside } B_i((1-u)r)) \\ &= e^{-\lambda(1-u)^2} \sum_{i=0}^{k-1} \frac{(\lambda(1-u)^2)^i}{i!} \\ &= e^{-\lambda(1-u)^2} \frac{(\lambda(1-u)^2)^{k-1}}{(k-1)!} \cdot (1+o(1)), \end{aligned} \tag{4.29}$$

where the last equality holds because $\lambda \to \infty$ and $i < k$ is assumed to be bounded, and thus the last term in the summation dominates all other (finitely many) terms.

Since there are at most ℓ^2/s^2 inner grids, the expectation of total number, X^I, of un-k-covered[1] inner grids, is

$$\begin{aligned} E[X^I] &\leq \frac{\ell^2}{s^2} EX_i \\ &= \frac{\ell^2}{2u^2r^2} e^{-\lambda(1-u)^2} \frac{(\lambda(1-u)^2)^{k-1}}{(k-1)!} \cdot (1+o(1)) \\ &= \frac{\pi\ell^2}{2u^2} e^{-\lambda(1-u)^2} \frac{(\lambda(1-u)^2)^{k-1}}{(k-1)!} \cdot (1+o(1)), \end{aligned}$$

where the last equality holds because $\pi r^2 = 1$. We take the logarithm (with natural bases) on both sides, and obtain

$$\begin{aligned} \log E[X^I] \leq\ & \log \ell^2 + \log(\pi/2) - 2\log u - \lambda(1-u)^2 + \\ & (k-1)(\log\lambda + 2\log(1-u)) - \log(k-1)! + o(1). \end{aligned} \tag{4.30}$$

Since $u = 1/\log\ell^2 \to 0$ as $\ell \to \infty$, $\log(1-u) \sim -u \to 0$. By the assumption, $\lambda = \log\ell^2 + 2k\log\log\ell^2 + c(\ell)$. As $c(\ell) = o(\log\log\ell^2)$, $\log\lambda = \log\log\ell^2 + o(1)$. Plugging these results into Eq. (4.30), we obtain

$$\begin{aligned} \log E[X^I] \leq\ & (2u-u^2)\log\ell^2 + (k+1-2k(1-u)^2)\log\log\ell^2 \\ & -(1-u)^2 c(\ell) + \log(\pi/2) - \log((k-1)!) + o(1). \end{aligned}$$

Thus if $c(\ell) \to \infty$ (actually a weaker condition suffices in this case), $\log E[X^I] \to -\infty$ and $E[X^I] \to 0$.

[1] A grid is un-k-covered iff at least one point in it is covered by less than k nodes.

Side grids For a side grid, part of the disk that is centered at the grid center and with radius $(1-u)r$ is out of the monitored region. We need to estimate how much of the disk area is contained in the monitored square region. We assign each side grid a row index according to its distance to the side of the square region. The row closest to the side has index 0.

For a side grid g at row j, the distance from its center to the closest side is $x = (j + 1/2)s$. Denote $B_g(t)$ as the disk centered at the center of the grid g and with radius t. Let v denote the area of the part of disk $B_g(t)$ that is contained in the monitored square region (assuming the disk $B_g(t)$ only intersects one side of the square). The bound of v is given in the following lemma.

Lemma 4.4.1 *$(\pi t^2 + \pi xt)/2 \le v \le \pi t^2$, and $v \le \pi t^2/2 + 2xt$.*

The first inequality follows from the result on the area of $B_2 - B_1$ in Eq. (A.11) in Appendix A.4, where B_1 and B_2 are two intersecting disks. The second inequality is due to the fact that a partial disk area is certainly not larger than the area of the whole disk, πt^2. The third inequality can be obtained by simple geometric analysis: if we draw a rectangle with side length $2r$ and x, the rectangle will clearly contain the intersection of R and the half disk that intersects with one side of the region R. We point out that a less stringent result $v \ge (\pi t^2 + 2xt)/2$ (for the first inequality) also suffices for the following proof. Since we are considering a disk centered at the center of a grid at row j with radius $r(1-u)$, the area of the part of disk that is inside the square region is

$$\begin{aligned} v &\ge \frac{\pi r^2(1-u)^2 + \pi r(1-u)(j+1/2)s}{2} \\ &\ge \frac{(1-u)^2 + j\sqrt{2}u(1-u)}{2} \end{aligned} \tag{4.31}$$

since $s = \sqrt{2}ur$ and $\pi r^2 = 1$. If a side grid g at row j is not k-covered, then there are less than k nodes in $B_g(r(1-u)) \cap R$ Therefore (note $\sum_{i=0}^{k-1} e^{-x}\frac{x^i}{i!}$ is a decreasing function of x),

$$\begin{aligned} &P(\text{a side grid at row } j \text{ is not } k\text{-covered}) \\ &\le \sum_{i=0}^{k-1} e^{-\lambda\frac{(1-u)^2+j\sqrt{2}u(1-u)}{2}} \frac{(\lambda((1-u)^2 + j\sqrt{2}u(1-u))/2)^i}{i!} \\ &= e^{-\lambda\frac{(1-u)^2+j\sqrt{2}u(1-u)}{2}} \frac{(\lambda((1-u)^2 + j\sqrt{2}u(1-u))/2)^{k-1}}{(k-1)!} \cdot (1+o(1)) \\ &\le e^{-\lambda\frac{(1-u)^2+j\sqrt{2}u(1-u)}{2}} \frac{(\lambda(1-u)^2)^{k-1}}{(k-1)!} \cdot (1+o(1)). \end{aligned} \tag{4.32}$$

Since there are four side regions in the square and at most r/s rows in each side region and at most ℓ/s grids in each row of a side region, the expectation of the number X^S of the side grids that are not

k-covered can be written as

$$\begin{aligned} E[X^S] &= \frac{4\ell}{s}\sum_{j=0}^{r/s} P(\text{a grid at row } j \text{ is not } k\text{-covered}) \\ &\le \frac{4\ell}{s}\sum_{j=0}^{r/s} e^{-\lambda\frac{(1-u)^2+j\sqrt{2}u(1-u)}{2}}\frac{(\lambda(1-u)^2)^{k-1}}{(k-1)!}\cdot(1+o(1)) \\ &\le \frac{4\ell}{s}e^{-\lambda\frac{(1-u)^2}{2}}\frac{(\lambda(1-u)^2)^{k-1}}{(k-1)!}\cdot\frac{1+o(1)}{1-e^{-\lambda\sqrt{2}u(1-u)/2}}. \end{aligned}$$

Again, we take the logarithm on both sides, and obtain (notice $s=\sqrt{2}ur=\sqrt{2/\pi}/\log\ell^2$)

$$\begin{aligned} \log E[X^S] \le\ & \log 4+\frac{1}{2}\log\ell^2+\frac{1}{2}\log(\pi/2)+\log\log\ell^2-\lambda\frac{(1-u)^2}{2} \\ & +(k-1)(\log\lambda+2\log(1-u))-\log((k-1)!)-\log(1-e^{-\lambda\sqrt{2}u(1-u)/2})+o(1). \end{aligned}$$

Since $\lambda=\log\ell^2+2k\log\log\ell^2+c(\ell))$ and $c(\ell)=o(\log\log\ell^2)$, we have $\log\lambda=\log\log\ell^2+o(1)$. Therefore,

$$\begin{aligned} \log E[X^S] \le\ & \frac{2u-u^2}{2}(\log\ell^2+2k\log\log\ell^2)-\frac{(1-u)^2}{2}c(\ell)+\frac{1}{2}\log(8\pi) \\ & +2(k-1)\log(1-u)-\log((k-1)!)-\log(1-e^{-\lambda\sqrt{2}u(1-u)/2})+o(1). \end{aligned}$$

Since k is assumed to be a fixed integer and $u=1/\log\ell^2$, as $\ell\to\infty$, most of the terms converge to a finite value except $-\frac{(1-u)^2}{2}c(\ell)$ which converges to $-\infty$. Therefore, $E[X^S]\to 0$ as $\ell\to\infty$.

Corner grids For a corner grid, if we draw a disk centered at the center of the grid and with radius $r(1-u)$, at least a quarter of the disk is inside the monitored square region. Therefore,

$$\begin{aligned} & P(\text{a corner grid is not } k\text{-covered}) \\ \le\ & \sum_{i=0}^{k-1}\frac{e^{-\lambda(1-u)^2/4}(\lambda(1-u)^2/4)^i}{i!} \\ =\ & \frac{e^{-\lambda(1-u)^2/4}(\lambda(1-u)^2/4)^{k-1}}{(k-1)!}(1+o(1)). \end{aligned} \tag{4.33}$$

The number of corner grids is $4\frac{r^2}{s^2}=\frac{2}{u^2}$. Hence, the expectation of the number X^C of the corner grids that are not k-covered is

$$E[X^C]\le\frac{2}{u^2}e^{-\lambda(1-u)^2/4}\frac{(\lambda(1-u)^2/4)^{k-1}}{(k-1)!}(1+o(1)). \tag{4.34}$$

Since $1/u=\log\ell^2$ is in the same order of λ, $E[X^C]\to 0$ as long as $\lambda\to\infty$.

Based on the analysis on the three types of grids, we conclude that the expectation of the total number

of un-k-covered grids $X = X^I + X^S + X^C$ converges to 0 as the side length $\ell \to \infty$ if λ is given as in the theorem. The theorem is thus proved. □

Necessary condition

Let the k-vacancy V_k denote the area of the region that is covered by less than k nodes, and $\chi_k(Z)$ denote the indicator function of whether a point Z is covered by less than k nodes, i.e.,

$$\chi_k(Z) = \begin{cases} 1, & \text{if less than } k \text{ nodes cover the point } Z; \\ 0, & \text{otherwise.} \end{cases} \tag{4.35}$$

To derive the necessary condition for k-coverage, we first derive the bounds on $E[V_k]$ and $E[V_k^2]$.

Proposition 4.4.1 *If $Dp = \lambda = \log \ell^2 + 2k \log\log \ell^2 + C$, where C is a constant, then*

$$E[V_k](\log \ell^2)^2 \geq \frac{\sqrt{\pi}}{e^{C/2} 2^{k-2}(k-1)!},$$

as $\ell \to \infty$.

Proof. Since we are interested in deriving a lower bound, we only consider the k-vacancy in the side area of the square, i.e., those locations which are at most r distance away from one side and at least r distance away from all other sides. Without loss of generality, we consider a point Z in the side area with coordinate (x, y), where $0 \leq x \leq r, r \leq y \leq \ell - r$. Now the expectation of the k-vacancy indicator function $\chi_k((x, y))$ is

$$\begin{aligned} & E[\chi_k((x,y))] \\ &= P((x,y) \text{ is not } k\text{-covered}) \\ &= P(B_{(x,y)}(r) \cap R \text{ contains less than } k \text{ nodes}), \end{aligned} \tag{4.36}$$

where $B_{(x,y)}(r)$ denotes the disk centered at (x, y) with radius r. Since the area of $B_{(x,y)}(r) \cap R$ is not larger than $\frac{1}{2} + 2xr$ by Lemma 4.4.1,

$$\begin{aligned} E[\chi_k((x,y))] &\geq e^{-\lambda(1/2+2xr)} \sum_{i=0}^{k-1} \frac{(\lambda(1/2+2xr))^i}{i!} \\ &\geq e^{-\lambda(1/2+2xr)} \sum_{i=0}^{k-1} \frac{(\lambda/2)^i}{i!}. \end{aligned} \tag{4.37}$$

Since there are four side regions in the square,

$$\begin{aligned} E[V_k] &\geq 4\int_0^r \int_r^{\ell-r} E[\chi_k(x,y)]dydx \qquad (4.38)\\ &\geq 4\int_0^r \int_r^{\ell-r} e^{-\lambda(1/2+2xr)} \sum_{i=0}^{k-1} \frac{(\lambda/2)^i}{i!} \\ &= 4(\ell-2r)\sum_{i=0}^{k-1} \frac{(\lambda/2)^i}{i!} e^{-\lambda/2} \frac{1-e^{-2\lambda r^2}}{2\lambda r} \\ &\geq 4(\ell-2r)\frac{(\lambda/2)^{k-1}}{(k-1)!} e^{-\lambda/2} \frac{1-e^{-2\lambda/\pi}}{2\lambda r}. \qquad (4.39) \end{aligned}$$

We take logarithm on both sides. Since $\log(\ell-2r) = \frac{1}{2}\log\ell^2 + o(1)$, $\lambda = \log\ell^2 + 2k\log\log\ell^2 + C$, and $\log\lambda = \log\log\ell^2 + o(1)$, we have

$$\begin{aligned} &\log E[V_k] \\ &\geq \log 4 + \frac{1}{2}\log\ell^2 + (k-1)\log(\lambda/2) - \log((k-1)!) \\ &\quad -\frac{\lambda}{2} + \log(1-e^{-2\lambda/\pi}) - \log\lambda - \log(2r) + o(1) \\ &= -2\log\log\ell^2 - \frac{C}{2} - \log((k-1)!) - (k-2)\log 2 \\ &\quad + \log\sqrt{\pi} + \log(1-e^{-2\lambda/\pi}) + o(1). \qquad (4.40) \end{aligned}$$

As $\ell\to\infty$, $\lambda\to\infty$, so $\log(1-e^{-2\lambda/\pi})\to 0$. Therefore,

$$E[V_k](\log\ell^2)^2 \geq \frac{\sqrt{\pi}}{e^{C/2}2^{k-2}(k-1)!} \qquad (4.41)$$

as $\ell\to\infty$. □

Proposition 4.4.2 *If $\lambda = \log\ell^2 + 2k\log\log\ell^2 + C$, where C is a constant, then*

$$\frac{E[V_k^2]}{E[V_k]^2} \leq 1 + \frac{32k(k+1)}{\lambda^2 E[V_k]}, \qquad (4.42)$$

as $\ell\to\infty$.

Proof. Several results derived in Appendix A.4 will be utilized here, and they are summarized in the following lemmas for the ease of understanding.

Lemma 4.4.2

$$E[V_k^2] \leq E[V_k]^2 + \int\int_{R^2\cap\{|Z_1-Z_2|\leq 2r\}} E[\chi_k(Z_1)\chi_k(Z_2)]dZ_1dZ_2 \qquad (4.43)$$

Lemma 4.4.3 *Let B_1 and B_2 denote the disks with radius r, centered at Z_1 and Z_2, respectively. If $|Z_1 - Z_2| = x \leq 2r$, then the area of $B_2 - B_1$ is*

$$||B_2 - B_1|| \geq x/(2r). \tag{4.44}$$

Lemma 4.4.4

$$\int_0^\infty e^{-\lambda u} \sum_{i=0}^{k-1} \frac{(\lambda u)^i}{i!} \cdot u du = \frac{1}{2} k(k+1)\lambda^{-2}. \tag{4.45}$$

Lemma 4.4.2 follows from Eqs. (A.5) and (A.6). Lemma 4.4.3 follows from Eq. (A.11). Lemma 4.4.4 follows from Eq. (A.14).

The challenge when we consider the boundary conditions is that now the area of $(B_2 - B_1) \cap R$ may be zero if B_2 is close to the boundary. We overcome this difficulty by exploiting the symmetric relation between Z_1 and Z_2. Let $Z_1 = (x_1, y_1), Z_2 = (x_2, y_2)$, and the ∞-norm distance $d_\infty(Z_1, Z_2)$ of the two points Z_1, Z_2 be denoted as

$$d_\infty(Z_1, Z_2) = \max(|x_1 - x_2|, |y_1 - y_2|). \tag{4.46}$$

Denote the center of the square region as O. Consider the event $Q = \{d_\infty(Z_1, O) \geq d_\infty(Z_2, O)\}$. Intuitively, if we draw a square centered at O and the boundary of the square goes through Z_1, then Q is the event that Z_2 is inside this square. For each pair of points $(Z_1, Z_2) \notin Q$, there is a unique pair of symmetric points $(Z_1', Z_2')(= (Z_2, Z_1)) \in Q$, and these two pairs of points contribute exactly the same to the integral in Eq. (4.43). Therefore, the second term in Eq. (4.43), denoted as I_0, can be written as

$$\begin{aligned} I_0 &\triangleq \int\int_{R^2 \cap \{|Z_1 - Z_2| \leq 2r\}} E[\chi_k(Z_1)\chi_k(Z_2)] dZ_1 dZ_2 \\ &= 2 \int\int_{R^2 \cap \{|Z_1 - Z_2| \leq 2r\} \cap Q} E[\chi_k(Z_1)\chi_k(Z_2)] dZ_1 dZ_2. \end{aligned} \tag{4.47}$$

We define the central, side, corner regions similar to those in Section 4.4.1. We further define the extended corner region C_E as those points which are within distance r from one side and within distance $3r$ from another side. We consider two possible cases: (i) $Z_1 \in C_E$ and (ii) $Z_1 \notin C_E$.

Case (i): $Z_1 \in C_E$

$$\begin{aligned}
&\int\int_{R^2\cap\{|Z_1-Z_2|\le 2r\}\cap Q\cap\{Z_1\in C_E\}} E[\chi_k(Z_1)\chi_k(Z_2)]dZ_1dZ_2 \\
&\le \int\int_{R^2\cap\{|Z_1-Z_2|\le 2r\}\cap Q\cap\{Z_1\in C_E\}} E[\chi_k(Z_1)]dZ_1dZ_2 \\
&\le 20r^2\cdot\pi(2r)^2\cdot e^{-\lambda/4}\sum_{i=0}^{k-1}\frac{(\lambda/4)^i}{i!} \\
&= \frac{80}{\pi}e^{-\lambda/4}\sum_{i=0}^{k-1}\frac{(\lambda/4)^i}{i!}, \qquad (4.48)
\end{aligned}$$

where in the third equation, $20r^2$ is the total area of C_E, $\pi(2r)^2$ is the maximum possible area of Z_2 for a given point Z_1, and the last factor is an upper bound of $E[\chi_k(Z_1)]$, since at least a quarter of the disk $B_{Z_1}(r)$ is inside the monitored region R.

Case (ii): $Z_1 \notin C_E$ If Z_1 is not in the extended corner, Z_2 is within distance $2r$ from Z_1, and Z_2 is inside the square centered at O whose boundary passes through Z_1, then Z_2 cannot be in the corner area, and moreover, at least half of the area $B_2 - B_1$ is inside the region R. This is the key to the proof. Now for any given $Z_1 \notin C_E$, let $Z_2 \in R^2 \cap \{|Z_1 - Z_2| \le 2r\} \cap Q$, and $x = |Z_1 - Z_2| \le 2r$. By lemma 4.4.3, the area of $(B_2 - B_1) \cap R$ is at least $x/(4r)$. Therefore,

$$\begin{aligned}
E[\chi_k(Z_1)\chi_k(Z_2)] &= P(\text{there are less than } k \text{ nodes in } B_1\cap R \\
&\quad \text{and there are less than } k \text{ nodes in } B_2\cap R) \\
&\le P(\text{there are less than } k \text{ nodes in } B_1\cap R \\
&\quad \text{and there are less than } k \text{ nodes in } (B_2-B_1)\cap R) \\
&\le P(\text{there are less than } k \text{ nodes in } B_1\cap R) \\
&\quad \cdot P(\text{there are less than } k \text{ nodes in } (B_2-B_1)\cap R) \\
&\le E(\chi_k(Z_1))\cdot e^{-\lambda x/(4r)}\sum_{i=0}^{k-1}\frac{(\lambda x/(4r))^i}{i!}, \qquad (4.49)
\end{aligned}$$

where the third equation results from that the number of nodes in $B_1 \cap R$ and that in $B_2 - B_1 \cap R$ are independent. Thus,

$$\begin{aligned}
&\int\int_{R^2\cap\{|Z_1-Z_2|\le 2r\}\cap Q\cap\{Z_1\notin C_E\}} E[\chi_k(Z_1)\chi_k(Z_2)]dZ_1dZ_2 \\
&\le \int_R E[\chi_k(Z_1)]dZ_1\int_0^{2r} e^{-\lambda x/(4r)}\sum_{i=0}^{k-1}\frac{(\lambda x/(4r))^i}{i!}2\pi x dx, \\
&= \int_R E[\chi_k(Z_1)]dZ_1\int_0^{1/2} e^{-\lambda u}\sum_{i=0}^{k-1}\frac{(\lambda u)^i}{i!}32u du,
\end{aligned}$$

$$\begin{aligned} &\leq E[V_k] \cdot \int_0^\infty e^{-\lambda u} \sum_{i=0}^{k-1} \frac{(\lambda u)^i}{i!} 32u du, \\ &= E[V_k] \cdot 16k(k+1)\lambda^{-2}, \end{aligned} \tag{4.50}$$

where the factor $2\pi x$ in the second equation comes from the conversion from a Cartesian coordinate system to a polar coordinate system, the third equation is obtained by changing variable $u = x/(4r)$, and the last equation comes from Lemma 4.4.4.

Note that the value in case (i), which converges to 0 in the exponential rate of λ, is dominated by the value in case (ii), which converges to 0 in the polynomial rate of λ (since $E[V_k]$ is in the same order of λ^{-2} from Proposition 4.4.1). Combining the results in the above two cases, as well as Eqs. (4.43) and (4.47), we obtain Eq. (4.42). □

It has been proved in Section 4.3 using Cauchy-Schwartz inequality,

$$P(V_k > 0) \geq \frac{E[V_k]^2}{E[V_k^2]}. \tag{4.51}$$

By Proposition 4.4.2, we have

$$P(V_k > 0) \quad \geq \quad \frac{1}{1 + 32k(k+1)/(\lambda^2 E[V_k])}. \tag{4.52}$$

By Proposition 4.4.1,

$$E[V_k](\log \ell^2)^2 \geq \frac{\sqrt{\pi}}{e^{C/2} 2^{k-2}(k-1)!}, \tag{4.53}$$

and $\lambda = (1 + o(1)) \log \ell^2$,

$$P(V_k > 0) \quad \geq \quad \frac{1}{1 + 32e^{C/2} 2^{k-2}(k+1)!/\sqrt{\pi}}, \tag{4.54}$$

as $\ell \to \infty$.

Based on the above derivation, we can establish the following necessary condition for k-coverage, which also leads to a sufficient condition on un-k-coverage.

Theorem 4.4.2 *Let $\lambda = \log \ell^2 + 2k \log\log \ell^2 + c(\ell)$. If $c(\ell) \leq C$, where C is a constant, then, as $\ell \to \infty$,*

$$P(\textit{the monitored square region } R \textit{ is } k\textit{-covered}) \leq 1 - \frac{1}{1 + 32e^{C/2} 2^{k-2}(k+1)!/\sqrt{\pi}} < 1. \tag{4.55}$$

In addition, if $c(\ell) \to -\infty$, P(the monitored square region is k-covered) tends to 0.

Proof. The proof follows from two observations. First, the fact that the region is k-covered implies $V_k = 0$. Therefore, $P(\text{the region is } k\text{-covered}) \leq P(V_k = 0) = 1 - P(V_k > 0)$. Second, $P(V_k > 0)$ is a non-increasing function of λ. Since we have proved the conclusion holds for $c(\ell) = C$, it also holds for $c(\ell) \leq C$. The second part of the theorem is obtained by letting $C \to -\infty$. □

4.4.2 Analysis in uniformly random deployment

In this model, we assume there are n nodes in the square region R with side length ℓ and each node's location is identically, independently distributed according to a uniformly random distribution. Each node has an independent probability p to be active. In this section we establish a sufficient and a necessary condition for k-coverage under such a model.

Sufficient condition

Theorem 4.4.3 *Under the uniform distribution model, let $np/\ell^2 = \log \ell^2 + 2k \log\log \ell^2 + c(\ell)$, where ℓ is the side length of the deployment square region R. If $c(\ell) \to \infty$, as $\ell \to \infty$, then $P(\text{the region } R \text{ is } k\text{-covered}) \to 1$.*

Proof. We still divide the area into small grids with side length $s = \sqrt{2}ur$ where $u = 1/\log \ell^2$. Let X_i denote the indicator function of whether a grid is *not* k-covered and X the total number of the un-k-covered grids (recall a grid is un-k-covered iff it is not completely k-covered). Again we proceed to compute the expectation of the number of grids that are not k-covered in the three types of regions: *inner* grids, *side* grids, and *corner* grids, respectively.

Inner grids For an inner grid i to be k-covered, it is sufficient that there are k active nodes inside the disk $B_i((1-u)r)$ (since the whole disk is in the region R). Let p_1 denote the probability that a node is inside $B_i((1-u)r)$ and active, i.e., $p_1 = p\pi((1-u)r)^2/\ell^2 = p(1-u)^2/\ell^2$. The number of active nodes inside the disk $B_i((1-u)r)$ follows a binomial distribution with parameter n and p_1. If an inner grid i is not k-covered, the number of active nodes inside the disk $B_i((1-u)r)$ is less than k. Hence,

$$E[X_i] \quad = \quad P(\text{grid } i \text{ is not } k\text{-covered}) \leq \sum_{i=0}^{k-1} \binom{n}{i} p_1^i (1-p_1)^{n-i}.$$

Again, since $n/\ell^2 \to \infty$ as $\ell \to \infty$, the term with $i = k-1$ dominates all others. Also since $\binom{n}{i} \leq n^i/i!$ and $(1-p_1)^{n-i} \leq e^{-p_1(n-i)}$,

$$E[X_i] \quad \leq \quad \binom{n}{k-1} p_1^{k-1} (1-p_1)^{n-k+1} (1+o(1))$$

$$\begin{aligned} &\leq \frac{(np_1)^{k-1}}{(k-1)!}e^{-p_1(n-k+1)}(1+o(1)) \\ &= \frac{(np(1-u)^2/\ell^2)^{k-1}}{(k-1)!}e^{-(n-k+1)p(1-u)^2/\ell^2}(1+o(1)). \end{aligned}$$

If we replace np/ℓ^2 with λ, the above equation is identical to Eq. (4.29) except for a factor $e^{(k-1)p(1-u)^2/\ell^2)}$, which converges to 1 as $\ell \to \infty$. Therefore, by following the same derivation in Section 4.4.1, we can obtain the expectation of the number X^I of the un-k-covered inner grids converges to 0 as $\ell \to \infty$ and $c(\ell) \to \infty$.

Corner grids For a corner grid, if we draw a disk centered at the center of the grid, and with radius $(1-u)r$, at least a quarter of the disk is inside the region R. If the corner grid is not k-covered, then it is necessary that the quarter of the disk that is inside the region R has less than k active nodes. Again, the number of the active nodes inside the quarter of the disk is a binomial random variable with parameter n and $p_2 = p(\frac{1}{4}\pi r^2(1-u)^2)/\ell^2 = p(1-u)^2/(4\ell^2)$. Therefore,

$$\begin{aligned} &P(\text{a corner grid is not } k\text{-covered}) \\ &\leq \sum_{i=0}^{k-1}\binom{n}{i}p_2^i(1-p_2)^{n-i} \\ &= (1+o(1))\binom{n}{k-1}p_2^{k-1}(1-p_2)^{n-k+1} \\ &\leq (1+o(1))\frac{(np_2)^{k-1}}{(k-1)!}e^{-p_2(n-k+1)}. \end{aligned}$$

The number of corner grids is at most $4r^2/s^2 = 2/u^2$ since there are 4 corners. Therefore, the expectation of the number X^C of the corner grids that are not k-covered is

$$E[X^C] \leq \frac{2}{u^2}\frac{(np_2)^{k-1}}{(k-1)!}e^{-p_2(n-k+1)}(1+o(1)). \tag{4.56}$$

Since $u = 1/\log\ell^2$, and $np_2 = np(1-u)^2/(4\ell^2) \to \infty$, it is not hard to verify that $E[X^C] \to 0$ as $\ell \to \infty$ and $c(\ell) \to \infty$.

Side grids Now consider a side grid at row j (row zero is the one closest to the boundary of the square region). Again, if we draw a disk centered at the center of the grid and with radius $r(1-u)^2$, the area of the disk that falls in the square region R is at least $((1-u)^2 + j\sqrt{2}u(1-u))/2$ by Eq. (4.31). The probability that a node falls in this area and is active is $p_3 = p((1-u)^2 + j\sqrt{2}u(1-u))/(2\ell^2)$, and the number of the active nodes in this area follows a binomial distribution with parameter n and p_3.

Therefore, we have

$$\begin{aligned}
&P(\text{a side grid at row } j \text{ is not } k\text{-covered}) \\
&\leq \sum_i \binom{n}{i} p_3^i (1-p_3)^{n-i} \\
&\leq \binom{n}{k-1} p_3^{k-1}(1-p_3)^{n-k+1}(1+o(1)) \\
&\leq \frac{n^{k-1}}{(k-1)!}\left(\frac{p((1-u)^2+j\sqrt{2}u(1-u))}{2\ell^2}\right)^{k-1} \\
&\quad \cdot e^{-(n-k+1)p((1-u)^2+j\sqrt{2}u(1-u))/(2\ell^2)}(1+o(1)) \\
&\leq \frac{(np(1-u)^2/\ell^2)^{k-1}}{(k-1)!} e^{-np((1-u)^2+j\sqrt{2}u(1-u))/(2\ell^2)} \\
&\quad \cdot e^{(k-1)p((1-u)^2+j\sqrt{2}u(1-u))/(2\ell^2)}(1+o(1)). \qquad (4.57)
\end{aligned}$$

Since $e^{(k-1)p((1-u)^2+j\sqrt{2}u(1-u))/(2\ell^2)}$ converges to 1 as $\ell \to \infty$, the remaining factors are identical to Eq. (4.32) if we replace np/ℓ^2 with λ. Since we have chosen the same value of np/ℓ^2 as that of λ in Section 4.4.1, we have obtained the same upper bound of P(a grid at row j is not k-covered) as that in Eq. (4.32). Therefore, following the same derivation as that in Section 4.4.1, we have $E[X^S] \to 0$ (where X^S is the number of un-k-covered side grids) as $\ell \to \infty$ and $c(\ell) \to \infty$. Therefore, the expectation of the total number of un-k-covered grids tends to 0 and P(the region R is k-covered) $\to 1$ as $\ell \to \infty$. □

Necessary condition

The necessary condition for uniformly random deployment is obtained by approximating the uniformly random node distribution with a Poisson point process. In this section, we use $E_U[Y]$ and $E_P[Y]$ to denote the expectation of the quantity Y in uniformly random deployment and that in Poisson process deployment. In particular, we shall show $E_U[V_k] \sim E_P[V_k]$ and $E_U[V_k^2] \sim E_P[V_k^2]$ with appropriately chosen n, ℓ, p in the uniformly random node distribution and the node density λ in Poisson process deployment.

Proposition 4.4.3 *If $np/\ell^2 = \lambda = \log \ell^2 + 2k \log\log \ell^2 + C$, where C is a constant, then*

$$E_U[V_k](\log \ell^2)^2 \geq \frac{\sqrt{\pi}}{e^{C/2}2^{k-2}(k-1)!} \qquad (4.58)$$

Proof. Let $\chi_k((x,y))$ denote the indicator function of whether a point (x,y) is covered by less than k nodes. Again, we only consider the case that (x,y) is in the side area of the square to obtain a lower bound. Without loss of generality, we assume $0 \leq x \leq r, r \leq y \leq \ell - r$. Thus the disk $B_{(x,y)}(r)$ has at most area $\frac{1}{2} + 2xr$ inside the square region R. Denote $p_1 \triangleq p(\frac{1}{2} + 2xr)/\ell^2$ as the probability that one

node falls in a region with area $\frac{1}{2} + 2xr$ and is active. Therefore,

$$\begin{aligned} E_U[\chi_k((x,y))] &= P((x,y) \text{ is not } k\text{-covered}) \\ &= P(B_{(x,y)}(r) \cap R \text{ contains less than } k \text{ active nodes}) \\ &\geq \sum_{i=0}^{k-1} \binom{n}{i} p_1^i (1-p_1)^{n-i} \\ &\sim \sum_{i=0}^{k-1} \frac{n^i}{i!} \left(\frac{p(\frac{1}{2}+2xr)}{\ell^2} \right)^i e^{(n-i)\log(1-p_1)} \\ &= \sum_{i=0}^{k-1} \frac{(\lambda(\frac{1}{2}+2xr))^i}{i!} e^{(n-i)\log(1-p_1)}. \end{aligned} \tag{4.59}$$

Since $i < k$ is bounded, $np/\ell^2 = \lambda$, $np_1 = \lambda(\frac{1}{2} + 2xr)$, and $p_1 = p(\frac{1}{2} + 2xr)/\ell^2 < 2/\ell^2 \to 0$ as $\ell \to \infty$, we have

$$\begin{aligned} (n-i)\log(1-p_1) &= (n-i)(-p_1 + O(p_1^2)) \\ &= -np_1 + O(np_1^2) + i(p_1 - O(p_1^2)). \end{aligned} \tag{4.60}$$

As $\ell \to \infty$, $np_1^2 = \lambda(\frac{1}{2} + 2xr)p_1 \lesssim (\frac{1}{2} + 2xr)(\log \ell^2)2/\ell^2 \to 0$, and $i(p_1 - O(p_1^2)) \to 0$. Therefore, by Eq. (4.60),

$$e^{(n-i)\log(1-p_1)} \sim e^{-np_1} = e^{-\lambda(\frac{1}{2}+2xr)}. \tag{4.61}$$

Plugging Eq. (4.61) into Eq. (4.59), we have

$$\begin{aligned} E_U[\chi_k((x,y))] &\geq \sum_{i=0}^{k-1} \frac{(\lambda(\frac{1}{2}+2xr))^i}{i!} e^{-\lambda(\frac{1}{2}+2xr)}(1+o(1)) \\ &\geq e^{-\lambda(\frac{1}{2}+2xr)} \sum_{i=0}^{k-1} \frac{(\lambda/2)^i}{i!}(1+o(1)). \end{aligned} \tag{4.62}$$

Comparing Eqs. (4.37) and (4.38), we can easily obtain

$$E_U[V_k](\log \ell^2)^2 \geq \frac{\sqrt{\pi}}{e^{C/2} 2^{k-2}(k-1)!}, \tag{4.63}$$

as $\ell \to \infty$. □

Proposition 4.4.4 *If $np/\ell^2 = \lambda = \log \ell^2 + 2k \log\log \ell^2 + C$, where C is a constant, then*

$$\frac{E[V_k^2]}{(E[V_k])^2} \leq 1 + \frac{32k(k+1)}{\lambda^2 E[V_k]}, \tag{4.64}$$

as $\ell \to \infty$.

Proof. Let $\chi_k(Z_1)$ denote the indicator function of whether a point Z_1 is not k-covered. We have $V_k = \int_R \chi_k(Z_1)dZ_1$. Therefore,

$$\begin{aligned} E_U[V_k^2] &= E_U\left[\int_R \int_R \chi_k(Z_1)\chi_k(Z_2)dZ_1dZ_2\right] \\ &= \int_R \int_R E[\chi_k(Z_1)\chi_k(Z_2)]dZ_1dZ_2 \end{aligned} \tag{4.65}$$

We still consider two cases in the integration. In the first case, $|Z_1 - Z_2| > 2r$,

$$E_U[\chi_k(Z_1)\chi_k(Z_2)] = \sum_{i=0}^{k-1}\sum_{j=0}^{k-1}\binom{n}{i,j}p_1^i p_2^j(1-p_1-p_2)^{n-i-j}, \tag{4.66}$$

where p_1 and p_2 are the probability that a node is active and falls in an area within range r from Z_1 and Z_2, respectively. Note that

$$\begin{aligned} &E_U[\chi_k(Z_1)]E_U[\chi_k(Z_2)] \\ &= \sum_{i=0}^{k-1}\binom{n}{i}p_1^i(1-p_1)^{n-i}\sum_{j=0}^{k-1}\binom{n}{j}p_2^j(1-p_2)^{n-j} \\ &= \sum_{i=0}^{k-1}\sum_{j=0}^{k-1}\binom{n}{i}\binom{n}{j}p_1^i p_2^j(1-p_1)^{n-i}(1-p_2)^{n-j}. \end{aligned} \tag{4.67}$$

Since $1/(4\ell^2) \le p_1, p_2 \le 1/\ell^2$, $np \sim \ell^2 \log \ell^2$, and $i, j < k$ is bounded, we have

$$(1-p_1-p_2)^{n-i-j} \sim (1-p_1)^{n-i}(1-p_2)^{n-j}, \tag{4.68}$$

and

$$\binom{n}{i,j} = \frac{n!}{i!j!(n-i-j)!} \sim \frac{n!n!}{i!(n-i)!j!(n-j)!} = \binom{n}{i}\binom{n}{j}.$$

Hence, in the case of $|Z_1 - Z_2| > 2r$,

$$E_U[\chi_k(Z_1)\chi_k(Z_2)] \sim E_U[\chi_k(Z_1)]E_U[\chi_k(Z_2)]. \tag{4.69}$$

Therefore, by Eq. (4.65),

$$\begin{aligned} E_U[V_k^2] &= E_U[V_k]^2(1+o(1)) \\ &\quad + \int\int_{R^2\cap\{|Z_1-Z_2|\le 2r\}} E[\chi_k(Z_1)\chi_k(Z_2)]dZ_1dZ_2. \end{aligned} \tag{4.70}$$

In the second case: $|Z_1 - Z_2| \leq 2r$, we follow the derivations similar to those in Section 4.4.1. First,

$$\begin{aligned}
&\int\int_{R^2 \cap \{|Z_1 - Z_2| \leq 2r\}} E[\chi_k(Z_1)\chi_k(Z_2)] dZ_1 dZ_2 \\
&= 2 \int\int_{R^2 \cap \{|Z_1 - Z_2| \leq 2r\} \cap Q} E[\chi_k(Z_1)\chi_k(Z_2)] dZ_1 dZ_2, \qquad (4.71)
\end{aligned}$$

where Q is the event that Z_2 is inside the square centered at the center of region and whose boundary goes through Z_1. Second, we only consider the dominating subcase when Z_1 is not in the extended corner region C_E. Let B_1, B_2 denote as the unit-area disks centered at Z_1, Z_2, respectively. Under all the above conditions ($R^2 \cap \{|Z_1 - Z_2| \leq 2r\} \cap Q$),

$$\begin{aligned}
E[\chi_k(Z_1)\chi_k(Z_2)] &= P(\text{there are less than } k \text{ active nodes in } B_1 \cap R \text{ and} \\
&\quad \text{there are less than } k \text{ active nodes in } B_2 \cap R) \\
&\leq P(\text{there are less than } k \text{ active nodes in } B_1 \cap R \text{ and} \\
&\quad \text{there are less than } k \text{ active nodes in } (B_2 - B_1) \cap R).
\end{aligned}$$

As have been proved in Section 4.4.1, the area of $(B_2 - B_1) \cap R$ is at least $x/(4r)$ where $x = |Z_1 - Z_2|$ and $r = 1/\sqrt{\pi}$ is the radius of the disk B_1, B_2. Let p_1 denote the probability that a node falls in $B_1 \cap R$ and is active, p_2 the probability that a node falls in $(B_2 - B_1) \cap R$ and is active. Therefore,

$$\begin{aligned}
E_U[\chi_k(Z_1)\chi_k(Z_2)] &= \sum_{i=0}^{k-1}\sum_{j=0}^{k-1} \binom{n}{i,j} p_1^i p_2^j (1 - p_1 - p_2)^{n-i-j} \\
&\sim \sum_{i=0}^{k-1} \binom{n}{i} p_1^i (1 - p_1)^{n-i} \sum_{j=0}^{k-1} \binom{n}{j} p_2^j (1 - p_2)^{n-j} \\
&= E_U[\chi_k(Z_1)] \sum_{j=0}^{k-1} \binom{n}{j} p_2^j (1 - p_2)^{n-j} \\
&\leq E_U[\chi_k(Z_1)] \sum_{j=0}^{k-1} \frac{(np_2)^j}{j!} e^{-(n-j)p_2} \\
&\sim E_U[\chi_k(Z_1)] e^{-np_2} \sum_{j=0}^{k-1} \frac{(np_2)^j}{j!} \\
&\leq E_U[\chi_k(Z_1)] e^{-\lambda x/(4r)} \sum_{j=0}^{k-1} \frac{(\lambda x/(4r))^j}{j!}, \qquad (4.72)
\end{aligned}$$

where the second equation follows from the derivation in the case of $|Z_1 - Z_2| > 2r$, and the last equation results from that $np_2 \geq np(x/(4r))/\ell^2 = \lambda x/(4r)$ and that the function $\sum_{j=0}^{k-1} \frac{x^j}{j!} e^{-x}$ is monotonically decreasing.

Now comparing Eqs. (4.72) and (4.49), and by Eq. (4.50), we have

$$\int\int_{R^2\cap\{|Z_1-Z_2|\le 2r\}\cap Q} E_U[\chi_k(Z_1)\chi_k(Z_2) \le E_U[V_k]\cdot 16k(k+1)\lambda^{-2}(1+o(1)). \tag{4.73}$$

Combining Eqs. (4.70), (4.71), and (4.73), we have

$$E_U[V_k^2] \quad = \quad E_U[V_k]^2(1+o(1)) + 32k(k+1)\lambda^{-2}E_U[V_k](1+o(1)).$$

Eq. (4.64) follows by taking $\ell \to \infty$. □

The following theorem follows immediately from Propositions 4.4.3 and 4.4.4. The proof is identical to that of Theorem 4.4.2.

Theorem 4.4.4 *Let $np/\ell^2 = \log \ell^2 + 2k\log\log \ell^2 + c(\ell)$. If $c(\ell) \le C$, where C is a constant value, then, as $\ell \to \infty$,*

$$\begin{aligned} &P(\textit{the monitored square region is k-covered}) \\ \le\ & 1 - \frac{1}{1+32e^{C/2}2^{k-2}(k+1)!/\sqrt{\pi}} \end{aligned} \tag{4.74}$$

In addition, if $c(\ell) \to -\infty$, P(the monitored square region is k-covered) tends to 0 as $\ell \to \infty$. □

4.4.3 Analysis in grid deployment

In this section, we consider grid deployment where $n = k^2$ nodes form regular square grids inside the square region R with side length ℓ. Each node is active with probability p, and $D = n/\ell^2$ denotes the node density. We prove the following lemma first.

Lemma 4.4.5 *for $0 \le p < 1$,*

$$p \le -\log(1-p) \le \frac{p}{1-p}. \tag{4.75}$$

Proof. Since $1-p \le e^{-p}$, taking logarithm, we have $\log(1-p) \le -p$ and hence the first inequality. To prove the second inequality, let $f(p) = p + (1-p)\log(1-p)$. It is simple to verify $f(0) = 0$ and $f'(p) \ge 0$ for $0 \le p < 1$. So $f(p) \ge 0$ for $0 \le p < 1$. Rearranging the equation, we have the second inequality. □

Sufficient condition

Theorem 4.4.5 *Assume $p \le 1-\epsilon < 1$ for some constant ϵ. Let*

$$\begin{aligned}&(-\log(1-p))n/\ell^2 = -D\log(1-p)\\ &= \log \ell^2 + 2k\log\log \ell^2 + 2\sqrt{-2\pi \log \ell^2 \log(1-p)} + c(\ell)\end{aligned} \tag{4.76}$$

and $c(\ell) \to \infty$ as $\ell \to \infty$, then P(the region R is k-covered) $\to 1$.

Proof. We still divide the square region into grids with side length $s = \sqrt{2}ur$, where $u = 1/\log \ell^2$. We now calculate the expected number of grids that are not k-covered. We shall only consider the grids in the side area of the region R since this area contributes most un-k-covered grids. Again, consider a side grid g at j rows away from the side (there are j other rows between the grid and the side of the square region R). Let m_j denote the number of nodes that are contained in the disk centered at the center of grid g with radius $r - s/\sqrt{2}$. Any one of the m_j nodes can completely cover the grid g if it is active (notice a node has sensing range r).

We first estimate the value m_j. If we draw a disk S_j with radius $t = r - s/\sqrt{2}$ centered at the center of grid g, the distance between the center of the disk and the closest side of the square R is $j(s+1/2) \ge js$. The area of the part of disk S_j that is inside R is at least $\pi t^2/2 + \pi jst/2$ by Lemma 4.4.1. Therefore, the number m_j of nodes that are inside the area is approximately $D(\pi t^2/2 + \pi jst/2)$. To obtain a bound on m_j, we envision all nodes are at the centers of disjoint small squares of side length $d = 1/\sqrt{D} = \ell/\sqrt{n}$. If we draw a disk S'_j with radius $t - d/\sqrt{2}$, then any point in disk S'_j must belong to some square whose center is covered by disk S_j. Hence, the area of S'_j is less than the total area of all the squares whose center is covered by disk S_j, i.e., $\pi(t - d/\sqrt{2})^2/2 + \pi js(t - d/\sqrt{2})/2 \le m_j d^2$. Therefore,

$$\begin{aligned}m_j \ge\ & D(\pi(t - d/\sqrt{2})^2/2 + \pi js(t - d/\sqrt{2})/2)\\ &= D(\pi t^2/2 - \pi td/\sqrt{2} + \pi d^2/4 + \pi jst/2 - \pi jsd/(2\sqrt{2}))\\ &\ge D\pi t^2/2 - \pi t\sqrt{D/2} + D\pi jst/2 - \pi js\sqrt{D/2}/2)\\ &\ge D(1-u)^2/2 + D\sqrt{\pi}js(1-u)/2 - \sqrt{2\pi D}\\ &\triangleq\ m_{j0},\end{aligned} \tag{4.77}$$

where the third equation results from $D = 1/d^2$, and the fourth equation results from $t = r - s/\sqrt{2} = r(1-u)$, $\pi t^2 = \pi r^2(1-u)^2 = (1-u)^2$, and $js \le r = 1/\sqrt{\pi}$. Notice that $m_{j0} \le D(1-u)^2$.

Let p_j denote the probability that grid g at row j is not k-covered. Clearly, p_j increases if m_j decreases (because p_j is the probability that out of m_j nodes, less than k of them are active),

$$\begin{aligned} p_j &= \sum_{i=0}^{k-1} \binom{m_j}{i} p^i (1-p)^{m_j - i} \\ &\leq \sum_{i=0}^{k-1} \binom{m_{j0}}{i} p^i (1-p)^{m_{j0} - i}. \end{aligned} \tag{4.78}$$

Denote the ith item in the above summation as T_i. We have

$$\frac{T_{i+1}}{T_i} = \frac{m_{j0} - i}{i+1} \cdot \frac{p}{1-p} \geq \frac{(m_{j0} - k)p}{k(1-p)}. \tag{4.79}$$

Since

$$\begin{aligned} (m_{j0} - k)p/(1-p) &\sim m_{j0}p/(1-p) \\ &\geq D(1-u)^2/2 \cdot (-\log(1-p)) \end{aligned}$$

(where the second equation results from Lemma 4.4.5 and $m_{j0} \geq D(1-u)^2/2$ by Eq. (4.77)) tends to infinity, T_i is dominated by T_{i+1} for $i < k$. Therefore,

$$\begin{aligned} p_j &\lesssim \binom{m_{j0}}{k-1} p^{k-1} (1-p)^{m_{j0} - k + 1} \\ &\leq \frac{(m_{j0}p/(1-p))^{k-1}}{(k-1)!} (1-p)^{m_{j0}} \\ &\leq \frac{(Dp(1-u)^2/(1-p))^{k-1}}{(k-1)!} (1-p)^{m_{j0}}, \end{aligned} \tag{4.80}$$

where the last equation results from $m_{j0} \leq D(1-u)^2$.

The expected number X^S of un-k-covered side grids is

$$\begin{aligned} E[X^S] &\leq \frac{4\ell}{s} \sum_{j=0}^{r/s} p_j \\ &\lesssim \frac{4\ell}{s} \sum_{j=0}^{r/s} \frac{(D(1-u)^2 p/(1-p))^{k-1}}{(k-1)!} \cdot (1-p)^{\frac{D(1-u)^2}{2} - \sqrt{2\pi D} + j\frac{D\sqrt{\pi}s(1-u)}{2}} \\ &\leq \frac{4\ell}{s} \frac{(D(1-u)^2 p/(1-p))^{k-1}}{(k-1)!} \cdot (1-p)^{\frac{D(1-u)^2}{2} - \sqrt{2\pi D}} \cdot \frac{1}{1-(1-p)^{D\sqrt{\pi}s(1-u)/2}}. \end{aligned} \tag{4.81}$$

The last factor $\frac{1}{1-(1-p)^{D\sqrt{\pi}s(1-u)/2}}$ in Eq. (4.81) converges to a constant since $D\sqrt{\pi}s(1-u)/2 \sim 1/(-\log(1-p)\sqrt{2})$ by Eq. (4.76), $(1-p)^{D\sqrt{\pi}s(1-u)/2} = (1-p)^{1/(-\log(1-p)\sqrt{2}(1+o(1)))} = e^{-1/\sqrt{2}(1+o(1))}$.

Notice $s = \sqrt{2}ur = \sqrt{2/\pi}/\log \ell^2$. We take logarithm on both sides, put all constant and $o(1)$ terms into C_1, and obtain

$$\begin{aligned}\log E[X^S] &\leq \frac{1}{2}\log \ell^2 + \log\log \ell^2 + (k-1)\log(\frac{Dp(1-u)^2}{1-p}) + (D\frac{(1-u)^2}{2} - \sqrt{2\pi D})\log(1-p) + C_1 \\ &= \frac{1}{2}\log \ell^2 + \log\log \ell^2 + (k-1)\log(\frac{Dp(1-u)^2}{1-p}) - \frac{(1-u)^2}{2}(\log \ell^2 + 2k\log\log \ell^2 \\ &\quad +2\sqrt{-2\pi \log \ell^2 \log(1-p)} + c(\ell)) - \sqrt{2\pi D}\log(1-p) + C_1, \end{aligned} \tag{4.82}$$

where the second equation is obtained by plugging in Eq. (4.76). Since $\log(1-p) \leq -p$, $Dp \leq -D\log(1-p) \sim \log \ell^2$, we have $(k-1)\log Dp \leq (k-1)\log\log \ell^2 + o(1)$. In addition, since $p < 1-\epsilon$, $\log \frac{(1-u)^2}{1-p} \leq \log \frac{1}{\epsilon}$ is bounded. Therefore,

$$\begin{aligned}\log E[X^S] &\leq (u - \frac{u^2}{2})(\log \ell^2 + 2k\log\log \ell^2) - \frac{(1-u)^2}{2}c(\ell) + C_2 \\ &\quad -(1-u)^2\sqrt{-2\pi \log \ell^2 \log(1-p)} - \sqrt{2\pi D}\log(1-p). \end{aligned} \tag{4.83}$$

Since

$$-\sqrt{2\pi D}\log(1-p) - \sqrt{-2\pi \log \ell^2 \log(1-p)} = \sqrt{-2\pi\log(1-p)}(\sqrt{-D\log(1-p)} - \sqrt{\log \ell^2})$$

and

$$\begin{aligned}\sqrt{-D\log(1-p)} - \sqrt{\log \ell^2} &= \frac{-D\log(1-p) - \log \ell^2}{\sqrt{-D\log(1-p)} + \sqrt{\log \ell^2}} \\ &\leq \frac{2k\log\log \ell^2 + 2\sqrt{-2\pi \log \ell^2 \log(1-p)} + c(\ell)}{\sqrt{-D\log(1-p)} + \sqrt{\log \ell^2}} \\ &\leq \text{constant}, \end{aligned}$$

the terms $-(1-u)^2\sqrt{-2\pi \log \ell^2 \log(1-p)} - \sqrt{2\pi D}\log(1-p)$ in Eq. (4.83) are bounded. Additionally, since $u = 1/\log \ell^2$, $(u - u^2/2)(\log \ell^2 + 2k\log\log \ell^2)$ converges to 1. Therefore, if $c(\ell) \to \infty$, $\log E[X^S] \to -\infty$ and $E[X^S] \to 0$. Since the number of un-k-covered side grids dominates that of un-k-covered grids in the inner and corner region, the expected number X of total un-k-covered grids converges to 0 as $\ell \to \infty$. By using the Markov inequality again, we have P(the whole region is completely k-covered) $\to 1$ as $\ell \to \infty$ if the number of nodes is given as in Eq. (4.76). □

Necessary condition

The derivation of the necessary condition in grid deployment follows a procedure similar to that in uniformly random deployment and Poisson process deployment. Again we need to estimate the bounds

on $E[V_k]$ and $E[V_k^2]$.

Proposition 4.4.5 *Assume $p \leq 1-\epsilon$, where $\epsilon > 0$. If*

$$\begin{aligned}(-\log(1-p))n/\ell^2 &= -D\log(1-p)\\ &= \log\ell^2 + 2(k-1)\log\log\ell^2 - 2\sqrt{-2\pi\log\ell^2\log(1-p)} - c(\ell),\end{aligned} \tag{4.84}$$

where $c(\ell)$ is slowly growing (i.e., $c(\ell)\to\infty$ and $c(\ell) = o(\log\log\ell^2)$) as $\ell\to\infty$ and k is fixed, then

$$E[V_k](\log\ell^2) \geq C_3 e^{c(\ell)/2}, \tag{4.85}$$

where C_3 is a constant.

Proof. Let $\chi_k((x,y))$ denote the indicator function of whether a point (x,y) is covered by less than k nodes. Again, we only consider the case that (x,y) is in the side area of square R to obtain a lower bound. Without loss of generality, we assume $0 \leq x \leq r, r \leq y \leq \ell - r$. Thus disk $B_{(x,y)}(r)$ has at most area $\frac{1}{2} + 2xr$ inside the square region R. The region $B_{(x,y)}(r)\cap R$ contains at most $M_x = D(\pi r^2/2 + 2xr + 2\pi rd/\sqrt{2}) = D(\frac{1}{2}+2xr) + \sqrt{2\pi D}$ nodes. Therefore,

$$\begin{aligned}E[\chi_k((x,y))] &\geq \sum_{i=0}^{k-1}\binom{M_x}{i}p^i(1-p)^{M_x-i}\\ &\sim \sum_{i=0}^{k-1}\frac{(M_xp/(1-p))^i}{i!}(1-p)^{M_x}\\ &= \sum_{i=0}^{k-1}\frac{(M_xp/(1-p))^i}{i!}e^{M_x\log(1-p)}.\end{aligned} \tag{4.86}$$

Since $M_x \geq D/2$, and $p/(1-p) \geq -\log(1-p)$, we have

$$\begin{aligned}E[\chi_k((x,y))] &\gtrsim \sum_{i=0}^{k-1}\frac{(-\frac{D}{2}\log(1-p))^i}{i!}e^{M_x\log(1-p)}\\ &\geq \sum_{i=0}^{k-1}\frac{(-\frac{D}{2}\log(1-p))^i}{i!}e^{(D/2+2xrD+\sqrt{2\pi D})\log(1-p)}\\ &\geq \frac{(-\frac{D}{2}\log(1-p))^{k-1}}{(k-1)!}e^{(D/2+2xrD+\sqrt{2\pi D})\log(1-p)}.\end{aligned} \tag{4.87}$$

Therefore,

$$\begin{aligned}E[V_k] &\geq 4\int_0^r\int_r^{\ell-r}E[\chi_k((x,y))]dydx\\ &\gtrsim 4\int_0^r\int_r^{\ell-r}\frac{(-\frac{D}{2}\log(1-p))^{k-1}}{(k-1)!}\cdot e^{(D/2+2xrD+\sqrt{2\pi D})\log(1-p)}dydx\end{aligned}$$

$$\geq \quad 4(\ell - 2r)\frac{(-\frac{D}{2}\log(1-p))^{k-1}}{(k-1)!} \cdot e^{(D/2+\sqrt{2\pi D})\log(1-p)} \frac{1 - e^{2r^2 D\log(1-p)}}{-2rD\log(1-p)}. \tag{4.88}$$

Since $-D\log(1-p) \sim \log \ell^2$ and $r^2 = 1/\pi$, $e^{2r^2 D\log(1-p)} \to 0$ as $\ell \to \infty$, by taking logarithm on both sides of Eq. (4.88), we obtain

$$\begin{aligned}
\log E[V_k] \geq & \frac{\log \ell^2}{2} + (k-1)\log(-\frac{D}{2}\log(1-p)) - \log((k-1)!) \\
& +(\frac{D}{2} + \sqrt{2\pi D})\log(1-p) - \log(-2rD\log(1-p)) + o(1) \\
\geq & -1\log\log \ell^2 + C_4 + c(\ell)/2,
\end{aligned} \tag{4.89}$$

where C_4 contains all constant and $o(1)$ terms. Therefore, we conclude that

$$E[V_k](\log \ell^2) \geq C_3 e^{c(\ell)/2}. \tag{4.90}$$

□

Proposition 4.4.6 *Given the same conditions as in Proposition (4.4.5),*

$$\frac{E[V_k^2]}{E[V_k]^2} \leq 1 + \frac{C_5(p + (\log \ell^2)^{-1})}{E[V_k]\log \ell^2}. \tag{4.91}$$

Proof. Similar to the proofs in Section 4.4.1,

$$\begin{aligned}
E[V_k^2] &= E[\int_R \int_R \chi_k(Z_1)\chi_k(Z_2) dZ_1 dZ_2] \\
&= \int_R \int_R E[\chi_k(Z_1)\chi_k(Z_2)] dZ_1 dZ_2.
\end{aligned} \tag{4.92}$$

We still consider two cases in the integral: case (i) $|Z_1 - Z_2| > 2r$; and case (ii) $|Z_1 - Z_2| \leq 2r$. In the first case, $\chi_k(Z_1)$ and $\chi_k(Z_2)$ are independent. Therefore,

$$\begin{aligned}
& \int\int_{R^2 \cap \{|Z_1 - Z_2| > 2r\}} E[\chi_k(Z_1)\chi_k(Z_2)] dZ_1 dZ_2 \\
& \leq \int\int_{R^2} E[\chi_k(Z_1)] E[\chi_k(Z_2)] dZ_1 dZ_2 \\
& = E[V_k]^2.
\end{aligned} \tag{4.93}$$

In the second case, $|Z_1 - Z_2| \leq 2r$, and we follow the derivation similar to that in Section 4.4.1.

$$\int\int_{R^2 \cap \{|Z_1 - Z_2| \leq 2r\}} E[\chi_k(Z_1)\chi_k(Z_2)] dZ_1 dZ_2$$

$$\leq 2 \int \int_{R^2 \cap \{|Z_1 - Z_2| \leq 2r\} \cap Q} E[\chi_k(Z_1)\chi_k(Z_2)] dZ_1 dZ_2, \tag{4.94}$$

where Q is the event that Z_2 is inside the square centered at the center of R and whose boundary crosses Z_1. Again, we only consider the dominating subcase when Z_1 is not in the extended corner region C_E (the extended corner region is the corner region and the side region that is at most $3r$ away from a second side of the region R). Let B_1, B_2 denote the unit-area disks centered at Z_1, Z_2, respectively. Under the above conditions (i.e., $R^2 \cap \{|Z_1 - Z_2| \leq 2r\} \cap Q$),

$$\begin{aligned}
&E[\chi_k(Z_1)\chi_k(Z_2)] \\
&\quad = P(\text{there are less than } k \text{ active nodes in } B_1 \cap R \text{ and} \\
&\qquad \text{there are less than } k \text{ active nodes in } B_2 \cap R) \\
&\quad \leq P(\text{there are less than } k \text{ active nodes in } B_1 \cap R\ ) \\
&\qquad \cdot P(\text{there are less than } k \text{ active nodes in } (B_2 - B_1) \cap R).
\end{aligned}$$

As has been proved in Section 4.4.1, the area of $(B_2 - B_1) \cap R$ is at least $x/(4r)$ and its perimeter length is at most $2\pi r$ (noticing the shape $B_2 - B_1$ has the same perimeter length as B_2 or B_1), Therefore, the number of nodes inside $(B_2 - B_1) \cap R$ is at least $m_x = \max(0, Dx/(4r) - \sqrt{2\pi D})$. Therefore, conditioning on $(R^2 \cap \{|Z_1 - Z_2| \leq 2r\} \cap Q)$, we have

$$E[\chi_k(Z_1)\chi_k(Z_2)] \quad \leq \quad E[\chi_k(Z_1)] \sum_{j=0}^{k-1} \binom{m_x}{j} p^j (1-p)^{m_x - j}. \tag{4.95}$$

Now we integrate over the space $(R^2 \cap \{|Z_1 - Z_2| \leq 2r\} \cap Q)$, and obtain

$$\begin{aligned}
&\int \int_{R^2 \cap \{|Z_1 - Z_2| \leq 2r\} \cap Q} E[\chi_k(Z_1)\chi_k(Z_2)] dZ_1 dZ_2 \\
&\leq \quad \int_R E[\chi_k(Z_1)] \int_{Z_2 : R \cap \{|Z_1 - Z_2| \leq 2r\} \cap Q} \sum_{j=0}^{k-1} \binom{m_x}{j} p^j (1-p)^{m_x - j} dZ_2 dZ_1 \\
&\leq \int_R E[\chi_k(Z_1)] dZ_1 \int_0^{2r} \sum_{j=0}^{k-1} \binom{m_x}{j} p^j (1-p)^{m_x - j} 2\pi x dx,
\end{aligned} \tag{4.96}$$

where the $2\pi x$ term in the last equation results from the conversion from a Cartesian coordinate system to a polar coordinate system. Notice a convention of $\binom{n}{m} = 0$ if $n < m$. Recall $r = 1/\sqrt{\pi}$ and $1/\sqrt{D}$ is the distance between two adjacent nodes. If $x \leq 4\sqrt{2/D}$, $m_x = 0$. Therefore, the integration in Eq. (4.96) can be divided into two parts.

$$\int_0^{2r} \sum_{j=0}^{k-1} \binom{m_x}{j} p^j (1-p)^{m_x - j} 2\pi x dx$$

$$
\begin{aligned}
&\leq \left(\int_0^{4\sqrt{2/D}} + \int_{4\sqrt{2/D}}^{2r}\right) \sum_{j=0}^{k-1} \binom{m_x}{j} p^j (1-p)^{m_x - j} 2\pi x dx \\
&= \int_0^{4\sqrt{2/D}} 2\pi x dx + \int_{4\sqrt{2/D}}^{2r} \sum_{j=0}^{k-1} \binom{m_x}{j} p^j (1-p)^{m_x - j} 2\pi x dx \\
&\leq 32\pi/D + \int_{4\sqrt{2/D}}^{2r} \sum_{j=0}^{k-1} \frac{(m_x p/(1-p))^j}{j!} (1-p)^{m_x} 2\pi x dx \\
&= 32\pi/D + \int_{4\sqrt{2/D}}^{2r} \sum_{j=0}^{k-1} \frac{((Dx/(4r) - \sqrt{2\pi D})p/(1-p))^j}{j!} \cdot (1-p)^{(Dx/(4r) - \sqrt{2\pi D})} 2\pi x dx \\
&\quad \text{(let } u = x/(4r) - \sqrt{2\pi/D}\text{)} \\
&= 32\pi/D + \int_0^{1/2 - \sqrt{2\pi/D}} \sum_{j=0}^{k-1} \frac{(uDp/(1-p))^j}{j!} \cdot (1-p)^{uD} 2\pi 4r(u + \sqrt{2\pi/D}) 4r du \\
&\quad \text{(since } p \leq -\log(1-p)\text{)} \\
&\leq 32\pi/D + (1-p)^{-k+1} \int_0^{\infty} \sum_{j=0}^{k-1} \frac{(-uD\log(1-p))^j}{j!} \cdot e^{uD\log(1-p)} 32(u + \sqrt{2\pi/D}) du. \qquad (4.97)
\end{aligned}
$$

Treating $-D\log(1-p)$ as λ, by Lemma 4.4.4 we obtain that

$$
\int_0^{\infty} \sum_{j=0}^{k-1} \frac{(-uD\log(1-p))^j}{j!} e^{uD\log(1-p)} 32u du = 16k(k+1)(-D\log(1-p))^{-2}, \qquad (4.98)
$$

and similarly

$$
\int_0^{\infty} \sum_{j=0}^{k-1} \frac{(-uD\log(1-p))^j}{j!} e^{uD\log(1-p)} 32\sqrt{2\pi/D} du = 32k\sqrt{2\pi/D}(-D\log(1-p))^{-1}. \qquad (4.99)
$$

Hence, combining Eqs. (4.97), (4.98) and (4.99), we have

$$
\begin{aligned}
&\int_0^{2r} \sum_{j=0}^{k-1} \binom{m_x}{j} p^j (1-p)^{m_x - j} 2\pi x dx \\
&\leq 32\pi/D + \epsilon^{-k+1}(16k(k+1)(-D\log(1-p))^{-2} + 32k\sqrt{2\pi/D}(-D\log(1-p))^{-1}) \\
&\leq (32\pi p + C_5(\log \ell^2)^{-1} + C_6\sqrt{p/\log \ell^2})(\log \ell^2)^{-1} \\
&\leq C_7(p + (\log \ell^2)^{-1})(\log \ell^2)^{-1}, \qquad (4.100)
\end{aligned}
$$

for some constant C_7.

Plugging Eq. (4.100) into Eq. (4.96), we obtain

$$
\int\int_{R^2 \cap \{|Z_1 - Z_2| \leq 2r\} \cap Q} E[\chi_k(Z_1)\chi_k(Z_2)] dZ_1 dZ_2 \leq E[V_k] C_7 (p + (\log \ell^2)^{-1})(\log \ell^2)^{-1}. \qquad (4.101)
$$

Combining Eq. (4.101) with Eqs. (4.92), (4.93), and (4.94), we have

$$E[V_k^2] \leq E[V_k]^2 + 2C_7 E[V_k](p + (\log \ell^2)^{-1})(\log \ell^2)^{-1}. \tag{4.102}$$

Therefore,

$$\frac{E[V_k^2]}{E[V_k]^2} \quad \leq \quad 1 + \frac{2C_7(p + (\log \ell^2)^{-1})}{E[V_k](\log \ell^2)} \tag{4.103}$$

Choosing $C_5 = 2C_7$ completes the proof. □

We are now in a position to show the following necessary condition of complete k-coverage in the case of grid deployment. The proof is almost identical to that of theorem 4.4.2 and is thus omitted.

Theorem 4.4.6 *Given the same conditions as in Proposition 4.4.5 except that $c(\ell)$ need not be $o(\log \log \ell^2)$ (it still needs to go to ∞), P(the region R is not k-covered) $\to 1$.*

Comments There is a gap between the necessary condition and the sufficient condition on the density requirement for k-coverage. However, the gap with the term $2\sqrt{-2\pi \log \ell^2 \log(1-p)}$ is caused by the uncertainty of the number of lattice points contained in a circle (called Gauss's circle problem [1]), which is most probably not closable. It is not clear whether the gap with the term $\log \log \ell^2$ is closable or not. However, if $p = O((\log \ell^2)^{-1})$, the gaps with both of the two terms diminish. The first gap diminishes obviously. The second gap diminishes because the conclusion in Proposition 4.4.6 reduces to

$$\frac{E[V_k^2]}{E[V_k]^2} \leq 1 + \frac{C_5}{E[V_k](\log \ell^2)^2}, \tag{4.104}$$

which is essential to close the gap on the term $\log \log \ell^2$.

4.4.4 Numerical validations

We have carried out a simulation study to validate the conditions required to maintain k-coverage under three different deployment strategies. As all of the conditions derived in Sections 4.4.1–4.4.3 are asymptotic, it is very difficult (if not impossible) to evaluate the level of coverage as the side length ℓ goes to infinity. Moreover, in all the asymptotic conditions, we have made an implicit assumption that $c(\ell)$ grows slower than (or equal to) $\log \log \ell^2$ (although the conclusions still hold without the assumption) because we do not want the term $c(\ell)$ to dominate the previous terms. In practical situation, it is very difficult to construct a term $c(\ell)$ that grows to infinity at a rate slower than $\log \log \ell^2$ since $\log \log \ell^2$ grows extremely

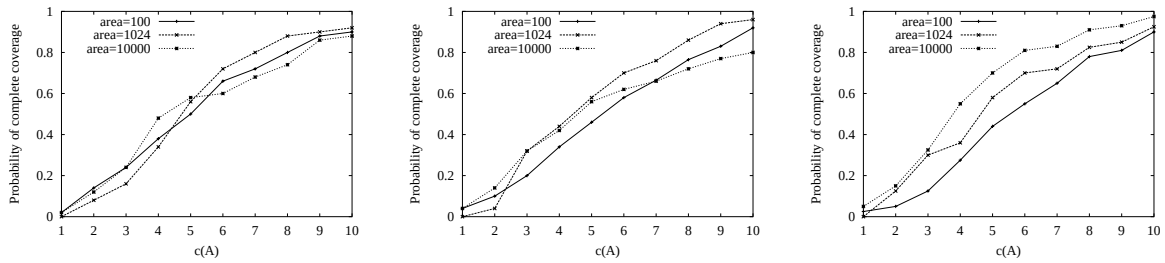

(a) Poisson process deployment with the density λ such that $\lambda p = \log \ell^2 + 2 \log \log \ell^2 + c(\ell)$.

(b) Uniformly random deployment with the number of nodes n such that $np/\ell^2 = \log \ell^2 + 2 \log \log \ell^2 + c(\ell)$.

(c) Grid deployment with the number of nodes n such that $-n \log(1-p)/\ell^2 = \log \ell^2 + 2 \log \log \ell^2 + c(\ell)$.

Figure 4.2: Probability of complete coverage vs. $c(\ell)$.

slow[2]. Therefore, we study instead the following questions:

1. For a given side length ℓ, what are the practical values of $c(\ell)$ that can lead to complete coverage?

2. For a given node density, which deployment method (random or regular) renders higher probability of complete coverage?

3. How does the coverage degree change as node density increases?

Let each node cover a unit-area disk. We consider three different network areas: 100, 1024, 10000. Each node has a probability 0.1 to be active. (We have experimented with other probabilities and the results exhibit the same trends.) For each parameter $c(\ell)$, we generate 100 network configurations for each deployment strategy (Poisson process deployment, uniformly random deployment, and grid deployment) and use the percent of the configurations that are completely covered as the probability of complete coverage.

Figure 4.2 shows the probability of complete coverage under each deployment strategy. Notice that for grid deployment, we have not used the sufficient condition derived in Section 4.4.3 because our simulation results indicate the sufficient condition tends to be too conservative. These figures show that as $c(\ell)$ grows from 1 to 10, the probability of complete coverage increases to a value that is close to 1.

In Fig. 4.3, we compare the probability of complete coverage under uniformly random deployment and grid deployment. In order to perform a fair comparison, we have used the same equation for the number of nodes: $np/\ell^2 = \log \ell^2 + 2 \log \log \ell^2 + c(\ell)$ and the node density in the figure is defined as n/ℓ^2. The figure shows that grid deployment renders a higher probability of complete coverage, which corroborates the theoretical analysis. Another observation is that the larger the values of p, the more

[2]Note that $\log \log 100000000 = 2.9$ and it is not quite possible to simulate a network with area 100000000 where each node covers 1 unit area.

significant difference in the probability of complete coverage under these two deployment strategies. Due to the space limit, we did not show this part of results.

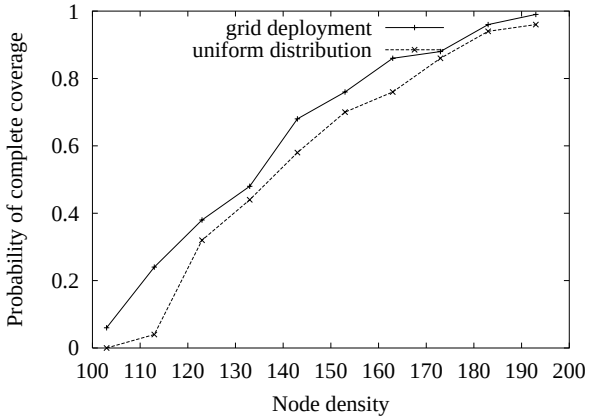

Figure 4.3: The probability of complete coverage under uniformly random deployment and grid deployment. The network area is 1024.

Figure 4.4 gives the average coverage degree over 50 runs in the case that the network area is 1024. We notice that the coverage degree linearly increases as node density increases, which is consistent with the theoretical results in the previous sub-sections (notice the network area is fixed here). Again, we observe that grid deployment renders a higher coverage degree than uniformly random deployment.

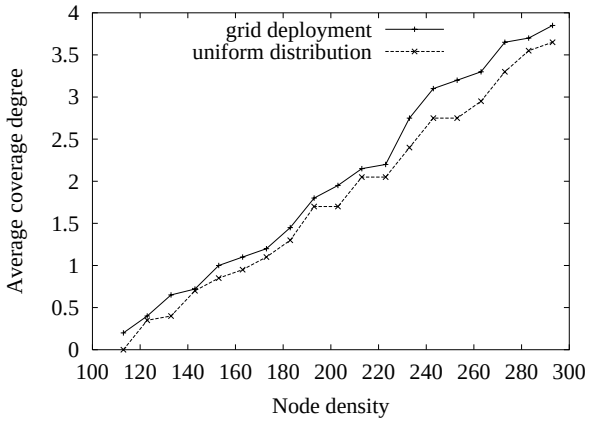

Figure 4.4: The coverage degree under uniformly random deployment and grid deployment. The network area is 1024.

4.5 Upper Bound of α-Lifetime in Finite Regions

The asymptotic upper bound of the 1-lifetime derived in Section 4.3 and 4.4 give the required node density in order to achieve complete coverage as the monitored area grows to infinity ($\ell \to \infty$). However,

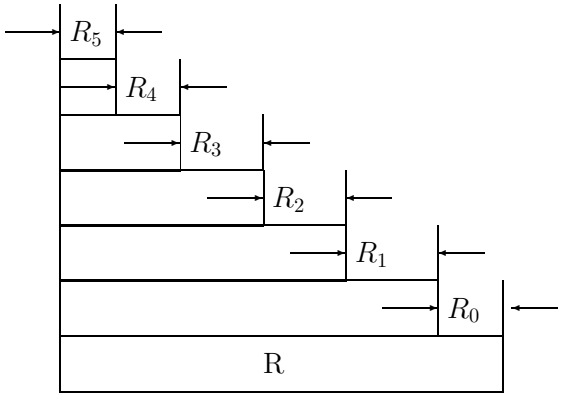

Figure 4.5: The entire region R can be divided into different sub-regions: $R_0, R_1, \cdots, R_n$, where all points in R_i are exactly covered by i nodes.

in practice one may be more interested in knowing how many nodes should be deployed (or, equivalently, what is the node density) in order to achieve the α-lifetime in a finite region. Results derived in Section 4.3 and 4.4 cannot be directly applied to answer this question, as they are derived for *complete* coverage for regions of *infinitely large* area.

In this section, we consider the α-lifetime in a finite region with a finite density of sensor nodes, where $0 < \alpha < 1$ and usually α is close to 1. We derive two bounds: (i) an upper bound of α-lifetime for a special family of algorithms in which the entire region is completely covered initially, and as large coverage ratio as possible is maintained until it drops below a certain threshold α; and (ii) an upper bound of α-lifetime that applies to algorithms that maintain the coverage ratio of α from the beginning of network deployment. The second bound applies to any algorithm.

4.5.1 Upper bound of α-lifetime for a special family of algorithms

We first derive the upper bound of α-lifetime for the family of algorithms that intend to completely cover the region initially and maintain as large coverage ratio as possible, until the drops below a certain threshold α.

We can divide the entire region R into several sub-regions $R_0, R_1, \cdots, R_n$, where all points in R_i are exactly covered by i sensor nodes (Fig. 4.5). Thus $V_k = \sum_{i=0}^{k-1} ||R_i||$, and $1 - V_k/\ell^2$ is the portion of the region in which each point is covered by at least k nodes. We can also divide the network lifetime into rounds with the duration for each round set to T. In each round, a minimum set of nodes which are not chosen in previous rounds and have maximum coverage is chosen to operate. Thus after k rounds, the maximum possible coverage ratio is at most $1 - V_{k+1}/\ell^2$. Clearly, if $\alpha > 1 - V_{k+1}/\ell^2$, the sensor network

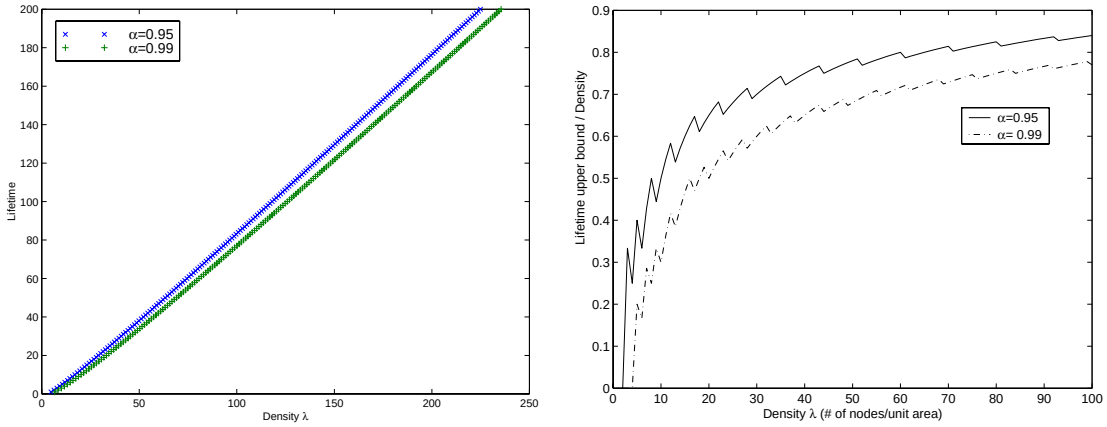

(a) Average α-lifetime upper bound v.s. density

(b) Average α-lifetime upper bound per unit of density v.s. density

Figure 4.6: Upper bounds of Average α-lifetime and α-lifetime per unit of density versus node density for the special class of algorithms that maintain as large coverage as possible.

can not provide coverage ratio α any more. Thus the upper bound of α-lifetime is

$$L(\lambda, \alpha) = \max\{k : \alpha \leq 1 - V_k/\ell^2\} \cdot T. \tag{4.105}$$

As V_k's are random variables whose distributions are difficult, if not impossible, to obtain, we use $E(V_k)$ to approximate V_k. That is, the resulting α-lifetime can be regarded as the average α-lifetime:

$$G(\lambda, \alpha) = \max\{k : \alpha \leq 1 - F(k, \lambda)\} \cdot T, \tag{4.106}$$

where

$$F(k, \lambda) = E(V_k)/\ell^2 = \exp(-\lambda) \left(\sum_{i=0}^{k-1} \frac{\lambda^i}{i!} \right). \tag{4.107}$$

As a matter of fact, $G(\lambda, \alpha)$ is not the expectation of $L(\lambda, \alpha)$. However, we prove in the following theorem that it suffices to approximate V_k with $E(V_k)$ in regions of large sizes.

Theorem 4.5.1 *As $\ell \to +\infty$ and $n/\ell^2 \to \lambda$, $V_k/\ell^2 \to F(k, \lambda)$ almost surely, where $F(k, \lambda)$ is defined in Eq. (4.107).*

Proof. Refer to Appendix A.5 for a detailed account of the proof.

Numerical examples Figure 4.6 depicts the upper bounds of the average α-lifetime $G(\lambda, \alpha)$ and the average α-lifetime per unit density $G(\lambda, \alpha)/\lambda$ versus the density λ under the cases of $\alpha = 0.95$ and 0.99,

where we let $T = 1$. The upper bound of the lifetime per unit density increases as the density increases in general, and slightly decreases at certain density values. This is because the upper bound of network lifetime does not change when the node density λ slightly increases at some points of λ.

4.5.2 Upper bound of α-lifetime for all algorithms

Several sensor network applications do not require full coverage of the entire monitored area. Instead it is sufficient to maintain the coverage ratio above a certain threshold α throughout the network operation. In this case, energy can be saved by maintaining α-coverage since system initialization. In this section, we derive the upper bound of the network lifetime in this case. Note that this upper bound can be applied to all algorithms that maintain α-coverage. For analysis tractability, again we use $E(V_k)$ to approximate V_k. The following theorem establishes the upper bound of the lifetime.

Theorem 4.5.2 *Let $\gamma_i \triangleq 1 - E(V_i)/l^2$ and $\beta_i \triangleq \gamma_i - \gamma_{i+1}$. Then the upper bound of α-lifetime for a sensor network with density λ is*

$$\left(\min_{k:\alpha>\gamma_k} H(k,\alpha) \triangleq \frac{\sum_{i=1}^{k-1} i\beta_i}{\alpha - \gamma_k} \right) \cdot T. \tag{4.108}$$

Proof. We still divide the entire region R into different sub-regions $R_0, R_1, \cdots$, where all points in R_i are exactly covered by i nodes. By definition, γ_k represents the portion of region R that is covered by at least k nodes and β_k represents the portion of region R that is covered by exactly k nodes. Thus $\beta_k = ||R_k||/||R||$.

For each k such that $\gamma_k < \alpha$, in each round of time T, the working nodes must cover α portion of the region R, among which at least $(\alpha - \gamma_k)$ portion must come from $R_1 \cup \cdots \cup R_{k-1}$ since $\cup_{i \geq k} R_i$ can provide at most γ_k coverage (and R_0 is not covered by any node). On the other hand, for each $i < k$, the total coverage contribution of region R_i throughout the lifetime is at most $i\beta_i$ (since it can provide β_i portion of coverage for i rounds). Hence, the total amount of coverage $R_1, R_2, \cdots, R_{k-1}$ can contribute throughout the lifetime over all rounds is $\sum_{i=1}^{k-1} i\beta_i$. Therefore, the maximum lifetime is upper bounded by

$$\frac{\sum_{i=1}^{k-1} i\beta_i}{\alpha - \gamma_k} \cdot T. \tag{4.109}$$

Since this is true for every k such that $\alpha > \gamma_k$, the α-lifetime is upper bounded by Eq. (4.108). □

As an example, as shown in Figure 4.7, in each round, $(\alpha - \gamma_3)$ portion of the region must come from region R_2 and R_1 to ensure α-coverage since $\alpha > \gamma_3$. The total lifetime "contribution" R_1 and R_2 can

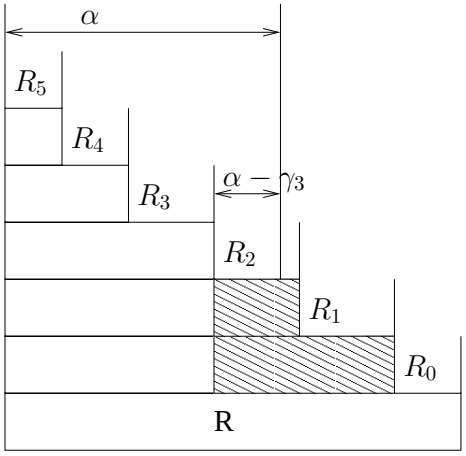

Figure 4.7: In each round, $\alpha - \gamma_3$ portion of the region must come from region R_2 and R_1 to ensure α-coverage. The total lifetime "contribution" R_1 and R_2 can make over all rounds is $\beta_1 + 2\beta_2$. Hence the α-lifetime is upper bounded by $T \cdot (\beta_1 + 2\beta_2)/(\alpha - \gamma_3)$.

make over all rounds is $\beta_1 + 2\beta_2$. Hence the α-lifetime is upper bounded by $T \cdot (\beta_1 + 2\beta_2)/(\alpha - \gamma_3)$.

Recall in the proof of Theorem 4.5.2, in each round we divide the entire region into two sub-regions. In the first sub-region, each point is covered by at least k nodes and in the second sub-region, each point is covered by at most $k-1$ nodes. The proof of Theorem 4.5.2 only considers the limit implied by the second sub-region. In what follows, we prove that the first sub-region can always provide γ_k portion coverage for at least $H(k,\alpha)$ rounds for the k that minimizes $H(k,\alpha)$.

Theorem 4.5.3 *Let* $k = \arg\min_{i:\alpha>\gamma_i} H(i,\alpha)$*, then*

$$k \geq H(k,\alpha).$$

Proof. To facilitate the proof, we first give several nice properties of $H(k,\alpha)$ in the next lemma.

Lemma 4.5.1 *For all* k *such that* $\alpha > \gamma_k$*,* $H(k,\alpha)$ *given in Eq. (4.108) has the following properties:*

(i) *If* $H(k,\alpha) > k$*,* $H(k,\alpha)$ *monotonically decreases as* k *increases;*

(ii) *If* $H(k,\alpha) < k$*,* $H(k,\alpha)$ *monotonically increases as* k *increases;*

(iii) *If* $H(k,\alpha) = k$*, then* $H(k,\alpha) = H(k+1,\alpha)$*;*

(iv) *If* $H(k,\alpha) > k$*, then* $H(k+1,\alpha) > k$*;*

(v) *If* $H(k,\alpha) = k$*, then* $H(k+1,\alpha) = k$*;*

(vi) *If* $H(k,\alpha) < k$*, then* $H(k+1,\alpha) < k$*.*

Please refer to Appendix A.6 for the proof of this Lemma.

Now since $k = \arg\min_{i:\alpha>\gamma_i} H(i,\alpha)$, if $H(k,\alpha) > k$, by property (i) in Lemma 4.5.1, $H(k,\alpha) > H(k+1,\alpha)$. Since $\gamma_{k+1} < \gamma_k < \alpha$, this contradicts our assumption that $k = \arg\min_{i:\alpha>\gamma_i} H(i,\alpha)$. So $H(k,\alpha) \leq k$. □

In many cases, we may be only interested in the integer part of the minimum $H(k,\alpha)$, i.e., $H_o(\lambda,\alpha) \triangleq \lfloor \min_{k:\alpha\geq\gamma_k} H(k,\alpha) \rfloor$ (where $H(k,\alpha)$ is given in Eq. (4.108)). For example, if whenever a node is schedule to be active, it is so until the end of its lifetime, the maximum achievable lifetime is upper bounded by H_oT. In this circumstance, we can have more efficient ways to calculate the lifetime upper bound H_oT, which is stated in the following Corollary.

Corollary 4.5.1 (i) $H_o(\lambda,\alpha) = \max_{\alpha>\gamma_k}\{k : H(k,\alpha) \geq k\}$,

(ii) $H_o(\lambda,\alpha) = \min_{\alpha>\gamma_k}\{k : H(k,\alpha) < k\} - 1$.

Before we give the proof of this corollary, we discuss its implications. Without this corollary, in order to find H_o, we need to evaluate $H(k,\alpha)$ for every k such that $\gamma_k < \alpha$. The maximal possible value of k can be the total number, n, of nodes. Hence the time complexity of finding H_o is $\Theta(n)$. However, with this corollary, we can perform binary division to reduce the time complexity of finding H_o to $\Theta(\log n)$. Due to the fact that γ_k monotonically decreases as k increases, we can find the minimum k_m such that $\gamma_{k_m} < \alpha$ using binary division. For any $k > k_m$, if $H(k,\alpha) \geq k$ we only need to look at those H_j's for $j \geq k$ and if $H(k,\alpha) < k$ we only need to look at those H_j's for $j < k$. As a result, we can perform binary division again.

Proof of Corollary 4.5.1. (i) By Lemma 4.5.1 (i), (v) and (vi), $j \equiv \max\{k : H(k,\alpha) \geq k\}$ exists and is unique. We consider two cases: $H(j,\alpha) = j$ and $H(j,\alpha) > j$.

If $H(j,\alpha) = j$, by the definition of j, $H(k,\alpha) < k$ for any $k > j$. By Lemma 4.5.1 (ii), (iii), and induction on k, $H(k,\alpha) \geq H(j,\alpha)$ for all $k > j$. For any $k < j$ such that $\alpha > \gamma_k$, we claim that $H(k,\alpha) > k$. Otherwise $H(k,\alpha) \leq k$. By Lemma 4.5.1 (v), (vi), and induction on all $m \geq k$, $H(m+1,\alpha) \leq m$. Thus $H(j,\alpha) < j$ and this contradicts the definition of j. Since $H(k,\alpha) > k$ for any $k < j$ such that $\alpha > \gamma_k$, by Lemma 4.5.1 (i) and induction, $H(k,\alpha) > H(j,\alpha)$. Thus, $H(j,\alpha) = j$ is the minimum of $H(k,\alpha)$ for all k such that $\alpha > \gamma_k$.

If $H(j,\alpha) > j$, by the definition of j, $H(k,\alpha) < k$ for all $k > j$. By Lemma 4.5.1 (ii) and induction on k, $H(k,\alpha) > H(j+1,\alpha)$ for all $k > j+1$. For any $k \leq j$ such that $\alpha > \gamma_k$, we claim that $H(k,\alpha) > k$. Otherwise, $H(k,\alpha) \leq k$. By Lemma 4.5.1 (v), (vi) and induction on all $m \geq k$, $H(m+1,\alpha) \leq m$. Hence $H(j,\alpha) < j$ and contradicts the definition of j again. So we can see that $H(j+1,\alpha)$ is the minimum of $H(k,\alpha)$ for all k such that $\alpha > \gamma_k$. In addition since $H(j,\alpha) > j$, by Lemma 4.5.1 (iv), $H(j+1,\alpha) > j$. By the definition of j, $H(j+1,\alpha) < j+1$. As a result, $H_o(\lambda,\alpha) = \lfloor H(j+1,\alpha) \rfloor = j$.

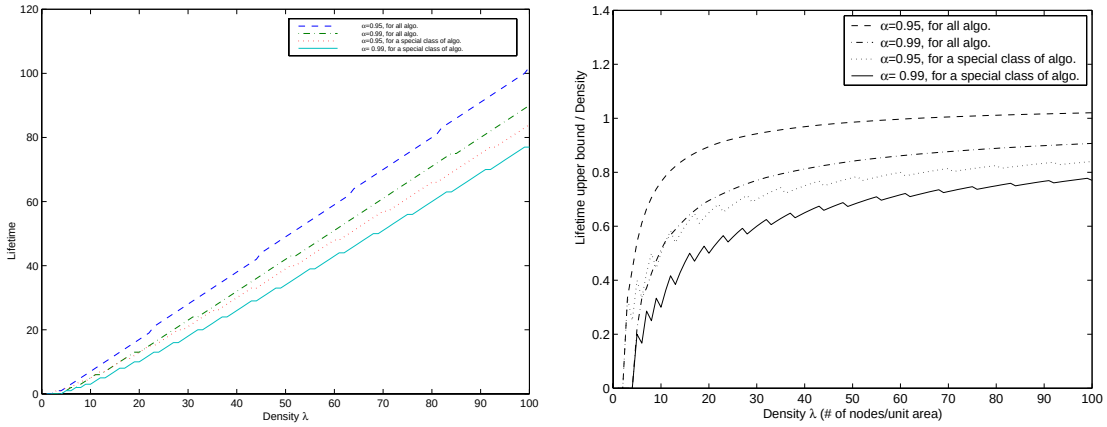

(a) Average α-lifetime upper bound v.s. density

(b) Average α-lifetime upper bound per unit of density v.s. the density

Figure 4.8: Upper bounds of average α-lifetime and α-lifetime per unit of density derived in Section 4.5.1 and in Section 4.5.2.

The proof for (ii) is similar, and is thus omitted. □

Numerical examples Figure 4.8 gives the upper bound of the lifetime derived in Section 4.5.1 and that in this subsection, and their respective upper bound of lifetime per unit of density. As compared with the upper bound of the lifetime derived in Section 4.5.1, the "universal" upper bound of the lifetime increases by 15% for 99%-coverage and over 20% for 95%-coverage. It is not surprising to observe that the lifetime per unit density can be more than 1 in some cases, because less than 100%-coverage is required in each round.

Another interesting finding is that although it is, in general, desirable to deploy sensors with high density to achieve a large lifetime per unit of nodal density, the increase in the lifetime per unit of nodal density levels off when the density exceeds certain threshold. The overhead incurred in maintaining coverage in a distributed manner dominates when the sensor density becomes very high.

4.6 Approaching the α-Lifetime Upper Bound

Although we have developed the α-lifetime upper bounds, it is not clear whether or to what extent, the derived upper bounds can be achieved. In this section, we devise an algorithm to (sub)-optimally schedule the wakeup and sleep schedule of each node to achieve a lifetime that is close to the (universal) upper bound. The algorithm makes use of the derived α-lifetime upper bounds and chooses a subset of nodes to be active in each round, with the objective of maximizing the universal lifetime upper bound of the remaining nodes that have not been scheduled to be active. We also carry out simulation to compare the

derived lifetime upper bounds, the actual lifetime achieved using the devised algorithm, and the lifetime achieved using a baseline algorithm where in each round a minimum number of nodes are chosen to meet the coverage requirement. The simulation results show that the devised algorithm can achieve nearly (and sometimes over) 90% of the universal lifetime upper bound in most cases, and it outperforms the baseline algorithm by 15-20%. These results imply that i) the derived universal lifetime upper bound is tight; and ii) the devised algorithm is effective in determining the achievable lifetime.

The significance of our study is that it shows that to improve the sensor network lifetime per unit of node density, one can either i) deploy sensor nodes with high density (as practically allowed by a distributed algorithm); or ii) allow a small portion of the area to be uncovered. For the second strategy, an algorithm should start with providing α-coverage from the beginning, where α is the percentage of the area that can be uncovered. Our study also suggests that choosing the minimum number of nodes to maintain coverage in each round is not always optimal with respect to maximizing the network lifetime. In general, it is better to choose a subset of nodes that maximizes the lifetime upper bound of the remaining nodes.

4.6.1 The algorithms

In this section we devise a centralized algorithm that maximizes α-lifetime. The algorithm is designed to maintain α-coverage from the very beginning. There are two purposes for devising a centralized algorithm. First, it can be used to investigate whether, or to what extent, the derived lifetime upper bound in Section 4.5.2 can be achieved under practical assumptions. Note that the tightness proof in Section 4.5.2 is based on the assumption that the coverage region of a node can be arbitrarily selected to provide α-coverage. In practice, at any time, a node's coverage region is either completely selected or completely unselected for providing α-coverage. Under this practical condition, in general the derived lifetime upper bound cannot be achieved exactly. A centralized algorithm can be used to investigate to what extent the lifetime upper bound can be achieved. Second, a good centralized algorithm provides a practical upper bound of the lifetime that can be possibly achieved by any distributed/localized algorithm, thus serving as a baseline of performance comparison for distributed algorithms.

To facilitate the description of the algorithm, we first define several notations:

Definition 4.6.1 *An* α-cover *is a set of nodes which can cover at least* α *portion of the monitored region.*

Definition 4.6.2 *A* minimal α-cover *is an* α*-cover from which removing any node will lead to a coverage ratio less than* α*.*

```
α-Lifetime Algorithm
1.  the remaining set of nodes = the set of all nodes,
2.  lifetime = 0,
3.  while (the remaining set of nodes have α coverage)
4.      find an initial minimal α-cover C,
5.      search for a minimal α-cover which maximizes the
            lifetime upper bound of the remaining nodes,
6.      lifetime += 1,
7.  endwhile
```

Figure 4.9: α-Lifetime algorithm

Definition 4.6.3 *A* trim operation *is an operation of reducing a α-cover to a minimal α-cover by iteratively visiting each node in the α-cover and removing the node if after removing the node, the remaining nodes can still provide α-coverage.*

The basic idea of the algorithm is that in each round, it tries to find a minimal α-cover which maximizes the α-lifetime upper bound of the remaining set of nodes (i.e., those which have not been selected in earlier rounds and the current round). The maximization is performed through a global, greedy search, while jumping out local minima.

The pseudo-code of the algorithm is listed in Figure 4.9-4.11. The algorithm continuously searches for minimal α-covers until the remaining set of nodes cannot provide α-coverage. In each round (line 4-6 in Figure 4.9), the algorithm seeks a minimal α-cover which maximizes the α-lifetime upper bound of the remaining set of nodes. The search in each round is composed of two steps. In the first step (Figure 4.10), it finds a minimal α-cover, which is obtained by first iteratively selecting the node that maximizes the coverage improvement of the current cover divided by the reduction of the lifetime upper bound of the remaining set of nodes (line 2-5 in Figure 4.10) and then performing a trim operation (line 6 in Figure 4.10).

In the second step (Figure 4.11), a global search is performed to further improve the lifetime upper

```
Finding an initial minimal α-cover C
1.  C = ∅, coverage = 0,
2.  while (coverage < α)
3.      Find the node in the remaining set of nodes that maximizes
            the coverage improvement of C divided by the reduction
            of the lifetime upper bound of the remaining nodes
            due to moving the node from the remaining set to C,
4.      move the node to C and update the coverage of C,
5.  endwhile
6.  trim the cover C,
7.  return C.
```

Figure 4.10: Procedure for finding an initial minimal α-cover

```
/* Search for a minimal α-cover which maximizes the
lifetime upper bound of the remaining nodes */
GlobalSearch(C)
1.  improved = true,
2.  while (improved)
3.      improved = false,
4.      for (each node in the remaining set)
5.          move the node to the α-cover C
6.          trim the cover C,
7.          if (there is improvement on the lifetime
                upper bound of the remaining set)
8.              keep the current α-cover C,
9.              improved = true,
10.         else
11.             revert to the original α-cover C.
12.         endif
13.     endfor
14. endwhile
```

Figure 4.11: Global search for a minimal α-cover that maximizes lifetime upper bound of the remaining nodes.

bound of the remaining set of nodes. In each iteration of the search, a node (sequentially chosen) in the remaining set is added to the found minimal α-cover (line 5 in Figure 4.11) and is followed by a trim operation (line 6 in Figure 4.11). If the new minimal α-cover leads to a larger lifetime upper bound, the new minimal α-cover is kept as the starting point for the next iteration; otherwise the original minimal α-cover is kept (line 7-12 in Figure 4.11). The global search finishes when adding to the minimal α-cover any node in the remaining set of nodes followed with a trim operation does not lead to any improvement on the lifetime upper bound of the remaining nodes. The lifetime is then the number of α-covers constructed.

Baseline Algorithm As a baseline algorithm for comparison, we have also implemented an algorithm that performs the same search for minimal α-covers except that the objective in each round of the algorithm is to find a minimal α-cover that minimizes the number of nodes in the α-cover.

4.6.2 Simulation study

In this section, we carry out several sets of simulations to validate the theoretical lifetime upper bound and to investigate to what extent the upper bound can be achieved by the algorithm we have developed. In addition, we are mostly interested in the lifetime achievable using algorithms that maintain α-coverage from the very beginning, although we will also compare it with the lifetime upper bound for algorithms that maintain as large coverage as possible.

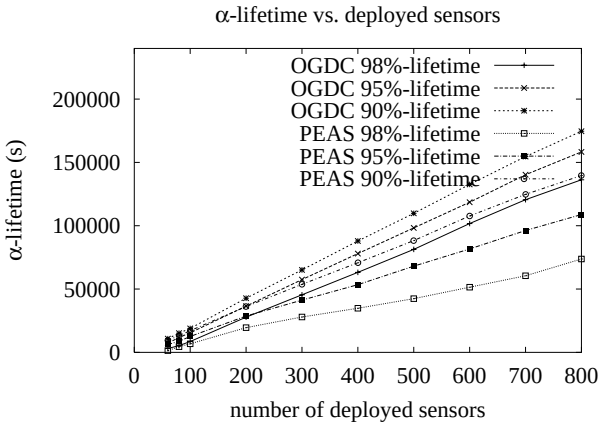

Figure 4.12: Average 95%-lifetime upper bounds and the achieved 95%-lifetime.

Simulation methodology

We randomly place N nodes in a square region R with 100×100 pixels. The positions of the nodes are independently and uniformly distributed in the square region. We assume that each node has a sensing range of r. For each pixel we count the number of disks that cover it. For each randomly generated instance, we calculate the k-vacancy V_k by counting the number of pixels that are not covered by at least k nodes. With the numerical value of V_i, we compute the upper bound of the lifetime for the special class of algorithms using Eq. (4.105), and that for all algorithms using Eq. (4.108). The lifetime of a single sensor T is set to 1. To accommodate the effect of sensing radius, the (normalized) network density is evaluated as $\frac{N\pi r^2}{10000}$. All the results reported below are averages of 10 simulation runs.

Note that decreasing the disk radius with the side length of the square area fixed has the same effect of increasing the side length of the square area with the disk radius fixed. For each value of α we vary the disk radii over different runs (but keep the radii of all disks fixed in each run) to investigate how the area size of the region affects the upper bound of the lifetime. For each value of α and disk radius, we vary the number of sensors to change the node density. The performance metrics we consider are the actual lifetime achieved and the ratio of the achieve lifetime to its corresponding upper bound.

Simulation results

Figure 4.12 compares various lifetime upper bounds and the actual lifetime achieved using our algorithm and that using the baseline algorithm. In this simulation, we set $\alpha = 0.95$ and the radius r=20. We define the *critical point* as the point in the surveillance region that is covered by the least number of sensors and the *coverage degree* as the number of sensors which cover the critical point. The coverage degree is an upper bound of lifetime for complete coverage.

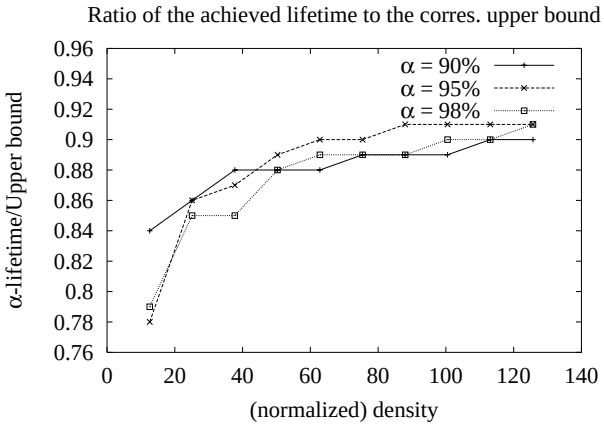

Figure 4.13: Average ratios of the achieved α-lifetime to the corresponding upper bound.

Several observations are in order. First, allowing a small portion of the region to be uncovered can lead to significant improvement on the system lifetime upper bound and the actual lifetime achieved. Even for the special class of algorithms that provide as much coverage as possible, the 95%-lifetime upper bound can improve by more than 100%. Second, the α-lifetime upper bound is significantly larger in the case that α-coverage is maintained from the very beginning (than in the case that as maximum coverage as possible is maintained until the coverage ratio drops below a certain threshold α. For α=95%, the improvement is usually more than 50%. Third, the actual lifetime achieved by the proposed algorithm is much larger than that by an algorithm that maintain as maximum coverage as possible at the beginning. Although we have not devised the latter algorithm, we can make this conclusion by observing that the former is much larger (usually by 30-40%) than the upper bound of the latter. This suggests that it is desirable to maintain α-coverage from the beginning of system operations, as long as this is acceptable to applications. Fourth, although it is in general a good choice to select a minimum subset of nodes to maintain α-coverage, this does not always lead to maximum lifetime. As a matter of fact, the proposed algorithm (which maximizes the lifetime upper bound of the remaining nodes) achieves over 20% longer lifetime than the baseline algorithm which minimizes the number of nodes used in each round. All these performance trends have been observed for different combinations of sensing radii and α values.

Note that the lifetime upper bound depicted in Figure 4.12 is smaller than that in Figure 4.8. This is because in Figure 4.8, we used $E(V_k)$ to replace V_k, which usually increases the lifetime upper bound. Also, we take into consideration of the boundary effect in Figure 4.12 — if some portion of the coverage area of a node falls outside of the monitored region, it does not contribute to the lifetime upper bound.

Figure 4.13 shows the average ratio of the actual lifetime achieved using our algorithm to the corresponding upper bound for three different values of α: 90%, 95% and 98%. The ratio increases as the

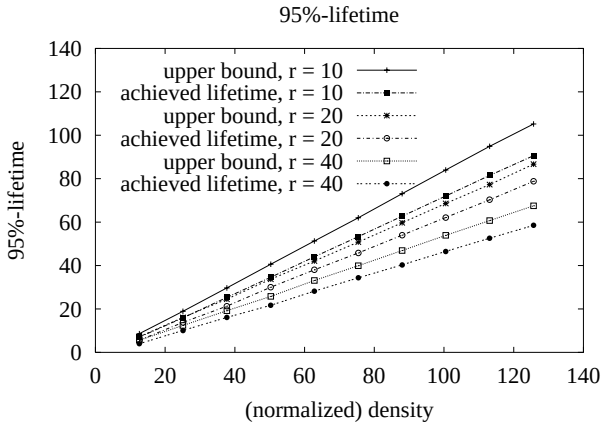

Figure 4.14: Achieved 95%-lifetime and corresponding upper bound for different values of sensing radii: 10, 20, 40.

node density increases, but levels off when the node density becomes sufficiently large. This is because when the density is too small, there is little room for optimizing the coverage usage. When the density is very high, the lifetime is limited by the upper bound and the practical physical constraint (i.e. a node's coverage area has to be either completely used or completely not used). This is another argument for deploying sensor nodes with a relatively high density. On the other hand, little difference has been observed in the average ratio with different values of α.

Figure 4.14 shows the actual 95%-lifetime achieved and the corresponding upper bound for three different values of sensing radii:10, 20, and 40. As the radii increase, both the actual lifetime achieved and its corresponding upper bound decrease. This is because as the radii increase, there is a higher chance that some portion of the coverage area of a node falls out of the monitored region, and thus

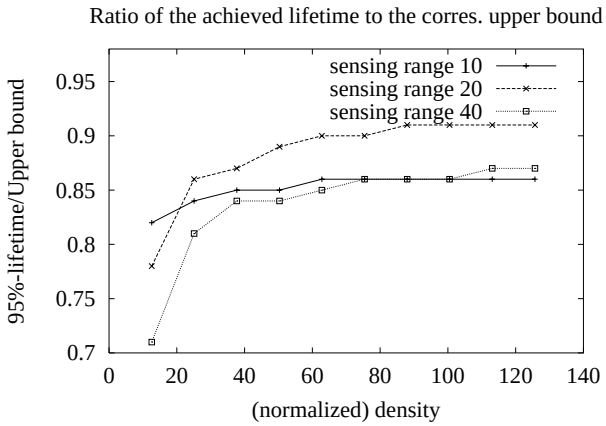

Figure 4.15: Average ratios of the achieved α-lifetime to the corresponding upper bound for different values of sensing radii.

the effective coverage areas given by all the nodes decrease. Figure 4.15 shows the average ratio of the achieved lifetime using the proposed algorithm to the corresponding upper bound for different values of sensing radii. It is a little surprising that the ratio decreases if the sensing radius is very large or very small. When the sensing radius is very large, the room for optimizing the coverage usage is small, leading to a low ratio of the actual lifetime achieved to its corresponding upper bound. When the sensing radius is very small, to maintain the same normalized density as in the case of large sensing radii, one has to deploy much more sensor nodes. When the number of nodes becomes very large, the optimization problem becomes more challenging. The search algorithm may easily get stuck at some local minima and fails to find the minimal α-cover that maximizes the lifetime upper bound of the remaining nodes. This is partially confirmed by the fact that in the low density case, the ratio with smaller radii is larger than that with larger radii in Figure 4.15.

4.7 Conclusions

In this chapter we have investigated the upper bound of α-lifetime for large scale sensor networks. We first derive the asymptotic node density required to ensure full coverage for the duration of k times the lifetime of a single sensor (in the almost surely sense) in large sensor networks, as the network size approaches infinity. We have considered several different model assumptions including Torus convention and non-Torus convention. We have also considered three different types of node deployment methods: Poisson process deployment, uniformly random deployment, and regular grid deployment. We have also derived two upper bounds of α-lifetime in a finite region with a finite density of nodes: (i) an upper bound of α-lifetime for a special family of algorithms in which the entire region is completely covered initially, and the coverage ratio is gradually reduced until it drops below a certain threshold α; and (ii) an upper bound of α-lifetime that applies to algorithms that maintain the coverage ratio of α from the beginning of network deployment. In addition, we have devised an algorithm that can approach the derived α-lifetime upper bounds. Simulation results show that our algorithm can achieve around 90% of the lifetime upper bounds when the node density is reasonably large.

With our derivation, we are able to determine, given the lifetime T of a single sensor node, how many sensor nodes have to be deployed in a region, in order to continuously monitor the region for a period of $k \cdot T$.

However, we observe that although it is, in general, desirable to deploy sensors with high density to achieve a large lifetime per unit of nodal density, the increase in the lifetime per unit of nodal density becomes marginal when the density exceeds certain threshold. In addition, as the node density increases,

the overhead of performing density control will increase. Specifically, as the density increases, the control packets may incur more collisions, and it may take more time (and more energy consumption due to packet retransmission) for the density control process to complete.

Another limitation of the work is that the sensing area of a node is assumed to be a uniform disk. In general, the sensing areas of different nodes may be different. Moreover, the sensing area of a node may be of an arbitrary shape. Investigating the lifetime upper bound and devising algorithms for maintaining coverage under the general case is the second subject of our future work.

Chapter 5

Critical Total Power for k-Connectivity of Wireless Networks

5.1 Introduction

One important issue in wireless ad hoc networks is how to reduce transmission power while maintaining network connectivity. Reducing transmission power not only saves energy, but also reduces MAC-level collision and hence increases network capacity. However, in order to maintain proper network operations, it is also necessary to ensure network connectivity. In many circumstances (such as in the presence of node failures or mobility), it is important that the networks are k-connected in order to enable robust communications.

The goal of this chapter is to quantify the asymptotic minimum power required for maintaining (k-)connectivity. Several other works [59, 35, 56, 57, 62, 73] study the asymptotic minimum common transmission range in order to ensure connectivity or k-connectivity.

In this chapter, instead of imposing the uniform assumption that all nodes are subject to the same common minimum power, we assume each node can choose different transmission power to ensure connectivity or k-connectivity. Under this assumption, we investigate the asymptotic bounds of the minimum total power (termed as *critical total power*) required for maintaining *k-connectivity* in a random wireless network on a unit square $S = [0,1]^2$. Specifically, let $W_{t,i}$ be the critical transmission power node i uses, and $R_{t,i}$ the corresponding transmission range of node i under the power model $W_{t,i} = R_{t,i}^c$, where $2 \le c \le 4$ is the path loss exponent. Then the critical total power of all the nodes is $W_c = \sum W_{t,i} = \sum R_{t,i}^c$, where the summation is taken over all the nodes in the network. Under the assumption that wireless nodes are distributed on a unit square $S = [0,1]^2$ according to a homogeneous Poisson point process with density λ, we show that the critical total power $W_c = \sum R_{t,i}^c$ for maintaining k-connectivity is $\Theta(\frac{\Gamma(c/2+k)}{(k-1)!}\lambda^{1-c/2})$ with probability approaching 1 as $\lambda \to \infty$.

We derive a lower bound and an upper bound of the critical total power. The lower bound is derived based on the necessary condition that every node must be able to reach its kth nearest neighbor in order to maintain strong k-connectivity. The upper bound is derived based on an assertion (which is also proved in this chapter) that the resulting network is strongly k-connected, if every node can reach at least k

nodes in each of its four quadrants as long as there are at least k nodes in that quadrant. (By "each of its four quadrants", we assume that every node has its own coordinate system which is obtained by shifting the origin of the $[0,1]^2$ plane to its own location.) In the case that there are less than k nodes in a quadrant, the transmission power of the node should be sufficiently large to reach all of them.

Our results suggest that the power saved using optimal, non-uniform transmission ranges is in an order of $(\log \lambda)^{c/2}$ as compared to that using optimal uniform transmission ranges. In a rescaled network where the node density is kept fixed and the size of the square region goes to infinity, our results indicate that the average power of each node is bounded if we allow each node to choose its own transmission power to maintain (k-)connectivity, while the average power of each node is unbounded if all nodes have to choose a common power to maintain (k-)connectivity. These results are not determined by a specific algorithm, but rather a fundamental property in wireless networks.

The rest of the chapter is organized as follows. In Section 5.2, we state the system model, formulate the problem, and present preliminary material that will be used in subsequent sections. We then derive in Sections 5.3–5.4 respectively, the lower and upper bounds on the critical total power. Following that, we compare our results with those derived under the uniform metric assumption and discuss the issue on the transmission power model in Section 5.5. We perform simulations to validate the derived results in Section 5.6. Finally, we conclude the chapter in Section 5.7.

5.2 Preliminaries

In this section we present the system model, and introduce notations that will be used throughout the chapter. We also define two frequently-used random variables: $R_{\lambda,k}(\alpha)$ and $R_{\lambda,k}(d,\alpha)$ (to be defined in Subsection 5.2.3), derive their probability distributions and prove two lemmas that will be used in subsequent sections. Finally we present Palm theory on Poisson point process that will be used in this chapter.

5.2.1 System model

We assume nodes are distributed on a unit square $S = [0,1]^2$ according to a (homogeneous) Poisson point process $\mathcal{P}_\lambda$ with density λ. It is well accepted that n nodes whose locations are independent random variables, each with a uniform distribution on S, are essentially a Poisson point process with density n if the network size is large ([36], page 39). For the ease of presentation, we first assume the Toroidal model (Torus convention) [56] to eliminate the boundary effects and we will remove this assumption later in this chapter. In the Toroidal model, the Euclidean metric $d(i,j) = |X_i - X_j|$ is replaced with

$d(i,j) = \min_{z\in\{0,1\}^2} |X_i - X_j - z|$, where X_i is the coordinate of node i. Under the Toroidal model assumption, each node can view the original plane $[0,1]^2$ as the plane $[-\frac{1}{2},\frac{1}{2}]^2$ in a coordinate system centered at itself.

Let R_i denote the (fixed) transmission range of node i. Different nodes may use different transmission power and hence have different transmission ranges. Node i can directly transmit to node j if and only if $d(i,j) \le R_i$. We further assume that the transmission power of node i is $W_i = R_i^c$, where $2 \le c \le 4$ is the path loss exponent (although our analysis applies to any $c > 0$). Hence the total power of all nodes is

$$W = \sum_{i\in\mathcal{P}_\lambda} W_i = \sum_{i\in\mathcal{P}_\lambda} R_i^c. \tag{5.1}$$

The network can be viewed as a directed graph where each wireless node is a vertex and a directed edge exists from vertex i to j if and only if node i can directly transmit to node j. The network is said to be k-connected if and only if the corresponding directed graph is strongly k-connected, i.e., there exists a directed path from any vertex i to any other vertex j even if we remove any $k-1$ nodes from the network. The *critical total power W_c for k-connectivity* is defined as the minimum total power of all nodes required to ensure strong k-connectivity in the formed directed graph. As we are mostly interested in k-connectivity in this chapter, the critical total power W_c is henceforth by default for k-connectivity.

Let $W_{t,i}$ be the *critical* transmission power node i uses, and $R_{t,i}$ the corresponding transmission range of node i, then $W_c = \sum W_{t,i} = \sum R_{t,i}^c$. We are interested in deriving the asymptotic bounds on the critical total power W_c as $\lambda \to +\infty$.

5.2.2 Notations

Table 5.1 gives the notations used throughout this chapter. Several comments are in order:

- We envision a (homogeneous) Poisson point process $\mathcal{P}_\lambda$ on a unit square area $S = [0,1]^2$. This is often related to a binomial point process $\mathcal{X}_n$, i.e., n independent, uniformly distributed random 2-dimensional vectors on S. We use X_i to denote node i's location (coordinate).
- We use C_j to represent a (constant) function independent of λ. Unless specified, C_j only depends on the path loss exponent c and sometimes k, both of which are assumed to be constant in this chapter. We may explicitly express c as the parameter of C_i when we need to use the function of C_i with a different parameter (such as $2c$).
- Let $f(X)$ be a function on a random variable X (which can be a vector). By probability theory, the expectation of $f(X)$ is simply the integral of $f(X)$ over the probability space of X, i.e., $E[f(X)] =$

Table 5.1: Notations used

$\mathbb{R}$	Real line, $(-\infty, +\infty)$
S	$[0,1]^2$
$\mathcal{X}_n$	A binomial process (n independent, uniformly distributed random 2-vectors)
$\mathcal{P}_\lambda$	A homogeneous Poisson point process with density λ; $\{X_1, X_2, \cdots X_{N_\lambda}\}$
X_i	Node i's coordinate/location
C_j	(Constant) function that does not depend on λ
$\bar{G}$	The complement set of G
$\mathbf{1}_G$	The indicator function of G
$E[f(X)]$	Expectation of $f(X)$, i.e., $E[f(X)] = \int f(X)dP$
$E_G[f(X)]$	Expectation of $f(X)$ with the restriction G, i.e., $E_G[f(X)] = \int_G f(X)dP$
$\mathcal{B}_X(r)$	Ball of radius r centered at location X
$\mathcal{C}_X(\alpha, \beta)$	Cone that is centered at X and with the starting angle α and the ending angle β
$\mathcal{C}_X^*(r, \alpha, \beta)$	$\mathcal{B}_X(r) \cap \mathcal{C}_X(\alpha, \beta)$
$R_{\lambda,k}(\alpha)$	Random variable for the distance from a point X to the kth nearest node in $\mathcal{C}_X(\theta, \theta+\alpha)$
$R_{\lambda,k}(d, \alpha)(= R_\lambda(d, \alpha))$	Random variable for the distance from a point X to the kth nearest node in $\mathcal{C}_X^*(d, \theta, \theta+\alpha)$
$\Gamma(s)$	Gamma function, i.e., $\Gamma(s) = \int_0^\infty t^{s-1}e^{-t}dt$
$F_{\Gamma(s)}(x)$	c.d.f. of the Gamma distribution function, i.e., $F_{\Gamma(s)}(x) = (\Gamma(s))^{-1}\int_0^x t^{s-1}e^{-t}dt$
$\approx_\lambda$	$g(\lambda) \approx_\lambda h(\lambda)$ is interpreted as $g(\lambda)/h(\lambda) \to 1$ as $\lambda \to \infty$

$\int f(X)dP$. The expectation, $E_G[f(X)]$, of a function $f(X)$ under restriction G is the integral of $f(X)$ over the subset G of the probability space, i.e., $E_G[f(X)] = \int_G f(X)dP = \int \mathbf{1}_G f(X)dP$, where $\mathbf{1}_G$ is the indicator function of G. With this definition, by the law of total probability, $E[f(X)] = E_G[f(X)] + E_{\bar{G}}[f(X)]$, where $\bar{G}$ denotes the complement set of G; and by the law of conditional probability, $E_G[f(X)] = E[f(X)|G]P(G)$, where $P(G)$ is the probability that G occurs.

- We define $\mathcal{B}_X(r)$ as the ball (disk in a 2-dimensional space) centered at X with radius r, and $\mathcal{C}_X(\theta, \theta+\alpha)$ as the cone centered at X, with starting angle θ, ending angle $\theta+\alpha$, where $0 \le \theta, \alpha \le 2\pi$. The degree of cone $\mathcal{C}_X(\theta, \theta+\alpha)$ is α. We use $\mathcal{C}_X^*(r, \theta, \theta+\alpha)$ to denote the region $C_X(\theta, \theta+\alpha) \cap \mathcal{B}_X(r)$.
- We write $g(\lambda) \approx_\lambda h(\lambda)$ if $g(\lambda)/h(\lambda) \to 1$ as $\lambda \to \infty$, $g(\lambda) = o(h(\lambda))$ if $g(\lambda)/h(\lambda) \to 0$ as $\lambda \to \infty$, and $g(\lambda) = O(h(\lambda))$ if $g(\lambda) \le C \cdot h(\lambda)$ as $\lambda \to \infty$ for some constant C (which may depend on the path loss exponent c).

5.2.3 $R_{\lambda,k}(\alpha)$ and $R_{\lambda,k}(d, \alpha)$ and their probability distributions

In an infinite region $\mathbb{R}^2$ with the Poisson point process $\mathcal{P}_\lambda$, we define $R_{\lambda,k}(\alpha)$ as a random variable that represents the distance from a node at X to its kth nearest neighbor in a cone centered at X and with degree α, i.e., $\mathcal{C}_X(\theta, \theta+\alpha)$. Clearly the distribution of $R_{\lambda,k}(\alpha)$ is independent of the choices of X and θ. $P(R_{\lambda,k}(\alpha) > r)$ is the probability that at most $k-1$ points in the Poisson point process $\mathcal{P}_\lambda$ fall in $\mathcal{C}_X^*(r, \theta, \theta+\alpha)$, and can be expressed as $\exp(-\lambda\alpha r^2/2)\sum_{i=0}^{k-1}\frac{(\lambda\alpha r^2/2)^i}{i!}$. The cumulative distribution function (c.d.f.) $F_{R_{\lambda,k}(\alpha)}$ and the probability density function (p.d.f.) $f_{R_{\lambda,k}(\alpha)}$ of $R_{\lambda,k}(\alpha)$ can then be

expressed as

$$F_{R_{\lambda,k}(\alpha)}(r) = P(R_{\lambda,k}(\alpha) \leq r) = \begin{cases} 1 - e^{-\lambda\alpha r^2/2} \sum_{i=0}^{k-1} \frac{(\lambda\alpha r^2/2)^i}{i!}, & \text{if } r \geq 0, \\ 0, & \text{otherwise;} \end{cases} \tag{5.2}$$

$$f_{R_{\lambda,k}(\alpha)}(r) = \begin{cases} \frac{(\lambda\alpha r^2/2)^{k-1}\lambda\alpha r}{(k-1)!} e^{-\lambda\alpha r^2/2}, & \text{if } r \geq 0, \\ 0, & \text{otherwise.} \end{cases} \tag{5.3}$$

Also, the expectation of $R^c_{\lambda,k}(\alpha)$ (for $c > 0$) can be calculated as

$$\begin{aligned} E[R^c_{\lambda,k}(\alpha)] &= \int_0^\infty f_{R_{\lambda,k}(\alpha)}(r) r^c dr \\ &= \int_0^\infty \frac{(\lambda\alpha r^2/2)^{k-1}\lambda\alpha r}{(k-1)!} e^{-\lambda\alpha r^2/2} r^c dr \\ &\quad \text{(changing variable } t = \lambda\alpha r^2/2) \\ &= \int_0^\infty e^{-t} \left(\frac{2t}{\lambda\alpha}\right)^{\frac{c}{2}} \frac{t^{k-1}}{(k-1)!} dt \\ &= \frac{\Gamma(c/2+k)}{(k-1)!} \left(\frac{2}{\lambda\alpha}\right)^{c/2}, \end{aligned} \tag{5.4}$$

where the Γ function is defined as $\Gamma(k) = \int_0^\infty t^{k-1} e^{-t} dt$.

Another closely related random variable $R_{\lambda,k}(d,\alpha)$ (for $d > 0$) is defined as

$$R_{\lambda,k}(d,\alpha) = \begin{cases} R_{\lambda,k}(\alpha), & \text{if } R_{\lambda,k}(\alpha) \leq d, \\ 0, & \text{otherwise.} \end{cases} \tag{5.5}$$

$R_{\lambda,k}(d,\alpha)$ can be interpreted as the distance from a node at X to the kth nearest neighbor in a cone centered at X, with degree α, and within radius d, i.e., $\mathcal{C}^*_X(d,\theta,\theta+\alpha)$, where θ is a fixed value. In the case that there are less than k nodes in the cone within radius d, $R_{\lambda,k}(d,\alpha)$ is defined to be 0. Thus, $R^c_{\lambda,k}(d,\alpha)$ is a restriction of $R^c_{\lambda,k}(\alpha)$, under the sub probability space that there are at least k nodes in $\mathcal{C}^*_X(d,\theta,\theta+\alpha)$. The expectation of $R^c_{\lambda,k}(d,\alpha)$ can be similarly calculated as

$$\begin{aligned} E[R^c_{\lambda,k}(d,\alpha)] &= \int_0^d f_{R_{\lambda,k}(\alpha)}(r) r^c dr \\ &= \frac{\Gamma(\frac{c}{2}+k)}{(k-1)!} \left(\frac{2}{\lambda\alpha}\right)^{c/2} F_{\Gamma(c/2+k)}(\lambda\alpha d^2/2), \end{aligned} \tag{5.6}$$

where $F_{\Gamma(c/2+k)}$ is the c.d.f. of the Gamma distribution with parameter $c/2+k$. With fixed values of $\alpha, d, c, k > 0$, $F_{\Gamma(c/2+k)}(\lambda\alpha d^2/2) \to 1$ as $\lambda \to \infty$. Hence, we obtain the following lemma (that will be used in subsequent sections).

Lemma 5.2.1 *For fixed values of $d > 0, c > 0, \alpha > 0$ and k positive integer,*

$$E[R^c_{\lambda,k}(d,\alpha)] \approx_\lambda E[R^c_{\lambda,k}(\alpha)] = \frac{\Gamma(\frac{c}{2}+k)}{(k-1)!}\left(\frac{2}{\lambda\alpha}\right)^{c/2}. \tag{5.7}$$

Let A, B be two given nodes in the Poisson point process $\mathcal{P}_\lambda$ in the square region S, and $R_{A,\lambda,k}(\alpha)(R_{B,\lambda,k}(\beta))$ be the distance from A (B) to its kth nearest neighbor in a cone of degree $\alpha > 0$. Specific choices of the cones and the locations of nodes A and B are not important in the following lemma.

Lemma 5.2.2

$$E[R^c_{A,\lambda,k}(\alpha)R^c_{B,\lambda,k}(\alpha)] \le C_0\lambda^{c(-1+\delta_1)} \tag{5.8}$$

for some $C_0 > 0$ and any given $\delta_1 > 0$, if λ is sufficiently large, where C_0 only depends on c and α but not on λ.

Proof. For notational convenience, we denote $R_{A,\lambda,k}(\alpha)$ and $R_{B,\lambda,k}(\alpha)$ respectively as R_A and R_B in the following derivation. For any given $\delta_1 > 0$, we can choose $\epsilon > 0$ such that $\alpha\epsilon^2/2 = \lambda^{-1+\delta_1}$. We first note that

$$\begin{aligned}
P(R_AR_B \le \epsilon^2) &\ge P(R_A \le \epsilon \text{ and } R_B \le \epsilon) \\
&= 1 - P(R_A > \epsilon \text{ or } R_B > \epsilon) \\
&\ge 1 - (P(R_A > \epsilon) + P(R_B > \epsilon)) \\
&\ge 1 - 2\exp(-\lambda\alpha\epsilon^2/2)\sum_{i=0}^{k-1}\frac{(\lambda\alpha\epsilon^2/2)^i}{i!} \\
&= 1 - 2\exp(-\lambda^{\delta_1})\sum_{i=0}^{k-1}\frac{(\lambda^{\delta_1})^i}{i!}.
\end{aligned} \tag{5.9}$$

Thus,

$$P(R_AR_B > \epsilon^2) \le 2\exp(-\lambda^{\delta_1})\sum_{i=0}^{k-1}\frac{(\lambda^{\delta_1})^i}{i!}. \tag{5.10}$$

Now $E[R^c_AR^c_B]$ can be expressed as

$$\begin{aligned}
E[R^c_AR^c_B] &= E[R^c_AR^c_B|R_AR_B \le \epsilon^2]P(R_AR_B \le \epsilon^2) + E[R^c_AR^c_B|R_AR_B > \epsilon^2]P(R_AR_B > \epsilon^2) \\
&\le E[\epsilon^{2c}|R_AR_B \le \epsilon^2]P(R_AR_B \le \epsilon^2) + E[1|R_AR_B > \epsilon^2]P(R_AR_B > \epsilon^2) \\
&\le \epsilon^{2c} + 2\exp(-\lambda^{\delta_1})\sum_{i=0}^{k-1}\frac{(\lambda^{\delta_1})^i}{i!} \\
&\le \left(2\lambda^{-1+\delta_1}/\alpha\right)^c + C_1\lambda^{c(-1+\delta_1)}
\end{aligned}$$

$$= \quad C_0 \lambda^{c(-1+\delta_1)}, \tag{5.11}$$

where the second inequality from the fact that $P(R_A R_B \leq \epsilon^2) \leq 1$ and Eq. (5.10). The third inequality results from the choice of ϵ ($\alpha\epsilon^2/2 = \lambda^{-1+\delta_1}$) and the fact that $e^{\lambda^{\delta_1}}$ grows much faster than any polynomial function of λ. The choice of C_1, C_0 is independent of λ and δ_1 if δ_1 is fixed and λ is sufficiently large. □

5.2.4 Palm theory on Poisson point process

As Palm theory on the Poisson point process is used in multiple places in the chapter, we state the theorem ([55], Theorem 1.6) below.

Theorem 5.2.1 *(Palm theory for Poisson processes) Let $\lambda > 0$. Suppose $j \in N$, and $h(\mathcal{Y}, \mathcal{X})$ is a bounded measurable function defined on all pairs of the form $(\mathcal{Y}, \mathcal{X})$ with $\mathcal{X}$ being a finite subset of $\mathbb{R}^d$ and $\mathcal{Y}$ a subset of $\mathcal{X}$, satisfying $h(\mathcal{Y}, \mathcal{X}) = 0$ except when $\mathcal{Y}$ has j elements. Then*

$$E[\sum_{\mathcal{Y} \subseteq \mathcal{P}_\lambda} h(\mathcal{Y}, \mathcal{P}_\lambda)] = \frac{\lambda^j}{j!} E h(\mathcal{X}_j, \mathcal{X}_j \cup \mathcal{P}_\lambda), \tag{5.12}$$

where the sum on the left-hand side is over all subsets $\mathcal{Y}$ of the random Poisson point set $\mathcal{P}_\lambda$, and on the right-hand side the set $\mathcal{X}_j$ is a binomial process with j nodes, independent of $\mathcal{P}_\lambda$.

5.3 Lower Bound on the Critical Total Power

In this section, we derive the lower bound on the critical total power W_c to maintain network k-connectivity.

Theorem 5.3.1 *For any given $\delta > 0$, $P(W_c \geq (1-\delta) C_2 \frac{\Gamma(\frac{c}{2}+k)}{(k-1)!} \lambda^{1-\frac{c}{2}}) \to 1$ as $\lambda \to \infty$, where $C_2 = \pi^{-\frac{c}{2}}$.*

The proof of Theorem 5.3.1 will be given through two propositions. Clearly, in order to maintain strong k-connectivity, every node must be able to reach at least k other nodes. Thus a lower bound on the critical total power is the summation of power incurred by each node such that each node can exactly reach its kth nearest neighbor. Specifically, let X_i be the location of node i, r_i the distance from X_i to node i's kth nearest neighbor, $W_i = r_i^c$, and N_λ the number of nodes in the Poisson point process $\mathcal{P}_\lambda$ in $[0,1]^2$. Then the total power $W_L = \sum_{i=1}^{N_\lambda} W_i = \sum_{i=1}^{N_\lambda} r_i^c$ serves as a lower bound on the critical total power required to maintain k-connectivity. In what follows, we estimate W_L. First, we derive the expectation of W_L.

Proposition 5.3.1

$$E[W_L] \approx_\lambda \frac{\Gamma(\frac{c}{2}+k)}{(k-1)!}\pi^{-\frac{c}{2}}\lambda^{1-\frac{c}{2}}. \tag{5.13}$$

Proof. By Palm theory for the Poisson point process,

$$E[W_L] = E[\sum_{i=1}^{N_\lambda} r_i^c] = \lambda E[r_0^c], \tag{5.14}$$

where the last expectation is taken over the probability space where node 0 is randomly placed with a uniform distribution on S, together with a set of nodes distributed according to a Poisson point process $\mathcal{P}_\lambda$ and independent of X_0. Under the Toroidal model assumption, node 0 views all the nodes in $\mathcal{P}_\lambda$ as if they reside in $[-\frac{1}{2},\frac{1}{2}]^2$ of a coordinate system with the origin at X_0. Thus the distribution of r_0 is independent of the choice of X_0. Let s be the distance from X_0 to node 0's kth nearest neighbor in $\mathcal{P}_\lambda$ in $\mathcal{B}_{X_0}(1/2)$ if there are at least k nodes in $\mathcal{B}_{X_0}(1/2)$; and 0 otherwise. Then s has the same distribution as $R_{\lambda,k}(\frac{1}{2},2\pi)$. In addition, if $s>0$ (which means there are at least k nodes in $\mathcal{B}_{X_0}(1/2)$), then $r_0 = s$. Thus $s \le r_0$ and $E[s^c] \le E[r_0^c]$. Also, since $r_0 < 1$,

$$\begin{aligned} E[r_0^c] &= E[r_0^c|s>0]P(s>0) + E[r_0^c|s=0]P(s=0) \\ &= E[s^c|s>0]P(s>0) + E[r_0^c|s=0]P(s=0) \\ &\le E[s^c] + P(s=0). \end{aligned} \tag{5.15}$$

Since $P(s=0) = e^{-\lambda\pi/4}\sum_{i=0}^{k-1}\frac{(\lambda\pi/4)^i}{i!} = o(\lambda^{-c/2})$ as $\lambda\to\infty$ and $E[s^c] \approx_\lambda \frac{\Gamma(\frac{c}{2}+k)}{(k-1)!}(\lambda\pi)^{-\frac{c}{2}}$ (by Lemma 5.2.1), we obtain

$$\begin{aligned} E[r_0^c] &\approx_\lambda \frac{\Gamma(\frac{c}{2}+k)}{(k-1)!}(\lambda\pi)^{-\frac{c}{2}}, \\ E[W_L] &= \lambda E[r_0^c] \approx_\lambda \frac{\Gamma(\frac{c}{2}+k)}{(k-1)!\pi^{\frac{c}{2}}}\lambda^{1-\frac{c}{2}}. \end{aligned} \tag{5.16}$$

□

As has been shown in Lemma 5.2.1, the restriction on the distance to the kth nearest neighbor in a fixed cone (such as in one quadrant) can be ignored when the node density λ approaches infinity. In all the subsequent discussion, we ignore this restriction and assume, whenever desirable, the distance to the kth nearest neighbor can go to infinity (although with a small probability).

In order to bound $|W_L - E[W_L]|$, we need to derive the second moment of W_L (so that Chebyshov's inequality can be applied).

Proposition 5.3.2

$$E[W_L^2] \leq E[W_L]^2 + C_3\lambda^{1-c+\delta_0} \text{ as } \lambda \to \infty, \tag{5.17}$$

where $\delta_0 > 0$ is arbitrary but fixed and C_3 is a constant independent of λ.

Proof.

$$\begin{aligned} E[W_L^2] &= E[(\sum_{i=1}^{N_\lambda} W_i)^2] \\ &= E[\sum_{i=1}^{N_\lambda} W_i^2] + 2E[\sum_{1\leq i<j\leq N_\lambda} W_i W_j] \end{aligned} \tag{5.18}$$

Since $W_i^2 = r_i^{2c}$, by Proposition 5.3.1 we obtain

$$E[\sum_{i=1}^{N_\lambda} W_i^2] = E[\sum_{i=1}^{N_\lambda} r_i^{2c}] \approx_\lambda \frac{\Gamma(c+k)}{(k-1)!}\pi^{-c}\lambda^{1-c}. \tag{5.19}$$

For the second term of Eq. (5.18), we apply Palm theory for the Poisson point process again and obtain

$$2E[\sum_{1\leq i<j\leq N_\lambda} W_i W_j] = \lambda^2 E[W_A W_B], \tag{5.20}$$

where the last expectation is taken over the probability space where A and B are uniformly and randomly distributed on S, together with a set of nodes distributed according to a Poisson point process $\mathcal{P}_\lambda$.

We first evaluate $E[W_A W_B]$ conditioning on the locations, X_A and X_B, of nodes A and B.

$$E[W_A W_B] = E[E[W_A W_B | X_A, X_B]]. \tag{5.21}$$

Given the location X_A and X_B, let $|X_A - X_B| \equiv d$. Let G_A be the event that there are at least k nodes in $\mathcal{B}_{X_A}(d/2)$, G_B the event that there are at least k nodes in $\mathcal{B}_{X_B}(d/2)$, and $G = G_A \cap G_B$. Then,

$$E[W_A W_B | X_A, X_B] = E_G[W_A W_B | X_A, X_B] + E_{\bar{G}}[W_A W_B | X_A, X_B]. \tag{5.22}$$

The first term of Eq. (5.22) can be expressed as

$$\begin{aligned} E_G[W_A W_B | X_A, X_B] &= E_G[r_A^c r_B^c | X_A, X_B] \\ &= E[r_A^c r_B^c \mathbf{1}_G | X_A, X_B] \\ &= E[r_A^c r_B^c \mathbf{1}_{G_A} \mathbf{1}_{G_B} | X_A, X_B] \end{aligned}$$

$$= \quad E[\tilde{r}_A^c \tilde{r}_B^c | X_A, X_B], \tag{5.23}$$

where

$$\tilde{r}_A = r_A \mathbf{1}_{G_A} = \begin{cases} r_A, & \text{if } r_A \le d/2, \\ 0, & \text{otherwise;} \end{cases}$$

$$\tilde{r}_B = r_B \mathbf{1}_{G_B} = \begin{cases} r_B, & \text{if } r_B \le d/2, \\ 0, & \text{otherwise.} \end{cases}$$

Given the locations X_A and X_B, $\tilde{r}_A$ and $\tilde{r}_B$ are completely determined by the node distribution in $\mathcal{B}_{X_A}(d/2)$ and that in $\mathcal{B}_{X_B}(d/2)$ respectively. Since the two regions $\mathcal{B}_{X_A}(d/2)$ and $\mathcal{B}_{X_B}(d/2)$ are disjoint, $\tilde{r}_A$ and $\tilde{r}_B$ are independent. Hence we can evaluate their expectations separately:

$$E_G[W_A W_B | X_A, X_B] = E[\tilde{r}_A^c | X_A, X_B] E[\tilde{r}_B^c | X_A, X_B]. \tag{5.24}$$

Note that the expectation of $\tilde{r}_A^c$ conditioned on X_A and X_B, $E_G[W_A W_B | X_A, X_B]$, is taken over the probability space of a Poisson point process $\mathcal{P}_\lambda$ on S. For each instance (realization) of $\mathcal{P}_\lambda$ on S, we can define $\hat{r}_A$ to be the kth nearest neighbor distance of node A with node B removed from S. Then $\tilde{r}_A \le \hat{r}_A$. Clearly, $\hat{r}_A$ is independent of node B's location. $\hat{r}_A$ is also independent of node A's location because of the homogeneous Poisson point process assumption and the Toroidal model assumption. Thus $E[\tilde{r}_A^c | X_A, X_B] \le E[\hat{r}_A^c | X_A, X_B] = E[\hat{r}_A^c]$. Finally, $\hat{r}_A$ is just the distance between node A (which is uniformly and randomly placed on S) and its kth nearest neighbor from $\mathcal{P}_\lambda$ on S. Thus $E[\hat{r}_A^c] = E[r_0^c]$, where $E[r_0^c]$ is given in Eq. (5.14). Therefore, $E[\tilde{r}_A^c | X_A, X_B] \le E[r_0^c]$. Similarly, $E[\tilde{r}_B^c | X_A, X_B] \le E[r_0^c]$. Since $E[W_L] = \lambda E[r_0^c]$ by Eq. (5.14), we obtain that

$$E[E_G[W_A W_B | X_A, X_B]] \le E[E[r_0^c]^2] = E[r_0^c]^2 = (E[W_L]/\lambda)^2 \tag{5.25}$$

It remains to evaluate the second term $E_{\bar{G}}[W_A W_B | X_A, X_B]$ in Eq. (5.22). Since $\bar{G} = \bar{G}_A \cup \bar{G}_B$, we have

$$\begin{aligned} E_{\bar{G}}[W_A W_B | X_A, X_B] &\le E_{\bar{G}_A}[W_A W_B | X_A, X_B] + E_{\bar{G}_B}[W_A W_B | X_A, X_B] \\ &= E_{\bar{G}_A}[r_A^c r_B^c | X_A, X_B] + E_{\bar{G}_B}[r_A^c r_B^c | X_A, X_B] \\ &= 2E_{\bar{G}_A}[r_A^c r_B^c | X_A, X_B], \end{aligned} \tag{5.26}$$

where the last equality is by symmetry.

The basic idea to bound $E_{\bar{G}_A}[r_A^c r_B^c | X_A, X_B]$ is that if the distance, d, between nodes A and B is large, $\bar{G}_A$ occurs with low probability, and that the probability that the distance d is small is low. Specifically, consider the restriction of $|X_A - X_B| = d > \epsilon$ where ϵ is chosen such that $\pi\epsilon^2 = \lambda^{-1+\delta_1}$ for any fixed $\delta_1 > 0$.

$$\begin{aligned}
E_{\{d>\epsilon\}}[E_{\bar{G}_A}[r_A^c r_B^c | X_A, X_B]] &\leq E_{\{d>\epsilon\}}[E_{\bar{G}_A}[1 | X_A, X_B]] \\
&\leq P(\bar{G}_A \cap \{d > \epsilon\}) \\
&\leq P(\text{There are less than } k \text{ nodes in } \mathcal{B}_A(\epsilon/2)) \\
&= \exp(-\lambda\pi(\epsilon/2)^2) \sum_{i=0}^{k-1} \frac{(\lambda\pi(\epsilon/2)^2)^i}{i!} \\
&= \exp(-\lambda^{\delta_1}/4) \sum_{i=0}^{k-1} \frac{(\lambda^{\delta_1}/4)^i}{i!} \\
&\leq C_4 \lambda^{-(1+c)}, \qquad (5.27)
\end{aligned}$$

for some $C_4 > 0$ when λ is sufficiently large. Note that the last inequality results from $\exp(\lambda^{\delta_1}/4)$ grows much faster than any polynomial function of λ as $\lambda \to \infty$.

Next by Lemma 5.2.2 (with $\alpha = 2\pi$), for any given $\delta_1 > 0$, if λ is sufficiently large, there exists some constant $C_5 > 0$ such that

$$E_{\bar{G}_A}[r_A^c r_B^c | X_A, X_B] \leq E[r_A^c r_B^c | X_A, X_B] \leq C_5 \lambda^{c(-1+\delta_1)}. \qquad (5.28)$$

Therefore,

$$\begin{aligned}
E_{\{d\leq\epsilon\}}[E_{\bar{G}_A}[r_A^c r_B^c | X_A, X_B]] &\leq E_{\{d\leq\epsilon\}}[C_5 \lambda^{c(-1+\delta_1)}] \\
&= P(d \leq \epsilon) \cdot C_5 \lambda^{c(-1+\delta_1)} \\
&= \pi\epsilon^2 \cdot C_5 \lambda^{c(-1+\delta_1)} \\
&= \lambda^{-1+\delta_1} \cdot C_5 \lambda^{c(-1+\delta_1)} \\
&= C_5 \lambda^{-1-c+\delta_1(1+c)}. \qquad (5.29)
\end{aligned}$$

By setting $\delta_1 = \delta_0/(c+1)$, we obtain

$$E_{\{d\leq\epsilon\}}[E_{\bar{G}_A}[r_A^c r_B^c | X_A, X_B]] \leq C_5 \lambda^{-1-c+\delta_0}. \qquad (5.30)$$

Combining Eqs. (5.27) and (5.30), we obtain

$$E[E_{\bar{G}_A}[r_A^c r_B^c | X_A, X_B]] \leq C_6 \lambda^{-1-c+\delta_0}. \tag{5.31}$$

Combining Eqs. (5.21), (5.22), (5.25) and (5.31), we obtain

$$E[W_A W_B] \leq (E[W_L]/\lambda)^2 + C_6 \lambda^{-(c+1)+\delta_0}. \tag{5.32}$$

Finally combining Eqs. (5.18)-(5.20) and (5.32), we obtain Eq. (5.17). □

We are now in a position to prove Theorem 5.3.1.

Proof of Theorem 5.3.1. By Chebyshov's inequality, for any given $\delta' > 0$, when $\lambda \to \infty$,

$$\begin{aligned} P(|W_L - E[W_L]| \geq \delta' E[W_L]) &\leq \frac{Var(W_L)}{\delta'^2 E[W_L]^2} \\ &= \frac{E[W_L^2] - E[W_L]^2}{\delta'^2 E[W_L]^2} \\ &\leq \frac{C_3 \lambda^{1-c+\delta_0}}{\delta'^2 E[W_L]^2} \\ &\approx_\lambda \frac{C_3 \lambda^{1-c+\delta_0}}{\delta'^2 \frac{\Gamma^2(c/2+k)}{((k-1)!)^2 \pi^c} \lambda^{2-c}}, \end{aligned} \tag{5.33}$$

where the last equation tends to 0 as λ goes to infinity if we choose $\delta_0 < 1$. Hence $P(W_L \geq (1-\delta')E[W_L]) \to 1$ as $\lambda \to \infty$. Since $W_c \geq W_L$, we have $P(W_c \geq (1-\delta')E[W_L]) \to 1$ as $\lambda \to \infty$. By Proposition 5.3.1, $E[W_L] \geq (1-\delta')\frac{\Gamma(\frac{c}{2}+k)}{(k-1)!\pi^{\frac{c}{2}}} \lambda^{1-\frac{c}{2}}$ for sufficiently large values of λ. Consequently we have

$$P\left(W_c \geq (1-\delta')^2 \frac{\Gamma(\frac{c}{2}+k)}{(k-1)!\pi^{\frac{c}{2}}} \lambda^{1-\frac{c}{2}}\right) \to 1, \tag{5.34}$$

as $\lambda \to \infty$. Given any $\delta > 0$, we can find $\delta' > 0$ such that $(1-\delta')^2 > (1-\delta)$, and hence as $\lambda \to \infty$,

$$P\left(W_c \geq (1-\delta) \frac{\Gamma(\frac{c}{2}+k)}{(k-1)!\pi^{\frac{c}{2}}} \lambda^{1-\frac{c}{2}}\right) \to 1, \tag{5.35}$$

for any given $\delta > 0$, which completes the proof. □

5.4 Upper Bound on the Critical Total Power

In this section, we derive an upper bound on the critical total power required to maintain k-connectivity. As will be shown later in this section, the upper bound turns out to be of the same order as the lower bound, not only in terms of λ but also in terms of k.

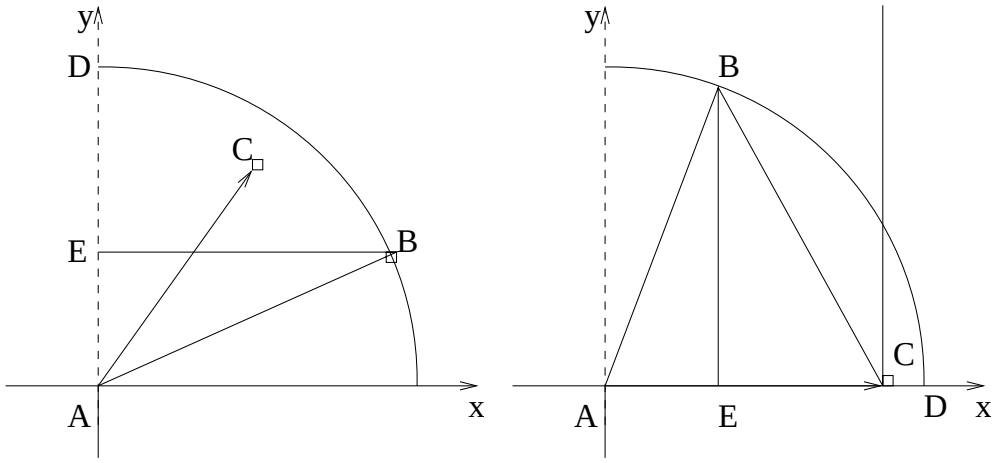

(a) Case (i) $y_B - y_A < x_B - x_A$ (b) Case (ii) $y_B - y_A \geq x_B - x_A$

Figure 5.1: Illustration for Lemma 5.4.1

Given the coordinates of all nodes in the plane $[0,1]^2$, each node can define its own coordinate system by only shifting the origin of the $[0,1]^2$ plane to its own location. We use (x_i, y_i) to represent the coordinate of a node i in the original coordinate system (i.e., the plane $[0,1]^2$), and define the p-norm distance d_p between two nodes A and B as

$$d_p(A,B) = (|x_A - x_B|^p + |y_A - y_B|^p)^{1/p}. \tag{5.36}$$

If $p = \infty$, $d_\infty(A,B) = \max(|x_A - x_B|, |y_A - y_B|)$. Clearly p-norm distance does not change under the conversion from the original plane to a new coordinate system with a new origin. Throughout this chapter, we use 2-norm distance as the "distance" unless otherwise specified, and $|AB|$ to represent $d_2(A,B)$. We first prove a geometric result on strong 1-connectivity.

Lemma 5.4.1 *Given the locations of all nodes on the plane $[0,1]^2$, if each node chooses its power level to reach at least one neighbor in each of the four quadrants in its own coordinate system as long as there exists one or more nodes in that quadrant, the resulting network is strongly (1-)connected. (To eliminate the ambiguity in which quadrant the axis lines belong to, we assign the positive x-axis to the first quadrant, the positive y-axis to the second quadrant, and so on.)*

Proof. We prove the lemma by contradiction. If the resulting network is not strongly connected, there exists at least a pair of nodes (i,j) such that there exists no (directed) path from node i to node j. Among all the pairs, we choose the one *with the smallest ∞-norm distance*. In case of a tie, we choose the pair with the smallest 2-norm distance. Let the chosen pair be nodes (A,B). It suffices to find a pair of disconnected nodes (Y,Z) such that $d_\infty(Y,Z) < d_\infty(A,B)$, or $d_\infty(Y,Z) = d_\infty(A,B)$ and

$d_2(Y,Z) < d_2(A,B)$.

Without loss of generality, we assume that there is no directed path from A to B, and node B is in the first quadrant in node A's coordinate system, i.e., $x_A < x_B, y_A \leq y_B$ (note that the first quadrant includes the positive x-axis but not the positive y-axis). Since there exists at least one node B in the first quadrant of node A's coordinate system, node A's power must be able to reach at least one other node C in the first quadrant of its coordinate system. Clearly $d_2(A,C) < d_2(A,B)$ since node A's power is not sufficient to reach node B. In addition, there exists no path from node C to node B; otherwise there would be a path from node A to node B. Now we consider two possible cases.

Case (i) $y_B - y_A < x_B - x_A$ **(Fig. 5.1 (a))** In this case $d_\infty(A,B) = x_B - x_A \equiv a$ and $|y_A - y_B| < a$. Let D be the intersection point of the cycle centered at A with radius $d_2(A,B)$ and the positive y-axis in node A's coordinate system. Let E be the intersection point of the y-axis in A's coordinate system and a horizontal line through node B. Then $|BE| = a$. As $y_C - y_A \leq |AC| < |AB|$ and $y_B - y_A = |AE|$, we have $y_C - y_B < |AB| - |AE| \leq |BE| = a$. On the other hand, $y_C \geq y_A$ and hence $y_C - y_B \geq y_A - y_B > -a$. Therefore $|y_C - y_B| < a$,

Similarly, $x_C > x_A$, and hence $x_C - x_B > x_A - x_B = -a$. In addition, as $x_C - x_A \leq |AC| < |AB|$ and $x_B - x_A = |BE|$, we have $x_C - x_B < |AB| - |BE| \leq |AE| \leq a$. Therefore $|x_C - x_B| < a$. As such, we conclude $d_\infty(B,C) = \max(|x_C - x_B|, |y_C - y_B|) < d_\infty(A,B)$, which violates the assumption on the pair of nodes (A,B).

Case (ii) $y_B - y_A \geq x_B - x_A$**(Fig. 5.1 (b))** In this case $d_\infty(A,B) = y_B - y_A \equiv a \geq |x_B - x_A|$. Let D be the intersection point of the cycle centered at A with radius $d_2(A,B)$ and the positive x-axis in node A's coordinate system. Let E be the intersection point of the x-axis in A's coordinate system and a vertical line through node B. Then $|BE| = a$. As $x_C > x_A$, we have $x_C - x_B > x_A - x_B \geq -a$. Also, since $x_C - x_A \leq |AC| < |AB|$ and $x_B - x_A = |AE|$, we have $x_C - x_B < |AB| - |AE| \leq |BE| = a$. Therefore $|x_C - x_B| < a$.

Since $y_C - y_A < |AB|$ and $y_B - y_A = |BE|$, we have $y_C - y_B < |AB| - |BE| \leq |AE| \leq |BE| = a$. Also, since $y_C \geq y_A$, we have $y_C - y_B \geq y_A - y_B = -a$. Therefore, $|y_C - y_B| \leq a$. As such, we conclude $d_\infty(B,C) \leq a = d_\infty(A,B)$ with equality held if and only if $y_C = y_A$. If $y_C \neq y_A$, we reach the contradiction.

Now assume $y_C = y_A$. By the way nodes A and B are selected, we have $x_C > x_B$ because otherwise $d_\infty(B,C) = d_\infty(A,B)$ and $d_2(B,C) < d_2(A,B)$, which violates the assumption on the pair of nodes (A,B). Now we obtain a disconnected pair of nodes (C,B) that also has the smallest ∞-distance among

all the disconnected node pairs, node B is in the second quadrant in node C's coordinate system, and

$$|x_C - x_B| < |y_C - y_B| \tag{5.37}$$

(as $\angle ACB > \pi/4$). Now we carry out the above analysis on the node pair (C, B). As the positive y-axis belongs to the second quadrant and by Eq. (5.37), we can only go to case (i). That is, we can find a pair of nodes (G, B) such that there exists no directed path from G to B and $d_\infty(G, B) < d_\infty(C, B) = d_\infty(A, B)$. This violates the assumption on the pair of nodes (A, B), and completes the proof. □

The above proof is primarily based on the distance metrics without use of the Toroidal model. However, it can be easily extended to the distance metrics under the Toroidal model. Please refer to [84] for a detailed account of the discussion.

Lemma 5.4.1 can be easily extended to accommodate the case of strong k-connectivity as follows.

Lemma 5.4.2 *Given the locations of all nodes on the plane $[0, 1]^2$, if each node chooses its power level to reach at least k neighbors in each of the four quadrants in its own coordinate system, as long as there exist k or more nodes in that quadrant (in the case that there are less than k nodes in a quadrant, the transmission power of the node is chosen to reach all of the nodes in that quadrant), the resulting network is strongly k-connected.*

Proof. After removing any $k - 1$ nodes from the network, each node can still reach at least one neighbor in each of its four quadrants, as long as that quadrant still contains some nodes. By Lemma 5.4.1, the remaining network is strongly connected. Therefore, the original network is at least strongly k-connected. □

Since the above simple topology control mechanism ensures strong k-connectivity in the underlying graph, the total power incurred based on this mechanism provides an upper bound on the critical total power required for k-connectivity. In what follows, we derive an upper bound on the critical total power based on the above topology control algorithm.

Let $W_U = \sum_{i=1}^{N_\lambda} W_i'$, where W_i' is the power consumed by node i under the topology control mechanism introduced in Lemma 5.4.2, and the summation is taken over all the points generated by a Poisson point process with density λ on $[0, 1]^2$. Clearly $W_c \le W_U$. We have the following major result.

Theorem 5.4.1 $P(W_c \le (1 + \delta)C_7(c)\lambda^{1-c/2}) \to 1$ *as* $\lambda \to \infty$, *for any* $\delta > 0$, *where*

$$C_7(c) = \frac{4\Gamma(\frac{c}{2} + k)}{(k-1)!} \left(\frac{4}{\pi}\right)^{\frac{c}{2}}. \tag{5.38}$$

The proof of Theorem 5.4.1 will be given through two propositions and one lemma. First we evaluate the expectation of W_U.

Proposition 5.4.1 *$E[W_U] \leq C_7(c)\lambda^{1-\frac{c}{2}}$ as $\lambda \to \infty$, where $C_7(c)$ is given in Eq. (5.38).*

Proof. By Palm theory for the Poisson point process, we have

$$E[W_U] = E[\sum_{i=1}^{N_\lambda} W_i'] = \lambda E[W_1'], \tag{5.39}$$

where the last expectation is taken over the probability space where node 1 is randomly placed with a uniform distribution on the region S, together with a set of nodes that are distributed according to a Poisson point process $\mathcal{P}_\lambda$ and independent of X_1.

Let R_{1_i}, $1 \leq i \leq 4$, be the distance from node 1 to its kth nearest neighbor in the ith quadrant of node 1's coordinate system, and $R_1 = \max\{R_{1_i}, 1 \leq i \leq 4\}$. The power required for node 1 is then $W_1' = R_1^c$. Since R_{1_i}'s are independent and have the same distribution as $R_{\lambda,k}(\pi/2)$[1] under the Poisson point process assumption, the expectation of W_1' can be expressed as

$$\begin{aligned} E[W_1'] &= E[R_1^c] \\ &\leq E[R_{1_1}^c + R_{1_2}^c + R_{1_3}^c + R_{1_4}^c] \\ &\approx_\lambda 4E[R_{\lambda,k}^c(\pi/2)] \\ &= \frac{4\Gamma(c/2+k)}{(k-1)!}\left(\frac{4}{\lambda\pi}\right)^{c/2}, \end{aligned} \tag{5.40}$$

where the last equality results from Eq. (5.4). Thus, by Eq. (5.39), we have

$$E[W_U] = \lambda E[W_1'] \leq C_7(c)\lambda^{1-\frac{c}{2}}. \tag{5.41}$$

□

In order to bound $|W_U - E[W_U]|$, we need to estimate the second moment of W_U.

Proposition 5.4.2

$$E[W_U^2] \leq E[W_U]^2 + C_8\lambda^{1-c+\delta_0} \text{ as } \lambda \to \infty \tag{5.42}$$

for any given $\delta_0 > 0$ and some constant $C_8 > 0$ that is independent of λ.

[1] More precisely, R_{1_i} is slightly different from $R_{\lambda,k}(\pi/2)$. By carrying out a proof similar to that in Proposition 5.3.1, we can show that the ratio of the expectations derived using $R_{\lambda,k}(\pi/2)$ to that using the precise version of R_{1_i} tends to 1 as $\lambda \to \infty$.

Proof.

$$\begin{aligned} E[W_U^2] &= E[\sum_{i=1}^{N_\lambda} W_i']^2 \\ &= E[\sum_{i=1}^{N_\lambda} W_i'^2] + 2E[\sum_{1\le i<j\le N_\lambda} W_i' W_j']. \end{aligned} \tag{5.43}$$

Since $W_i'^2 = R_i^{2c}$, by Proposition 5.4.1 we have

$$E[\sum_{i=1}^{N_\lambda} W_i'^2] = E[\sum_{i=}^{N_\lambda} R_i'^{2c}] = C_7(2c)\lambda^{1-c}. \tag{5.44}$$

It remains to determine the second term of Eq. (5.43). Applying Palm theory for the Poisson point process, we have

$$2E[\sum_{1\le i<j\le N_\lambda} W_i' W_j'] = \lambda^2 E[W_A' W_B'], \tag{5.45}$$

where the last expectation is taken over the probability space where nodes A and B are uniformly randomly distributed in the region S, together with a set of nodes that are distributed as a Poisson point process with density λ and is independent of the locations of nodes A and B.

First we evaluate $E[W_A' W_B']$ conditioning on the locations, X_A and X_B, of nodes A and B, i.e.,

$$E[W_A' W_B'] = E[E[W_A' W_B' | X_A, X_B]]. \tag{5.46}$$

Given the locations X_A, X_B, let $d = |X_A - X_B|$. For each $i \in \{1,2,3,4\}$, let T_{A_i} be the event that at least k nodes from $\mathcal{P}_\lambda$ fall in node A's ith quadrant within radius $d/2$, and T_{B_i} the event that at least k nodes from $\mathcal{P}_\lambda$ fall in node B's ith quadrant within radius $d/2$. Let $T_A = \cap_{i=1}^4 T_{A_i}$, $T_B = \cap_{i=1}^4 T_{B_i}$, and $T = T_A \cap T_B$. That is, T denotes the event that at least k nodes in the Poisson point process $\mathcal{P}_\lambda$ fall in each of the four quadrants within radius $d/2$ in node A's coordinate system and in each of the four quadrants within radius $d/2$ in node B's coordinate system. By the law of total probability,

$$E[W_A' W_B' | X_A, X_B] = E_T[W_A' W_B' | X_A, X_B] + E_{\bar{T}}[W_A' W_B' | X_A, X_B]. \tag{5.47}$$

The first term in the above Eq. (5.47) can be written as

$$\begin{aligned} E_T[W_A' W_B' | X_A, X_B] &= E_T[R_A^c R_B^c | X_A, X_B] \\ &= E[\mathbf{1}_T R_A^c R_B^c | X_A, X_B] \end{aligned}$$

$$
\begin{aligned}
&= E[\mathbf{1}_{T_A}\mathbf{1}_{T_B}R_A^cR_B^c|X_A,X_B] \\
&= E[\tilde{R}_A^c\tilde{R}_B^c|X_A,X_B], \qquad (5.48)
\end{aligned}
$$

where $\tilde{R}_A = R_A\mathbf{1}_{T_A} = R_A\mathbf{1}_{\{R_A\le d/2\}}$, and $\tilde{R}_B = R_B\mathbf{1}_{T_B} = R_B\mathbf{1}_{\{R_B\le d/2\}}$. Now, clearly $\tilde{R}_A$ and $\tilde{R}_B$ are independent because they depend on the node distributions in two disjoint regions, $\mathcal{B}_{X_A}(d/2)$ and $\mathcal{B}_{X_B}(d/2)$, respectively. Therefore, we can evaluate their expectations separately, i.e.,

$$
E_T[W_A'W_B'|X_A,X_B] = E[\tilde{R}_A^c|X_A,X_B]E[\tilde{R}_B^c|X_A,X_B]. \qquad (5.49)
$$

By a similar argument to that in Proposition 5.3.2, we obtain

$$
\begin{aligned}
E[\tilde{R}_A^c|X_A,X_B] &\le E[R_1^c] = E[W_U]/\lambda, \\
E[\tilde{R}_B^c|X_A,X_B] &\le E[R_1^c] = E[W_U]/\lambda. \qquad (5.50)
\end{aligned}
$$

Thus

$$
E_T[W_A'W_B'|X_A,X_B] \le (E[W_U]/\lambda)^2. \qquad (5.51)
$$

Combining Eqs. (5.46), (5.47) and (5.51), we obtain

$$
E[W_A'W_B'] \le (E[W_U]/\lambda)^2 + E[E_{\bar{T}}[W_A'W_B'|X_A,X_B]] \qquad (5.52)
$$

Now it remains to determine the second term of Eq. (5.52), which we denote as I_2, i.e.,

$$
\begin{aligned}
I_2 &\equiv E[E_{\bar{T}}[W_A'W_B'|X_A,X_B]] \\
&= E[E_{\bar{T}}[R_A^cR_B^c|X_A,X_B]]. \qquad (5.53)
\end{aligned}
$$

Since

$$
\bar{T} = (\cup_{l=1}^4 \bar{T}_{A_l}) \cup (\cup_{l=1}^4 \bar{T}_{B_l}), \qquad (5.54)
$$

it follows that

$$
\begin{aligned}
I_2 &\le E\sum_{l=1}^4 E_{\bar{T}_{A_l}}[R_A^cR_B^c|X_A,X_B] + E\sum_{l=1}^4 E_{\bar{T}_{B_l}}[R_A^cR_B^c|X_A,X_B] \\
&= 2E\sum_{l=1}^4 E_{\bar{T}_{A_l}}[R_A^cR_B^c|X_A,X_B], \qquad (5.55)
\end{aligned}
$$

where the last equality is by symmetry.

Since $R_A = \max_{1\le i\le 4} R_{A_i}$, $R_B = \max_{1\le j\le 4} R_{B_j}$, where R_{A_i} (R_{B_j}) is the distance from node A (B) to node A's (B's) kth nearest neighbor in the ith (jth) quadrant of A's (B's) coordinate system, we have $R_A^c \le \sum_{i=1}^4 R_{A_i}^c$ and $R_B^c \le \sum_{j=1}^4 R_{B_j}^c$. Hence,

$$I_2 \le 2E\left[\sum_{l=1}^4\sum_{i=1}^4\sum_{j=1}^4 E_{\bar{T}_{A_l}}[R_{A_i}^c R_{B_j}^c | X_A, X_B]\right]. \tag{5.56}$$

There are a total of 64 possible combinations of (l,i,j) in Eq. (5.56). We show in the following lemma that each of the 64 terms is at most of the order $\lambda^{-(1+c)+\delta_0}$.

Lemma 5.4.3 *For any $(l,i,j) \in \{1,2,3,4\}^3$,*

$$E[E_{\bar{T}_{A_l}}[R_{A_i}^c R_{B_j}^c | X_A, X_B]] \le C_9 \lambda^{-(1+c)+\delta_0}, \tag{5.57}$$

for any $\delta_0 > 0$ and some constant C_9 if λ is sufficiently large, where C_9 only depends on c, k and not on λ.

The proof of Lemma 5.4.3 pretty much follows that in Proposition 5.3.2. On one hand, if the distance d between nodes A and B is large, the probability that T_{A_l} occurs is low. On the other hand, the probability that the distance d is small is low. The proof also uses the result in Lemma 5.2.2. The interested reader is referred to [84] for a detailed account of the proof.

Combining Lemma 5.4.3 with Eqs. (5.52), (5.53) and (5.56), we obtain

$$E[W_A' W_B'] \le (E[W_U]/\lambda)^2 + 128 C_9 \lambda^{-(1+c)+\delta_0}. \tag{5.58}$$

With Eqs. (5.43)–(5.45) and (5.58), we obtain Eq. (5.42). □

With Propositions 5.4.1 and 5.4.2, We can prove Theorem 5.4.1 in a similar manner to Theorem 5.3.1.

5.5 Discussions

5.5.1 Interpretation of derived results

By Theorem 5.3.1 and 5.4.1, we reach the following corollary.

Corollary 5.5.1 *As $\lambda \to \infty$,*

$$W_c = \Theta\left(\frac{\Gamma(c/2+k)}{(k-1)!}\lambda^{1-\frac{c}{2}}\right) \tag{5.59}$$

with probability approaching 1, where W_c is the critical total power required for maintaining k-connectivity.

In general, the path loss exponent is $2 \leq c \leq 4$, although our proof applies to any $c > 0$. In the case of $c > 2$, Corollary 5.5.1 indicates that if the density is sufficiently large, the increase in the density reduces the critical total power, and in addition, the critical total power decreases as the path loss exponent increases.

It has been shown by Penrose in [57] that if λ nodes are uniformly randomly placed on a Torus unit square, and r_λ represents critical common transmission range required by all nodes in order to ensure k-connectivity, then

$$P(\lambda\pi r_\lambda^2 - \log\lambda - (k-1)\log\log\lambda + \log((k-1)!) \leq \tau) = \exp(-e^{-\tau}).$$

By this equation, if

$$\pi r_\lambda^2 = \frac{\log\lambda + (k-1)\log\log\lambda - \log((k-1)!) + \tau}{\lambda} \tag{5.60}$$

and $\tau \to \infty$ as $\lambda \to \infty$, the network has k-connectivity with probability approaching one.

Comparing with the critical total power derived under the uniform metric assumption (given in Eq. (5.60) and a similar equation in [73]), we conclude that the critical total power can be reduced by a factor of $\Theta((\log\lambda)^{c/2})$ by allowing nodes to optimally choose different levels of transmission power. This is not subject to any specific algorithm, but rather a fundamental property in wireless networks.

5.5.2 Legitimacy of the system model

We claim that the assumption of a unit area region is an abstraction of the real world. The unit area is not necessarily 1 meter^2, but instead can be used to model a L^2meter^2 area. That is, we can rescale the unit area to a square area with side length L and network density λ_0. In this rescaled network, every pair of nodes have a small chance to be very close to each other. A one-to-one correspondence between the values in the unit-area network and those in the rescaled network can be made and is given in Table 5.2.

Consider the average power consumed by each node. In the unit-area network, the average power consumed by each node is of order $\lambda^{-c/2}$ (the constant that contains k is ignored). In the rescaled network, since each edge is rescaled by a factor of L, the power consumption should be multiplied by a factor of L^c. However, if we consider the side length L to be one unit, the node density in the corresponding

Table 5.2: One-to-one correspondence between the values in the unit-area square and those in the $L \times L$ square.

in the unit-area square	in the $L \times L$ square
1	L
r	Lr
$\lambda = \lambda_0 L^2$	λ_0

unit-area square becomes $\lambda = \lambda_0 L^2$. Hence the average power consumption (in the rescaled network) is now $\lambda^{-c/2} L^c = (\lambda_0 L^2)^{-c/2} L^c = \lambda_0^{-c/2}$, which only depends on the density λ_0 in the rescaled network and not on the side length L of the area. On the other hand, if we assume a common critical transmission power among nodes for k-connectivity in the rescaled network, each node has to consume power in the order of $\lambda_0^{-c/2} (\log \lambda_0 L^2)^{c/2}$,[2] which tends to infinity if λ_0 is fixed and $L \to \infty$.

5.5.3 Boundary conditions

So far, our discussion is based on Torus convention, which eliminates boundary conditions. We now address the problem introduced by boundary conditions. For the lower bound, the introduction of boundaries will only increase the nearest neighbor distance. Therefore, the lower bound we have derived for Torus convention still hold when boundary conditions are considered. So we will focus on how the upper bound is affected by boundary conditions.

At the first glance, boundary conditions may significantly increase the upper bound. As in Figure 5.2, where the axes of each node's coordinate system is in parallel with the side of the square region, the node O is very close to the right side of the region. The first quadrant of its coordinate system is a narrow rectangle. Therefore, it is quite possible that the nearest neighbor in the first quadrant has a long distance to the node O itself.

However, if we rotate the square region by 45 degree, as shown in Figure 5.3, no quadrant of any node is a long narrow rectangle. If a node is around the boundary of the monitored region, the main quadrant that is affected by the boundary is the one facing the boundary (e.g., the fourth quadrant of node O in Fig. 5.3). However, if the distance between the node and the boundary d is small, the kth nearest neighbor distance in this quadrant is upper bounded by $\sqrt{2}d$, which is also small. The other two quadrants affected by the boundary (e.g., the first and the third quadrant of node O in Fig. 5.3) both contain a cone with angle $\pi/4$. Therefore, the kth nearest neighbor distance in these two quadrants is no larger than $R_{\lambda,k}(\pi/4)$ (refer to Table 5.1). Overall, the chance of having a kth nearest neighbor with

[2]By Eq. (5.60), each node needs power $r_\lambda^c = \Theta((\frac{\log \lambda}{\lambda})^{c/2})$ (ignoring the less significant terms) in the unit-area network. Rescaling to the large network with side length L, each node needs power $r_\lambda^c L^c = \Theta(\lambda_0^{-c/2} (\log(\lambda_0 L^2))^{c/2})$. Although the Eq. (5.60) (comes from [57]) assumes n independently randomly placed nodes while our results are based on Poisson point processes, they are comparable through Poissonization and De-Poissonization techniques (see [55]).

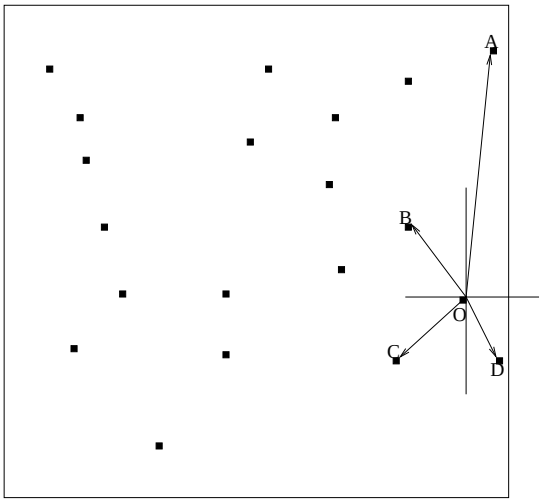

Figure 5.2: The axes of each node's coordinate system are in parallel with the side of the square region.

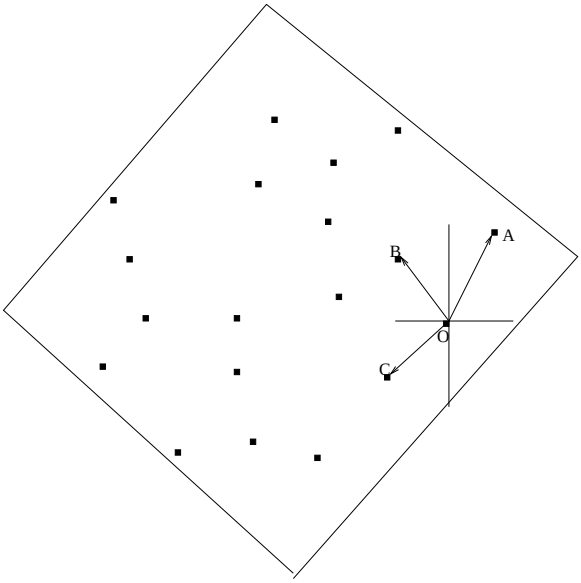

Figure 5.3: The axes of each node's coordinate system and the side of the square region are of 45 degree.

long distance in any quadrant is small. Therefore, the upper bound derived in the previous section is still valid even with boundary conditions.

5.6 Numerical Validation

We perform simulations to validate the theoretically derived results. In a unit-area square,[3] λ nodes are randomly generated, where λ ranges from 10 to 10240. The location of each node is uniformly randomly distributed and is independent of each other (here we use a uniformly random process to approximate the Poisson process). As we are considering a unit-area network, the node density is also the number of nodes in the field. We evaluate the lower bound and upper bound of the critical total power for 1-connectivity and 3-connectivity. We consider power loss exponent $c = 2$, 3, and 4 and the transmission power of a node is r^c where r is the transmission range.

Figures 5.4 and 5.5 show the critical total power required for maintaining 1-connectivity and 3-connectivity, respectively. The linear relationship in the log-log plot clearly demonstrates the power relation between the critical total power W_c and the node density λ. The slope of the curves shows the exact power exponent (i.e. $1 - c/2$) of the power relationship.

To further verify the exact power exponent of the power relationship, we plot the curves $W_c/\lambda^{1-c/2}$ vs. λ in Figures 5.6 and 5.7, which clearly show W_c is proportional to $\lambda^{1-c/2}$.

[3]All the numerical results in this section can be readily rescaled to a square region with arbitrary side length.

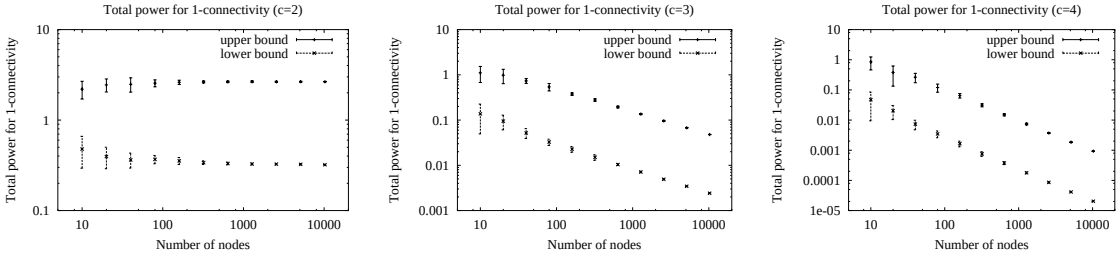

(a) c = 2 (b) c = 3 (c) c = 4

Figure 5.4: Lower bounds and upper bounds of critical total power required for maintaining 1-connectivity

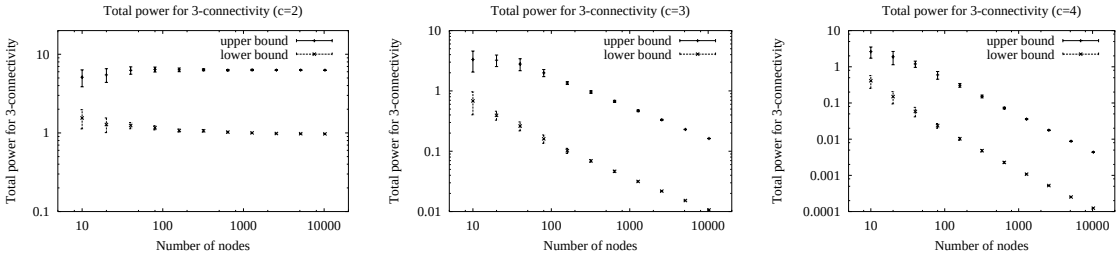

(a) c = 2 (b) c = 3 (c) c = 4

Figure 5.5: Lower bounds and upper bounds of critical total power required for maintaining 3-connectivity

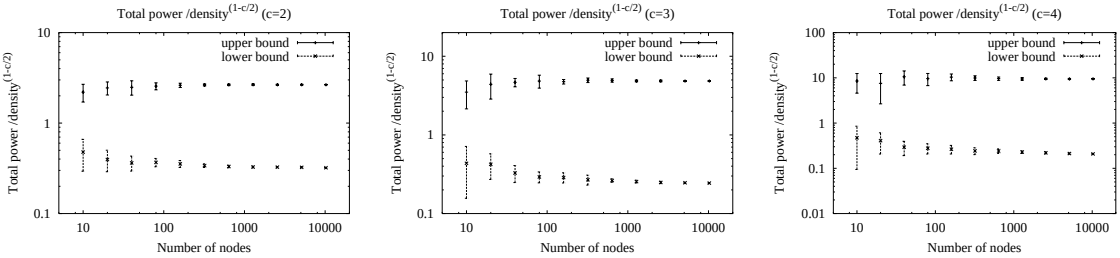

(a) c = 2 (b) c = 3 (c) c = 4

Figure 5.6: For 1-connectivity: lower bounds and upper bounds of $W_c/\lambda^{1-c/2}$, where W_c is the critical total power required for maintaining 1-connectivity.

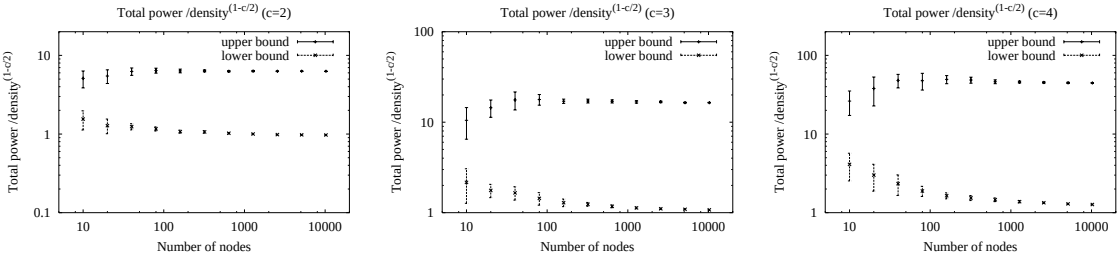

(a) c = 2 (b) c = 3 (c) c = 4

Figure 5.7: For 3-connectivity: lower bounds and upper bounds of $W_c/\lambda^{1-c/2}$, where W_c is the critical total power required for maintaining 3-connectivity.

5.7 Conclusion

We have shown in this chapter that in a heterogeneous wireless network in which wireless nodes are distributed in a unit square region $[0,1]^2$ according to a Poisson point process with density λ and nodes may transmit with different levels of power, the critical total power required to maintain k-connectivity is $\Theta(\frac{\Gamma(c/2+k)}{(k-1)!}\lambda^{1-c/2})$ with probability approaching 1, where c is the path loss exponent. This result is obtained by deriving a lower bound and an upper bound on the critical total power. By comparing the result against those obtained when all nodes use the uniform critical transmission power for k-connectivity [57, 73], we conclude that with the use of (optimal) power control, the critical total power can be reduced by a factor of $\Theta((\log \lambda)^{c/2})$, irregardless of the power/topology control algorithm used.

Chapter 6

Asymptotic Minimum Transporting Energy and its Implication on Wireless Network Capacity

6.1 Introduction

In wireless sensor networks, reducing power and energy consumption is always an important issue because sensors are often powered with onboard batteries. The problem of power saving is often formulated into minimizing the total power consumption while maintaining network connectivity or k-connectivity as discussed in the previous chapter.

In this chapter, we approach the problem from a different angle. Since the primary function of a wireless network is to transport data packets and maintaining network connectivity is merely the underlying mechanism to support data transport, we consider the problem of minimizing energy consumption *when transporting a packet from a source to a destination in a wireless network*. Algorithmically, the problem can be solved using any shortest-path algorithm such as Dijkstra's algorithm. However, it has been left unattended *what is the asymptotic minimum energy*[1] *required to carry a packet from a source to a destination in a wireless network*, and especially, how this quantity scales as the network size goes to infinity. In this chapter we address the problem under the assumption that nodes are distributed as a Poisson point process with density n in a unit square area, and the source and the destination are separated by at least a constant distance.

We solve the formulated problem by deriving, based on percolation theory, an upper bound and a lower bound on the asymptotic minimum energy required to transport a packet from a source to a destination in a random network in a unit-square region. We show that if the source-destination distance is of order $\Theta(1)$, both the upper and lower bounds are of order $\Theta(n^{(1-\alpha)/2})$ with probability approaching one as the network density goes to infinity, where α is the path-loss exponent.

After the bounds are derived, we discuss how to extend the results to accommodate the cases (i) that the network density is kept as constant but the network size goes to infinity, and (ii) that both the transmitting and receiving operations consume energy. In particular, we obtain the following more general result in (i): in a network where nodes are distributed according to a Poisson point process

[1] which is termed as the *minimum transporting energy* in this chapter.

with density n on an infinite plane, the minimum energy required to carry a packet from a source to a destination with distance l is $\Theta(n^{(1-\alpha)/2}l)$ with high probability if $nl^2 \to \infty$.

We also demonstrate how to apply the derived results to solve other related problems. In particular, the derived results can be used to determine the capacity bound in the case that directional antennas are used for spatial reuse and the capacity bound in the case of ultra wide band (UWB) communications. This is because in both cases the limiting factor for the capacity bound is the system energy. The derived results can also be used to determine an upper bound on the network lifetime of wireless sensor networks.

We carry out simulations to both validate the theoretical derivation and estimate the associated constant in the derived asymptotic function. The simulation results suggest that the minimum energy required for transporting a data packet converges to $n^{(1-\alpha)/2}l$ with high probability, where l is the source-destination distance and n is the node density.

The rest of the chapter is organized as follows. In Section 6.2, we discuss the system model and assumptions we have made for the rest of the chapter. We prove the lower bound on the minimum energy required to transport a packet in Section 6.3 and the upper bound in Section 6.4. Following that, we discuss the extensions in Section 6.5 and the applications of the derived results to network capacity and lifetime bounds in Section 6.6. Finally, we present simulation results in Section 6.7, and conclude the chapter in Section 6.8.

6.2 Model Assumptions

The network is composed of a set of wireless nodes that are distributed according to a Poisson point process with density n in a two-dimensional unit square region $[0,1]^2$. We assume that the energy required to directly transmit a packet from a sender to a receiver with distance d is d^α,[2] where $2 \leq \alpha \leq 4$ is the path loss exponent (although in our derivation of the minimum transporting energy, we only require $\alpha \geq 1$). Let X_i denote the location of the ith node. Let R denote the minimum energy route for a given source-destination pair, i.e, $R = [X_0, X_1, \cdots, X_k]$. The minimum energy of the route (which is also termed as transporting energy in this chapter) is thus

$$Q \triangleq \sum_{i=0}^{k-1} |X_i - X_{i+1}|^\alpha, \tag{6.1}$$

where $|X_i - X_{i+1}|$ denotes the Euclidean distance between X_i and X_{i+1}. The objective of this chapter is to determine the asymptotic bounds of Q. The results are shown to hold with high probability (*w.h.p.*),

[2]Clearly, the energy also depends on the packet size and the transmission rate. We assume these factors contribute to a constant factor, and hence are ignored in the derivation.

which means the probability approaching 1 as the density $n \to \infty$. We assume the distance between the source and the destination is $\Theta(1)$.

6.3 Lower Bound on the Energy Requirement

In this section, we establish a lower bound on Q. The key to the derivation is that, if it is possible for the route R to be composed of mostly short hops, then potentially the minimum energy (Q) of a route can be very small. Thus, our major task is to show that there is a *sufficiently* large number of long hops. The proof is based on the site percolation model.

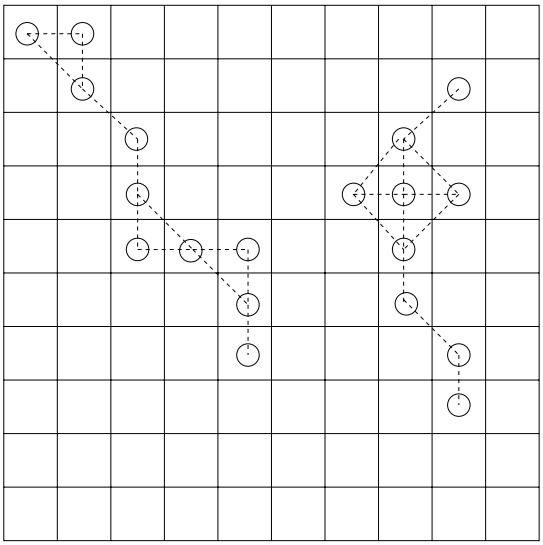

Figure 6.1: Construction of the site percolation model. We divide the region into grids of edge length $c_0/\sqrt{n}$. A grid is said to be open if there is at least one Poisson point inside it; and closed otherwise. Two grids are said to be adjacent if two grids share an edge or a vertex, i.e., grid (i, i) is adjacent to $(i-1, i-1), (i-1, i), (i-1, i+1), (i, i-1), (i, i+1), (i+1, i-1), (i+1, i), (i+1, i+1)$. An open grid is denoted with a circle inside it. The dashed lines show all the possible open links.

6.3.1 Construction of the site percolation model

We divide the square region into grids of edge length $c_0/\sqrt{n}$ as depicted in Fig. 6.1. By adjusting the constant c_0, we can adjust the probability that a grid contains at least one node:

$$P(\text{a grid contains at least one node}) = 1 - e^{-c_0^2} \triangleq p. \tag{6.2}$$

A grid is said to be *open* if it contains at least one node, and *closed* otherwise. Two grids are said to be *adjacent* if they share an edge or a vertex. Any grid is thus adjacent to eight other grids. For notational convenience, we use (i) a *path* to refer to a list of grids such that any two neighboring grids in the list are

adjacent; and (ii) a *route* to refer to a list of wireless nodes that are actually used to transport packets from a source to a destination. By the convention in graph theory, we assume a path does not include any grid twice, except that its first grid may be the same as the last grid. A path is said to be *open* (*closed*) if all the grids on the path are open (closed).

Important Properties of the Site Percolation Model As a first step, we observe that if there is an open path in the percolation model from the grid containing the source to the grid containing the destination, then we can form a route from the source to the destination by picking one node from each grid on the path. Every hop on this route is bounded from above by $2\sqrt{2}c_0/\sqrt{n}$. On the other hand, if there is no such open path in the percolation model, then on any route (including the minimum energy route) from the source to the destination, at least one hop is of length at least $c_0/\sqrt{n}$. Indeed, if c_0 and consequently p are sufficiently small, and the distance, d, between the source and the destination is sufficiently large, there exists no open path between them in the percolation model *w.h.p.*. We formally state and prove the above property in the lemma below.

Lemma 6.3.1 *Let p be the probability that a grid is open in the site percolation model we have defined (Eq. (6.2)). Then the probability that there exists an open path of length m starting from a source is upper bounded by*

$$P(N(m) \geq 1) \leq \frac{8}{7}(7p)^m, \tag{6.3}$$

where $N(m)$ is the number of open paths of length m starting from a given source.

Proof. The total number of paths of length m is upper bounded by $8 \cdot 7^{m-1}$, because for the first hop there are at most 8 choices, and for each subsequent hop there are at most 7 choices. Each path of length m is open with a probability of p^m. Thus, the expected number of open paths of length m starting from a given source is $E[N(m)] = 8 \cdot 7^{m-1} \cdot p^m$. It then follows by the Markov inequality that

$$P(N(m) \geq 1) \leq E[N(m)] = \frac{8}{7}(7p)^m. \tag{6.4}$$

□

If we choose $p < 1/7$ and the distance (in terms of grids) between the source and the destination goes to infinity, then *w.h.p.* there is no open path between them.

The next result is patterned on the results derived in [31] (Eq. (2.49)) in which the bond percolation model is used. Note, however, that we consider the *site* percolation model, and hence the proof is not

exactly the same.

Lemma 6.3.2 *Let A be the event that there exists an open path of length m starting from a given source and F_A the minimum number of grids that need to be turned open from closed in order for the event A to take place. Then we have*

$$P_p(A) \geq \left(\frac{p-p'}{1-p'}\right)^r P_{p'}(F_A \leq r) \tag{6.5}$$

for any $0 < p' < p < 1$, where P_p ($P_{p'}$) denote the probability measure with the site-open probability p (p'), which is the probability that a grid is open .

Proof. See Appendix A.7.

6.3.2 Derivation of the lower bound

We are now in a position to prove the following major result.

Theorem 6.3.1 *Assume that nodes are distributed in a unit square area according to a Poisson point process with density n. If the distance between a source-destination pair is $d \geq \epsilon > 0$, the energy Q (defined in Eq. (6.1)) of the minimum energy route between them is at least $c_1 n^{(1-\alpha)/2}$* w.h.p. *for some constant $c_1 > 0$. Specifically,*

$$P(Q \geq c_1 n^{(1-\alpha)/2}) \geq 1 - \frac{8}{7} \cdot \exp(-c_2\sqrt{n}), \tag{6.6}$$

as $n \to \infty$, for some constant $c_1, c_2 > 0$.

Proof. For any route between the source and the destination, we can construct a walk (which may include some grids more than once) in the site percolation model, by including all the grids that intersect with the route. The walk can be further trimmed into a path which contains the minimum number of closed grids by removing unnecessary grids. The trimming process is illustrated in Fig. 6.2. We denote T^* as an optimally trimmed path that contains the minimum number of closed grids. In what follows, we derive a bound on the probability that the optimally trimmed path T^* contains at most $c_3\sqrt{n}$ closed grids, where c_3 is a constant yet to be determined.

Note that the distance between the source-destination pair in terms of grids is at least $m \triangleq d/(\sqrt{2}c_0/\sqrt{n}) = d\sqrt{n}/(\sqrt{2}c_0)$. This implies the path length of T^* is at least m.

If T^* contains at most $c_3\sqrt{n}$ closed grids, then we can construct an open path from the source to the destination, by turning at most $c_3\sqrt{n}$ closed grids into open grids. This further indicates that by turning

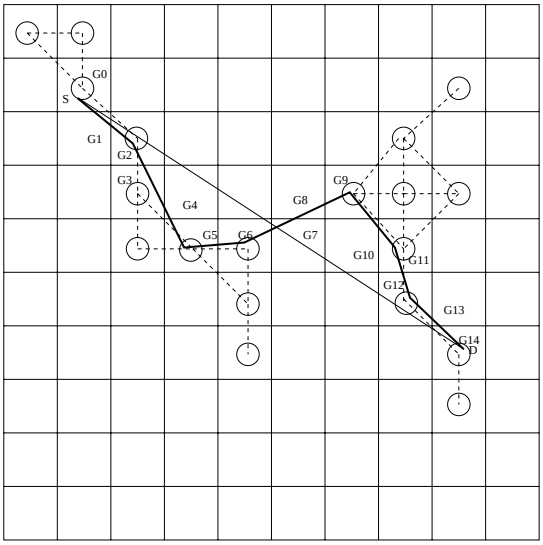

Figure 6.2: The bold lines show a route from source S to destination D. We can construct a walk (which is also a path) that is composed of grids that intersect with the route: $[G_0, G_1, G_2, G_3, G_4, G_5, G_6, G_7, G_8, G_9, G_{10}, G_{11}, G_{12}, G_{13}, G_{14}]$. Some of the grids can be removed from the path. For example, G_1 can be removed because G_0 and G_2 are connected (in our percolation model). Similarly, G_4, G_8, G_{10}, G_{13} can all be removed. There are multiple ways of trimming the path. For example, we can also remove G_3, G_5 but keep G_4. Among all the trimmed paths, we pick as T^* the one that contains the minimum number of closed grids. Ties are broken arbitrarily. In the above example, the path $[G_0, G_2, G_3, G_5, G_6, G_7, G_9, G_{11}, G_{12}, G_{14}]$ contains minimum number (which is 1 in this case) of closed grids.

at most $c_3\sqrt{n}$ closed grids into open ones, we can obtain an open path of length at least m starting from the source. Now we apply Lemma 6.3.2. Let A denote the event that there is an open path of length m starting from the source, and F_A the minimum number of closed grids that need to be turned into open in order for event A to take place. We conclude that $F_A \leq r = c_3\sqrt{n}$ if the trimmed path T^* contains at most $c_3\sqrt{n}$ closed grids. By Lemma 6.3.2,

$$P_{p'}(F_A \leq c_3\sqrt{n}) \quad \leq \quad P_p(A)\left(\frac{p-p'}{1-p'}\right)^{-c_3\sqrt{n}}. \tag{6.7}$$

By Lemma 6.3.1,

$$P_p(A) = \frac{8}{7}\cdot(7p)^m = \frac{8}{7}\cdot(7p)^{d\sqrt{n}/(\sqrt{2}c_0)}. \tag{6.8}$$

We can choose c_0 such that $p = 1 - e^{-c_0^2} < 1/7$. After fixing c_0 and p, we can choose $k > 1/p$ and $p' = \frac{kp-1}{k-1} < p$. Now plugging the expression of p' and Eq. (6.8) into Eq. (6.7), we have

$$P_{p'}(F_A \leq c_3\sqrt{n}) \quad \leq \quad \frac{8}{7}\cdot(7p)^{d\sqrt{n}/(\sqrt{2}c_0)}\cdot k^{c_3\sqrt{n}}$$

$$= \frac{8}{7} \cdot \exp\left(\sqrt{n}\left(\frac{d\log(7p)}{\sqrt{2}c_0} + c_3 \log k\right)\right). \tag{6.9}$$

If we choose $0 < c_3 < -\frac{\epsilon \log(7p)}{\sqrt{2}c_0 \log k} < -\frac{d\log(7p)}{\sqrt{2}c_0 \log k}$, we obtain

$$P_{p'}(F_A \le c_3\sqrt{n}) \le \frac{8}{7} \cdot \exp(-c_2\sqrt{n}) \to 0 \tag{6.10}$$

as $n \to \infty$, where

$$c_2 = -\frac{\epsilon \log(7p)}{\sqrt{2}c_0} - c_3 \log k > 0. \tag{6.11}$$

Hence, the optimally trimmed path T^* contains more than $c_3\sqrt{n}$ closed grids with probability at least

$$p_1 \triangleq 1 - \frac{8}{7} \cdot e^{-c_2\sqrt{n}} \tag{6.12}$$

if we choose the grid size $c_0'/\sqrt{n}$ such that $1 - e^{-c_0'^2} = p'$.

We claim that for each closed grid on T^*, there is exclusively one line segment with length at least $c_0'/\sqrt{n}$ completely contained in a link on the minimum energy route. This is because, for each such closed grid g, there must be a link l on the route that crosses the grid g either from two parallel sides of g or from two adjacent sides of g. (An illustration is given in Fig. 6.3.) In the former case, the line segment on the link and contained inside the grid g has length at least $c_0'/\sqrt{n}$. In the latter case, we consider two neighbor grids of g that also intersect with the link l. At least one of them is either not closed or not on the optimally trimmed path T^* (otherwise, we can remove the closed grid g from the path T^*). The line segment on the link contained inside the grid g and the neighbor grid that is either not on the path T^* or not closed has length at least $c_0'/\sqrt{n}$. By induction on the number of grids intersecting a given link, we can prove that any part of the above obtained line segment will not be reclaimed by other closed grids on T^*. An illustration is given in Fig. 6.3.

Therefore, we conclude that for each closed grid on T^*, there is a link on the minimum energy route that intersects with it. In addition, if a link on the route intersects with j closed grids on T^*, the link has length at least $jc_0'/\sqrt{n}$. To derive the lower bound of the energy of the route, we can assume each link only intersects at most one grid in T^*, because if a link intersects with j closed grids on T^*, its energy will be greater than the energy of j links each with length $c_0'/\sqrt{n}$ since its length is at least $jc_0'/\sqrt{n}$.[3] Thus the route contains at least $c_3\sqrt{n}$ links each with length at least $c_0'/\sqrt{n}$ with probability at least p_1 (defined in Eq. (6.12)). Hence the total energy of the route is at least $c_3\sqrt{n} \cdot \left(\frac{c_0'}{\sqrt{n}}\right)^\alpha = c_3 c_0'^\alpha n^{(1-\alpha)/2}$

[3]Here we make use of the assumption $\alpha \ge 1$; otherwise, the statement may not hold.

with probability at least p_1. Denoting $c_1 = c_3 c_0'^{\alpha}$, we obtain

$$P(Q \geq c_1 n^{(1-\alpha)/2}) \geq p_1 = 1 - \frac{8}{7} \cdot \exp(-c_2\sqrt{n}). \tag{6.13}$$

□

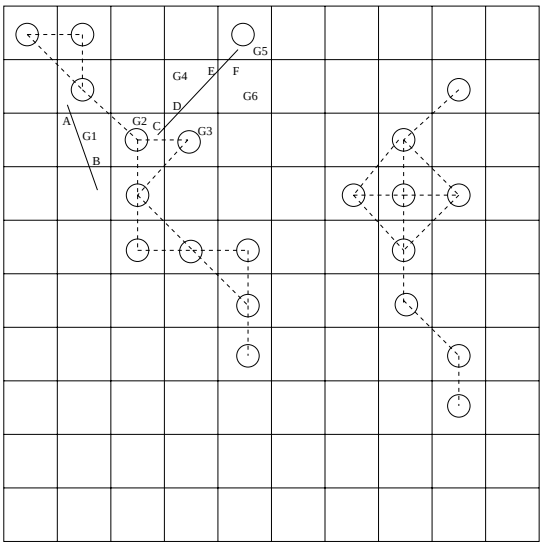

Figure 6.3: Illustration that for each closed grid on T^*, there exists exclusively one line segment completely contained in a link on the minimum energy route with length at least $c_0'/\sqrt{n}$. If a link crosses a closed grid at the two opposite edges (as in the grid G_1), the line segment (AB) on the link that is contained by the grid have length at least $c_0'/\sqrt{n}$. Hence without loss of generality, we can assume a link enters a closed grid from its bottom and exits from its right (such as grid G_4). If grid G_3 is on the path T^*, then G_6 is either not on the path T^* or open, because otherwise G_4 can be removed from the path. In this case, the line segment DF has length at least $c_0'\sqrt{n}$. Similarly if G_2 but not G_3 is on the path T^*, the line segment CE has length at least $c_0'\sqrt{n}$. If a link intersects more than one grid on the path T^*, similar analysis can be performed.

6.4 An Upper Bound on the Minimum Energy Consumption

In order to derive an upper bound on the minimum energy required to transport a packet over a wireless network, we leverage the routing scheme devised in [26, 27] and show that there exists a routing scheme that can achieve the energy bound. As will be discussed later, the energy bound turns out to be of the same order of the lower bound that we have derived in Section 6.3.

6.4.1 Construction of the backbone network

The routing scheme lays a wireless backbone network that carries packets across the network at the desired rate. The backbone network is composed of mostly short hops (and hence consumes low energy),

and is obtained through the percolation theory.

To construct the backbone network, we divide the area into square grids of edge length $c_5/(\sqrt{2n})$. The new grid system is depicted in Fig. 6.4 (a). Note that the grid system is constructed differently from that in Section 6.4: grids in this grid system are not arranged in a vertical-horizontal fashion, but are 45 degree tilted. Then, as depicted in Fig. 6.4 (b), for each of the one half of grids in the system, we draw a horizontal edge across it and for each of the other half of grids, a vertical edge across it. (Both the horizontal and vertical edges are depicted in thick lines in Fig. 6.4 (b).) An edge is said to be open if there exists at least one node (from the Poisson point process) in the grid that contains the edge and closed otherwise. In this fashion we obtain a bond percolation model. The probability that an edge is open is independent of all other edges, and can be expressed as

$$p = 1 - e^{-c_5^2/2}. \tag{6.14}$$

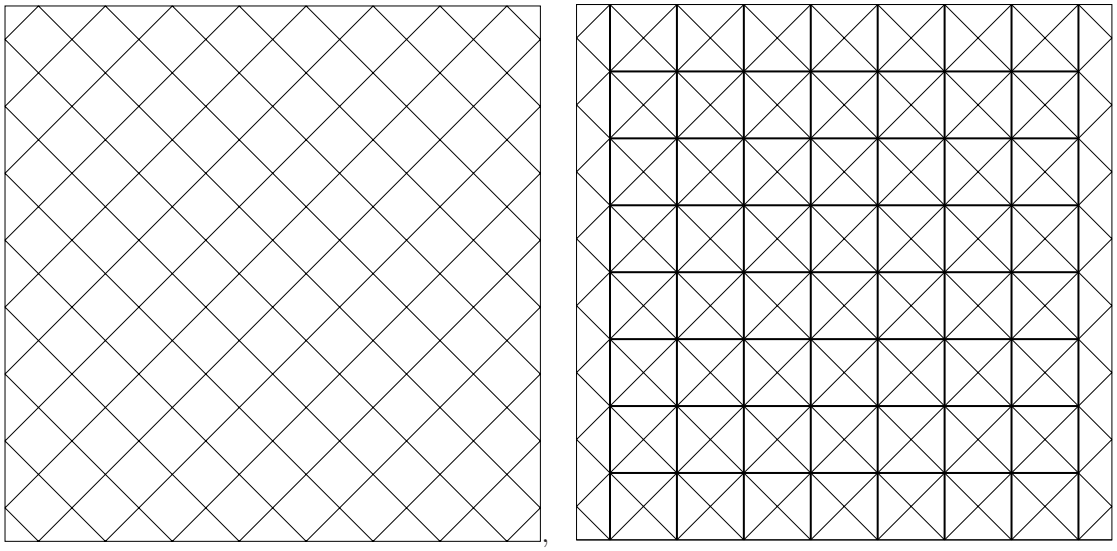

(a) New grid system (b) Edges for the bond percolation model

Figure 6.4: Construction of the bond percolation model. We divide the unit square area into square grids of side length $c_5/(\sqrt{2n})$. A grid is said to be *open* if it contains at least one point in the Poisson point process and *closed* otherwise. The edge that crosses an open (closed) grid is said to be *open* (*closed*).

Next we divide the network area into horizontal rectangles, $\bar{R}_n$, of size $1 \times \frac{c_5}{\sqrt{n}} \log \frac{\sqrt{n}}{c_5}$. Each of the rectangles thus has $m \times \log m$ grids in the bond percolation model, with $m = \sqrt{n}/c_5$ (as the edges have length $\frac{1}{m}$). As proved in [26] (Theorem 1), there exist many open paths from left to right inside each such rectangle $\bar{R}_n$.

Lemma 6.4.1 *(Theorem 1 in [26]) If c_5 is sufficiently large, there exists a constant $\beta = \beta(c_5) > 0$ such*

that w.h.p. *there are* $\beta \log m = \beta \log \frac{\sqrt{n}}{c_5}$ *disjoint open paths that cross each rectangle* $\bar{R}_n$ *from left to right.*

This result does not give a bound on the length of the paths. However, we can bound the length of the shortest open path in each rectangle $\bar{R}_n$ as follows.

Lemma 6.4.2 *If* c_5 *is sufficiently large, there exists a constant* $\beta = \beta(c_5) > 0$ *such that* w.h.p. *the shortest open path crossing each rectangle* $\bar{R}_n$ *has length not larger than* $2m/\beta$.

Proof By Lemma 6.4.1, *w.h.p.*, there are $\beta \log m$ *disjoint* open paths in each rectangle $\bar{R}_n$. If every open path in a rectangle has a length greater than $2m/\beta$, the total number of edges held by all the disjoint, open paths in the rectangle is larger than $2m \log m$. However, the total number of edges in each rectangle is equal to the number of original grids (as depicted in Fig. 6.4(a)) in that rectangle, which is $2m \log m$. By the pigeonhole principle, we reach a contradiction, and hence at least one open path in each rectangle has length not greater than $2m/\beta$ and so does the shortest open path. □

We can also divide the area into vertical rectangles and obtain the same results for paths that cross the area from the bottom to the top. With the use of a simple union bound argument, we conclude that there exist at least one horizontal open path and one vertical open path with length at most m/β in each horizontal rectangle and vertical rectangle simultaneously *w.h.p.*. These paths constitute the backbone network we are going to use in the routing scheme.

6.4.2 Routing scheme

The routing scheme operates as follows. Packets are transported from the source to the destination in the above backbone network via three phases: the *draining phase*, the *backbone phase*, and the *delivery phrase*. In the first (draining) phase, the source sends packets directly to a node on a horizontal open path of the backbone network. In the second (backbone) phase, packets are transported along the horizontal open path and reach a vertical open path. In the third (delivery) phase, a node in the vertical open path sends packets directly to the destination. In what follows we discuss the detailed operations in each phase.

Draining phase

In the draining phase, packets are carried from the source to the backbone network. We first evenly divide the square area into $m/\log m$ horizontal slabs of width $\frac{\log m}{m}$, where $m = \sqrt{n}/c_5$. Now since there are exactly as many slabs as the rectangles, we can enforce nodes in the ith slab to send their packets using the shortest open path in the ith rectangle. More precisely, an entry point in the ith horizontal

path can be assigned to each source in the ith slab. As shown in Fig. 6.5, the entry point is chosen to be the node on the shortest open path in the ith horizontal rectangle that is closest to the vertical line drawn from the source point. By Lemma 6.4.1, the distance between a source and its corresponding entry point is never larger than $(c_5/\sqrt{n})\log(\sqrt{n}/c_5) + c_5/\sqrt{n}$ (since the source and the entry point are in the same rectangle $\bar{R}_n$ their vertical distance is at most $(c_5/\sqrt{n})\log(\sqrt{n}/c_5)$, and their horizontal distance is at most $c_5/\sqrt{n}$ by the choice of the entry point).

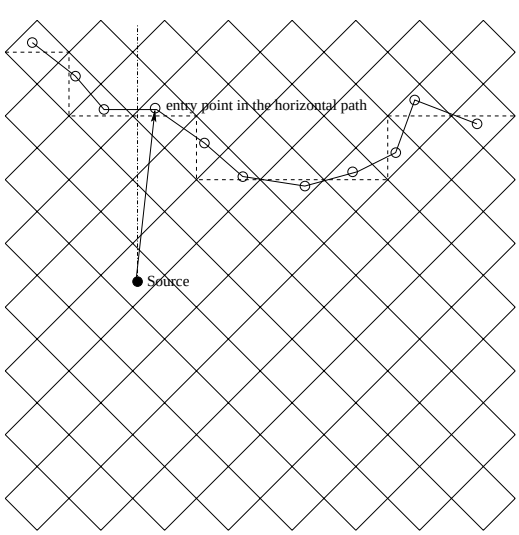

Figure 6.5: A source transmits packets directly to the entry point on a horizontal open path.

Backbone phase

Similarly we can divide the square area into $m/\log m$ vertical slabs. Once a packet is transmitted to the entry point, it is carried along the corresponding horizontal path until it reaches the crossing point with the target vertical open path. The target vertical open path is determined by the vertical slab that contains the destination node, i.e, if the destination is in the ith vertical slab, the target vertical open path is the shortest open path in the ith vertical rectangle.

Delivery phase

In the delivery phase, packets are transported from the *exit point* of the vertical open path to the destination directly, where the exit point for a given destination is defined as a node in the grid on the vertical open path whose center (i.e., the center of the grid) is closest to the horizontal line drawn from the destination. Again by a similar line of argument, the destination from the exit point to the destination is at most $(c_5/\sqrt{n})\log(\sqrt{n}/c_5) + c_5/\sqrt{n}$.

6.4.3 Energy consumption for transporting a packet

We now show that the energy consumed to transport a packet using the routing scheme presented in Section 6.4.2 is $O(n^{\frac{1-\alpha}{2}})$. Clearly it is sufficient to show this is true in each phase of the routing scheme.

Draining phase

Since the distance from each source X to the entry point X_1 is never larger than $\frac{c_5}{\sqrt{n}}(\log\frac{\sqrt{n}}{c_5}+1)$, the required energy in this hop is

$$\begin{aligned} q_1 &= |X-X_1|^\alpha \\ &\leq \left(\frac{c_5(1+\log(\sqrt{n}/c_5))}{\sqrt{n}}\right)^\alpha \\ &\leq c_6 n^{(1-\alpha)/2}. \end{aligned} \tag{6.15}$$

Clearly the last inequality holds if n is sufficiently large for any $c_6 > 0$.

Backbone phase

By Lemma 6.4.2, a message needs to travel at most $2m/\beta$ hops on a horizontal open path and at most $2m/\beta$ hops on a vertical open path before it reaches the exit point. Since each hop length is at most $2c_5/\sqrt{n}$, the total energy consumption on the backbone phase is

$$\begin{aligned} q_2 &\leq 2\cdot 2m/\beta\cdot(2c_5/\sqrt{n})^\alpha \\ &= \frac{4}{\beta}\sqrt{n}/c_5(2c_5/\sqrt{n})^\alpha \\ &= \frac{2^{\alpha+2}}{\beta}c_5^{\alpha-1}\cdot n^{\frac{1-\alpha}{2}}. \end{aligned} \tag{6.16}$$

Delivery phase

In the delivery phase, an exit point on the vertical path sends packets to the destination node directly. Again, the distance from the exit point to the destination node is upper bounded by $(c_5/\sqrt{n})(\log(\sqrt{n}/c_5)+1)$. With a similar analysis performed in the draining phase, we can upper bound the energy consumption by

$$q_3 \leq c_6 n^{(1-\alpha)/2}, \tag{6.17}$$

if n is sufficiently large for any given $c_6 > 0$.

Summing up the energy consumption in all three phases, we obtain an upper bound on the energy

required to transport a packet in a network from source to destination.

Theorem 6.4.1 *With the assumptions we have made in Section 6.2, the minimum energy required to transport a packet from a source to a destination in a unit-square area is upper bounded by* $c_7(n^{(1-\alpha)/2})$ w.h.p.*, where* $c_7 = 2c_6 + 2^{\alpha+2}c_5^{\alpha-1}/\beta$ *is independent of* n.

Remarks on load balancing In the derivation, we do not consider the issue of load balancing, as our focus is on the minimum energy required to transport a packet between a source-destination pair. However, load balancing can be achieved, while maintaining the same order of minimum energy consumption. By applying the pigeonhole principle, for any $0 < \gamma < \beta$ (where β is defined in Lemma 6.4.1), one can show that *w.h.p.* at least $\gamma \log m$ disjoint open paths in each rectangle have a length of at most $2m/(\beta - \gamma)$. Combining all the open paths in all rectangles, we can obtain γm disjoint horizontal open paths and γm disjoint vertical open paths, all of which are of length at most $2m/(\beta - \gamma)$. Thus we can evenly distribute the traffic on the γm open paths to balance the traffic load while still consuming the minimum order of energy.

Combining Theorems 6.3.1 and 6.4.1, we reach the major conclusion in this chapter.

Corollary 6.4.1 *Assume that nodes are distributed in a unit square area according to a Poisson point process with density* n*. If the distance between a source-destination pair is* $\Theta(1)$*, the minimum energy required to transport a packet from the source to the destination is* $\Theta(n^{(1-\alpha)/2})$ w.h.p..

6.5 Extensions

In this section, we discuss how to extend the results to accommodate the case (i) that the network density is kept as a constant but the area of the network goes to infinity, and (ii) that both the transmitting and receiving operations consume energy.

6.5.1 Extension to the case that the network size grows

One may wonder if the derivation holds true in the case of very short distance scale (e.g., of order less than or equal to $n^{-1/2}$), as the energy, d^α, incurred in transmission may not be accurate in this case (where d is the distance between a sender and a receiver). Our understanding is that the unit area square (which is widely used) is a miniature of the real world and can be "resized" to obtain parameters of interest. That is, we consider a (rescaled) network with a fixed node density D in a square region with side length $l \to \infty$. If we scale such a network back to unit-area with side length 1, the node density in the unit-area network is now Dl^2 (Table 6.1 shows the corresponding values in the rescaled network and those in the

Table 6.1: Corresponding values in the rescaled (large) square and those in the original unit-area square.

values of interest	in the rescaled square	in the unit-area square
side length	l	$l' = 1$
density	D	$\lambda' = Dl^2$

original one). By Corollary 6.4.1, the minimum energy required in the unit-area disk is $(Dl^2)^{(1-\alpha)/2}$. As compared with the unit-area network, each edge in the rescaled (large) network is multiplied by l, and the energy consumed at each hop (and hence the total energy consumption) is multiplied by l^α. Therefore, the energy consumed to carry a packet from a source to a destination with distance $\Theta(l)$ in the rescaled network is

$$\Theta((Dl^2)^{(1-\alpha)/2} \cdot l^\alpha) = \Theta(D^{(1-\alpha)/2} l). \tag{6.18}$$

It is interesting to observe that although the energy consumed at a single hop scales as l^α, the energy consumed through multiple hops scales linearly with l and decreases as the node density increases. We also note that Eq. (6.18) does not require that D be constant. Instead, the only assumption required (for the asymptotic proof in Section 6.3 and 6.4) is that Dl^2 goes to infinity.

More generally, for any given source destination pair with distance l, we can construct a square with a side length of $\Theta(l)$ which contains both the source and the destination. Therefore, we can easily obtain the following result.

Corollary 6.5.1 *Assume that nodes are distributed as a Poisson point process with density D in an infinite plane. If the distance between a source-destination pair is l, the minimum energy required to transport a packet from the source to the destination is* $\Theta(D^{(1-\alpha)/2} l)$ w.h.p., *as* $Dl^2 \to \infty$.

6.5.2 Extension to the case that both transmitting and receiving operations consume power

In the derivation in Sections 6.3–6.4, we only consider the energy consumption incurred in the transmission activities. It has been indicated (e.g. [9]) that a wireless node also consumes energy when it receives packets. As the amount of energy consumed in receiving a packet is usually a constant,[4] the total energy consumed at the receivers only depends on the number of hops.

To figure in the energy consumed in receiving packets, we consider the rescaled network as above.

[4]The energy consumed in transmitting a packet also contains a constant term (in addition to the d^α term), and can be figured in together with the receiving energy.

The number of hops has been shown to be upper bounded by $O(\sqrt{Dl^2})$. Therefore the total energy required to transport a packet from a source to a destination with distance $\Theta(l)$ is upper bounded by $O(D^{1/2}(1+D^{-\alpha/2})l)$ *w.h.p.*. The original lower bound in the case that does not consider receiving energy, $\Omega(D^{(1-\alpha)/2}l)$, still serves as a lower bound in the case that considers both transmitting and receiving energy. Notice that, if the node density D is no more than a constant, the two bounds are still in the same order.

6.6 Application to Other Energy-Related Problems

In this section, we demonstrate how to apply the results derived in earlier sections to solve other energy-related problems. We give (i) an network capacity bound (that is more improved than that derived in [54]) under Ultra Wide Band (UWB) communication, (ii) a network capacity bound using directional antennas (which is equivalent to the result obtained in [5]), and (iii) a new asymptotic network lifetime upper bound.

In the following discussions, we return to the case of a unit-square area which is used in the literature, so that a fair and meaningful comparison can be made.

6.6.1 Network capacity in the case of UWB

Negi and Rajeswaran [54] derived the capacity bounds of power constrained ad-hoc networks, and showed that under the assumption that arbitrarily large bandwidth can be used, the per node capacity in a wireless network in a unit square is upper bounded by $O((n \log n)^{(\alpha-1)/2}$ and lower bounded by $\Omega(\frac{n^{(\alpha-1)/2}}{(\log n)^{(\alpha+1)/2}})$. We now derive tighter bounds using the bounds we have obtained in Section 6.3–6.4. For the ease of understanding, we will first provide necessary background and several results in [54] that pertain to our derivation.

Background

Additional assumptions on the system model We still consider a square of unit area, in which nodes are distributed according to a Poisson point process with density n. In addition, we make the following assumptions: (i) each node has a power constraint W_0; (ii) the underlying communication system has an arbitrarily large bandwidth B (i.e., $B \to \infty$); (iii) an ambient Gaussian noise model with the power spectral density of $N_0/2$ and the signal noise power loss of $1/d^\alpha$ is used, where d is the distance and $\alpha > 2$ is the distance loss exponent; and (iv) capacity-achieving Gaussian channel codes are assumed for each link. Thus, each link can support a data rate determined by the Shannon capacity of that

link [18], i.e., $r = B\log(1 + SINR)$. Similar to [54], we use $\log(\cdot)$ to denote $\log_e(\cdot)$ and the capacity is expressed in units of nats [18]. The $SINR$ of the transmission from node i to node j can be computed as

$$SINR = \frac{W_i g_{ij}}{BN_0 + \sum_{k \in I} W_k g_{kj}}, \tag{6.19}$$

where W_i denotes the transmission power of node i, $g_{ij} = |X_i - X_j|^{-\alpha}$ denotes the power loss between node i and j, and I is the set of nodes that are simultaneously transmitting.

Performance metric All nodes send traffic at a rate of $r(n)$ nats per second to their corresponding destinations. The source-destination pairs are uniformly and randomly selected, so that each node is exactly the destination of one source. A uniform throughput $r(n)$ is feasible if there exists a routing and scheduling scheme that can satisfy the throughput requirement of $r(n)$ nats per second for each source-destination pair. The maximum feasible uniform throughput is the uniform throughput capacity, and is the performance metric studied in this section.

The objective is to bound the uniform throughput capacity by a function of n. We say that the uniform throughput capacity $r(n)$ is of order $\Theta(f(n))$ if there exist deterministic constants $c_1 > c_0 > 0$ (w.r.t. n) such that

$$\lim_{n\to\infty} \text{Prob}(r(n) = c_0 f(n)) \text{ is feasible }) = 1, \tag{6.20}$$

$$\lim_{n\to\infty} \text{Prob}(r(n) = c_1 f(n)) \text{ is feasible }) < 1. \tag{6.21}$$

If only Eq. (6.20) is satisfied, we say that the uniform throughput capacity $r(n)$ is of order (or lower bounded by) $\Omega(f(n))$. If only Eq. (6.21) is satisfied, we say that the uniform throughput capacity $r(n)$ is of order (or upper bounded by) $O(f(n))$.

Bandwidth requirement An additional interesting question is how fast the bandwidth B should grow in order to satisfy the derived capacity bounds. It has been shown in [54] that the bandwidth should grow at least as fast as $\Theta(n^{(\alpha+1)/2})$ in order to obtain the capacity bounds thus derived. Later in this chapter we will show: (i) for the upper bound, the bandwidth requirement is arbitrary (i.e., the upper bound holds even for finite value of B), (ii) for the lower bound, the bandwidth requirement is $\Omega(n^{\alpha/2})$.

Upper bound of the capacity

To prove an upper bound of the capacity, we first establish a relation between power consumption and the transmission rate. Assume node i transmits to node j with power W_i and the transmission rate r_{ij}

(according to the Shannon capacity) is

$$\begin{aligned} r_{ij} &= B\log(1+\frac{W_i g_{ij}}{BN_0+\sum_{k\in I} W_k g_{kj}}) \\ &\leq B\log(1+\frac{W_i g_{ij}}{BN_0}) \\ &\leq \frac{W_i g_{ij}}{N_0} \\ &= \frac{W_i}{N_0|X_i-X_j|^\alpha}, \end{aligned} \tag{6.22}$$

where the first inequality results from ignoring the interference term, the second inequality results from $\log(1+x)\leq x$, and the last equation follows from the definition of g_{ij}. Therefore,

$$W_i \geq r_{ij}N_0|X_i-X_j|^\alpha.$$

Now consider an arbitrary route $R_i=[X_{i_1},X_{i_2},\cdots X_{i_K}]$ from a source to a destination. Let r_i denote the achieved throughput on the route R_i. Then, by Eq. (6.22), the total power consumption on this route is

$$W(R_i)\triangleq\sum_{j=1}^{k-1}W_{i_j} \quge r_i(n)\cdot N_0\sum_{k=1}^{K-1}|X_{i_k}-X_{i_{k+1}}|^\alpha = r_i(n)N_0Q_i \tag{6.23}$$

where the last equation results from the definition of Q (Eq.(6.1)). Intuitively, since the average power consumption on each route is bounded, the achievable rate r_i is determined by Q_i. As we have shown that Q_i is lower bounded by $\Omega(n^{(1-\alpha)/2})$ w.h.p., the achievable rate r_i is upper bounded by $O(n^{(\alpha-1)/2})$. Now we present a rigorous analysis.

Lemma 6.6.1 *(i)* W.h.p.*, the number of nodes in the field is between $n/2$ and $2n$.*
(ii) With our ways of choosing source-destination pairs, there exists $\epsilon>0$ such that the number of pairs with distance at least ϵ is at least $n/8$ w.h.p..

Proof: Refer to Appendix A.8.

We now give the major result in this section.

Theorem 6.6.1 *With the assumptions we have made in Section 6.6.1, the network capacity is upper bounded by $O(n^{(\alpha-1)/2})$* w.h.p. *as $n\to\infty$.*

Proof. Let J denote the set of routes with the distance between the source-destination pair at least ϵ. By Lemma 6.6.1, we have $n/8\leq|J|\leq 2n$ *w.h.p.*. Summing up the power consumption (Eq. (6.23))

over all the routes in J, we have

$$\sum_{i\in J} W(R_i) = \sum_{i\in J} r_i(n) N_0 Q_i. \tag{6.24}$$

Since we are interested in the uniform capacity bound $r(n)$ achieved by all routes, we have

$$\sum_{i\in J} W(R_i) \geq r(n) \sum_{i\in J} N_0 Q_i. \tag{6.25}$$

In Theorem 6.3.1, we have shown that there exist $c_1, c_2 > 0$ such that

$$P(Q_i \leq c_1 n^{(1-\alpha)/2}) \leq \frac{8}{7}\exp(-c_2\sqrt{n}) \tag{6.26}$$

for a given source destination pair i with distance at least ϵ. Without loss of generality, we can assume $|J| \leq 2n$ because otherwise we may only keep the first $2n$ routes in J. Thus

$$P(\exists i \in J, \text{ s.t. } Q_i \leq c_1 n^{(1-\alpha)/2}) \leq 2n \cdot \frac{8}{7}\exp(-c_2\sqrt{n}). \tag{6.27}$$

Note that the right term in the above expression converges to 0 as $n \to \infty$, and hence *w.h.p.* we have at least $n/8$ routes, each with at least power $c_1 n^{(1-\alpha)/2}$. In addition, *w.h.p.* the total power of all routes in J is at most $2nW_0$ by Lemma 6.6.1(i). Plugging these results into Eq. (6.25), we obtain that *w.h.p.*

$$r(n) \leq \frac{2W_0}{N_0 c_1 n^{(1-\alpha)/2}/8} = \frac{16W_0}{N_0 c_1} \cdot n^{(\alpha-1)/2}. \tag{6.28}$$

This completes our proof. □

Two remarks are in order for the upper bound. First, the upper bound is derived under the assumption of arbitrary value of B (including finite value). Second, the upper bound is sharper than that presented in [54].

Lower bound of the capacity

A lower bound on the network capacity in the case of UWB communication can be obtained in a similar way as in the derivation of the upper bound on the minimum energy required to transport a packet between a source-destination pair. Specifically, a packet is still delivered in three phases as discussed in Section 6.4.2. In what follows, we discuss each of the three phases, with emphasis on the difference between schemes used in Section 6.4.2 and here, and show that any source-destination pair can achieve a throughput of order $n^{(\alpha-1)/2}$ via the routing strategy.

Draining phase In the first phase, we now divide the region into $\beta\sqrt{n}/c_5$ (which is equal to the number of disjoint horizontal paths) horizontal slabs, and let a source node in the ith slab directly send its message to the node (called entry point) with the shortest horizontal distance in the ith horizontal path.

By Lemma 6.4.1, the distance between a source and its corresponding entry point is never larger than $(c_5/\sqrt{n})(\log(\sqrt{n}/c_5)+1)$ (since the source and the entry point are in the same rectangle $\bar{R}_n$ their vertical distance is at most $(c_5/\sqrt{n})\log(\sqrt{n}/c_5)$, and their horizontal distance is at most $c_5/\sqrt{n}$ by the choice of the entry point). The achievable rate from each source X_i to the entry point is

$$r_i = \frac{W_0}{N_0|X_i - X_{i_1}|^\alpha} \geq \frac{W_0}{N_0}\left(\frac{\sqrt{n}}{c_5(1+\log\sqrt{n}/c_5)}\right)^\alpha \geq c_6 n^{(\alpha-1)/2}. \tag{6.29}$$

Clearly the last inequality holds if n is sufficiently large for any given $c_6 > 0$. Therefore, the rate $c_6 n^{(\alpha-1)/2}$ is achievable as long as there are $\beta\log(\sqrt{n}/c_5)$ horizontal paths in every rectangle $\bar{R}_n$. Since the latter takes place *w.h.p.*, the rate $c_6 n^{(\alpha-1)/2}$ is achievable *w.h.p.*

Backbone phase Similarly we divide the region into $\beta\sqrt{n}/c_5$ vertical slabs. In the second phase, once a packet is transmitted to a horizontal path, it is carried along the path until it reaches the target vertical path, where the target vertical path is determined by the vertical slab that contains the destination node (i.e., if a destination is in the jth vertical slab, its target vertical path is the jth vertical path).

The following lemma has been proved in [26],

Lemma 6.6.2 *The probability that each slab contains less than $c_5\sqrt{n}/\beta$ nodes tends to one when $n \to \infty$.*

Therefore, *w.h.p.*, every node in the backbone (on the horizontal path, the vertical path, or both), will need to relay traffic at a rate $r_i \leq 2\cdot(c_5\sqrt{n}/\beta)\cdot c_6 n^{(\alpha-1)/2} = 2\sqrt{2}c_5c_6n^{\alpha/2}/\beta$. In the backbone phase, a node only needs to transmit packets to its next hop node and the transmission distance is at most $c_5/\sqrt{n}$. Thus, the power consumption on each node W_i is

$$\begin{aligned} W_i &\leq r_i N_0 (c_5/\sqrt{n})^\alpha \\ &\leq (2\sqrt{2}c_5c_6n^{\alpha/2}/\beta)\cdot N_0(c_5/\sqrt{n})^\alpha \\ &= 2c_6(c_5\sqrt{2})^{\alpha+1}N_0/\beta. \end{aligned} \tag{6.30}$$

If we choose $c_6 \leq \frac{W_0\beta}{2N_0(c_5\sqrt{2})^{\alpha+1}}$, we have $W_i \leq W_0$. Thus, the backbone can support a rate of $c_6 n^{(\alpha-1)/2}$ for each source *w.h.p.*.

Delivery phase The routing strategy is identical to that used for minimizing the transporting energy and the analysis is almost identical to that in the first phase. Hence we do not elaborate on the arguments.

In summary, we have proved the lower bound of the network capacity as follows.

Theorem 6.6.2 *With the assumptions we have made in Section 6.2, the network capacity is lower bounded by* $\Omega(n^{(\alpha-1)/2})$ w.h.p..

Bandwidth requirement

As mentioned in Section 6.6.1, the upper bound of the capacity applies to arbitrary values of bandwidth B (including finite values). Hence we only need to focus on the bandwidth requirement for ensuring the lower bound of the capacity. Clearly it is sufficient to show with the required bandwidth, each phase can still support throughput of the same order of magnitude. In what follows we only address the achievable throughput in the second (backbone) phase because it is the bottleneck phase which limits the network capacity.

By the Shannon capacity, the link rate on a hop from node i to j in the second phase is

$$r_{ij} = B\log(1 + \frac{W_i d_{ij}^{-\alpha}}{BN_0 + \sum_{k\in I} W_k d_{kj}^{-\alpha}}), \tag{6.31}$$

where d_{ij} represents the distance between node i and j. To reduce the interference, we first apply a simple TDMA scheme in which when a node j is in the receiving mode, no node in any of its neighboring grids transmits except node i. With this TDMA scheme, each node can transmit with a constant fraction of time. To bound the total interference, all interfering nodes must have a distance of at least $g \triangleq c_5/\sqrt{2n}$ (where g is the grid size) from the receiving node j. Also, consider the grids surrounding the grid containing j and divide them into nested rectangular rings based on their (infinite-norm) distance from the grid containing j. With this division, the innermost ring contains 8 grids, the second innermost ring contains 16 grids, and in general the kth innermost ring contains $8k$ grids.

Since each grid has at most one node transmitting and a node in the kth ring has a distance of at least $(k-1)g$ from the receiving node j, the total interference can be bounded by (noticing that nodes in the innermost ring do not transmit except node i)

$$\begin{aligned}
\sum_{k=2}^{\infty} 8k((k-1)g)^{-\alpha} &= g^{-\alpha}\sum_{k=2}^{\infty} 8k((k-1))^{-\alpha} \\
&\le g^{-\alpha}\int_1^{\infty}(x^{-\alpha} + x^{1-\alpha}) \\
&= g^{-\alpha}(\frac{1}{1-\alpha} + \frac{1}{2-\alpha}) \\
&= c_8 n^{\alpha/2},
\end{aligned} \tag{6.32}$$

where $c_8 = c_5^{-\alpha} 2^{\alpha/2} (\frac{1}{1-\alpha} + \frac{1}{2-\alpha})$. Under the assumption that $\alpha > 2$, we have

$$r_{ij} \geq B \log(1 + \frac{W_i d_{ij}^{-\alpha}}{BN_0 + c_8 n^{\alpha/2}}). \tag{6.33}$$

Since each node can transmit with power W_0 and $d_{ij} \leq 2\sqrt{2}g = 2c_5/\sqrt{n}$,

$$r_{ij} \geq B \log(1 + \frac{W_0 (2c_5)^{-\alpha} n^{\alpha/2}}{BN_0 + c_8 n^{\alpha/2}}). \tag{6.34}$$

Since the function $x \log(1 + a/(x + c))$ is an increasing function of x for any given positive values of a, c, if we let $B \geq c_9 n^{\alpha/2}$, we have

$$\begin{aligned} r_{ij} &\geq c_9 n^{\alpha/2} \log(1 + \frac{W_0 (2c_5)^{-\alpha}}{c_9 N_0 + c_8}) \\ &= c_{10} n^{\alpha/2}, \end{aligned} \tag{6.35}$$

which is the desired throughput. In conclusion, under the assumption $\alpha > 2$, the bandwidth required for achieving the network capacity of order $\Theta(n^{(\alpha-1)/2})$ is $\Omega(n^{\alpha/2})$.

6.6.2 Network capacity with the use of directional antennas

Peraki and Servetto [5] studied the problem of network capacity in wireless networks with directional antennas. By the assumption in [5] that directional antennas can generate arbitrarily narrow beams, wireless interference can be ignored and the major constraint for limiting the network capacity is the energy consumption. One of the major results obtained in [5] is that the network capacity with the use of directional antennas is upper bounded by $\Theta(\sqrt{n \log n})$ if all nodes choose a common power to maintain connectivity. As given in [35], the common transmission radius r required to maintain connectivity satisfies

$$\pi r^2 = \frac{\log n + \eta_n}{n}, \tag{6.36}$$

for some $\eta_n \to \infty$ as $n \to \infty$.

Now we show how the results derived in this chapter can be used to obtain the same capacity bound. Normally we assume the transmission power for a transmission radius r is r^α. The transmission power is just the transmission energy per unit of time. Based on Eq. (6.36), in any one unit of time, the total available transmission energy in the network is $\Theta(n \cdot (\frac{\log n}{n})^{\alpha/2})$. As we have proved in Sections 6.3–6.4, for each source-destination with distance at least $\epsilon > 0$, the minimum energy required to transport a packet

from a source to a destination is $\Theta(n^{(1-\alpha)/2})$. Therefore, the total network capacity is upper bounded by

$$\frac{\Theta(n \cdot (\frac{\log n}{n})^{\alpha/2})}{\Theta(n^{(1-\alpha)/2})} = \Theta(\sqrt{n(\log n)^{\alpha}}). \tag{6.37}$$

At the first glance, this bound is higher than the upper bound $\Theta(\sqrt{n \log n})$ given in [5] since usually $2 \leq \alpha \leq 4$ in practice. However, throughout the derivation in Sections 6.3–6.4 we only assume $\alpha \geq 1$. Taking $\alpha = 1$, we obtain the same upper bound as that in [5].

6.6.3 Upper bound of the lifetime of wireless sensor networks

If a power management scheme can be properly deployed in a wireless sensor network to determine when sensor nodes should go to sleep (in the lack of communications/sensing activities) and when they should wake up (to perform their sensing/communications tasks), we can assume that energy is only consumed when a sensor transmits/receives data packets. In such a power-managed sensor network, the results derived in Sections 6.3–6.4 can be used to obtain an upper bound on the network lifetime. For example, if we assume each sensor node has a constant initial energy and each node transmits to a random destination at a constant rate, then the network lifetime is upper bounded by $\Theta(\frac{1}{Q}) = \Theta(n^{(\alpha-1)/2})$. (Even in the case that a power management scheme is not used and all the sensor nodes are kept awake consuming energy in their idle states, the derived upper bound on the network lifetime still serves as an upper bound.)

6.7 Simulation Results

We have carried out a simulation study to validate the derived results and to estimate the associated constant in the energy equation $\Theta(n^{(1-\alpha)/2})$ in Corollary 6.4.1. The reason for validating the derived results is because the network behavior/property is analyzed in the asymptotic sense (e.g., as the network size grows to infinity). It is not clear whether or not the results hold in a finite region (or, alternatively, beyond what network size the network will exhibit the asymptotic properties).

Energy vs distance A total of 10 simulation runs are carried out in a unit-area square with a node density 100 nodes per unit-area. The node positions are uniformly and randomly distributed. In each simulation run we randomly choose 10 source-destination pairs and calculate the minimum energy required to transport packets between each source-destination pair using Dijkstra's algorithm. Figure 6.6 shows the minimum energy versus the source-destination distance under different values of path loss exponent

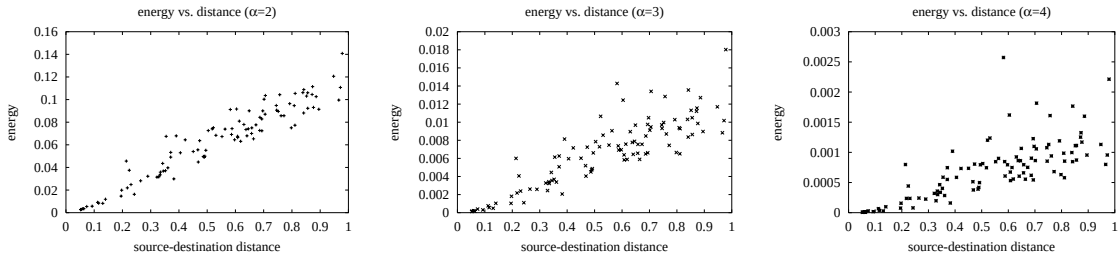

(a) $\alpha = 2$ (b) $\alpha = 3$ (c) $\alpha = 4$

Figure 6.6: The relationship between the minimum energy incurred on a multiple-hop path and the source-destination distance.

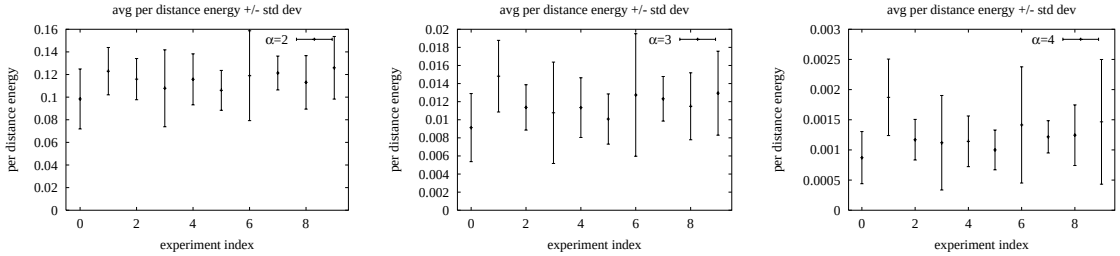

(a) $\alpha = 2$ (b) $\alpha = 3$ (c) $\alpha = 4$

Figure 6.7: The average, energy incurred per unit of distance on a multi-hop, minimum-energy path and its standard deviation. Note that the size of the error bar is twice the standard deviation.

α. As shown in Figure 6.6, there exists a clear linear relationship between the minimum energy and the source-destination distance. Such a relationship has been predicted in Eq. (6.18).

To remove the effect of the source-destination distance, we consider the *energy consumed per unit of distance*, defined as the minimum energy divided by the source-destination distance. For each of the 10 experiments, we evaluate the average energy consumed per unit of distance among the 10 source-destination pairs as well as its standard deviation. As shown in Figure 6.7, for a fixed node density, the energy consumed per unit of distance is some constant value.

Energy consumed per unit of distance vs node density Now we study how the energy consumed per unit of distance changes as the node density increases. This set of simulation runs are similar to the first set, except that the node density is varied from 10 to 10^5. Then we carry out 10 simulation runs, in each of which 10 source-destination pairs are randomly selected. For each value of node density, we calculate the average energy consumed per unit of distance, and its standard deviation, over all source-destination pairs that are apart from each other by a distance of at least 0.5.[5] Figure 6.8 gives the energy consumed per unit of distance versus the node density. The linear relation in the double log scale graph

[5]This complies with the assumption in our theoretical analysis that the distance between a source and a destination is non-diminishing as the node density increases. This assumption is necessary because if the source-destination distance is extremely small such that they are one-hop away on the the minimum energy route, the minimum energy required to transport packets between them is l^α, and is independent of n.

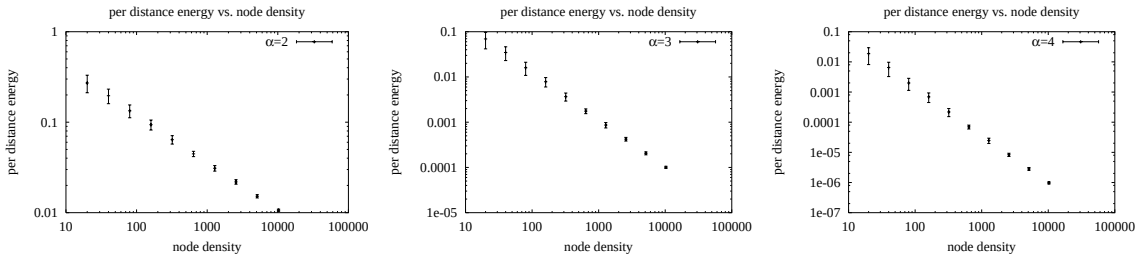

(a) $\alpha = 2$ (b) $\alpha = 3$ (c) $\alpha = 4$

Figure 6.8: The relationship between the energy consumed per unit of distance on a multi-hop, minimum energy path and the node density.

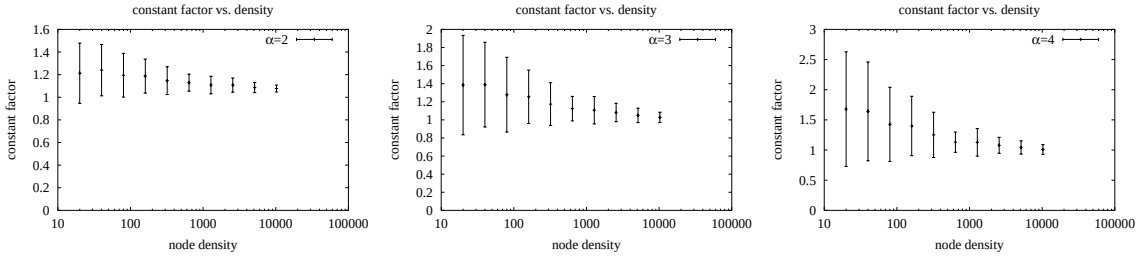

(a) $\alpha = 2$ (b) $\alpha = 3$ (c) $\alpha = 4$

Figure 6.9: The relationship between the constant factor and the node density.

suggests a power relation between the energy and the node density. Again this has been predicted in Eq. (6.18) as well as Corollary 6.4.1.

Finally we would like to quantify the constant associated with Eq. (6.18) and study whether or not the constant converges. Figure 6.9 gives $\frac{E}{n^{(1-\alpha)/2}l}$ vs. the node density, where E is the minimum energy required to transport packets, n the node density, and l the source-destination distance. The value, $c_n \triangleq \frac{E}{n^{(1-\alpha)/2}l}$, shown in the y-axis is the *constant factor* in Eq. (6.18). As shown in Figure 6.9, the constant factor converges to 1 with high probability as the node density goes to infinity (because the standard deviation becomes smaller and smaller as the density increases). Based on the observation, we make the following conjecture.

Conjecture 6.7.1 *Assume that nodes are distributed in a unit square area according to a Poisson point process with density n. Given a fixed source-destination pair and their distance $l \geq \epsilon > 0$, the minimum energy required to transport a packet from the source to the destination is $n^{(1-\alpha)/2}l$* w.h.p.*, as the density $n \to \infty$.*

6.8 Conclusion

In this chapter, we have derived both the lower and upper bounds of the asymptotic minimum energy required to transport packets from a source to a destination in a random wireless network. Under the

assumption that nodes are deployed according to a Poisson point process with node density n in a unit square area and the source-destination distance is non-diminishing, we prove, based on the percolation theory, that the minimum energy required to transport a data packet from a source to a destination is $\Theta(n^{(1-\alpha)/2})$ *w.h.p.*, where α is the path loss exponent. We have also discussed how to extend the results to accommodate the cases (i) that the network density is kept as constant but the network size goes to infinity, and (ii) that both the transmitting and receiving operations consume energy.

We have demonstrated how to leverage derived results to derive the network capacity of wireless networks equipped with directional antennas, the network capacity of wireless networks that operate in UWB, and the upper bound of the lifetime of wireless sensor networks. We believe the results and the proof techniques can be applied to derive the asymptotic conditions on other parameters in wireless networks, as long as the limiting factor for the parameters of interest is the energy.

Finally, we have carried out simulations to validate the derived results and to estimate the constant factor associated with the bounds on the minimum energy. Based on the simulation results, we conjecture that the minimum energy required to transport packets between a source-destination pair that is separated by the distance l converges to $n^{(1-\alpha)/2}l$ *w.h.p.*. This is subject to further theoretical investigation.

Chapter 7

Conclusion and Future Work

In this thesis, we have investigated several issues related to the performance limits of wireless sensor networks with respect to coverage, connectivity, lifetime, power, and network capacity. Specifically, we have studied the following questions:

(1) We have investigated the issues of maintaining coverage and connectivity by choosing a minimum subset of sensor nodes to operate in the active mode in wireless sensor networks. We first derive the relationship between coverage and connectivity, and show that if the radio range is at least twice the sensing range, then complete coverage implies connectivity. Hence, if the condition holds, we only need to consider the coverage problem. Then, we derive a set of optimality conditions to minimize the overlap (which will in turn minimizes the number of working nodes) while ensuring coverage. Based on the optimality conditions, we then devise a decentralized and localized density control algorithm, OGDC. OGDC is fully localized and can maintain coverage as well as connectivity, regardless of the relationship between the radio range and the sensing range. *Ns-2* simulations show that OGDC outperforms several existing algorithms with respect to the number of working nodes and network lifetime, and achieves almost the same coverage as the best algorithms.

(2) We have investigated the lifetime upper bound of of wireless sensor networks. We have first derived necessary and sufficient conditions on the node density required to ensure k-coverage (in the asymptotically almost sure sense) in large sensor networks, as the network size approaches infinity. We have considered several different model assumptions including Torus convention and non-Torus convention. We have also considered three different types of node deployment methods: Poisson process deployment, uniformly random deployment, and regular grid deployment. Then, given the coverage degree k, the sensor network lifetime is upper bounded by k times the lifetime of a single sensor.

We have also derived two upper bounds of α-lifetime in a finite region with a finite density of nodes: (i) an upper bound of α-lifetime for a special family of algorithms which maintain as large coverage as possible; and (ii) an upper bound of α-lifetime that applies to algorithms that maintain the coverage

ratio of α from the beginning of network deployment. In addition, we have devised an algorithm that can approach the derived α-lifetime upper bounds. Simulation results show that our algorithm can achieve around 90% of the lifetime upper bounds when the node density is reasonably large.

With our derivation, we are able to determine, given the lifetime T of a single sensor node, how many sensor nodes have to be deployed in a region, in order to continuously monitor the region for a period of $k \cdot T$.

Based on the analytic and simulation results, we suggest the following sensor network deployment and design strategies. First, a sensor network should be deployed with a reasonably high density in order to achieve a large lifetime per unit of nodal density and to optimize the coverage usage of sensor nodes. Second, as far as the lifetime is concerned, a sensor network should not cover the entire monitored region, but merely maintain α-coverage from the beginning of systems operations, where α is the minimum percentage required by applications. Third, the criteria for choosing a working set of nodes may not necessarily be the number of nodes. Instead, it is desirable to choose a set of working nodes that maximizes the lifetime upper bound of the remaining set of nodes.

(3) We have derived the critical total power required for maintaining k-connectivity in a random wireless networks under the assumption that nodes may choose different transmission power. Comparing the result against those obtained when all nodes use the uniform critical transmission power for k-connectivity [57, 73], our results suggest that with the use of (optimal) power control, the critical total power can be reduced by a factor of $\Theta((\log \lambda)^{c/2})$, irregardless of the power/topology control algorithm used.

(4) We have derived both the lower and the upper bound of the asymptotic minimum energy required to transport packets from a source to a destination in a random wireless network. Under the assumption that nodes are deployed according to a Poisson point process with node density λ in a unit square area and the source-destination distance is non-diminishing, we prove, based on the percolation theory, that the minimum energy required to transport a data packet from a source to a destination is $\Theta(\lambda^{(1-\alpha)/2})$ *w.h.p.*, where α is the path loss exponent. We have also discussed how to extend the results to accommodate the cases (i) that the network density is kept as constant but the network size goes to infinity, and (ii) that both the transmitting and receiving operations consume power.

We have also demonstrated how to leverage the derived results to obtain the network capacity of wireless networks equipped with directional antennas, the network capacity of wireless networks that operate in UWB, and the upper bound of the lifetime of wireless sensor networks. We believe the results and the proof techniques can be applied to derive the asymptotic conditions on other parameters in wireless networks, as long as the limiting factor for the parameters of interest is the energy.

In addition, we have carried out simulations to validate the derived results and to estimate the constant factor associated with the bounds on the minimum energy. Based on the simulation results, we conjecture that the minimum energy required to transport a packet between a source-destination pair that is separated by the distance l converges to $n^{(1-\alpha)/2}l$ *w.h.p.*

We have identified the following research avenues for the future work. For the short term, we plan to improve our current results by considering more general assumptions, imposing additional constraints, and obtaining stronger results.

More specifically, for the problem of maintaining coverage and connectivity, we are interested in developing conditions satisfying coverage and connectivity under more general assumptions of sensing and transmission range (e.g., the transmission range may be less than twice the sensing range, and/or different nodes may have different sensing and transmission range).

Another interesting direction is that when transmission range is less than sensing range, ensuring coverage and connectivity may not be sufficient since when a sleeping node wakes up, it may need to communicate with at least one working node in order to probe its neighborhood. Under this circumstance, it may be important to construct a set of nodes maintaining coverage, connectivity, and also dominating other nodes.

In our problem formulation of α-coverage, we have not considered the coverage issue in the time domain. As a result, some locations may not be covered for a very long time. An interesting future problem is to impose an additional constraint in the time domain. For example, we may want to require every point to be covered at least once in every certain period.

Another interesting problem is to jointly consider the issue of coverage and connectivity with an additional temporal dimension. We assume that an event, once it occurs, will persist for a period of time. This is true for, for example, vehicle tracking, habitat monitoring, and environment monitoring applications. When a vehicle or an animal (to be monitored) shows up (or a fire takes place), it will not disappear immediately. As a matter of fact, the duration during which the event persists (or the time interval until which the event must be detected) may be profiled (or at least characterized by a lower bound). In this setting, the set of working nodes needs not cover the entire region at *all* times, but only need to provide, for each point, intermittent coverage with the inactive period less than or equal to the given bound. There is clearly a tradeoff between energy conservation and efficiency of detecting events of interests.

For the problem of deriving critical total power, a problem that remains is that in our constructive proof, the maximum transmission range and transmission power are unbounded. An interesting question is whether we can bound both the total power and the maximum transmission power and what is the

tradeoff between them.

We are also interested in analytically proving our conjecture on the minimum transporting energy: the minimum energy required to transport a packet between a source-destination pair with distance l converges to $n^{(1-\alpha)/2}l$ *w.h.p.*

For the long term, our goal is to apply the analytical techniques in other related problems. We are interested in analyzing performance limits of networks with more resources and more advanced communication technologies. For example, each node may have multiple antennas and can use multiple channels. Recent advance of communication technologies such as MIMO and OFDM can also improve the networking performance. We are also interested in understanding network performance taking into consideration of specific protocol stacks (e.g., the effects of wireless MAC protocols and TCP on networking performance). Finally, we are interested in understanding the effects of detailed physical channel model on networking performance by both analysis and measurement.

Appendix A

Background and Proof of Lemmas

A.1 Proof of Lemma 3.3.2

We prove the Lemma by showing that given the conditions stated in the lemma, the number of working sensor nodes and the overlap have a linear relationship with a positive slope.

Let the indicator function of a working node i, $I_i(x)$, be defined as

$$I_i(x) = \begin{cases} 1, & \text{if } x \text{ is within the coverage area of node } i, \\ 0, & \text{otherwise.} \end{cases}$$

Let R' be a region that contains R and the coverage areas of all sensor nodes. Then the coverage area of a sensor node i is a disk with the size $\int_{R'} I_i(x)dx \stackrel{\triangle}{=} |S_i|$, where $|S_i|$ denotes the size of the area S_i covered by sensor node i. By condition (ii), $|S_i| = |S|$ for all i. With the definition of $I_i(x)$, the overlap at point x can be written as

$$L(x) = \sum_{i=1}^{N} I_i(x) - I_R(x), \tag{A.1}$$

where N is the number of working nodes, and the overlap of sensing areas of all the sensor nodes, L, can be written as

$$\begin{aligned} L &= \int_{R'} L(x)dx \\ &= \int_{R'} (\sum_{i=1}^{N} I_i(x) - I_R(x))dx \\ &= \sum_{i=1}^{N} \int_{R'} I_i(x)dx - |R| \\ &= N|S| - |R|, \end{aligned} \tag{A.2}$$

where condition (i) is implied in the first equality and condition (ii) is implied in the fourth equality. Eq. (A.2) states that minimizing the number of working nodes N is equivalent to minimizing the overlap

of sensing areas of all the sensor nodes L. □

A.2 Proof of Lemma 3.3.3

There are multiple coverage areas centered at C_i's and they all intersect at point O. We assume that the centers of these coverage areas are labeled as C_i, with the index i increasing clockwise. (Fig. 3.3 gives the case of $k = 3$, where $C_1 = A$, $C_2 = B$, and $C_3 = C$.) Now we have $\sum_{i=1}^{k} \angle C_i O C_{(i \mod k)+1} = 2\pi$ and $\angle C_i O C_{(i \mod k)+1} + \alpha_i = \pi$. From the above equations, we have $\sum_{i=1}^{k} \alpha_i = (k-2)\pi$. □

Table A.1: Radio transmission range of Berkeley Motes [53]

Product	Transmission Range
MPR300*	30m
MPR400CB	150m
MPR410CB	300m
MPR420CB	300m
MPR500CA	150m
MPR510CA	300m
MPR520CA	300m

$*$ MPR300 is the second generation sensors, while the rest are the third generation sensors.

Table A.2: Sensing range of several typical sensors

Product	Sensing Range	Typical Applications
HMC1002 Magnetometer sensor [40]	5m	Detecting disturbance from automobiles
Reflective type photoelectric sensor [4]	1m	Detecting targets of virtually any material
Thrubeam type photoelectric sensor [4]	10m	Detecting targets of virtually any material
Pyroelectric infrared sensor (RE814S) [64]	30m	Detecting moving objects
Acoustic sensor on Berkeley Motes * [40]	$\sim$ 1m	Detecting acoustic sound sources

* This result is based on our own measurement on Berkeley motes [40].

A.3 Results of Coverage Processes

We summarize some of the results on asymptotic coverage drawn from [36] that pertain to our derivation in Section 4.3 and 4.4.

Let the vacancy $V(\ell, \lambda)$ denote the area that is not covered by any node, S_i the coverage disk of node i, and $\chi(x)$ an indicator function of whether a point x is covered by any coverage disk, i.e.,

$$\chi(x) = \begin{cases} 1, & \text{if for all } i, x \notin S_i, \\ 0, & \text{otherwise.} \end{cases}$$

When all nodes are randomly placed on the region R, V is a random variable that can be expressed as

$$V = V(R) = \int_R \chi(x)dx. \tag{A.3}$$

To calculate the expectation of V, we use Fubini's theorem and take the expectation within the integral in Eq. (A.3). That is,

$$\begin{aligned} E(V) &= \int_R E(\chi(x))dx \\ &= ||R||E(\chi(x))dx \\ &= \ell^2 \exp(-\lambda). \end{aligned} \tag{A.4}$$

We have used interchangeably the terms "complete coverage" and "vacancy area is 0" throughout Chapter 4. This is supported by the following theorem (Theorem 3.3 in [36]).

Theorem A.3.1 *Let C be a Boolean model in R^k in which covering shapes are distributed as S. If R is an open subset of R^k, S is a random closed set with $E(||S||) < +\infty$, and V is the vacancy area, then*

$$P(V = 0; R \textit{ is not completed covered}) = 0.$$

Although the theorem requires R be an open subset, it can be generalized to the case that R is closed and regular. The interested reader is referred to the discussions after the theorem in [36].

A.4 Proof of Lemma 4.3.1

By the definition of V_k (as in Eq. (4.3)), we have

$$\begin{aligned} E(V_k^2) &= E\left(\int\int_{R^2} \chi_k(x_1)\chi_k(x_2)dx_1dx_2\right) \\ &= \int\int_{R^2} E\left(\chi_k(x_1)\chi_k(x_2)\right)\, dx_1dx_2 \\ &\equiv I_1 + I_2, \end{aligned} \tag{A.5}$$

where $\chi_k(x)$ is the indicator function of whether x is covered by less than k sensors, and

$$\begin{aligned} I_1 &\equiv \int\int_{R^2\cap\{|x_1-x_2|>2r\}} E\left(\chi_k(x_1)\chi_k(x_2)\right) dx_1dx_2, \quad \text{and} \\ I_2 &\equiv \int\int_{R^2\cap\{|x_1-x_2|\le 2r\}} E\left(\chi_k(x_1)\chi_k(x_2)\right) dx_1dx_2. \end{aligned}$$

For $|x_1 - x_2| > 2r$,$\chi_k(x_1)$ and $\chi_k(x_2)$ are independent, and $E(\chi_k(x)) = e^{-\lambda}\sum_{i=0}^{k-1}\lambda^i/i!$ for all x. Hence,

$$\begin{aligned} I_1 &\equiv \int\int_{R^2\cap\{|x_1-x_2|>2r\}} E\left(\chi_k(x_1)\chi_k(x_2)\right) dx_1dx_2 \\ &= \int\int_{R^2\cap\{|x_1-x_2|>2r\}} E\chi_k(x_1)E\chi_k(x_2)dx_1dx_2 \\ &\le \int\int_{R^2} E\chi_k(x_1)E\chi_k(x_2)dx_1dx_2 \\ &= \left(\ell^2 e^{-\lambda}\sum_{i=0}^{k-1}\frac{\lambda^i}{i!}\right)^2 = \left(E(V_k)\right)^2. \end{aligned} \tag{A.6}$$

What is left is the derivation of I_2. Let B_1 and B_2 denote the unit-area disks centered at x_1 and x_2, respectively. If $|x_1 - x_2| = x \le 2r$ and x_1 and x_2 are given, then

$$\begin{aligned} E\left(\chi_k(x_1)\chi_k(x_2)\right) &= P(\text{Both } B_1 \text{ and } B_2 \text{ contain less than } k \text{ nodes}) \\ &\le P(B_1 \text{ contains less than } k \text{ nodes}, B_2 - B_1 \text{ contains less than } k \text{ nodes}) \\ &= P(B_1 \text{ contains less than } k \text{ nodes}) \times P(B_2 - B_1 \text{ contains less than } k \text{ nodes}) \end{aligned} \tag{A.7}$$

The last equality results from the fact that B_1 and $B_2 - B_1$ are disjoint and thus the number of nodes that are located in them are independent (under the Poisson point process assumption) of each other. The first term in Eq. (A.7) can be expressed as

$$P(B_1 \text{ contains less than } k \text{ nodes}) = e^{-\lambda}\sum_{i=0}^{k-1}\frac{\lambda^i}{i!}. \tag{A.8}$$

Let $B(u)$ denote the intersection area of the two unit-area disks whose centers are $2u$ apart. Then,

$$B(u) = 4\int_u^1 (1-y^2)^{1/2}dy = \pi - 4\int_0^u (1-y^2)^{1/2}dy \tag{A.9}$$

Now the second term of Eq. (A.9) can be expressed as

$$\begin{aligned}\int_0^u (1-y^2)^{1/2}dy &= (u/2)\left\{u^{-1}\arcsin u + (1-u^2)^{1/2}\right\} \\ &\geq (u/2)\arcsin 1 = (\pi/4)u,\end{aligned} \tag{A.10}$$

since $u^{-1}\arcsin u + (1-u^2)^{1/2}$ is decreasing on (0,1). Hence the area of $B_2 - B_1$ is

$$\begin{aligned}||B_2 - B_1|| &= r^2(\pi - B(x/(2r))) \\ &\geq r^2 \cdot 4(\pi/4)\cdot x/(2r) = x/(2r).\end{aligned} \tag{A.11}$$

Therefore,

$$\begin{aligned}P(B_2 - B_1 \text{ contains less than } k \text{ nodes}) &= e^{-\lambda||B_2-B_1||}\sum_{i=0}^{k-1}\frac{(\lambda||B_2-B_1||)^i}{i!} \\ &\leq e^{-\lambda x/(2r)}\sum_{i=0}^{k-1}\frac{(\lambda x/(2r))^i}{i!},\end{aligned} \tag{A.12}$$

since $e^{-x}\sum_{i=0}^{k-1} x^i/i!$ is decreasing on $[0,+\infty)$.

By Eqs. (A.7), (A.8) and (A.12), we can express I_2 as

$$\begin{aligned}I_2 &\equiv \int\int_{R^2\cap\{|x_1-x_2|\leq 2r\}} E\{\chi_k(x_1)\chi_k(x_2)\}dx_1dx_2 \\ &\leq \int_R dx_1\int_0^{2r}\left(e^{-\lambda}\sum_{i=0}^{k-1}\frac{\lambda^i}{i!}\right)\left(e^{-\lambda x/(2r)}\sum_{i=0}^{k-1}\frac{(\lambda x/(2r))^i}{i!}\right)2\pi x dx \\ &= \ell^2\left(e^{-\lambda}\sum_{i=0}^{k-1}\frac{\lambda^i}{i!}\right)\left(\int_0^1 e^{-\lambda u}\sum_{i=0}^{k-1}\frac{(\lambda u)^i}{i!}8udu\right),\end{aligned} \tag{A.13}$$

where the last equality is obtained by changing variable $u = x/(2r)$. The third factor in Eq. (A.13) can be further simplified as follows.

$$\begin{aligned}\int_0^1 e^{-\lambda u}\sum_{i=0}^{k-1}\frac{(\lambda u)^i}{i!}\cdot 8udu &\leq \int_0^{+\infty} e^{-\lambda u}\sum_{i=0}^{k-1}\frac{(\lambda u)^i}{i!}\cdot 8udu \\ &= \int_0^{+\infty} e^{-\lambda u}\sum_{i=0}^{k-1}\frac{\lambda^i u^{i+1}}{i!}\cdot 8du\end{aligned}$$

$$
\begin{aligned}
&= \sum_{i=0}^{k-1} \frac{\lambda^{-2}\Gamma(i+2)}{i!} \cdot 8 \\
&= \lambda^{-2} \sum_{i=0}^{k-1} (i+1) \cdot 8 \\
&= 4k(k+1)\lambda^{-2}. \qquad \text{(A.14)}
\end{aligned}
$$

Hence we have

$$
I_2 \leq 4k(k+1)\lambda^{-2}\ell^2 \left(e^{-\lambda} \sum_{i=0}^{k-1} \frac{\lambda^i}{i!} \right). \qquad \text{(A.15)}
$$

Combining Eqs. (A.5), (A.6) and (A.15), we have

$$
E(V_k^2) \leq (EV_k)^2 + 4k(k+1)\lambda^{-2}\ell^2 \left(e^{-\lambda} \sum_{i=0}^{k-1} \frac{\lambda^i}{i!} \right). \qquad \text{(A.16)}
$$

□

A.5 Proof of Theorem 4.5.1

Without loss of generality, we assume l is an integer. We can divide the region $R = [0, l] \times [0, l]$ into unit grids: $R = \cup_{0 \leq i,j \leq l-1,} D(i, j)$, where $D(i, j) = [i, i + 1] \times [j, j + 1]$. Now, let $V_k(i, j) = V_k \cap D(i, j)$. Since each disk is of radius $r = 1/\sqrt{\pi}$, if two grids $D(i, j)$ and $D(i', j')$ are separated by at least $2r$, then $V_k(i, j)$ and $V_k(i', j')$ are independent variables by the assumption of Poisson point process. Thus we can divide the $V_k(i, j)$'s into (finite) m groups $\mathcal{I}_1, \mathcal{I}_2, \cdots, \mathcal{I}_m$, and V_k's in each group are independent of each other. As such, we can write

$$
\begin{aligned}
\sum_{0 \leq i,j \leq l-1} V_k(i, j) = &\sum_{(i,j) \in \mathcal{I}_1} V_k(i, j) + \cdots \\
&+ \sum_{(i,j) \in \mathcal{I}_m} V_k(i, j), \qquad \text{(A.17)}
\end{aligned}
$$

where for each p the variables $\{V_k(i, j) : (i, j) \in \mathcal{I}_p\}$ are stochastically independent. The number n_p of elements in each $\mathcal{I}_p$ go to $+\infty$ while the number m of groups is a finite constant as $l \to +\infty$, and $\cup_p \mathcal{I}_p = [0, l] \times [0, l]$. By the strong law of large numbers,

$$
n_p^{-1} \sum_{(i,j) \in \mathcal{I}_p} V_k(i, j) \to F(k, \lambda) \qquad \text{(A.18)}
$$

almost surely as $l \to +\infty$ for $1 \le p \le m$. Hence,

$$\begin{aligned}
&\lim_{l\to+\infty} \frac{V_k}{l^2} \\
&= \lim_{l\to+\infty} \frac{\sum_p \sum_{(i,j)\in\mathcal{I}_p} V_k(i,j)}{\sum_p n_p} \\
&= \lim_{l\to+\infty} \sum_p \frac{\sum_{(i,j)\in\mathcal{I}_p} V_k(i,j)}{n_p} \cdot \frac{n_p}{\sum_p n_p} \\
&= \lim_{l\to+\infty} \sum_p \frac{n_p}{\sum_p n_p} \cdot F(k,\lambda) \\
&= F(k,\lambda)
\end{aligned} \tag{A.19}$$

almost surely. This completes the proof. □

A.6 Proof of Lemma 4.5.1

First we prove (i) $H(k,\alpha)$ monotonically decreases as k increases if $H(k,\alpha) > k$. We need to show that $H(k,\alpha) > H(k+1,\alpha)$. Since we only consider k such that $\alpha > \gamma_k$,

$$\begin{aligned}
& H(k,\alpha) > H(k+1,\alpha) \\
\Leftrightarrow\quad & \frac{\sum_{i=1}^{k-1} i\beta_i}{\alpha-\gamma_k} > \frac{\sum_{i=1}^{k} i\beta_i}{\alpha-\gamma_{k+1}} \\
\Leftrightarrow\quad & (\alpha-\gamma_{k+1})(\sum_{i=1}^{k-1} i\beta_i) > (\alpha-\gamma_k)(\sum_{i=1}^{k} i\beta_i) \\
\Leftrightarrow\quad & (\gamma_k-\gamma_{k+1})(\sum_{i=1}^{k-1} i\beta_i) > k\beta_k\alpha - k\gamma_k\beta_k \\
\Leftrightarrow\quad & \beta_k(\sum_{i=1}^{k-1} i\beta_i) > k\beta_k\alpha - k\gamma_k\beta_k \\
\Leftrightarrow\quad & \sum_{i=1}^{k-1} i\beta_i > k(\alpha-\gamma_k) \\
\Leftrightarrow\quad & H(k,\alpha) > k.
\end{aligned} \tag{A.20}$$

So the first part of the Lemma is proved. In order to prove (ii), we only need to reverse the inequality directions in the above proof. For (iii), we only need to change the inequality sign to equality sign in (i). Next we prove (iv). Since $H(k,\alpha) > k$, we have $\sum_{i=1}^{k-1} i\beta_i > k(\alpha-\gamma_k)$. Hence,

$$\begin{aligned}
H(k+1,\alpha) &= \frac{\sum_{i=1}^{k} i\beta_i}{\alpha-\gamma_{k+1}} \\
&= \frac{\sum_{i=1}^{k-1} i\beta_i + k\beta_k}{(\alpha-\gamma_k)+\beta_k} \\
&> \frac{k(\alpha-\gamma_k)+k\beta_k}{(\alpha-\gamma_k)+\beta_k}
\end{aligned}$$

$$= \quad k. \tag{A.21}$$

In order to prove (v) and (vi) we only need to change the “>” sign in (iv) to “=” and “<” sign respectively.

□

A.7 Proof of Lemma 6.3.2

We prove a generalized version of Lemma 6.3.2 in the context of the site percolation model. Let $\Omega = \Pi_{s\in\mathbb{Z}^d}\{0,1\}$ be the sample space in the underline probability space, where $\mathbb{Z} = \{\cdots, -1, 0, 1, \cdots\}$. Points in Ω are represented as $\omega = (\omega(s) : s \in \mathbb{Z}^d)$ and called *configurations*. The value $\omega(s) = 0$ corresponds to the site (grid) s being closed and $\omega(s) = 1$ corresponds to the site s being open. An event A is called *increasing* if $I_A(\omega) \le I_A(\omega')$ whenever $\omega \le \omega'$, where I_A is the indicator function of the event A. (Interested readers should refer to [31] for more details of the definitions.) Let A be an increasing event. For $\omega \in \Omega$, let $F_A(\omega)$ denote the "distance" of ω from A, i.e.,

$$F_A(\omega) = \inf\left\{\sum_s(\omega'(s) - \omega(s)) : \omega' \ge \omega, \omega' \in A\right\}. \tag{A.22}$$

Note that $F_A(\omega) = 0$ if $\omega \in A$. The generalized version of Lemma 6.3.2 is

$$P_{p_2}(A) \ge \left(\frac{p_2 - p_1}{1 - p_1}\right)^r P_{p_1}(F_A \le r) \tag{A.23}$$

for any $0 < p_1 < p_2 < 1$. With Eq. (A.23), Lemma 6.3.2 is obvious since the event that there is an open path of length m starting from a given source is an increasing event.

Proof. Suppose that $X(s) : s \in \mathbb{Z}^d$ is a family of independent random variables indexed by the grid (site) set $\mathbb{Z}^d$, where each $X(s)$ is uniformly distributed on [0,1]. We may couple together all the site percolation processes on $\mathbb{Z}^d$ in the following way. Let $0 \le p \le 1$ and define $\eta_p \in \Omega$ by

$$\eta_p(s) = \begin{cases} 1 & \text{if} X(s) \le p, \\ 0 & \text{otherwise.} \end{cases} \tag{A.24}$$

We may think of η_p as the random outcome of the site percolation process on $\mathbb{Z}^d$ with the site-open probability p. It is clear that $\eta_{p_1} \le \eta_{p_2}$ whenever $p_1 < p_2$. Thus we may couple two percolation processes with site-open probability p_1 and p_2 in such a way that the set of open sites of the first process is a subset of the set of the open sites of the second.

Suppose that $0 \le p_1 \le p_2 \le 1$ and A is an increasing event. Denote $I_r(A) = \{\omega : F_A(\omega) \le r\}$. If $\eta_{p_1} \in I_r(A)$, there exists a (random) collection $C = C(\eta_{p_1})$ of sites such that

(a) $|C| \le r$;

(b) $\eta_{p_1}(s) = 0$ for all $s \in C$; and

(c) the configuration η obtained from η_{p_1} by declaring all sites in C to be open, satisfies $\eta \in A$.

Suppose now that every s in the set C satisfies $p_1 \leq X(s) \leq p_2$. It follows from (c) above that $\eta_{p_2} \in A$. Conditioning on (b) above, the probability of $p_1 \leq X(s) \leq p_2$ is $((p_2 - p_1)/(1 - p_1))^{|C|}$. Therefore,

$$P(\eta_{p_2} \in A | \eta_{p_1} \in I_r(A)) \geq \left(\frac{p_2 - p_1}{1 - p_1} \right)^r , \tag{A.25}$$

since $|C| \leq r$. Eq. (A.23) follows easily.

A.8 Proof of Lemma 6.6.1

(i) follows directly from Lemma 1.2 in [55]. Alternatively, this can be proved using Chernoff bound.

(ii) Let N be the number of nodes in the field. By (i) *w.h.p.*, $N \geq n/2$. Now conditioning on $N \geq n/2$, all nodes' locations are uniformly independently distributed on the unit square area. Let d_i be the distance between the ith source-destination pairs and d_i' be the distance between the ith source-destination pairs under Torus convention (for a definition, see [83]). Clearly $d_i \geq d_i'$. Let $I(\cdot)$ denote an indicator function. For any $0 < \epsilon < 1/2$,

$$I(d_i \geq \epsilon) \geq I(d_i' \geq \epsilon) = 1 - \pi\epsilon^2. \tag{A.26}$$

Among the N source-destination pairs, we can pick $N' = N/3$ pairs such that any two of them do not share a node. Since nodes' locations are independently uniformly distributed, if two source-destination pairs i, j do not share nodes, their distance d_i, d_j (and d_i', d_j', respectively in the Torus convention) is independent. Without loss of generality, we can assume the first N' pairs do not share nodes. Thus $I_i \triangleq I(d_i' \geq \epsilon)$ is *i.i.d.* Bernoulli random variable with parameter $1 - \pi\epsilon^2$. Let $S_{N'} = \sum_{i \leq N'} I_i$. By Chernoff inequality, for any $\theta < 0, a > 0$,

$$\begin{aligned} P(S_{N'} \leq aN') &\leq E[\exp(\theta(S_{N'} - aN'))] \\ &= \exp(N'(\log E[e^{\theta I_i}] - \theta a)) \\ &= \exp(N'(\log(\pi\epsilon^2 + (1 - \pi\epsilon^2)e^{\theta}) - \theta a) \end{aligned} \tag{A.27}$$

Let $\theta = -1, a = 3/4$ and ϵ sufficiently small, we have $\delta \triangleq \log(\pi\epsilon^2 + (1 - \pi\epsilon^2)e^{\theta}) - \theta a < 0$ and

$$P(S_{N'} \leq 3N'/4) \leq \exp(N'\delta) \to 0 \text{ as } N' \to \infty. \tag{A.28}$$

Thus *w.h.p.*, the number of pairs with distance at least ϵ is at least $3N'/4 = N/4 \geq n/8$. □

References

[1] Gauss's circle problem. http://mathworld.wolfram.com/GausssCircle Problem.html.

[2] ns-2 network simulator. *http://www.isi.edu/nsnam/ns*.

[3] I. F. Akyildiz, W. Su, Y. Sankarasubramaniam, and E. Cayirci. Wireless sensor networks: A survey. *Computer Networks*, 38(4):393–422, March 2002.

[4] KEYENCE America. http://www.keyence.com/products/sensors.html.

[5] C. Peraki and. S. Servetto. On the maximum stable throughput problem in random wireless networks with directional antennas. In *ACM Mobihoc*, 2003.

[6] A. Arora and *et al.* A line in the sand: A wireless sensor network for target detection, classification, and tracking. Technical Report OSU-CISRC-12/03-TR17, Ohio State University, 2003.

[7] N. Bansal and Z. Liu. Capacity, delay and mobility in wireless ad-hoc networks. In *Proc. of IEEE Infocom*, 2003.

[8] M. Bhardwaj and A. P. Chandrakasan. Upper bounds on the lifetime of wireless sensor networks. In *Proc. of IEEE International Conference on Communications (ICC) 01*, 2001.

[9] M. Bhardwaj and A. P. Chandrakasan. Bounding the lifetime of sensor network via optimal role assignments. In *Proc. of IEEE Infocom*, 2002.

[10] D. M. Blough and P. Santi. Investigating upper bounds on network lifetime extension for cell-based energy conservation techniques in stationary ad hoc networks. In *Proc. of ACM Mobicom 2002*, 2002.

[11] D.M. Blough, M. Leoncini, G. Resta, and P. Santi. On the symmetric range assignment problem in wireless ad hoc networks. In *Proc. of the 2nd IFIP International Conference on Theoretical Computer Science*, pages 71–82, Montreal, Aug. 2002.

[12] N. Bulusu. *Self-Configuring Localization Systems*. PhD thesis, University of California, Los Angeles, 2002.

[13] N. Bulusu, J. Heidemann, and D. Estrin. GPS-less low cost outdoor localization for very small devices. *IEEE Personal Communications Magazine*, 7(5):28–34, October 2000.

[14] A. Cerpa and D. Estrin. Ascent: Adaptive self-configuring sensor networks topologies. In *Proc. of Infocom 2002*.

[15] B. Chen, K. Jamieson, H. Balakrishnan, and R. Morris. Span: An energy-efficient operation in multihop wireless ad hoc networks. In *Proc. of ACM MobiCom'01*, 2001.

[16] A. E.F. Clementi, P. Penna, and R. Silvestri. On the power assignment problem in radio networks. *Mobile Networks and Applications*, 9(2), April 2004.

[17] S. Coleri, M. Ergen, and T. J. Koo. Lifetime analysis of a sensor network with hybrid automata modelling. In *First ACM International Workshop on Wireless Sensor Network and Applications (WSNA02)*, Sep. 2002.

[18] T.M. Cover and J. A. Thomas. *Elements of Information Theory*. John Wiley, 1991.

[19] A. Dana and B. Hassibi. Power bandwidth trade-off in sensory and ad-hoc wireless networks. In *Proc. of International Symposium on Information Theory (ISIT)*, Chicago, IL, USA, June, 2004.

[20] A. Dana and B. Hassibi. Power bandwidth trade-off in sensory and ad-hoc wireless networks. In *Fourth Annual Workshop on Advanced Networking*, Pasadena, CA, USA, May, 14, 2004.

[21] R. S. Diggavi, M. Grossglauser, and D. Tse. Even one-dimensional mobility increases adhoc wireless capacity. In *Proc. of IEEE Int. Symp. Information Theory (ISIT)*, Lausanne, Switzerland, June 2002.

[22] L. Doherty, L. El Ghaoui, and K. S. J. Pister. Convex position estimation in wireless sensor networks. In *Proc. of IEEE Infocom 2001*, Anchorage, AK, April 2001.

[23] O. Dousse and P. Thiran. Connectivity vs capacity in dense ad hoc networks. In *Proc. IEEE Infocom*, 2004.

[24] D. Estrin, R. Govindan, J. S. Heidemann, and S. Kumar. Next century challenges: Scalable coordination in sensor networks. In *Proc. of ACM MobiCom'99*, Washington, August 1999.

[25] L. Feeney and M. Nilsson. Investigating the energy consumption of a wireless network interface in an ad hoc networking environment. In *Proc. of IEEE Infocom 2001*, 2001.

[26] M. Franceschetti, O. Dousse, D. Tse, and P. Thiran. Closing the gap in the capacity of random wireless networks. *Preprint under submission*, 2004.

[27] M. Franceschetti, O. Dousse, D. Tse, and P. Thiran. Closing the gap in the capacity of random wireless networks. In *Proc. of IEEE International Symposium on Information Theory (ISIT'04)*, June 2004.

[28] A. El Gamal, J. Mammen, B. Prabhakar, and D. Shah. Throughput-delay trade-off in wireless networks. In *Proc. of IEEE Infocom*, 2004.

[29] M. Gastpar and M. Vetterli. On the capacity of wireless networks: the relay case. In *proc. of IEEE Infocom*, 2002.

[30] J. Gomez and A. Campbell. A case for variable-range transmission power control in wireless multihop networks. In *Proc. of IEEE Infocom 2004*.

[31] G. Grimmett. *Percolation*. Springer, 1998.

[32] M. Grossglauser and D. Tse. Mobility increases the capacity of ad-hoc wireless networks. In *proc. of IEEE Infocom 2001*, 2001.

[33] H. Gupta, S. Das, and Q. Gu. Connected sensor cover: Self-organization of sensor networks for efficient query execution. In *Proc. of Mobihoc 2003*, 2003.

[34] P. Gupta and P. R. Kumar. The capacity of wireless networks. *IEEE Transactions and Information Theory*, March 2000.

[35] P. Gupta and P.R. Kumar. Critical power for asymptotic connectivity in wireless networks. *Stochastic Analysis, Control, Optimization and Applications: A Volume in Honor of W.H. Fleming, 1998*.

[36] P. Hall. *Introduction to the Theory of Coverage Processes*. John Wiley and Sons, 1988.

[37] W. B. Heinzelman, A. P. Chandrakasan, and H. Balakrishnan. An application-specific protocol architecture for wireless microsensor networks. *IEEE Transactions on Wireless Communications*, (4), October 2002.

[38] C. F. Huang and Y. C. Tseng. The coverage problem in a wireless sensor network. In *ACM International Workshop on Wireless Sensor Networks and Applications (WSNA)*, 2003.

[39] C. F. Huang and Y. C. Tseng. The coverage problem in a wireless sensor network. *ACM Mobile Networks and Applications (MONET) special issue on Wireless Sensor Networks*, 2004.

[40] Crossbow Technology Inc. http://www.xbow.com/support/support_pdf_files/mts-mda_series_user_manual_revb.pdf.

[41] J. M. Kahn, R. H. Katz, and K. S. J. Pister. Next century challenges: Mobile networking for "smart dust". In *Proc. of ACM MobiCom'99*, August 1999.

[42] S. Kandula and J. C. Hou. Hierarchical clustering for data-centric sensor networks. Technical report, University of Illinois at Urbana, Champaign, August 2002.

[43] U. Kozat and L. Tassiulas. Throughput capacity of random ad hoc networks with infrastructure support. In *Proc. of ACM Mobicom*, 2003.

[44] S. Kumar, T. H. Lai, and J. Balogh. On k-coverage in a mostly sleeping sensor network. In *ACM Mobicom 2004*.

[45] J. Li, C. Blake, D. S. J. De Couto, H. Lee, and R. Morris. Capacity of ad hoc wireless networks. In *proc. of ACM Mobicom'01*, Sep. 2001.

[46] L. Li, J. Halpern, V. Bahl, Y.M. Wang, and R. Wattenhofer. Analysis of a cone-based distributed topology control algorithm for wireless multi-hop networks. In *Proceedings of ACM Symposium on Principle of Distributed Computing (PODC)*, pages 264–273, 2001.

[47] X. Li, P. Wan, and O. Frieder. Coverage in wireless ad-hoc sensor networks. In *ICC 2002*, New York City, April 28 – May 2nd 2002.

[48] K. Lieska, E. Laitinen, and J. Lahteenmaki. Radio coverage optimization with genetic algorithms. In *IEEE International Sysmpsium on Personal, Indoor and Mobile Radio Communications*, volume 1, pages 318–22, Sep. 1998.

[49] B. Liu, Z. Liu, and D. Towsley. On the capacity of hybrid wireless networks. In *Proc. of IEEE Infocom 2003*, March 2003.

[50] A. Mainwaring, J. Polastre, R. Szewczyk, and D. Culler. Wireless sensor networks for habitat monitoring. In *First ACM International Workshop on Wireless Workshop in Wireless Sensor Networks and Applications (WSNA 2002)*, August 2002.

[51] S. Meguerdichian, F. Koushanfar, M. Potkonjak, and M. B. Srivastava. Coverage problems in wireless ad-hoc sensor networks. In *IEEE Infocom*, pages 1380–1387, 2001.

[52] A. Molina, G. E. Athanasiadou, and A.R. Nix. The automatic location of base-station for optimized cellular coverage: a new combinatiorial approach. In *IEEE 49th Vehicular Technology Conference*, volume 1, pages 606–10, May 1999.

[53] Motes. http://www.xbow.com/products/wireless_sensor_networks.htm.

[54] R. Negi and A. Rajeswaran. Capacity of power constrained ad-hoc networks. In *Proc. of IEEE Infocom 2004*, March 2004.

[55] M. Penrose. *Random Geometric Graphs*. Oxford University Press, 2003.

[56] M.D. Penrose. The longest edge of the random minimal spanning tree. *Annals of Applied Probability*, 7:340–361, 1997.

[57] M.D. Penrose. On k-connectivity for a geometric random graph. *Random Structures & Algorithms*, 15:145–164, 1999.

[58] E. Perevalov and R. Blum. Delay limited capacity of ad hoc networks: asymptotically optimal transmission and relaying strategy. In *Proc. of IEEE Infocom 2003*, March 2003.

[59] T. K. Philips, S. S. Panwar, and A. N. Tantawi. Connectivity properties of a packet radio network model. *IEEE Transaction on Information Theory*, 35(5):1044–1047, 1989.

[60] B. Rengarajan, J. Chen, S. Shakkottai, and T. S. Rappaport. Connectivity of sensor networks with power control. In *Proc. of 37th Asilomar Conference on Signals, Systems and Computers*, November 2003.

[61] S. G. Samko, A. A. Kilbas, and O. I. Marichev. *Fractional Integrals and Derivatives*, page 9. Yverdon, Switzerland: Gordon and Breach, 1993.

[62] P. Santi and D. M. Blough. The critical transmitting range for connectivity in sparse wireless ad hoc networks. *IEEE transactions on Mobile Computing*, 2(1):25–39, 2003.

[63] A. Savvides, C. Han, and M. Strivastava. Dynamic fine-grained localization in ad-hoc networks of sensors. In *Proc. of ACM MOBICOM'01*, pages 166–179. ACM Press, 2001.

[64] Infrared Sensor. http://www.interq.or.jp/japan/se-inoue/e_pyro.htm.

[65] S. Shakkottai, R. Srikant, and N. Shroff. Unreliable sensor grids: Coverage, connectivity and diameter. In *Proc. of IEEE Infocom 2003*.

[66] E. Shih, S. Cho, N. Ickes, R. Min, A. Sinha, A. Wang, and A. Chandrakasan. Physical layer driven protocol and algorithm design for energy-efficient wireless sensor networks. In *Proc. of ACM MobiCom'01*, Rome, Italy, July 2001.

[67] S. Slijepcevic and M. Potkonjak. Power efficient organization of wireless sensor networks. In *ICC 2001*, Helsinki, Finland, June 2001.

[68] J. M. Steele. Growth rates of euclidean minimal spanning trees with power weighted edges. *The Annals of Probability*, 16(4), 1988.

[69] D. Tian and N. D. Georganas. A coverage-preserving node scheduling scheme for large wireless sensor networks. In *First ACM International Workshop on Wireless Sensor Networks and Applications*, Georgia, GA, 2002.

[70] S. Toumpis. Capacity bounds for three classes of wireless networks: Asymmetric, cluster and hybrid. In *Proc. of ACM Mobihoc 2004*, May 2004.

[71] S. Toumpis and A. J. Goldsmith. Large wireless networks under fading, mobility and delay constraints. In *Proc. of IEEE Infocom 2004*, March 2004.

[72] P. Wan and C. Yi. Coverage by randomly deployed wireless sensor networks. Submitted to Special Issue of the IEEE Transactions on Information Theory and the IEEE/ACM Transactions on Networking, 2005.

[73] P-J. Wan and C. Yi. Asymptotic critical transmission radius and critical neighbor number for k-connectivity in wireless ad hoc networks. In *ACM Mobihoc 2004*.

[74] X. Wang, G. Xing, Y. Zhang, C. Lu, R. Pless, and C. Gill. Integrated coverage and connectivity configuration in wireless sensor networks. In *ACM Sensys'03*, Nov. 2003.

[75] L. Xie and P.R. Kumar. A network information theory for wireless communication: Scaling laws and optimal operation. *IEEE Transactions on Information Theory*, 50(5):748–767, May 2004.

[76] G. Xing, X. Wang, Y. Zhang, and C. Lu. Integrated coverage and connectivity configuration for energy conservation in sensor networks. 2005.

[77] Y. Xu, J. Heidemann, and D. Estrin. Geography-informed energy conservation for ad hoc routing. In *Proc. of ACM MOBICOM'01*, Rome, Italy, July 2001.

[78] F. Xue and P.R. Kumar. The number of neighbors needed for connectivity of wireless networks. *Wireless Networks*, 2003. URL:http://decision.csl.uiuc.edu/ prkumar.

[79] F. Ye, G. Zhong, S. Lu, and L. Zhang. Energy efficient robust sensing coverage in large sensor networks. Technical report, UCLA, 2002.

[80] F. Ye, G. Zhong, S. Lu, and L. Zhang. Peas: A robust energy conserving protocol for long-lived sensor networks. In *The 23nd International Conference on Distributed Computing Systems (ICDCS)*, 2003.

[81] S. Yi, Y. Pei, and S. Kalyanaraman. On the capacity improvement of ad hoc wireless networks using directional antenna. In *ACM Mobihoc*, 2003.

[82] J. E. Yukich. Asymptotics for weighted minimal spanning trees on random points. *Stochastic Processes and Their Applications*, 85:123–128, 2000.

[83] H. Zhang and J. Hou. On deriving the upper bound of α-lifetime for large sensor networks. In *Proc. of ACM MobiHoc 2004*, May 2004.

[84] H. Zhang and J. Hou. On the critical total power for asymptotic k-connectivity in wireless networks. Technical Report UIUCDCS-R-2004-2454, Computer Science Department, University of Illinois at Urbana, Champaign, http://lion.cs.uiuc.edu/ hzhang3/papers/k-connect_tech.ps, July 2004.

[85] H. Zhang and J. C. Hou. Maintaining sensing coverage and connectivity in large sensor networks. Technical Report UIUCDCS-R-2003-2351, Department of Computer Science, University of Illinois at Urbana-Champaign, June 2003.

Author's Biography

Honghai Zhang was born in Chaohu, Anhui, China, in 1975. He graduated from the Special Class for Gifted Young in the University of Science and Technology of China with a degree in Computer Science. He completed a Master of Science in Computer Science at University of Illinois in 2001.

His research interests include protocol design, performance analysis, and simulation and modeling in wireless networks, sensor networks, mesh networks, and WIMAX.